Development of a human 3D immune competent full-thickness skin model for the identification and characterization of sensitizers and drug discovery

Inaugural-Dissertation

zur Erlangung des Doktorgrades
der Mathematisch-Naturwissenschaftlichen Fakultät
der Heinrich-Heine-Universität Düsseldorf

vorgelegt von

Johanna Maria Hölken
aus Münster

Düsseldorf, Mai 2024

aus dem Institut für Pharmazeutische Biologie und Biotechnologie
der Heinrich-Heine-Universität Düsseldorf

durchgeführt an dem Institut für Pharmazeutische Biologie und Biotechnologie
der Heinrich-Heine-Universität Düsseldorf

und

an dem Institut für Gesundheitsforschung und Bildung, Abteilung Biomedizinische
Grundlagen der Universität Osnabrück

Gedruckt mit der Genehmigung der
Mathematisch-Naturwissenschaftlichen Fakultät der
Heinrich-Heine-Universität Düsseldorf

Berichterstatter:

1. Frau Prof. Dr. Nicole Teusch

2. Frau Prof. Dr. Stefanie Scheu

Tag der mündlichen Prüfung: 29.10.2024

Summary

In the past decades, toxicological testing, skin sensitization risk assessments, and drug development studies have been conducted primarily using animal models. However, the species-specific differences in anatomy, pathophysiology, and especially immune cell population are enormous, resulting in frequent failure to transfer the findings to human tissue. Thus, great efforts have been made to develop new non-animal approach methods (NAMs). However, since skin sensitization is a complex inter- and intracellular mechanism, the single-endpoint test methods developed to date are insufficient to completely replace animal models for assessing the sensitivity potential of chemicals. Hence, we aimed to develop a physiologically relevant 3D immune competent full-thickness skin equivalent (FTSE) for the identification and characterization of sensitizers and drug candidates. To achieve this, we first established a robust and highly reproducible protocol for the differentiation of the human leukemia monocyte cell line THP-1 into surrogates for immature dendritic cells (iDCs). The functionality of THP-1-derived iDCs was demonstrated by their ability to phagocytose exogenous particles as well as by the sensitizer-induced expression of Interleukin (IL)-12p40, which is required for T cell activation. The strong induction of the surface marker expression of the cluster of differentiation (CD)54 and CD86 upon sensitizer treatment indicated the applicability of iDCs to identify potentially sensitizing substances. In terms of drug discovery, this thesis demonstrates the promising anti-inflammatory potential of Pseudopterosin A-D in skin sensitization, reflected by the significant reduction of sensitizer-induced upregulation of surface markers such as CD54 and CD86. Additionally, the inhibition of the secretion of inflammatory cytokines such as IL-8, IL-6, and TNF-α to a similar extent as dexamethasone and the blockade of the sensitizer-induced activation of the inflammatory signaling pathways nuclear factor (NF)-κB and p38 mitogen-activated protein kinase (MAPK) support the relevance of Pseudopterosin A-D in skin sensitization.

Notably, THP-1-derived iDCs could be integrated into a FTSE as $CD11^+$ and $CD14^-$-derived dermal dendritic cell surrogates (DDCs). Topical treatment of the newly developed FTSE with nickel sulfate ($NiSO_4$) induced the upregulation of the surface markers CD54 and CD86 on the tissue-integrated DDC surrogates, which could be suppressed by pre-treatment with dexamethasone, thereby proving immune-competence on the one hand and the applicability for sensitizer identification and drug discovery on the other hand. To generate a physiologically relevant immune-competent skin model comprising Langerhans cells (LCs) and DDCs, THP1-derived DDC surrogates could be co-integrated into an FTSE together with LC surrogates, differentiated from the human myeloid leukemia cell line Mutz-3. Remarkably, treatment of the FTSE with incorporated LC and DDC surrogates showed an early sensitizer-induced response, reflected by increased numbers of CD1a-positive cells in the epidermis and dermis 8 hours after exposure.

Overall, our newly developed FTSE, which includes integrated LC and DDC surrogates, has great potential for studying dendritic cell (DC) activation as well as for the identification and characterization of sensitizers and drug candidates according to the 3Rs (“Replacement,” “Reduction,” and “Refinement”).

Zusammenfassung

In den vergangenen Jahrzehnten wurden toxikologische Tests und Risikobewertungen von Hautsensibilisatoren sowie Studien zur Arzneimittelentwicklung hauptsächlich an Tiermodellen durchgeführt. Die artspezifischen Unterschiede in der Anatomie, der Pathophysiologie und insbesondere in der Immunzellpopulation sind jedoch enorm, so dass die Ergebnisse häufig nicht auf menschliches Gewebe übertragen werden können. Daher wurden große Bemühungen unternommen, neue tierversuchsfreie Methoden (NAMs) zu entwickeln. Da es sich bei der Hautsensibilisierung jedoch um einen komplexen inter- und intrazellulären Mechanismus handelt, reichen die bisher entwickelten Einzelendpunkt-Testmethoden als eigenständige Methoden nicht aus, um Tiermodelle zur Beurteilung des Sensibilisierungspotenzials von Chemikalien vollständig zu ersetzen. Unser Ziel war es daher, ein humanphysiologisch relevantes immunkompetentes 3-D-Vollhautäquivalent (FTSE) für die Identifizierung und Charakterisierung von Sensibilisatoren und Wirkstoffkandidaten zu entwickeln.

Zu diesem Zweck haben wir zunächst ein robustes und in hohem Maße reproduzierbares Protokoll für die Differenzierung der menschlichen Leukämie-Monozyten-Zelllinie THP-1 in Surrogate für unreife dendritische Zellen (iDCs) etabliert. Die Funktionalität von THP-1-abgeleiteten iDCs wurde durch die Fähigkeit zur Phagozytose exogener Partikel sowie durch die Sensibilisator-induzierte Expression von Interleukin (IL)-12p40, welches für die T-Zell-Aktivierung erforderlich ist, nachgewiesen. Die starke Induktion der Expression der Oberflächenmarker Cluster of Differentiation (CD)54 und CD86 nach der Behandlung mit Sensibilisatoren deutet auf die Anwendbarkeit von iDCs zur Identifizierung potenziell sensibilisierender Substanzen hin. Im Hinblick auf die Entdeckung von Wirkstoffkandidaten zeigte diese Arbeit ein vielversprechendes entzündungshemmendes Potenzial von Pseudopterosin A-D bei Hautsensibilisierung, welches durch eine signifikante Verringerung der Sensibilisator-induzierten Hochregulierung von Oberflächenmarkern wie CD54 und CD86 sowie durch die Hemmung der Sekretion inflammatorischen Zytokine wie IL-8, IL-6 und TNF-α in ähnlichem Ausmaß wie Dexamethason und durch die Blockade der durch Sensibilisatoren induzierten Aktivierung der inflammatorischen Signalwege Nuklearfaktor (NF)-κB und p38 mitogen-aktivierte Proteinkinase (MAPK) nachgewiesen wurde.

Darüber hinaus konnten THP-1-abgeleitete iDCs erfolgreich als $CD11^+$ und $CD14^-$ dermale dendritische Zellsurrogate (DDCs) in ein FTSE integriert werden. Die topische Behandlung der neu entwickelten FTSE mit Nickelsulfat ($NiSO_4$) führte zu einer Hochregulierung der Oberflächenmarker CD54 und CD86 auf den gewebeintegrierten DDC-Surrogaten, die durch eine Vorbehandlung mit Dexamethason unterdrückt werden konnte, was einerseits die Immunkompetenz und andererseits die Anwendbarkeit für die Identifizierung und Charakterisierung von Sensibilisatoren und Wirkstoffkandidaten beweist. Um ein physiologisch relevantes immunkompetentes Hautmodell mit Langerhans-Zellen (LCs) und DDCs zu erzeugen, wurden THP-1 abgeleitete DDC-Surrogate zusammen mit LC-Surrogaten, die aus der menschlichen myeloischen Leukämiezelllinie Mutz-3 differenziert wurden, in ein FTSE integriert. Bemerkenswerterweise zeigte die Behandlung des FTSE mit inkorporierten LC- und DDC-Surrogaten eine frühe Sensibilisierungsreaktion, die sich in einer erhöhten Anzahl CD1a-positiver Zellen in der Epidermis und Dermis acht Stunden nach der Exposition zeigte.

Insgesamt birgt unser neu entwickeltes FTSE, das integrierte LC- und DDC-Surrogate enthält, großes Potenzial für die Untersuchung der Aktivierung dendritischer Zellen (DC) sowie für die Identifizierung und Charakterisierung von Sensibilisatoren und Wirkstoffkandidaten nach den 3R-Prinzipien ("Replacement", "Reduction" und "Refinement").

Table of Contents

1 Introduction

1.1 Skin sensitization and allergic contact dermatitis

Skin sensitization is caused by chemicals, leading to an immunological response that results in allergic contact dermatitis (ACD). Clinically, ACD is defined as a form of T cell-mediated Type IV delayed hypersensitivity [1, 2], which often causes contact-dependent local skin reactions characterized by redness (erythema), swelling (oedema) and itching (pruritus), rashes, eczema, and sometimes blisters [3-5]. Overall, ACD is a prevalent skin condition, affecting up to 20% of the general population in industrialized countries [6]. Common sources of sensitizing agents include metals, personal care products, cosmetics, hair dyes, or rubber materials [7, 8]. Notably, ACD, together with irritant contact dermatitis (ICD), accounts for the majority of occupational skin conditions due to close and repeated contact with common allergens among mechanics, assemblers, metal workers, construction workers, healthcare workers, food handlers, and hairdressers [9-11]. Today, the most prevalent allergens are nickel sulfate ($NiSO_4$), fragrance mix, (chloro)-methylisothiazolinone, and cobalt chloride [12, 13]. Industrialization and modern lifestyles have increased exposure to consumer products containing substances that can cause contact allergies, leading to constantly evolving trends and shifts in allergen exposure [14]. ACD is a chronic, lifelong disease that can affect any part of the body and is therefore associated with high personal burdens and an impact on quality of life [15-17]. Strong negative emotions such as annoyance, frustration, and embarrassment can lead to psychological stress and depression, often impairing social and interpersonal relationships [16, 17]. Furthermore, sleep disturbances due to pruritus and skin pain [17, 18] as well as reduced productivity at school or work have been reported [15, 17]. Accordingly, ACD leads to significant public health burdens, including increased medical costs, prolonged sick leave, loss of employment, and worker compensation, resulting in socioeconomic costs with an estimated range from the hundreds of millions up to one billion dollars per year [16, 19, 20]. Hence, skin sensitization is acknowledged as a significant occupational and environmental health concern due to its prevalence, persistence, and impact on quality of life [21]. To ensure human and environmental safety, various demands and regulations have been put in place (reviewed in Chapter 1.2) to screen and evaluate the potential hazards of new chemicals and drugs.

1.2 Regulatory demands and commitment to 3R research

In the European Union (EU), the regulation on registration, evaluation, authorization, and restriction of chemicals (REACH) provides the legal basis for the protection of human health and the environment from potentially hazardous chemicals [22]. Before receiving authorization, every chemical must comply with the legal requirements defined by the REACH regulation (EC 1907/2006) [23], while cosmetics must comply with the requirements of the EU Cosmetic regulation (EC 1223/2009) [24]. Chemical safety reports and hazard assessments, including skin sensitization using reliable test methods are mandatory for approval [25, 26]. Furthermore, potency prediction according to the UN Global Harmonized System (GHS) or the European Union's Classification, Labelling and Packing (CLP) Regulation (EC 1272/2008) is required to discriminate and classify categories of 1A (strong) and 1B (other/non-) sensitizers [27, 28].

Toxicological testing and risk assessment for skin sensitization have traditionally been accomplished using animal models, such as the mouse local lymph node assay (LLNA) [29, 30], the Buehler assay (BA) [31], and the guinea pig maximization test (GPMT) [32]. However, toxicological testing and assessment of skin sensitization potential in animal models has several limitations. First of all, the species-specific differences in the anatomy, pathophysiology, and immune cell population are tremendous [33]. Compared to mouse skin, human skin has larger areas of interfollicular skin, fewer hair follicles, and a thicker dermis and epidermis with more cellular layers [33, 34], which needs to be considered in terms of sensitizer penetration and drug delivery studies [34, 35]. Even more importantly, the substantial differences in the cutaneous dendritic cell (DC) subsets of humans and mice, which are not only distinguished by their surface marker phenotype but also according to their ontogeny and transcriptomic signature—and thus according to their specialization and capacity in antigen presentation—have become more explicit in recent years [36-38]. For example, the surface marker molecule cluster of differentiation (CD)1a, which is highly abundant on human Langerhans cells (LCs) and was reported to be involved in antigen presentation to T cells, is not expressed on murine or rat LCs [39-41]. Furthermore, mice fail to develop CHS upon exposure to nickel, the most frequent sensitizer, as binding of nickel to toll-like receptor (TLR) 4 requires the presence of two non-conserved histidine residues (H456 and H458), which are not expressed on murine TLR4 [42]. Notably, comparing human and murine skin transcriptomes reveals that humans and mice share approximately only 30% of skin-associated genes [43]. Taken together, these vast differences in skin biology often result in a failure to translate the findings from mouse models to human tissue. Indeed, when compared to human data, the overall predictive accuracy of the GMPT or LLNA was ~ 72% [44]. Hence, not only in terms of ethical concerns and animal welfare but also in terms of human (consumer) health and safety, the development of alternative non-animal methods is strongly recommended.

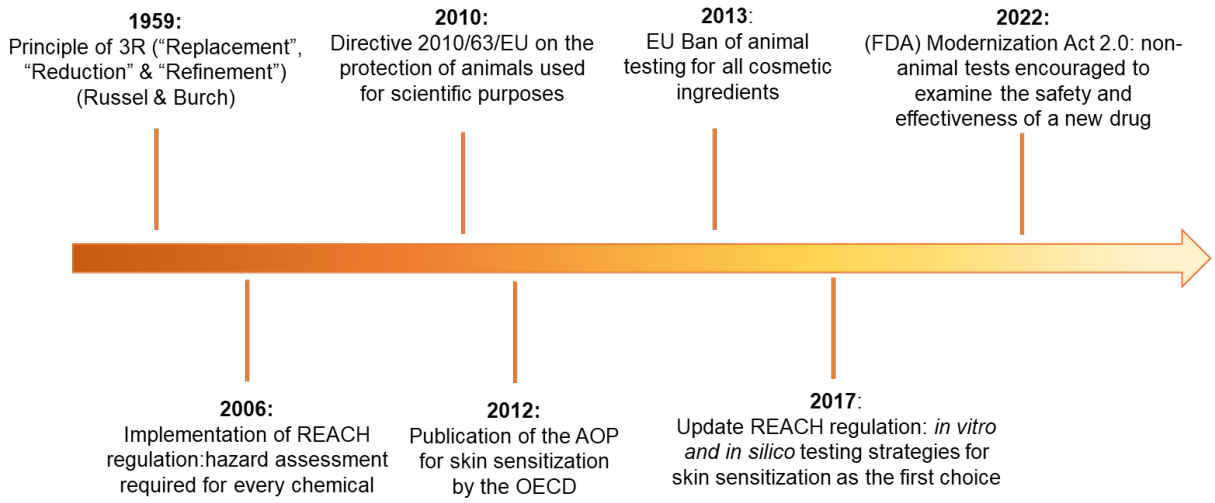

Figure 1.2-1 Timeline of selected milestones towards the implementation of the 3R principles ("Replacement," "Reduction," and "Refinement") for hazard identification and risk assessment in skin sensitization.

In 1959, Russell and Burch introduced the 3R principles of "Replacement," "Reduction," and "Refinement" as a framework for animal welfare in scientific testing [45]. Since then, these principles have become the basis for national and international regulations on the use of animals in scientific experiments, especially in terms of toxicological testing, including skin sensitization, and safety assessment of new chemicals and drugs (Figure 1.2-1). Indeed, in 2010 the principles of 3R were implemented for the first time in "Directive 2010/63/EU on the protection of animals used for scientific purposes," which demanded a reduction in the use of animals wherever possible without compromising the outcome of the scientific results [46]. In 2013, the European Union's 7th Amendment to the Cosmetic Directive enforced a complete ban on animal testing for all cosmetic ingredients [24]. Furthermore, the REACH regulation was also updated in 2017 and now requires non-animal-based *in vitro* and *in silico* testing strategies for skin sensitization as the first choice [47]. Most recently, in 2022 the United States Food and Drug Administration (FDA) Modernization Act 2.0 was signed. This amendment to the 1938 Federal Food, Drug, and Cosmetic Act removes the mandatory use of mammalian animal studies for toxicity assessment to obtain a license for biosimilar or interchangeable biological products. Furthermore, the implementation of human-biology-based non-animal tests, such as cell-based assays, organoids and tissue equivalents, organ on chips and microphysiological systems, bioprinted or computer models, and artificial intelligence (AI), is encouraged to investigate the safety and effectiveness of a new drug [48-50].

Overall, this progress in international regulations and legislation represents a significant change toward adopting new human-biology-based methods to assess the toxicity and safety of chemicals and drugs. This approach may more accurately predict human responses based on the most recent scientific discoveries rather than relying exclusively on increasingly outdated animal testing [48].

Alongside this progress in regulations and legislation, various efforts to develop non-animal methods have been made. From 2004 to 2007, the U.S. National Research Council's (NRC) Committee on Toxicity Testing and Assessment of Environmental Agents reviewed the current toxicity-testing methods and strategies to improve and advance the science of toxicity testing. To achieve substantial progress, the NRC proposed broadening the scope of chemical(s) (mixtures), results, and life stages to decrease testing times and costs, scale down the number of utilized animals, and create a stronger scientific basis for evaluating the health effects of environmental agents. To achieve these aims, the NRC recommended evaluating cellular response pathways that are expected to result in adverse health effects (so-called toxicity pathways) by using new computational and human-biology-based *in vitro* methods [51, 52]. In 2010, Ankley and colleagues reconceptualized toxicity pathways as adverse outcome pathways (AOPs) [53], and this term was later adopted by the Organization for Economic Co-operation and Development (OECD) [54]. An AOP is an analytical concept and framework that represents current understanding of the causal linkages between a molecular initiating event (MIE), a series of biological activities (key events) at each level of biological organization (molecular, organelle, cellular, organ and organism levels) that is essential for toxicological progression, and a final adverse (health or ecotoxicological) outcome (AO) that is relevant to a risk assessment or regulatory decisions [53, 55]. As a proof of concept, one of the first AOPs published by the OECD (in 2012) aimed to address the underlying molecular and cellular mechanisms crucial to the toxicological endpoint of skin sensitization [56] (reviewed in Chapter 1.4).

1.3 Anatomy of the human skin

Anatomically, the skin is composed of three layers: the epidermis, dermis, and hypodermis (Figure 1.3-1A). The hypodermis, or subcutaneous tissue, is the lowest layer of the skin. It covers and cushions the underlying tissue, acts as energy storage, and is crucial for the body's thermal isolation. The predominant cell type is adipocytes, which are arranged into lobules divided by fibrous connective tissue septa. These septa are highly innervated and vascularized, providing oxygenation and nutrient supply to nourish the dermis [57, 58].

The dermis is located above the hypodermis and beneath the epidermis and provides structural and nutritional support for the epidermis. The main component of the dermis is the extracellular matrix (ECM) composed of collagen and elastic fibers secreted by fibroblasts, the primary cell type within the dermis. In particular, collagen type I and type III are the main components, accounting for up to 70% of the dermis and providing dermal stability and tensile strength [59, 60]. In contrast, elastic fibers, consisting of fibrillin and elastin microfibrils, allow the stretching and recoiling of fibers and therefore maintain the required elasticity, flexibility, and resilience

of the dermis [60, 61]. Notably, fibroblasts continuously degrade and synthesize the ECM's fibrous and non-fibrous components, resulting in constant remodeling of the dermis, which is accompanied by the migration of fibroblasts through the dermis [60]. Furthermore, the dermis is traversed by a dense network of nerves, blood vessels, and lymph vessels. While blood vessels are required for the recruitment of immune cells, lymph vessels allow the emigration of activated immune cells towards the draining lymph nodes upon cutaneous inflammation or sensitization. Dermal immune cells include skin-resident cells such as dermal dendritic cells (DDCs); mast cells or macrophages; and passenger cells recruited upon inflammation such as T cells, monocytes, and neutrophils (Figure 1.3-1A) [62].

The epidermis is the outermost layer of the skin and comprises mainly keratinocytes, which undergo a constant differentiation process resulting in four strata (from top to bottom): stratum corneum, stratum granulosum, stratum spinosum, and stratum basale (Figure 1.3-1B). The stratum basale consists of one layer of basal, undifferentiated keratinocytes with stem cell-like properties, which proliferate constantly and are responsible for the continuous cell renewal process of the epidermis [63]. To start the maturation process, basal keratinocytes separate and migrate to the stratum spinosum but continue to proliferate to keep the basal layer replenished. Throughout their maturation process and migration into the stratum spinosum and stratum granulosum, their shape changes from columnar to polygonal, and they begin to increase production of distinct keratins, proteins, and lipids [64]. The stratum corneum and outermost layer of the epidermis contains terminally differentiated keratinocytes, which are devoid of the nucleus and cell organelles and referred to as corneocytes [64]. Further specialized cells in the epidermis include Merkel cells, which act as mechanoreceptors; melanocytes, responsible for the production of melanin to protect the keratinocytes' nucleus from UV radiation; and epidermal dendritic cells, also known as LCs, which are the sole skin-resident antigen-presenting cells (APC) in the epidermis [65, 66] (Figure 1.3-1A).

1.3.1 Antigen-presenting cells of the skin

Cutaneous APCs include DCs, monocytes, and macrophages [67]. However, in skin sensitization and ACD, DCs have emerged as the predominant key regulators in the initiation of the immune response [68, 69]. DCs are a heterogenous group accounting for a large number of subtypes, which are mainly distinguished by their anatomical distribution and surface marker expression. In general, cutaneous DCs are divided into epidermal LCs and dermal DCs [67, 70]. LCs account for approximately 3%–5% of the epidermal cell population and are primarily suprabasally located in the stratum spinosum, with prolonged cell protrusions into the stratum corneum [70, 71]. Furthermore, LCs are characterized by a high surface marker expression of CD1a; type II transmembrane C-type lectin Langerin (CD207); and Birbeck granules, which are cytoplasmic organelles uniquely found in LCs [40, 72]. Due to their epidermal location, LCs

were long believed to be the sole regulators of the cutaneous immune response [73]. However, research from the past decades has revealed a central role of DDCs in contact hypersensitivity (CHS) [74, 75]. Although DDCs reside at different sites throughout the dermis, they are primarily located beneath the epidermal-dermal junction [76]. In contrast to LCs, no specific marker exclusively expressed on all DDC subsets has been reported to date. Thus, to discriminate between DDCs from dermal monocytes and macrophages, the majority of researchers refer to a low expression of CD14 and a high expression of CD11c [77, 78]. Accordingly, in this thesis all DDC subtypes are summarized and referred to as $CD14^{-}$ $CD11c^{+}$ DDCs.

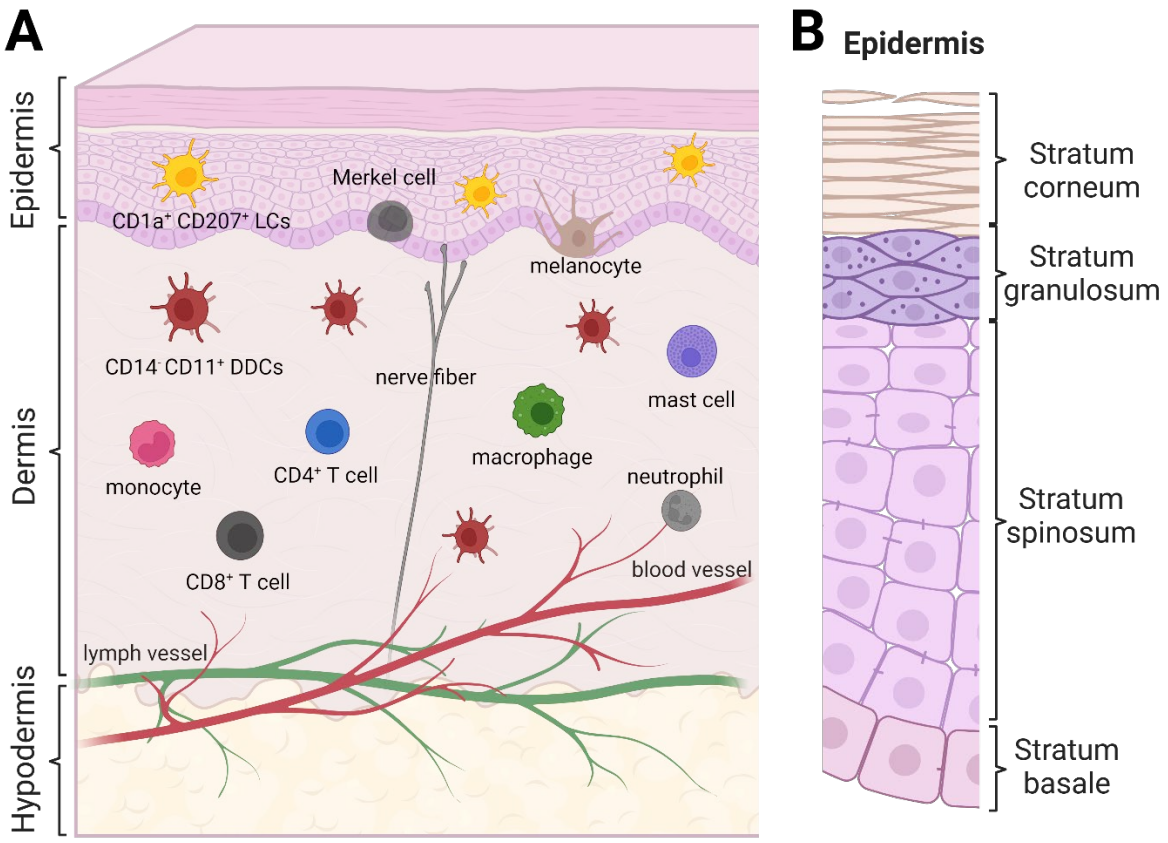

Figure 1.3-1 Anatomy and immune cell population of the human skin. **(A)** The human skin is composed of three layers: the epidermis, dermis, and hypodermis. **(B)** The epidermis consists mainly of keratinocytes in different stages of maturity, forming four layers: the stratum corneum, stratum granulosum, stratum spinosum, and stratum basale. **(A)** The epidermis is populated by specialized cells such as melanocytes, Merkel cells and LCs. The dermal immune cell population includes DDCs, mast cells, macrophages, monocytes, neutrophils and T cells. Created with BioRender.com

1.4 Molecular events of skin sensitization according to the adverse outcome pathway

According to the AOP published by the OECD, skin sensitization is divided into four key events (KEs): the covalent binding of a chemical to endogenous proteins of the skin (KE1), which leads to the activation of cyto-protective pathways in keratinocytes, and the release of pro-inflammatory cytokines (KE2), followed by the activation, maturation, and migration of DCs (KE3) to present the processed antigens to naive T cells resulting in the proliferation of memory T cells (KE4) (Figure 1.5-1) [56].

1.4.1 Key event 1 - Haptenation

Initiation of the first (induction) phase requires the penetration of small electrophilic molecules with low molecular weights (< 500 Da) through the stratum corneum to the viable cells of the epidermis [79]. However, some chemicals need to be converted into electrophilic molecules via air oxidation (pre-hapten) or cutaneous metabolism including enzymatic modification (pro-hapten) first [80]. Subsequently, a process called haptenation is induced, and nucleophilic amino acid residues (mainly cysteine, lysine, and histidine residues) of epidermal self-proteins are targeted and covalently bound to form hapten-carrier complexes [81, 82].

1.4.2 Key event 2 – Activation of keratinocytes

Upon skin contact with sensitizing chemicals, keratinocytes are the first cells that are encountered; as such, they are associated with important functions in haptenation processes and the activation of DCs [83]. In terms of haptenation, it was proposed that sensitizers can either directly or indirectly react with the highly cysteine residues of the cytosensor Kelch-like ECH-associated protein 1 (Keap1) in keratinocytes [84, 85]. Covalent modification of Keap1 leads to the release of the transcription factor nuclear factor erythroid 2 (Nrf2), which translocates to the nucleus [86] and heterodimerizes with various small musculoaponeurotic fibrosarcoma (MAF) proteins. Subsequently, binding to the antioxidant response element (ARE) in the promotor region of various genes, such as haeme oxygenase (hmox1), initiates the transcription of downstream genes [87, 88]. However, some sensitizers, such as metal ions, most prominently nickel, can directly activate inflammatory signaling cascades [89, 90]. Indeed, it has been demonstrated that Ni^{2+} directly binds to human TLR4, resulting in activation of the NF-κB pathway [42]. Likewise, classical sensitizers such as DNCB or Trinitrochlorobenzene (TNCB) were also associated with increased TLR4 expression [91], leading to downstream activation of nuclear factor (NF)-κB [91], followed by an increased expression of the NOD-like receptor family pyrin domain-containing 3 (NLRP3) inflammasome

and consequently a caspase-1-mediated cleavage of the immature pro-Interleukin (IL)-1ß and pro-IL-18 cytokines into their active forms [92, 93]. Secondly, independent activation of the NRLP3 inflammasome via sensitizer-induced intracellular stress, including the release of damage-associated molecular patterns (DAMPs) such as reactive oxygen species (ROS) or adenosine triphosphate (ATP) as second messengers by damaged keratinocytes has been described [91, 94]. Furthermore, increased release of ROS promotes the cutaneous degradation of hyaluronic acid (HA), which is recognized via TLR2 and TLR4, thereby contributing to the activation of the NF-κB-NLRP3 cascade in keratinocytes [91, 95]. Furthermore, sensitizer-induced secretion of not only the IL-1 family (including IL-1α [96, 97], IL-1β [92, 98], and IL-18 [92]) but also IL-6 [96] and IL-8 [97, 99] strongly contributes to activation of the surrounding DCs [100, 101].

1.4.3 Key event 3 – Activation of cutaneous DCs

One of the most crucial events of skin sensitization is the presentation of antigens by DCs to contact allergen-specific T cells [68]. While some sensitizers were reported to directly penetrate into DCs, hapten-carrier complexes need to be internalized via endocytosis or phagocytosis [102, 103]. Upon intracellular processing, the antigens are loaded to major histocompatibility complex (MHC) class I or class II and transported to the cell surface for recognition by $CD8^+$ T cells or $CD4^+$ T cells, respectively [104-106]. In addition, the antigen presentation of lipid antigens to T cells via CD1 molecules—including CD1a, which is highly abundant on LCs—has been increasingly reported [39, 40, 107]. Simultaneously, maturation of DCs is associated with high expression of adhesion molecules, such as CD54, and co-stimulatory molecules, such as CD80 and CD86 [108, 109]. Furthermore, intracellular pathways such as the mitogen-activated protein kinase (MAPK), extracellular signal-regulated kinase (ERK), c-Jun N-terminal kinase (JNK), and/or the NF-κB pathway are activated early in the process of DC activation [110-115]. It is important to note that sensitizer-induced DC maturation and therefore upregulation of CD80, CD86, and CD83, as well as the sensitizer-induced upregulation and secretion of inflammatory cytokines such as IL1, TNF-α, IL-6, IL-8, or IL-12p40 by DCs, were reported to be dependent on the phosphorylation of p38 MAPK and/or the NF-κB pathway [111-113]. Furthermore, it is assumed that in DCs, similar to what is described for KCs, exposure to other sensitizer-induced danger signals (DAMPs) such as HA-fragments, ROS, or ATP released by chemically damaged keratinocytes induces the activation of the NLRP3-caspase1 inflammasome cascade, resulting in the secretion of IL-1ß [116] and promoting DC maturation [117].

To present the MHC-loaded antigens to naïve T cells, LCs must migrate towards the dermis. In steady-state conditions, the adhesion of Langerhans cells to keratinocytes is presumed to be mediated by E-cadherin [118]. Thus, the sensitizer-induced secretion of IL-1 and TNF-α by

keratinocytes is proposed to abolish the E-Cadherin-mediated adhesion between LCs and KCs, thereby contributing to LC mobilization and emigration [119]. Furthermore, high expression of the C-X-C chemokine receptor type 4 (CXCR4) on mature LCs allows chemotactic migration towards the sensitizer-induced secretion of stromal cell-derived factor 1 (SDF1) by dermal fibroblasts and lymphatic endothelial cells [120-122]. Migration of LCs and DDCs towards local lymph nodes is mediated via additional C-C chemokine ligand (CCL)19 and CCL21 secretion by lymphatic endothelial cells, inducing CCR7-dependent migration of DCs and naïve T cells [120, 123-125].

1.4.4 Key event 4 – T cell activation and proliferation

Upon migration from the dermis to the skin-draining lymph nodes, DCs present antigens either via the MHC I complex to $CD8^+$ T cells or via the MHC II complex to $CD4^+$ T cells [106]. Antigen presentation via CD1 molecules was demonstrated for $CD4^+$ and $CD8^+$ T cells [39, 107, 126, 127]. However, to fully prime naïve T cells, a simultaneous interaction with co-stimulatory molecules is required. To this end, the intercellular adhesion molecule CD54 expressed on DCs forms a cell-cell adhesion, the so-called immunological synapse (IS), with its T cell ligands leukocyte function-associated antigen 1 (LFA-1) alpha (CD11a) and beta-2 (CD18) [128]. Further co-stimulation of naïve T cells is mediated via the binding of CD80 (B7-1) and CD86 (B72) expressed by DCs to their counter-receptors CD28 and cytotoxic T-lymphocyte-associated protein 4 (CTLA-4)/(CD152) on T cells [129]. Depending on the dominating cytokines secreted during DC-T cell interactions into the local environment, primed T cells can differentiate into different subsets of helper/effector or regulatory/ suppressive T cells, namely T_H1, T_H2, T_H17, T_H3 or Tr1 T cells, expressing unique transcription factors and cytokines. Thus, secretion of IL-12 and IFN-γ was associated with the generation of T_H1 cells and IL-4 with the generation of T_H2 cells. The presence of IL-6, TGF-β, IL-21, and IL-23 was reported for differentiation into T_H17 cells. Development of Tr1 cells or T_H3 cells is assumed to be mediated by the absence of danger signals and the secretion of IL-2 and TGF-β; or IL-10 and TGF-β, respectively [102]. However, the molecular mechanisms driving the polarization of T cells upon DC-T cell interaction are still not fully understood as these mechanisms rely on several factors such as the type of DC subset, the nature of the presented antigens, and the secreted cytokine cocktails [130]. Furthermore, the relative contribution of $CD4^+$ T cells or $CD8^+$ T cells in ACD is still debated [131].

1.5 New approach methodologies to predict skin sensitization

The AOP for skin sensitization is the most widely used AOP and has become a key example and valuable framework for the development of new approach methodologies (NAMs) [132]. NAMs comprise any technologies, methodologies, approaches, or combinations, including *in silico*, *in chemico*, *in vitro*, and *ex vivo* approaches, that can provide information on chemical hazards and risk assessment without utilizing animals [133]. Notably, the OECD has been a huge resource in defining, processing, and validating NAM concepts and test guidelines according to AOPs [132, 134]. In fact, a great number of non-animal test methods addressing one or more of the first three key events of skin sensitization have been developed up to this point [135, 136]. However, the test methods that have been submitted are being applied at various stages of development. While some approaches are in the optimization and standardization stages, others are undergoing peer review or validation [133, 137, 138].

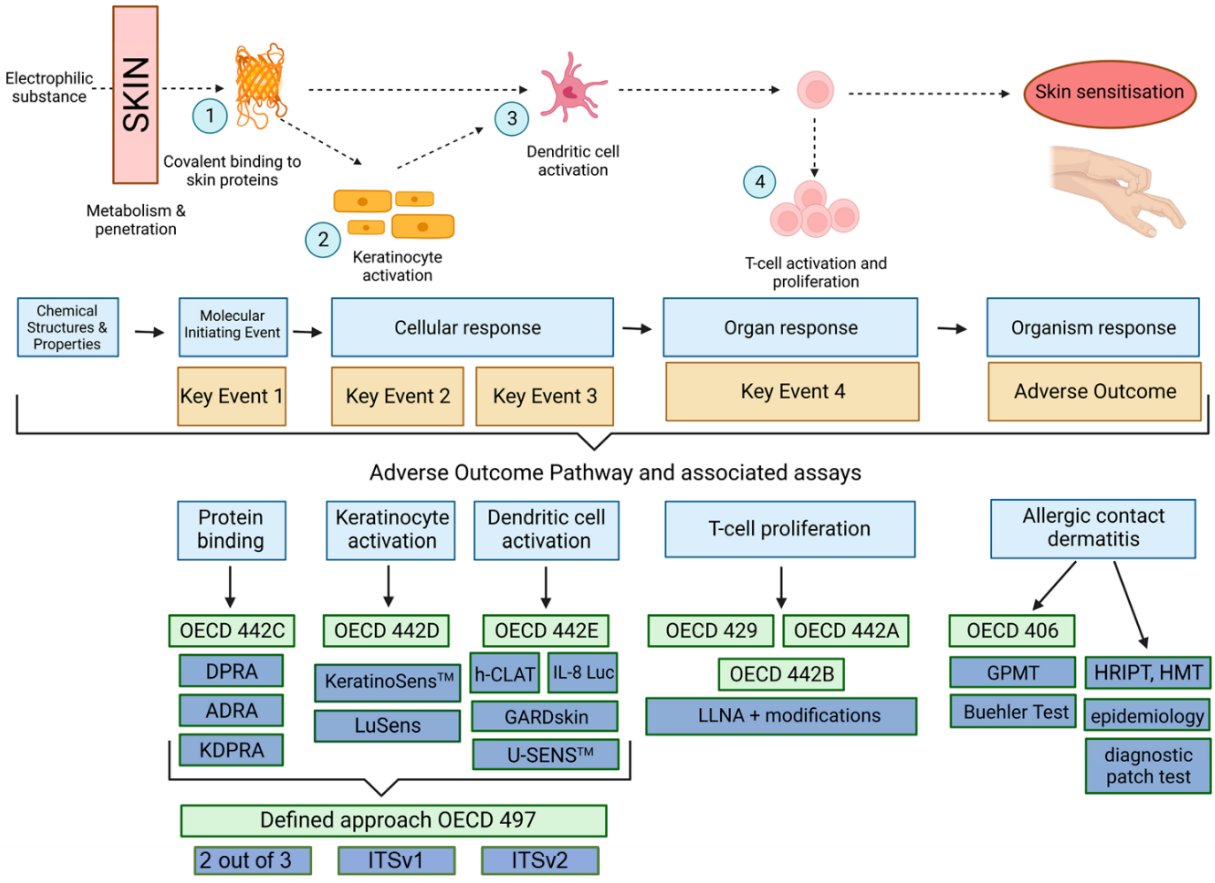

Figure 1.5-1 Adverse outcome pathway (AOP) concept of skin sensitization, including the four key events (KEs): haptenation (KE1), keratinocyte activation (KE2), dendritic cell activation (KE3) and T cell activation and proliferation (KE4), along with the respective OECD-approved test methods for skin sensitization [139]. Adapted from Bialas et al. (2023) [139].

To date, the OECD has validated and published nine different non-animal test guidelines addressing the AOP-defined key events of skin sensitization (Figure 1.5-1 and Table 1.5-1). The haptenation and therefore first KE (Chapter 1.4.1) can be addressed by the direct peptide reactivity assay (DPRA) [140, 141], the amino acid derivative reactivity assay (ADRA) [142, 143], or the kinetic direct peptide reactivity assay (kDPRA) [84, 144], which are based on the *in chemico* covalent binding of proteins [145, 146]. While all three methods allow the classification of a chemical into UN GHS category 1, only the kDPRA allows discrimination between UN GHS subcategories 1A and 1B or no category [144, 145].

The second KE, activation of keratinocytes (Chapter 1.4.2), is described in the OECD Test Guideline 442D. The KeratinoSens™ as well as the LuSens are *in vitro* test systems based on the activation of the Keap1-Nrf2-ARE pathway in keratinocytes, or more precisely, luciferase reporter cell lines [147-150].

Activation of DCs (KE3) (Chapter1.4.3) is one of the major events in skin sensitization and is usually assessed by the expression of specific cell surface markers, genomic transcripts, chemokines, and cytokines. To discriminate between sensitizers and non-sensitizers based on utilizing DC activation mechanisms, four *in vitro* test methods have been developed: the human cell line activation test (h-CLAT), the U937 cell line activation test (U-SENS), the Interleukin-8 Reporter Gene Assay (IL-8 Luc assay), and the Genomic Allergen Rapid Detection (GARD™) assay. All four test methods are based on utilizing immortal human cell lines as DC surrogates [151]. The h-CLAT quantifies the changes in the surface marker expression of the DC activation markers CD54 and CD86 on the human monocytic leukemia cell line THP-1 [151, 152]. The U-SENS focuses on the change in the surface marker expression of CD86 on the human histiocytic lymphoma cell line U-937 [151, 153]. The IL-8 Luc analyses the IL-8-induced expression in the THP-1-derived IL-8 reporter cell line [151, 154, 155]. The GARD assay evaluates the transcriptional patterns of an endpoint-specific genomic biomarker signature (=196 genes), referred to as the GARDskin Genomic Prediction Signature (GPS) in a subclone (SenzaCell) of the human acute myeloid leukemia cell line Mutz-3 [151, 156, 157].

Table 1.5-1 Outcome, accuracy and reproducibility of the OECD-approved NAM test systems to address the first three key events of skin sensitization

Test system/ method	OECD Guideline	Outcome	Accuracy (comp. to LLNA)	Reproducibility	Ref.
Key event 1 – Haptenation					
DPRA	442C	Positive/negative	80%	80%–85%	[140, 141, 145]
ADRA	442C	Positive/negative	76%	100%	[142, 143, 145]
kDPRA	442C	Positive/negative quantitative information: Cat 1A/Cat 1B/NS	85%	88%–96%	[144-146]
Key event 2 – Keratinocyte activation					
KeratinoSens (KS)	442D	Positive/negative	77%	85%	[147, 149]
LuSens	442D	Positive/negative	74%	71%–85%	[147, 150]
Key event 3 – Dendritic cell response					
h-CLAT	442E	Positive/negative	85%	80%	[151, 152]
U-SENS	442E	Positive/negative	86%–88%	79%–95%	[151, 153]
IL-8 Luc	442E	Positive/negative	81%–88%	88%	[151, 154, 155]
GARD^{TM} skin	442E	Positive/negative quantitative information: Cat 1A/Cat 1B/NS	88%	79%–92%	[151, 156, 157]
Combining key events 1, 2, and 3					
2 out of 3 DA (DPRA, KS & h-CLAT)	497	Positive/negative	83%	-	[158]
ITSv1 DA	497	Positive/negative quantitative information: Cat 1A/Cat 1B/NS	70%	-	[158]
ITS v2 DA	497	Positive/ negative quantitative information: Cat 1A/Cat 1B/NS	67%	-	[158]

Despite the great efforts made to develop these NAMs, they still have limitations. Even though no predictive toxicology test will ever be 100% accurate, the number of false negative or positive results remains high, while accuracy and reproducibility are still too low, leading to an overall unsatisfactory accuracy and predictability [135, 159]. These limitations are mainly caused by the poor (water) solubility and stability of some substances and/or the solvent/vehicle choice [160, 161], with the consequence that not all classes of test substances and severity effects can be covered [159]. Moreover, the test systems are mostly based on a

single isolated cell type and therefore represent only one or a few steps of the complex sensitization cascade [162]. In addition, none of the test systems can provide information about the absorption, distribution, or metabolism of the test substances [162-164]. Thus, existing single-endpoint methods are not sufficient for use as standalone methods or as drop-in replacements to assess chemicals for skin sensitization [165].

To overcome some of the limitations and increase predictivity, efforts were made to combine several OECD test guidelines, resulting in the three so-called defined approaches (DAs): 2 out of 3 DA, Integrated Testing Strategy (ITS)v1 DA, and ITSv2 DA, implemented in the OECD 497 test guideline [158]. The 2o3 DA provides a hazard assessment of skin sensitization based on at least two concordant, non-borderline results from the DPRA, KeratinoSens, and h-CLAT. Based on the DPRA and h-CLAT combined with computional/ *in silico* prediction, the ITSv1 and ITSv2 DA provide skin sensitization hazard assessment and potency classification according to the UN GHS system [158, 159, 166]. The limitations of the DAs are based on the limitations of the isolated single-endpoint measurement assays, including the limitations resulting from the poor solubility of some substances; the lack of information about the absorption, distribution, or metabolism of the test substances; as well as restrictions to mono-constituent substances as mixtures (solutions or suspensions of more than two different chemical substances) or formulations cannot be tested [162, 166, 167]. In conclusion, two-dimensional (2D) single-endpoint test methods as well as the combination of three independent *in vitro* test systems depicting the single key events of skin sensitization cannot capture the complex intercellular communication of the epidermal, dermal, and immune cells of the native human skin.

1.6 Current 3D tissue equivalents to predict skin sensitization

To overcome the limitations of the two-dimensional single-endpoint test methods reviewed in Chapter 1.5, engineering of three-dimensional (3D) tissue equivalents of the skin has become more prominent. Since the 1980s, several academic laboratories have developed reconstructed human epidermal equivalents (RHEEs) based on stimulation of primary human basal keratinocytes to differentiate and form a fully stratified epidermis [168, 169]. Over the years, the reconstruction of RHEEs has been improved and standardized, leading to the development of multiple commercially available RHEEs from different suppliers. Notably, the OECD has validated and accepted several commercially available RHEEs, such as EpiSkin™, EpiDerm™, SkinEthic™, LabCyte EPI-MODEL24 SI, or epi-Cs®, to assess skin corrosion (OECD TG 431) and skin irritation (OECD TG 439) [170, 171]. Furthermore, based on some of the commercially available RHEE models, gene-expression-based test methods for predicting skin sensitization such as the SENS-IS (based on EpiSkin™) or EpiSensA (based

on EpiDerm™) were developed [172-174]. In 2024, the development of an epidermal model based on a stably transfected Nrf2 reporter cell line derived from immortalized human primary keratinocytes for skin sensitization assessment was reported [175].

Hence, compared to the OECD-validated single-endpoint test methods, RHEEs allow the assessment of skin sensitization and address the first two key events of the AOP in just one model. Furthermore, 3D models better resemble the tissue-like structure of the native human skin. In particular, epidermal stratification allows the simple application and assessment of mixtures (solutions or suspensions of more than two different chemical substances) and formulations, as well as hydrophobic chemicals and chemicals of poor solubility [176-178]. Furthermore, information about the penetration, absorption, distribution, or metabolism of the test substances can be obtained [178-181].

However, RHEEs have important limitations as they comprise only one cell type (keratinocytes) and cannot mimic intercellular crosstalk with dermal fibroblasts or immune cells, which are crucial mediators in skin sensitization and the cutaneous immune response. [182]. Hence, to mimic the first three KEs of skin sensitization, a full-thickness skin equivalent (FTSE) including keratinocytes, fibroblasts, and DCs is required. Considering LCs as the first immunological sentinels to encounter a hazardous agent, the integration of LC surrogates is a promising concept to overcome the limitations of common FTSE. As such, in recent years skin equivalents containing LC surrogates derived from various cell sources, including cord-blood-derived $CD34^+$ hematopoietic progenitor cells [183, 184], $CD14^+$ peripheral blood mononuclear cells (PBMCs) [185, 186], and the human myeloid leukemia-derived cell line Mutz-3 [186-189], have been reported. In addition, topical application of sensitizers on FTSE with incorporated Mo-LCs (PBMC-derived) or Mutz-LCs could induce the typical LC migration from the epidermis to the dermis [186, 188, 189]. However, LC-containing FTSE are still in the early stages of development, and the identification and validation of robust and reproducible readout parameters for the identification of sensitizers are still required. Furthermore, capturing the full extent of sensitizer-induced DC activation requires additional integration of DDC surrogates into a FTSE as both DC cell types (LCs and DDCs) are considered crucial in the events of skin sensitization [74, 75]. There is therefore an urgent need for 3D, immune-competent tissue equivalents of the human skin that will allow for analysis of the molecular events of skin sensitization *in vitro* and consequently the robust and reproducible identification of sensitizers and potential new drug candidates including solutions, or suspensions of more than two different chemical substances (mixtures) and formulations.

1.7 Pseudopterosin as a potential natural anti-inflammatory drug candidate in skin sensitization

Pseudopterosin is a marine diterpene glycoside isolated from the octocoral sea whip *Antillogorgia elisabethae* (formerly *Pseudopterogorgia elisabethae*), which is located at coral reefs 15 to 35 meters below sea level [190, 191]. To date, at least 31 chemical derivatives of pseudopterosin have been discovered [192] from different specimens collected in the Bahamas [191, 193] Bermuda [194], the Florida Keys [195], and Columbia [196, 197]. Distinct pseudopterosin derivates have been reported to possess a variety of promising biological activities, including anti-inflammatory and analgesic effects [191, 195, 198, 199]. On a molecular level, pseudopterosin's anti-inflammatory mechanism of action is partially mediated by targeting different enzymes of the arachidonic acid (AA) pathway, such as phospholipase A2, cyclooxygenase-1 (COX-1), and lipoxygenases (LOXs), resulting in attenuated production of eicosanoids such as prostaglandins and leukotrienes [190, 199, 200]. Furthermore, a mixture including Pseudopterosins A-D (PsA-D) was demonstrated to inhibit activation of the NF-κB pathway via activation of the glucocorticoid receptor alpha (GRα), leading to decreased expressions of pro-inflammatory cytokines such as TNF-α, IL-8, IL-6, and MCP-1 [201, 202].
In terms of skin disorders, pseudopterosins and the semi-synthetic PsA methyl ether derivate have proven to be potent compounds for wound healing, increasing angiogenesis, reepithelization, and enhanced wound repair [203-206]. Furthermore, the semi-synthetic PsA methyl ether derivate (methopterosin/OAS1000) has completed Phase I and II clinical trials as a wound healing agent [207, 208]. Importantly, pseudopterosins have been utilized as an additive in Estée Lauder's Resilience® cosmetic care product to prevent skin irritation from sunlight or chemicals [209]. However, the potential of pseudopterosins to attenuate or suppress skin sensitization has not been reported yet.

1.8 Aims and Objectives

In the past decades, predictive identification of potentially sensitizing agents has been performed almost exclusively via animal models, such as the guinea pig test, the Buehler test, or the murine lymph node assay. However, species-specific differences in the anatomy, and especially in the cutaneous DC subsets, often result in failure to transfer findings from animal models to human tissue. Although great efforts have been made to establish alternative *in vitro* test systems to assess skin sensitization, most of the OECD-approved test systems are based on a single isolated cell type and can therefore represent only one or a few steps of the complex sensitization cascade. Furthermore, these test systems lack information about the absorption, distribution, or metabolism of the test substances and do not allow the assessment of substances with poor solubility, solvents, or suspensions based on more than two substances or the topical application of formulations. To overcome this, multi-layered human FTSEs have been developed, but these mostly lack immune cells, including LC and DDC surrogates, which are crucial mediators in skin sensitization and the cutaneous immune response. Hence, we aimed to engineer a human 3D immune competent tissue equivalent comprising functional LC and DDC surrogates for the identification and characterization of sensitizers and drug candidates. To achieve this aim, the following main objectives were defined:

I. Identification, differentiation, and characterization of potential LC and DDC surrogates
II. Determination of readout parameters, including surface marker expression, inflammatory pathways, and cytokine secretion, for the identification of sensitizers and drug candidates
III. Generation of an immune competent FTSE by incorporating LC and DDC surrogates
IV. Confirmation of the immune competence of the newly developed FTSE, including its applicability for the identification and characterization of skin sensitizers and drug candidates
V. Investigation of Pseudopterosin A-D as a potential natural anti-inflammatory drug candidate in skin sensitization

2 Publications and manuscripts

2.1 The Monocytic Cell Line THP-1 as a Validated and Robust Surrogate Model for Human Dendritic Cells

Johanna Maria Hölken[1] and Nicole Teusch[1]

[1]Institute of Pharmaceutical Biology and Biotechnology, Heinrich-Heine University Düsseldorf, Universitätsstraße 1, 40225 Düsseldorf, Germany

Published in: *International Journal of Molecular Sciences*
Hölken, J.M.; Teusch, N.: The Monocytic Cell Line THP-1 as a Validated and Robust Surrogate Model for Human Dendritic Cells. Int. J. Mol. Sci. 2023, 24, 1452. doi.org/10.3390/ijms24021452

Keywords: dendritic cells; THP-1; DC maturation; cytokine; sensitization; phagocytosis; nickel sulfate; $NiSO_4$; h-CLAT; 1-chloro-2,4-dinitrobenzene; DNCB; interleukin-12; IL-12

Own contributions to the manuscript: 90%

- Conceptualization of the experiments (50%) together with Nicole Teusch
- Methodology (100%), Investigation (100%), Validation (100%), Data curation (100%), Formal analysis (100%) and Visualization (100%) of the following experiments:
    - Surface marker characterization of iDCs and mDCs (100%)
    - Morphological characterization (imaging) of iDCs and mDCs (100%)
    - Surface marker characterization of iDCs upon sensitizer treatment (100%)
    - Phagocytosis assay (100%)
    - qPCR to determine the sensitizer-induced mRNA levels of IL-12p40 (100%)
- Writing and drafting the manuscript (100%)

Abstract

We have implemented an improved, cost-effective, and highly reproducible protocol for a simple and rapid differentiation of the human leukemia monocytic cell line THP-1 into surrogates for immature dendritic cells (iDCs) or mature dendritic cells (mDCs). The successful differentiation of THP-1 cells into iDCs was determined by high numbers of cells expressing the DC activation markers CD54 (88%) and CD86 (61%), and the absence of the maturation marker CD83. The THP-1-derived mDCs are characterized by high numbers of cells expressing CD54 (99%), CD86 (73%), and the phagocytosis marker CD11b (49%) and, in contrast to THP-1-derived iDCs, CD83 (35%) and the migration marker CXCR4 (70%). Treatment of iDCs with sensitizers, such as $NiSO_4$ and DNCB, led to high expression of CD54 (97%/98%; GMFI, 3.0/3.2-fold induction) and CD86 (64%/96%; GMFI, 4.3/3.2-fold induction) compared to undifferentiated sensitizer-treated THP-1 (CD54, 98%/98%; CD86, 55%/96%). Thus, our iDCs are highly suitable for toxicological studies identifying potential sensitizing or inflammatory compounds. Furthermore, the expression of CD11b, CD83, and CXCR4 on our iDC and mDC surrogates could allow studies investigating the molecular mechanisms of dendritic cell maturation, phagocytosis, migration, and their use as therapeutic targets in various disorders, such as sensitization, inflammation, and cancer.

Introduction

Dendritic cells (DC) are sentinel leukocytes mediating the innate and adaptive immune response in mammalian solid tissue. Dendritic cells play fundamental roles in infections [1,2], inflammation [3], skin sensitization [4], and allergy [5], as well as in cancer [6–8] and are, therefore, of great interest in research [9]. The DCs are a heterogenous population of cells, specialized in antigen presenting. Upon exposure to, for example, pro-inflammatory cytokines, such as tumor-necrosis factor alpha (TNF-α), bacterial agents, such as lipopolysaccharides (LPS), or chemically-derived haptens, such as from nickel sulfate ($NiSO_4$), maturation and migration of DCs is initiated. The DCs initially transform into immature dendritic cells (iDCs) with high endocytic activity and low T cell activation potential [10,11]. The first steps of phagocytosis and maturation are accompanied by up- regulation of the major histocompatibility complex (MHC) class II, such as the Human Leukocyte Antigen–DR isotype (HLA-DR) [12,13]. The MHC II molecules are synthesized on the cytosolic surface of the endoplasmic reticulum and are chaperoned by the invariant chain (Ii) to the late endosomal compartment where they encounter and fuse with endosomes loaded with the exogenous protein of presenting, building lysosome-like antigen processing compartments [14–16]. In order to bind antigens, the Ii peptide is cleaved. After loading a peptide derived from the exogenous protein, the class II molecules are exported to the cell surface for recognition by $CD4^+$ T cells [15]. In addition, internalized antigens can be loaded onto MHC I molecules for cross-presentation to $CD8^+$ T

cells [17,18]. Simultaneously, expression of adhesion molecules, such as clusters of differentiation (CD)54 and co-stimulatory molecules, such as CD80 and CD86, are upregulated and transported to the cell surface, inducing dendritic cell maturation [19,20]. Furthermore, DC maturation is accompanied by upregulation of migration markers, such as the C-X-C chemokine receptor type 4 (CXCR4) and C-C chemokine receptor type 7 (CCR7), resulting in antigen presentation to T cells in lymphoid tissues [21,22]. Overall, migration of DCs is a complex process which depends on chemokines, such as stromal cell-derived factor 1 (SDF-1), chemokine (C-C motif) ligand (CCL) 19, and CCL21 [23–26]. The SDF-1 is secreted by fibroblasts and endothelial cells in the dermis after antigen exposure, inducing chemotactic migration of CXCR4-expressing DCs to lymphatic vessels in the dermis [23,24]. Contrarily, CCL19 and CCL21 are secreted by lymph nodes, inducing CCR7 dependent migration of DCs and naïve T cells [25–27].

The activation of naïve $CD4^+$ T cells is initiated by the interaction of T cell receptors (TCRs) with the antigen-loaded MHC II complexes [28,29]. However, to fully prime naïve $CD4^+$ T cells, the simultaneous interaction with DC-expressing CD54, CD80, and CD86 is required [30,31]. In order to form a stable signaling structure between dendritic cells and naïve $CD4^+$ T cells, the intracellular adhesion molecule (ICAM-1)/CD54 forms with its partners, leukocyte function-associated antigen 1 (LFA-1) alpha (CD11a) and beta-2 (CD18), a cell–cell adhesion, the so-called immunological synapse (IS) [32,33]. Subsequently, high expression of the surface molecules CD80 (B7-1) and CD86 (B7-2) on antigen-presenting cells (APCs) allows the co-stimulation of naïve $CD4^+$ T cells via their CD28 and cytotoxic T-lymphocyte-associated protein 4 (CTLA-4)/(CD152) receptors [34,35]. Upon the cell– cell contact between dendritic cells and T cells, several signal cascades in both T cells and dendritic cells are initiated, depending on the stability and duration of the cell-cell contact, and the number of MHC complexes and co-stimulatory molecules enhancing the transfer [36]. In immature dendritic cells, CD83 is not expressed on the cell surface, but is stored in the Golgi complex and endocytic vesicles, and the receptor can be transported to the cell surface immediately upon maturation [37,38]. Notably, CD83 knockout studies revealed a severe reduction in $CD4^+$ T cells, proving the essential role of CD83 for the development of $CD4^+$ T cells [39,40]. By binding to the membrane-associated RING-CH8 (MARCH-8) ubiquitin ligase, which is responsible for the internalization of MHC II, CD83 stabilizes the MHC II surface expression [41]. In addition, transmembrane regulation of the MARCH-1 ubiquitin ligase promotes the upregulation of surface MHC-II and CD86 on activated DCs [42,43], ensuring the stimulation, proliferation, and maturation of naïve T cells into primed effector and memory T-lymphocytes in the draining lymph nodes [44]. In the past decades, the predictive identification of potentially sensitizing agents has been performed via the guinea pig Buehler test or the murine lymph node assay LLNA. However, due to the differences between human and guinea pig/murine skin physiology

and immune biology many agents were classified as false positive or negative [45,46]. Hence, there was an urgent need for alternative robust human-derived models. In this context, various protocols generating dendritic cell surrogates derived from human donor-derived peripheral blood monocytes (PBMCs) to study skin sensitization and inflammation have been reported [47–50]. However, the isolation and differentiation of PBMCs comes with various technical and biological limitations, such as the amount, availability, and donor heterogeneity [51,52]. In 2006, the human cell line activation test (h-CLAT) was developed by Ashikaga et al. [53,54]. The h-CLAT addresses one of the key events of the skin sensitization, by measuring CD54 and CD86 as markers for dendritic cell activation on the monocytic cell line THP-1 [53], originally isolated from peripheral blood of an acute leukemia patient [55]. The method is designed to distinguish between sensitizing and non-sensitizing agents, where the chemicals 1-chloro-2,4-dinitrobenzene (DNCB) and nickel sulfate ($NiSO_4$), both acting as strong sensitizers, are the positive controls. In order to be classified as a sensitizer, the relative fluorescence intensity (RFI) has to exceed a defined threshold, which is CD54 ≥ 200 or CD86 ≥ 150 in at least two out of three independent measurements [56,57]. Due to high intra- and inter-laboratory reproducibility (80%) [57,58], the h-CLAT was validated and authorized by the European Union Reference Laboratory on Alternatives to Animal Testing (EURL ECVAM) and by the Organization for Economic Co-Operation and Development (OECD) for the toxicological assessment of skin sensitization potential [58,59]. In conclusion, THP-1 cells bring along various advantages for differentiation into dendritic cell surrogates.

In most studies to date, THP-1 cells have been differentiated into macrophages [60,61], and only very few publications have converted THP-1 cells into iDCs and mDCs (Table 2.1-1). Similar to human PBMCs, THP-1 cells could be differentiated into iDCs with cytokines, such as GMC-SF and IL-4 [62–65]. Maturation of THP-1 into mDCs was achieved via GM- CSF, IL-4, TNF-α, and ionomycin exposure in (serum-free) medium for 24 h to 72 h [62,66], or by cultivating THP-1-derived iDCs for an additional 24–72 h in (serum-free) medium supplemented with GM-CSF and/or IL-4, TNF-α, and ionomycin [64,65]. However, as these protocols differ in cell numbers, basic media composition, media supplementation, the number of days for differentiation, the frequency of media exchange and, most importantly, the cytokine concentrations in the differentiation cocktail, it becomes highly challenging to identify the appropriate method.

Thus, our aim was to establish robust and highly reproducible standard operating procedures addressing THP-1-derived iDC and mDC surrogates for *in vitro* toxicological studies as well as for investigating the underlying mechanisms of human skin sensitization and inflammation.

Table 2.1-1 Literature review of the differentiation of THP-1 into iDCs or mDCs

Cultivation Conditions	iDCs	mDCs	Ref.
Cytokine concentrations	100 ng/mL (1500 U/mL) GM-CSF 100 ng/mL (1500 U/mL) IL-4	100 ng/mL (1500 U/mL) GM-CSF 200 ng/mL (3000 U/mL) IL-4 20 ng/mL (2000 U/mL) TNF-α 200 ng/mL ionomycin	[64]
Medium	RPMI, 10% serum,	RPMI, serum-free,	
Cell number	2 × 10^5 cells/ ml, 20 mL	2 × 10^5 cells/ ml, 20 mL	
Time of differentiation	5 d of cultivation	24–72 h of cultivation	
Cytokine concentrations	150 ng/mL GM-CSF 50 ng/mL IL-4	Exposure of generated iDCs to: 10 ng/mL IL-1β 10 ng/mL TNF-α 2 µg/mL PGE_2 25% MCM Or 1 µg/mL LPS	[65]
Medium	RPMI, 10% serum,	RPMI, 10% serum	
Cell number	5 × 10^5 cells/ mL	Cell number not indicated	
Time of differentiation	7 d of cultivation	48 h of cultivation	
Cytokine concentrations	-	100 ng/mL (1500 U/mL) GM-CSF 200 ng/mL (3000 U/mL) IL-4 20 ng/mL (3000 U/mL) TNF-α 200 ng/mL ionomycin	[68]
Medium		DMEM, serum-free	
Cell number	-	2 × 10^5 cells/ ml, 20 mL	
Time of differentiation		48 h of cultivation	
Cytokine concentrations	100 ng/mL GM-CSF 100 ng/mL IL-4	Exposure of generated iDCs to: 100 ng/mL GM-CSF 100 ng/mL IL-4 20 ng/mL TNF-α 200 ng/mL ionomycin	[66]
Medium	RPMI, 10% serum	RPMI, serum-free	
Cell number	Not indicated	Not indicated	
Time of differentiation	5 d of cultivation	72 h of cultivation	
Cytokine concentrations	1500 U/mL GM-CSF 1500 U/mL IL-4	Exposure of generated iDCs to: 3000 U/mL IL-4 2000 U/mL TNF-α 200 ng/mL ionomycin	[67]
Medium	RPMI, 10% serum	RPMI, 10% serum	
Cell number	2 × 10^5 cells/mL, 20 mL	Not indicated	
Time of differentiation	5 d of cultivation	24 h of cultivation	

Results

The differentiation of THP-1 cells into dendritic cells has been described using RPMI or DMEM as a cultivation medium (Table 2.1-1). Both RPMI and DMEM are basal mediums which do not contain proteins or growth promoting agents and, as such, require supplementation with a serum, such as FBS. However, RPMI contains high concentrations of vitamins, as well as amino acids, such as asparagine, proline, biotin, and vitamin B12, which are not incorporated in DMEM [67]. On the other hand, DMEM contains higher concentrations of calcium (1.8 mM)

and a lower concentration of phosphate (1 mM), compared to RPMI (0.8 mM calcium, 5 mM phosphate, respectively). While DMEM is selected for adherent cells, RPMI is widely used for suspension cells [68–70]. In line with this, RPMI is the recommended culture medium by the American Type Culture Collection (ATCC) and Deutsche Sammlung von Mikroorganismen und Zellkulturen (DSMZ) for THP-1 cells. Furthermore, PBMCs cultured in RPMI showed more efficient differentiation into DCs compared to PBMCs cultured in DMEM [71]. Based on these specifications, we decided to implement our differentiation protocols using RPMI.

The differentiation of THP-1 into iDCs and mDCs has been described using cytokine concentrations in ng/mL or in U/mL concentrations. However, by converting the indicated cytokine concentrations from ng/mL into U/mL and vice versa for the cytokines to be supplemented (Table 2.1-2), apparently significant differences become obvious. Thus, to systematically compare supplementation differences, we differentiated THP-1 cells into iDCs and mDCs by supplementing the medium with cytokines in either ng/mL or U/mL concentrations in parallel.

Table 2.1-2 Cytokine concentrations applied for the differentiation of THP-1 cells into iDCs or mDCs, calculated by referring to the biological activity published by the manufacturer

Cytokine	ng/ml	U/ml
GM-CSF [ImmunoTools, ##11343125]	100 ng/ml 166,67 ng/ml	900 U/ml 1500 U/ml
IL-4 [ImmunoTools, #11340045]	100 ng/ml 200 ng/ml 65,22 ng/ml 130,44 ng/ml	2300 U/ml 4600 U/ml 1500 U/ml 3000 U/ml
TNF-α [PromoKine, #C-63719]	20 ng/ml 100 ng/ml	400 U/ml 2000 U/ml

Differentiating THP-1 cells into iDCs in the presence of 100 ng/mL GM-CSF (≙ 900 U/mL) and 100 ng/mL IL-4 (≙ 2300 U/mL) resulted in a significantly higher number of cells expressing the surface markers CD54 (~95%), CD86 (~61%), and CD11b (~20%) (Figure 2.1-1A) compared to the undifferentiated control (CD54, ~58%; CD86, ~30%; CD11b, 3%). Furthermore, a pronounced higher geometric mean fluorescence intensity (GMFI) for HLA-DR (3.7-fold), CD54 (16.5-fold), and CD11b (3.1-fold) (Figure 2.1-1B) compared to the undifferentiated control could be detected. Supplementing the medium with 1500 U/mL GM-CSF and 1500 U/mL IL-4 induced the expression of CD54 (~88%), CD86 (~50%), and CD11b (~14%) on a significantly higher number of cells compared to the undifferentiated control (CD54, ~46%; CD86, ~24%; CD11b, ~3%) (Figure 2.1-1C) and a demonstrably higher GMFI for HLA-DR (4.1-fold), CD54 (14.6-fold), and CD11b (7.1-fold) (Figure 2.1-1D) compared to the undifferentiated control.

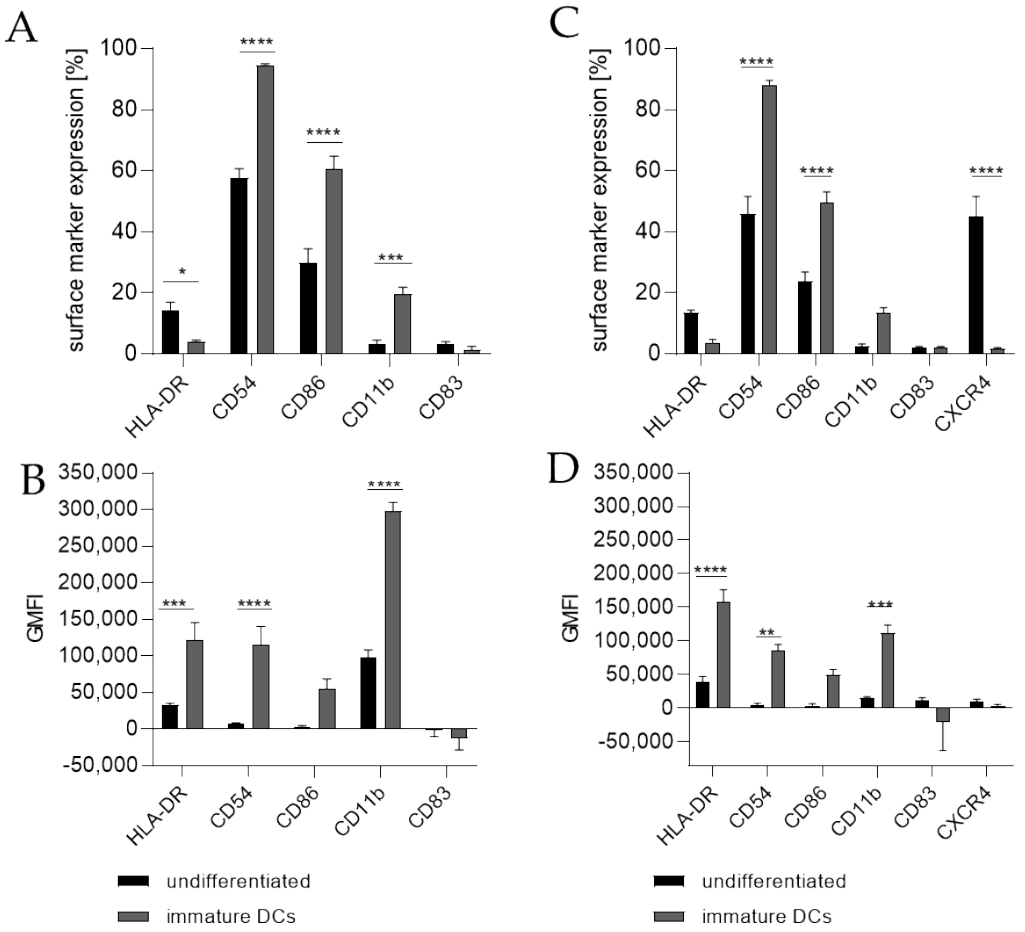

Figure 2.1-1 Surface marker expression of THP-1-derived iDCs, as follows: ng/mL **(A, B)** versus U/mL **(C, D)**. Here, 2 × 10^5 THP-1 cells/mL were seeded in 5 mL RPMI supplemented with 10% FBS, 1% PenStrep, and 0.05 mM 2-mercaptoethanol into a T25 flask. **(A, B)** For differentiation into iDCs, 100 ng/mL rhGM-CSF and 100 ng/mL rhIL-4 were added. **(C, D)** For differentiation into iDCs, 1500 U/mL rhGM-CSF and 1500 U/mL rhIL-4 were added. Cells were cultivated for 5 days, with medium exchange and addition of fresh cytokines after 72 h. Surface marker expression of at least 10,000 viable cells was analyzed via flow cytometry. Error bars indicate the standard errors of the mean (n = 3 independent experiments with * = $p \leq 0.05$, ** = $p \leq 0.01$, *** = $p \leq 0.001$, and **** = $p \leq 0.0001$).

For the differentiation of THP-1 cells into mDCs, various protocols have been published. The main difference between those protocols is the direct differentiation of THP-1 cells into mDCs versus the differentiation of THP-1 cells into iDCs followed by further subsequent differentiation steps towards mDCs. Again, protocols using cytokine concentrations in ng/mL, as well as protocols based on concentrations in U/mL and various differentiation durations, have been published (Table 2.1-2).

Thus, we differentiated THP-1 in a one-step protocol into mDCs for 48 h with supplementation of 100 ng/mL GM-CSF (≙ 900 U/mL), 200 ng/mL IL-4 (≙ 4600 U/mL), 20 ng/mL (≙ 400 U/mL) TNF-α, and 200 ng/mL ionomycin and with supplementation of 1500 U/mL GM-CSF, 3000 U/mL IL-4, 2000 U/mL TNF-α, and 200 ng/mL ionomycin for 48 h as well as for 72 h. The surface marker expression of mDCs generated from THP-1 cells cultivated in serum-free medium for 48 h was significantly higher for CD54 (ng/mL, ~100%; U/mL, ~99%), CD86 (ng/mL, ~73%; U/mL, ~73%), CD11b (ng/mL, ~44%; U/mL, ~52%), and CD83 (ng/mL, ~29%; U/mL, ~50%), but significantly lower for CXCR4 (ng/mL, ~2%; U/mL, ~3%) compared to the

undifferentiated controls (CD54, ~75–77%; CD86, ~44–48%; CD11b, ~3–4%; CD83, 0%; CXCR4, 33–35%) (Figure 2.1-2A, C). The differentiation of THP-1 cells into mDCs for 72 h using U/mL concentrations led to significantly higher numbers of cells expressing CD86 (~78%), CD11b (~49%), and CD83 (~35%), as well as CXCR4 (~70%), compared to the undifferentiated control (CD86, ~49%; CD11b, ~6%; CD83, ~0%; CXCR4, ~35%) (Figure 2.1-2E). Notably, a higher GMFI could only be observed for CD54 at a similar level (~415-fold) for all three differentiation approaches (Figures 2.1-2B, D, F).

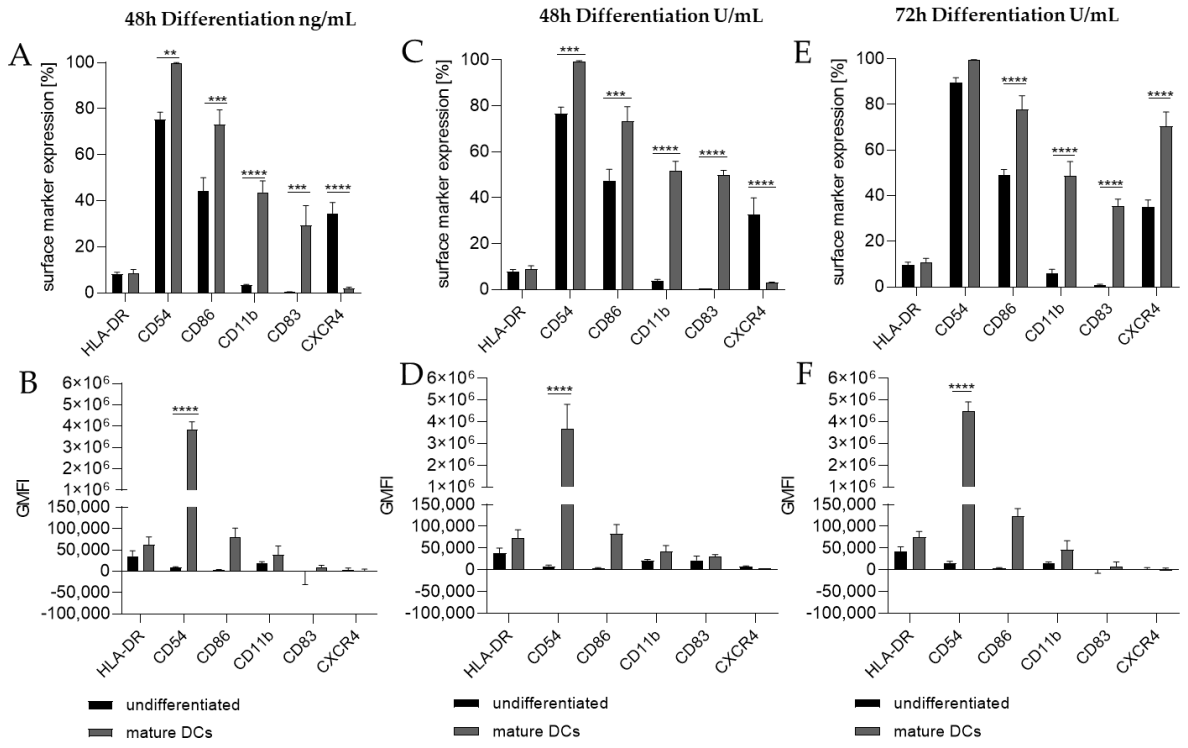

Figure 2.1-2 Surface marker expression of THP-1-derived mDCs, as follows: ng/mL **(A, B)** versus U/mL **(C–F)**. Here, 2 × 10^5 THP-1 cells/mL were seeded in 5 mL serum-free RPMI supplemented with 1% PenStrep, and 0.05 mM 2-mercaptoethanol into a T25 flask. **(A, B)** For differentiation into mDCs, 100 ng/mL rhGM-CSF, 200 ng/mL rhIL-4, 20 ng/mL TNF-α, and 200 ng/mL ionomycin were added. **(C, D, E, F)** For differentiation into mDCs, 1500 U/mL rhGM-CSF, 3000 U/mL rhIL-4, 2000 U/mL TNF-α, and 100 ng/mL ionomycin were added. Cells were cultivated for 48 h or 72 h. Surface marker expression of at least 10,000 viable cells was analyzed via flow cytometry. Error bars indicate the standard errors of the mean (n = 3 independent experiments, with ** = p ≤ 0.01, *** = p ≤ 0.001, and **** = p ≤ 0.0001).

Since the morphology of mDCs could be differentiated between floating and adherent populations (Figure 2.1-4), we also investigated the impact of a floating versus an adherent status on surface marker expression (Figure 2.1-3). Both floating and adherent mDCs expressed the surface markers CD54 (floating, ~99; adherent, ~98%), CD86 (floating, ~81; adherent, ~80%), and CD83 (floating, ~25; adherent, ~26%) at significantly higher rates than undifferentiated THP-1 cells (CD54, ~79%; CD86, ~41%; CD83, ~0%). Furthermore, although the numbers of cells expressing CXCR4 and CD11b was significantly higher on floating mDCs (CXCR4, ~46%; CD11b, ~29%), compared to undifferentiated THP-1 cells (CXCR4. ~20%;

CD11b, ~3%), the surface marker expression of CXCR4 (~29%) and CD11b (~3%) on the adherent mDC population was not significantly higher compared to undifferentiated THP-1 cells (CXCR4, ~20%; CD11b, ~3%) (Figure 2.1-3A). However, significant changes in the GMFI for CD54 were detected for floating (273-fold) as well as for adherent (225-fold) mDCs. Although the number of cells expressing HLA-DR was not increased, the GMFI for floating cells was elevated (2.3-fold) and was even higher for adherent mDCs (5.8-fold) compared to the undifferentiated control (Figure 2.1-3B). Thus, the differentiation of THP-1 cells with GM-CSF, IL-4, TNF-α, and ionomycin leads to two different populations, namely floating and adherent, which both reflect the marker expression of mature dendritic cells (CD54, CD86, and CD83), but display significant differences in CD11b and CXCR4 expression, which might be accompanied by different phagocytotic and migratory potential.

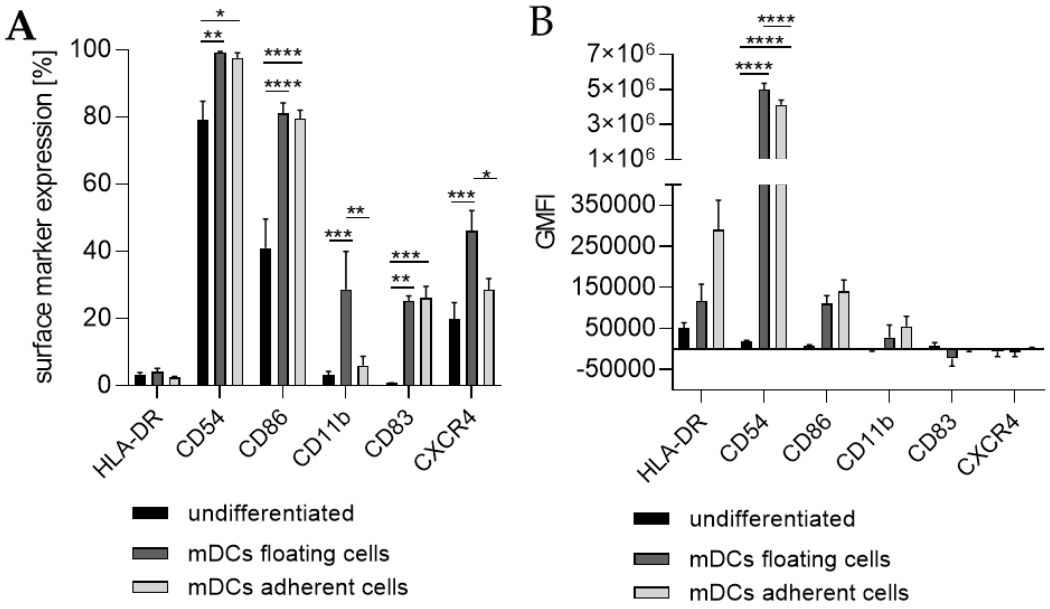

Figure 2.1-3 Surface marker expression of THP-1-derived mDCs. Floaters versus adherent cells. **(A)** Surface marker expression [%]. **(B)** Geometric mean fluorescence intensity (GMFI) 2 × 10^5 THP-1 cells/mL were seeded in 20 mL serum-free RPMI supplemented with 1% PenStrep and 0.05 mM 2-mercaptoethanol into a T75 flask. For differentiation, 1500 U/mL rhGM-CSF, 3000 U/mL rhIL-4, 2000 U/mL TNF-α, and 200 ng/mL ionomycin were added. Cells were cultivated for 72 h at 37 °C, 5% CO_2. Surface marker expression of at least 10,000 viable cells was analyzed via flow cytometry. Error bars indicate the standard errors of the mean (n = 3 independent experiments with * = $p \leq 0.05$; ** = $p \leq 0.01$; *** = $p \leq 0.001$; and **** = $p \leq 0.0001$).

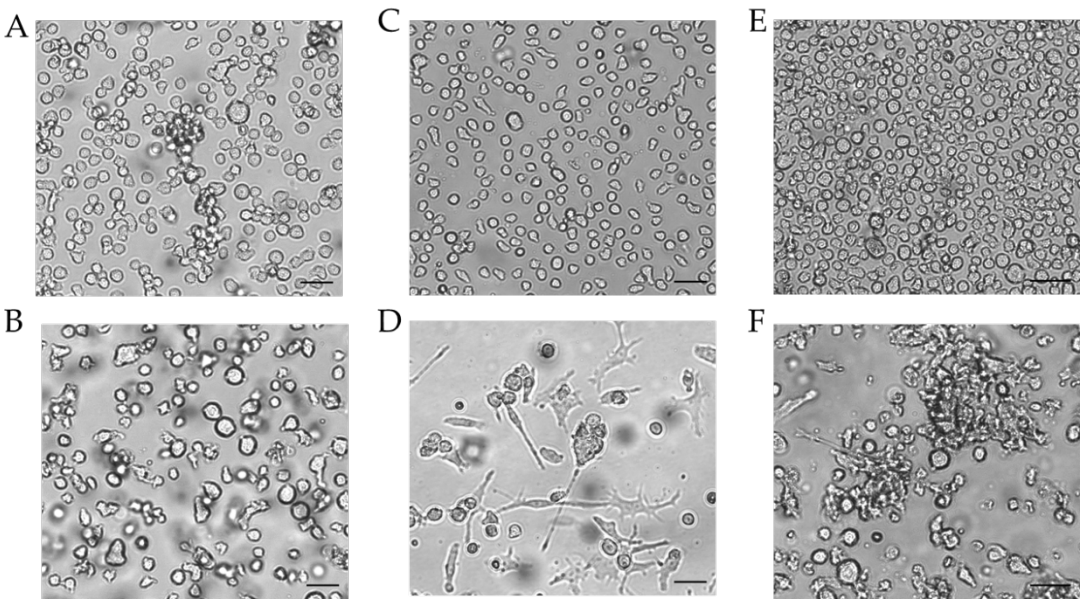

Figure 2.1-4 Morphology of THP-1-derived iDCs and mDCs using cytokine concentrations in U/mL. Morphology of undifferentiated THP-1 cells **(A,C,E)** according to the respective culture conditions of the differentiated cells. **(B)** Morphology of THP-1-derived immature dendritic cells (iDCs) (T25, U/mL, 5 d). **(D)** Morphology of THP-1-derived mDCs (T25, U/mL, 72 h). **(F)** Morphology of mDCs generated from THP-1-derived iDCs (T25, ng/mL, 48 h). Scale bar = 50 µm.

Next, we differentiated THP-1-derived iDCs further into mDCs (Figure 2.1-5). The differentiation of iDCs into mDCs led to a significantly higher number of cells expressing CD54 (~99%), CD86 (~54%), and CD11b (~21%) compared to undifferentiated THP-1 cells (CD54, ~63%; CD86, ~33%; CD11b, ~2%). Notably, the CXCR4 expression was completely diminished. The number of cells expressing CD11b was significantly higher in iDCs (~27%) as well as in mDCs (~21%) compared to undifferentiated THP-1 cells (~2%), but lower in mDCs (~21%) compared to iDCs (~27%). Expression of CD83 on mDCs from THP-1- derived iDCs could not be induced (Figure 2.1-5A). The GMFI for CD54 was 29.8-fold induced on iDCs and 128-fold induced on iDC-derived mDCs. However, the GMFI for HLA-DR was increased at similar levels for iDCs (8.3-fold) and mDCs (8.0-fold), and the GMFI induction for CD86 was lower for mDCs (16.4-fold), than for iDCs (26.2-fold) (Figure 2.1-5B). Furthermore, the morphology of mDCs differentiated from THP-1-derived iDCs, as depicted in Figure 2.1-4F, reveals mainly loosely adherent cell clusters.

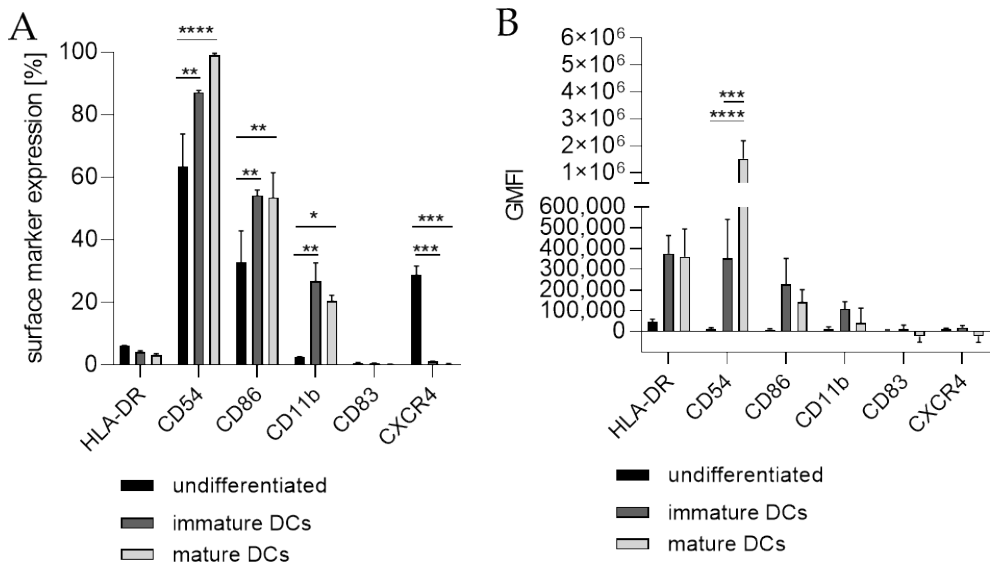

Figure 2.1-5 Surface marker expression of mDCs generated from-THP-1-derived iDCs. **(A)** Surface marker expression [%]. **(B)** Geometric mean fluorescence intensity (GMFI). Here, 2 × 10^5 THP-1 cells/mL were seeded in 5 mL RPMI supplemented with 10% FBS, 1% PenStrep, and 0.05 mM 2-mercaptoethanol into a T25 flask and differentiated into iDCs. For further differentiation into mDCs, the medium was removed and fresh medium containing 100 ng/mL rhGM-CSF, 200 ng/mL rhIL-4, 20 ng/mL TNF-α, and 200 ng/mL ionomycin was added. Cells were cultivated for 48 h at 37 °C, 5% CO_2. Surface marker expression of at least 10,000 viable cells was analyzed via flow cytometry. Error bars indicate the standard errors of the mean (n = 2 independent experiments with * = $p \leq 0.05$, ** = $p \leq 0.01$, *** = $p \leq 0.001$, and **** = $p \leq 0.0001$).

To investigate the ability of THP-1-derived iDCs to identify potential sensitizers, iDCs in comparison to undifferentiated THP-1 cells were treated for 24 h with either 20 µM 1-chloro-2,4-dinitrobenzene (DNCB) or 380 µM nickel sulfate ($NiSO_4$), the defined positive controls of the h-CLAT assay. As expected, the treatment of THP-1 cells with $NiSO_4$ led to a significantly higher expression of the h-CLAT key markers CD54 (~98%) and CD86 (~55%) and induced the expression of the maturation marker CD83 (~17%). Furthermore, treatment of iDCs with $NiSO_4$ resulted in a significant upregulation in CD54 (~97%), CD86 (~64%), and CXCR4 (~23%) (Figure 2.1-6A). The GMFI for CD54 was significantly higher (13.7-fold) after $NiSO_4$ treatment on THP-1 cells, but not as high as on iDCs after $NiSO_4$ treatment (29.2-fold) compared to untreated THP-1 cells. The GMFI for HLA-DR on iDCs was decreased after $NiSO_4$ treatment (1.5-fold), but not as much as on THP-1 cells with (6.4-fold) or without $NiSO_4$ treatment (5.6-fold) (Figure 2.1-6B). Furthermore, an increased GMFI (1.3-fold) for CD83 was observed after treatment of iDCs with $NiSO_4$.

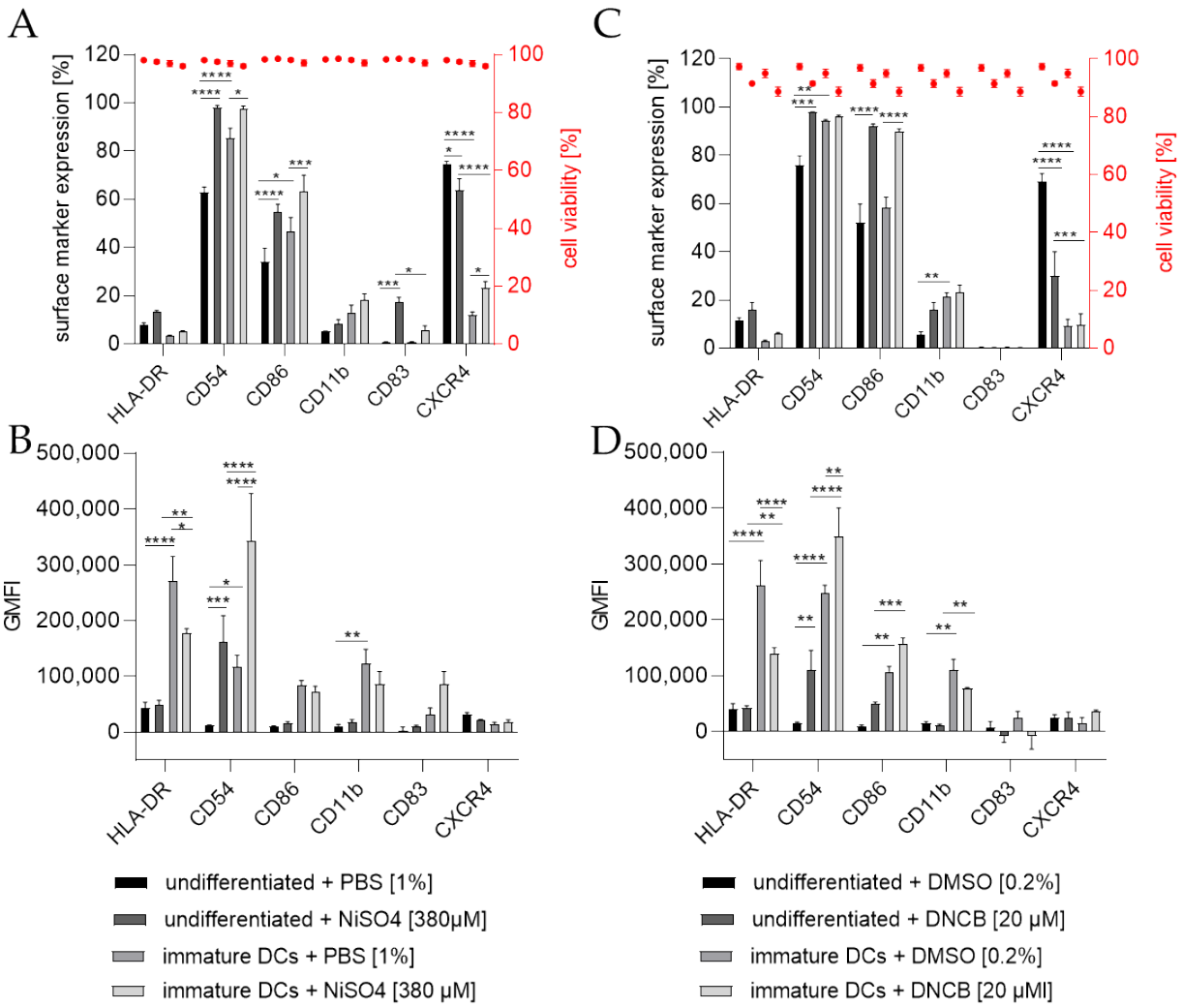

Figure 2.1-6 Surface marker expression of THP-1 cells or iDCs after sensitization according to the h-CLAT assay. **(A, C)** surface marker expression [%]. **(B, D)** Geometric mean fluorescence intensity (GMFI). Here, THP-1 cells or THP-1-derived iDCs were seeded with 1 × 10^6 cells/mL in 1 mL RPMI supplemented with 10% FBS, 1% PenStrep, and 0.05 mM 2-mercaptoethanol into a 24-well plate. Cells were treated with 20 µM 1-Chloro-2,4-dinitrobenzene (DNCB) and 380 µM nickel sulfate ($NiSO_4$) or their respective solvent control, namely DMSO or PBS. Surface marker expression of at least 10,000 viable cells was analyzed via flow cytometry. Error bars indicate the standard errors of the mean (n = 3 independent experiments with * = p ≤ 0.05, ** = p ≤ 0.01, *** = p ≤ 0.001, and **** = p ≤ 0.0001).

Treatment of THP-1 cells with 20 µM DNCB also resulted in significantly more cells expressing the h-CLAT markers CD54 (~98%) and CD86 (~96%), but significantly fewer cells expressing CXCR4 (~30%). Treatment of iDCs with DNCB resulted in significantly more cells expressing CD86 (~90%) (Figure 2.1-6C). Similar to the expression pattern of $NiSO_4$-treated iDCs, treatment with DNCB led to a significantly higher GMFI for CD54 (3-fold) and lower GMFI for HLA-DR (1.9-fold) compared to untreated iDCs. However, compared to DNCB-treated THP-1 cells, the GMFI for HLA-DR is 3.3-fold higher, and the GMFI for CD11b is 7.2-fold higher on DNCB-treated iDCs (Figure 2.1-6D).

In order to prove the capability of our THP-1-derived DCs to phagocytose exogenous pathogen-derived particles, the DC surrogates were incubated with pHrodo Red-labeled zymosan, an insoluble β-1,3-glucan polysaccharide extracted from the cell wall of

Saccharomyces cerevisiae. As pHrodo Red is a pH indicator dye, it is weakly fluorescent at neutral pH, but increases its fluorescence with decreasing pH during phagosomal acidification. As depicted in Figure 2.1-7 and as expected, significantly higher numbers of iDCs are able to phagocytose zymosan (~45%) compared to undifferentiated THP-1 cells (~17%) and to mDCs (~9%).

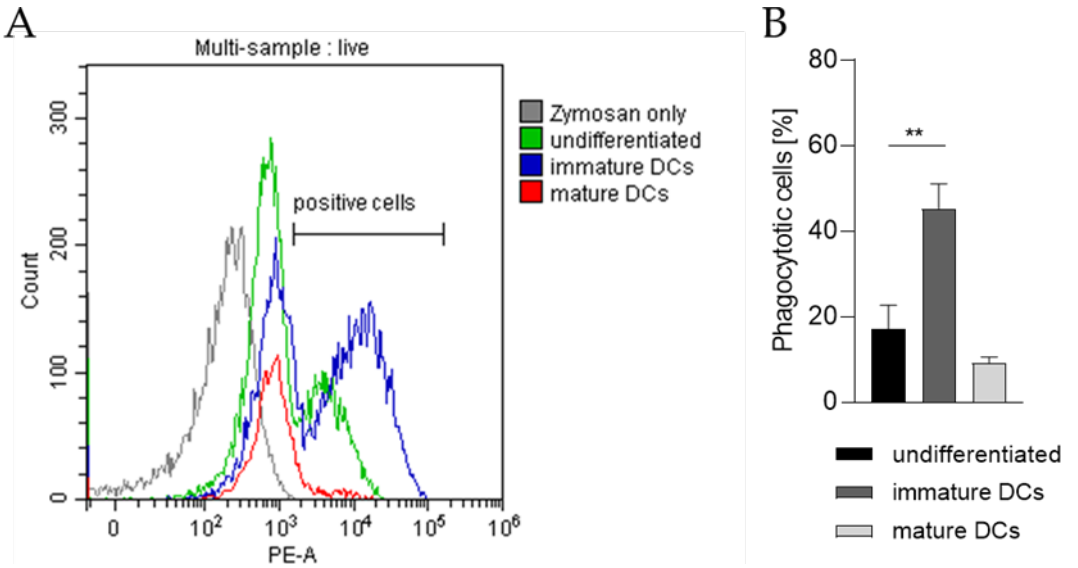

Figure 2.1-7 Phagocytotic capability of undifferentiated THP-1 cells, iDCs, and mDCs. Here, iDCs, as well as mDCs, were differentiated according to the U/mL protocols. After 5 days and 72 h respectively, 2 × 10^5 cells were resuspended in 100 µL pHrodo Red zymosan bioparticles, seeded into 96-well plates, and cultivated for 1 h at 37 °C, 5% CO_2. Then, DAPI was added before analysis of 10,000 living cells per sample via flow cytometry (Ex/Em, 560/585). **(A)** Gating strategy. **(B)** Number of cells (%) positive for phagocytosis. Error bars indicate the standard errors of the mean (n = 3 independent experiments, with ** = p ≤ 0.01).

Moreover, the ability of iDCs to initiate T cell activation was investigated by analyzing the mRNA expression of the p40 chain of interleukin (IL)-12 via quantitative real-time PCR. For this, iDCs as well as undifferentiated THP-1 cells, were treated for 6 h with either 20 µM DNCB or 380 µM $NiSO_4$, respectively. As expected, treatment of undifferentiated THP-1 cells with DNCB or $NiSO_4$ did not significantly alter the expression of IL-12p40 (Figure 2.1-8A). In contrast, mRNA expression of IL-12p40 was significantly higher in iDCs after DNCB treatment (4.5-fold), and 1.3-fold higher after $NiSO_4$ treatment, compared to the solvent control (Figure 2.1-8B), proving that differentiation of THP-1 cells into iDCs is required to study dendritic cell-mediated T cell activation.

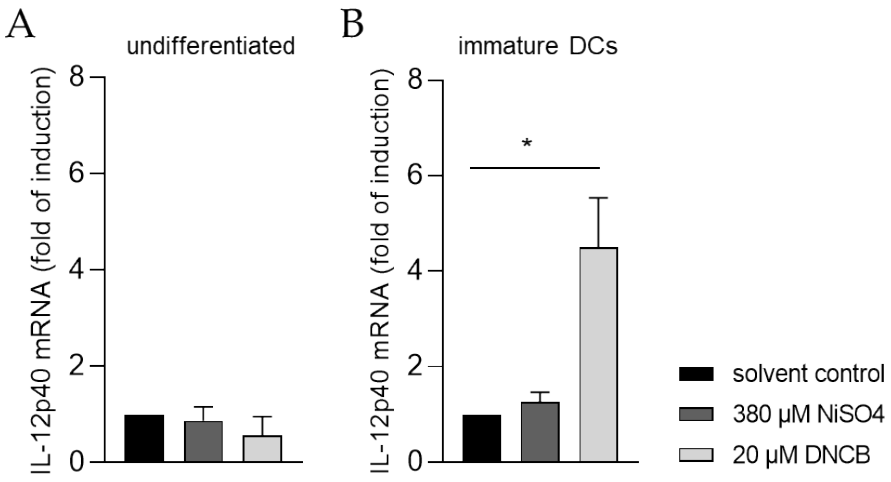

Figure 2.1-8 IL-12p40 mRNA expression of **(A)** THP-1 cells and **(B)** immature dendritic cells (iDCs) after sensitizer treatment. Here, THP-1 cells or THP-1-derived iDCs were seeded with 1 × 10^6 cells/mL in 1 mL RPMI supplemented with 10% FBS, 1% PenStrep, and 0.05 mM 2-mercaptoethanol into a 24-well plate. Cells were treated with 20 µM DNCB or 380 µM $NiSO_4$ for 6 h. Results were expressed as fold of induction compared to the solvent control and normalized to the expression of the housekeeping gene GAPDH. Error bars indicate the standard errors of the mean (n = 3 independent experiments with * = $p \leq 0.05$).

Discussion

The aim of this study was to generate robust, highly reproducible, and cost-effective protocols providing THP-1-derived iDC as well as mDC surrogates for *in vitro* human- based toxicological studies and for investigating the underlying mechanisms of sensitization and inflammation. In mediating the immune response, dendritic cells undergo various phenotypical changes, such as the upregulation of co-stimulatory molecules, maturation markers, and receptors regulating migratory behavior. In order to evaluate a conclusive differentiation of THP-1 cells into iDCs and mDCs as well as their potential for toxicological studies, we focused mainly on the DC activation markers CD54 and CD86, CD11b as marker for phagocytosis, the maturation marker CD83, and the migration maker CXCR4. The differentiation of THP-1 cells into iDCs resulted in a significant upregulation in the surface markers CD54, CD86, and CD11b. The upregulation of CD54 together with CD86 are the key readout parameters of the h-CLAT aiming to mimic dendritic cell activation in order to predict skin sensitization [58,59]. Furthermore, co-stimulatory molecules, such as CD86, as well as CD80, often working in tandem, are upregulated during DC maturation, promoting CD 4^+ T cell activation [34,72]. The upregulation of CD86 as well as CD80 have been shown for THP-1-derived iDCs [62,64]. However, contrarily, Galbiati et al. described CD80 as well as CD86 expression below 15% on iDCs [65], not matching our results. It is known that CD11b plays an important role in phagocytosis [73], and its upregulation on THP-1-derived iDCs has been revealed by Czernek et al. [64], a study which confirms our data. Furthermore, HLA-DR is one of the MHC class II cell surface receptors, presenting the internalized and processed antigens to CD 4^+ T cells [74]. Even though our results displayed a low number of iDCs expressing HLA-DR, the GMFI for HLA-DR

was significantly higher compared to undifferentiated cells, verifying an upregulation of HLA-DR molecules on HLA-DR-positive iDCs. This result matches the findings of Czernek et al., reporting a substantially higher MFI for HLA-DR on iDCs; unfortunately, Czernek et al. did not indicate the number of positive cells for HLA-DR [64]. However, as long as iDCs have not been exposed to antigens, MHC II molecules are retained by the invariant chain Ii in the late endosomal compartment [14]. In addition, it has been reported that only very few MHC II molecules are localized on the membrane of iDCs, and up to 75% of all MHC II molecules reside in the antigen processing compartments [15], confirming our results revealing low numbers of iDCs expressing HLA-DR on their surface. Furthermore, the differentiation of THP-1 cells into iDCs did not induce the expression of CD83, a principal marker for cell maturation [75], matching the literature [62] and proving their immature status. To date, most protocols differentiating THP-1 cells into iDCs were performed in T75 flasks and 20 mL medium [62,65,66]. In contrast, we are the first to prove the differentiation of THP-1 cells into iDCs in T25 flasks, using 5 mL medium and, thus, only one quarter of the amount of the required cytokines, confirming our cost-effective approach.

For the generation of THP-1-derived mDCs, various protocols have been published, differentiating THP-1 cells directly into mDCs for 24 h [62], 48 h [62,66], 72 h [62], or generating mDCs from iDCs [63–65]. Differentiating THP-1 cells directly into mDCs for 48 h resulted in significantly higher numbers of cells expressing CD54, CD86, CD11b, and CD83, but a significantly lower (almost none) expression of CXCR4. Contrarily, the differentiation of THP-1 cells into mDCs for 72 h led to significantly enhanced numbers of CXCR4 expressing cells compared to the undifferentiated control. Furthermore, CXCR4 is one receptor for CXCL12/SDF-1, which is constitutively expressed and secreted in lymphoid tissues and other non-lymphoid tissues by bone marrow-, lymph node-, skin-, muscle-, and lung-derived fibroblasts, as well as by endothelial cells, liver and kidney cells, and the central nervous system [76–79]. Furthermore, various organs respond to tissue damage by increasing SDF-1 expression and secretion via hypoxia-inducible factor-1 (HIF-1) binding to the hypoxia-responsive region of the SDF-1 promotor [80]. Based on knockout studies or pharmacological blockade, CXCR4 has been proven to have a key role in DC differentiation [81], as well as in DC and Langerhans cell migration [23,24,82]. We are the first to prove CXCR4 expression on THP-1-derived mDCs. Coherent, upregulation of CXCR4 surface expression on mature dendritic cells has been shown for PBMC-derived dendritic cells [83] as well as for bone marrow-derived dendritic cells [84]. Furthermore, low CXCR4 mRNA levels for PBMC-derived iDCs and high CXCR4 levels for PBMC-derived mDCs have been detected by Sallusto et al. [21], confirming the CXCR4 expression pattern on our iDCs and mDCs. However, CXCR4 is not only expressed on mDCs, but also on naïve T cells and B lymphocytes [85], which may favor co-localization of those cells at sites where SDF-1 is secreted due to inflammation and

tissue damage. Noteworthily, the direct differentiation of THP-1 cells into mDCs for 72 h led to two different subpopulations, namely floating and adherent cells. In both cell populations, CD83, the marker molecule for mature dendritic cells, was expressed by a similar quantity of cells, indicating no difference in maturation status. While the floating cells showed significantly higher expression of CXCR4 and CD11b than the undifferentiated THP-1 cells, the expression of CXCR4 and CD11b on adherent mDCs was only marginally higher than on undifferentiated THP-1 cells and significantly lower compared to the floating mDCs. Since CXCR4 is necessary for migration [23,24,82] and CD11b is involved in phagocytosis [73], it is coherent with the morphology and higher expression on floating cells which might be still in a steady state for the phagocytosis of antigens and migration to distinct sides. Furthermore, mDCs generated from THP-1-derived iDCs also display a different morphology compared to the mDCs which have been generated directly from THP-1 cells. While the directly generated mDCs were mostly strongly adherent and developed dendritic shaped branches, mDCs generated from iDCs formed loosely adherent cell clusters. Furthermore, CD11b expression was slightly lower than on iDCs and they expressed neither CD83 nor CXCR4. Based on these results we are confident that mDCs generated from THP-1-derived iDCs are not mDCs. Unfortunately, all publications which generated mDCs from THP-1-derived iDCs did not investigate the expression of CD83 or CXCR4, as successful maturation was assumed from high CD80 and CD86 expression [63–65]. Thus, only mDCs generated directly from THP-1 cells match the dendritic morphology and express the relevant maturation markers CD86 and CD83 as well as the migration marker CXCR4. However, for CXCR4 expression, it is mandatory to differentiate the THP-1 cells for 72 h and not as stated otherwise for 24 h or 48 h. Furthermore, comparing the differentiation results for iDCs and mDCs, expression levels for CD54, CD11b, and CD83 were different using cytokine concentrations indicated in ng/mL versus U/mL. Since the biological activity differs from supplier to supplier and occasionally between lots, the indication of applied cytokine concentrations in U/mL is more precise and strongly advised for reproducible data. Complementary to the iDC protocols, most protocols for mDC generation were performed in T75 flasks in a volume of 20 mL medium. We are the first to prove differentiation of THP-1 cells into iDCs in T25 flasks, using 5 mL medium and, thus, only one quarter of the cytokines, thereby generating a cost-effective protocol.

As mentioned before, the upregulation of co-stimulatory molecules, as well as maturation markers in response to sensitizing and inflammation inducing agents, has become one of the key parameters to identify and predict the potential sensitizing and inflammatory capacity of substances. One of the most prominent assays is the h-CLAT, predicting sensitizers via CD54 and CD86 upregulation. The accuracy of the h-CLAT to distinguish sensitizers from non-sensitizers has been calculated as being between 76% and 83% [58,86,87]. In order to be classified as sensitizer, the relative fluorescence intensity (RFI) has to exceed a defined

threshold, namely CD54 ≥ 200 or CD86 ≥ 150 [56,59]. However, detection of chemicals as false-negatives in the h-CLAT have been reported [54,87]. Our data reveals that the expression of CD54 as well as CD86, including percent positive cells and GMFI, is significantly higher for iDCs after sensitizer treatment compared to undifferentiated cells, which might allow a higher accuracy in detecting and subsequently categorizing sensitizers by decreasing rates of false-negative results and which might provide benefits for animal-free toxicological studies.

In order to demonstrate the functionality of our iDCs, their capability to phagocytose exogenous pathogen-derived particles as well as their potential to activate T cells was investigated. In their immature state, DCs are able to endocytose pathogens, which are further processed, initiating DC activation and maturation accompanied by the expression of surface markers, such as MHC II, CD54, and CD86. During the maturation process this ability decreases as DCs acquire primarily potent antigen presenting functions [12,88]. To assess the phagocytic potential of our DCs, cells were treated with zymosan, derived from the cell wall of *Saccharomyces cerevisiae*. While some undifferentiated THP-1 cells were able to phagocyte zymosan (17%), the number of phagocytotic iDCs was significantly higher (45%), whereas the number of mDCs phagocyting zymosan decreased (9%). In line with our findings, high phagocytotic capability for iDCs has been reported for PBMC-derived as well as bone-marrow-derived iDCs [89–91]. Furthermore, lower phagocytotic capability of mDCs upon maturation has been shown for mDCs derived from PBMCs [91].

In order to activate naïve $CD4^+$ T cells, DCs secrete IL-12, leading to upregulation of the transcription factor T-box expressed in T cells (T-bet) promoting their differentiation into interferon-γ producing T helper 1 cells (Th1) [92,93]. Treatment of our THP-1-derived iDCs with DNCB resulted in significantly higher mRNA levels of IL-12p40 and in moderate higher mRNA levels of IL-12p40 in the presence of $NiSO_4$. Overall, we are able to demonstrate and prove the potential of THP-1-derived iDCs to induce T cell activation. Previous studies have shown IL-12p40 expression induction upon $NiSO_4$ treatment of PBMC-derived iDCs [94,95], but not after DNCB treatment [94,96]. Contrarily, cutaneous treatment of mice with DNCB led to significantly enhanced IL-12p40 mRNA levels in local lymph nodes [97,98], as well as in spleens and the skin [99], tending to confirm our findings. In conclusion, we were able to downscale the differentiation approaches by three-quarters, thereby generating robust, highly reproducible, and cost-effective protocols providing THP-1-derived iDC and mDC surrogates. The strong induction of CD54 as well as CD86 expression on iDCs after sensitizer treatment are applicable for *in vitro* toxicological studies, identifying potential sensitizing or inflammatory compounds and, in further steps, for assessing the anti-inflammatory potential of novel drug candidates. Based on the observed expression induction rates of CD11b, CD83, and CXCR4 as well as the IL-12p40 expression upon sensitizer treatment and the phagocytotic capability, our iDC and mDC surrogates are beneficial to study the molecular mechanisms of dendritic

cell-mediated phagocytosis [73,100], dendritic cell maturation [101], as well as migration [22] and, furthermore, their use as therapeutic model systems in various disorders, such as sensitization, inflammation [102,103], as well as cancer [104] and the tumor microenvironment [105], should not be discounted.

Materials and Methods

Cell Line Cultivation

The human monocytic leukemia cell line THP-1 (#TIB202, LOT:70025047) was purchased from ATCC (Manassas, VA, USA) (The THP-1 cells were maintained in T75 flasks (Greiner, #658195, Frickenhausen, Germany) in 20 mL RPMI (Gibco, #22400089, Grand Island, NY, USA) supplemented with 10% FBS (Gibco, #10270-106), 1% penicillin–streptomycin (PenStrep) (Gibco, #15140122), and 0.05 mM 2-mercaptoethanol (Gibco, #21985023) in a humidified incubator at 37 °C and 5% CO_2. Cell density was maintained between 1 × 10^5 cells/mL and 5 × 10^5 cells/mL and cells were split every 2–3 days.

Differentiation of THP-1 cells into iDCs

For the generation of iDCs 2 × 10^5 THP-1 cells/mL were seeded in 5 mL RPMI supplemented with 10% FBS, 1% PenStrep, and 0.05 mM 2-mercaptoethanol into a T25 flask. For differentiation, according to the published ng/mL concentrations, the following concentrations of cytokines were added: 100 ng/mL (=900 U/mL) rhGM-CSF (ImmunoTools, #11343125, Friesoythe, Germany), and 100 ng/mL (=2300 U/mL) rhIL-4 (ImmunoTools, #11340045). For differentiation using U/mL concentrations, 1500 IU/mL rhGM-CSF (ImmunoTools, #11343125) and 1500 IU/mL rhIL-4 (ImmunoTools, #11340045) were added. The cells were incubated for 5 days at 37 °C, 5% CO_2, with medium exchange and addition of fresh cytokines on day 3.

Differentiation of THP-1 cells into mDCs

For differentiation of THP-1 cells into mDCs 2 × 10^5 cells/mL in 5 mL or 20 mL serum-free RPMI supplemented with 1% PenStrep and 0.05 mM 2-mercaptoethanol was placed into a T25 flask or T75 flask. For differentiation according to ng/mL cytokine concentrations, the following concentrations were added: 100 ng/mL (=900 U/mL) rhGM-CSF (ImmunoTools, #11343125), 200 ng/mL (=4600 U/mL) rhIL-4 (ImmunoTools, #11340045), 20 ng/mL (=400 U/mL) TNF-α (PromoKine, C63719), and 200 ng/mL ionomycin (Sigma- Aldrich, #I0634). For differentiation using U/mL concentrations, the following cytokines were added: 1500 IU/mL rhGM-CSF (ImmunoTools, #11343125), 3000 IU/mL rhIL-4 (ImmunoTools, #11340045), 2000 IU/mL TNF-α (PromoKine, #C63719, Heidelberg, Germany), and 200 ng/mL ionomycin (Sigma-Aldrich, #I0634, Darmstadt, Germany). The cells were cultivated for 48 h and 72 h at

37 °C, 5% CO_2. For flow cytometry analysis, adherent cells were detached with accutase (Sigma-Aldrich, #A6964).

Differentiation of THP-1-derived iDCs into mDCs

The THP-1-derived iDCs were generated as stated in in the Section “Differentiation of THP-1 cells into iDCs”. On day 5, for further differentiation into mDCs, the medium was removed, and fresh medium containing 100 ng/mL (=900 U/mL) rhGM-CSF (ImmunoTools, #11343125), 200 ng/mL (=4600 U/mL) rhIL-4 (Immuno-Tools, #11340045), 20 ng/mL (=400 U/mL) TNF-α (PromoKine, #C63719), and 200 ng/mL ionomycin (Sigma-Aldrich, #I0634) was added. The cells were cultivated for 48 h at 37 °C, 5% CO_2. For flow cytometry analysis, adherent cells were detached with accutase (Sigma-Aldrich, #A6964).

Sensitization Assay According to the h-CLAT

The THP-1 cells or THP-1-derived iDCs were seeded and treated accordingly to the h-CLAT assay. Briefly, 1 × 10^6 cells/mL were seeded in 1 mL RPMI supplemented with 10% FBS, 1% PenStrep, and 0.05 mM 2-mercaptoethanol into a 24-well plate. Cells were treated with 20 µM 1-chloro-2,4-dinitrobenzene (DNCB) (Sigma-Aldrich, #237329, Darmstadt, Germany) and 380 µM nickel sulfate ($NiSO_4$) (Sigma-Aldrich, #227676) or their respective solvent control, namely dimethylsulfoxide (DMSO) or Dulbecco’s phosphate buffered saline (PBS). After 24 h, the cells were harvested, and surface marker expression was determined via flow cytometry.

Surface Marker Detection via Flow Cytometry

Cells were harvested after differentiation and washed thrice in autoMACS running buffer (Miltenyi Biotec, #130-091-221, Gladbach, Germany). Cells were transferred to 96- well plates with 2 × 10^5 cells for each antibody panel. Cells were stained with the following antibodies: diluted 1:50, REA Control (S)-VioGreen (Miltenyi Biotec, #130-113-444), REA Control (S)-PE (Miltenyi Biotec, #130-113-438), REA Control (S)-APC (Miltenyi Biotec, #130- 113-434); REA Control (S)-PE-Vio770, (Miltenyi Biotec, #130-113-440); HLA-DR-VioGreen (Miltenyi Biotec, #130-111-795), CD54-APC (Miltenyi Biotec, #130-121-342); CXCR4-PE- Vio770 (Miltenyi Biotec, #130-116-161); CD11b-VioGreen (Miltenyi Biotec, #130-110-617); CD83-PE (Miltenyi Biotec, #130-110-561); CD86-APC (Miltenyi Biotec, #130-116-161) for 10 min at 4 °C in the dark. Afterwards, cells were washed thrice with autoMACS running buffer and stained with DAPI (Sigma, #D9542), to exclude dead cells for the determination of the cell viability.

Phagocytosis Assay

Phagocytosis assays were performed using pHrodo red zymosan particles (InvitrogenTM, #P35364, Waltham, MA, USA), dissolved in RPMI supplemented with 10% FBS, 1% PenStrep,

and 0.05 mM 2-mercaptoethanol at a concentration of 0.5 mg/mL. Cells were harvested after differentiation and 2 × 10^5 cells were resuspended in 100 µL pHrodo red zymosan particles and seeded into 96-well plates. The cells were cultivated for 1 h at 37 °C, 5% CO_2. Then, DAPI was added before the analysis of 10,000 living cells per sample via flow cytometry (Ex/Em, 560/585).

Analysis of IL-12p40 mRNA Expression by Quantitative Real-Time PCR

The THP-1 cells or THP-1-derived iDCs were seeded and treated according to the h-CLAT assay. Briefly, 1 × 10^6 cells/mL were seeded in 1 mL RPMI supplemented with 10% FBS, 1% PenStrep, and 0.05 mM 2-mercaptoethanol into a 24-well plate. Cells were treated with 20 µM 1-chloro-2,4-dinitrobenzene (DNCB) (Sigma-Aldrich, #237329) and 380 µM nickel sulfate ($NiSO_4$) (Sigma-Aldrich, #227676) or their respective solvent control, namely dimethylsulfoxide (DMSO) or Dulbecco's phosphate buffered saline (PBS) for 6 h. Total RNA was extracted according to the manufacturer's instructions using the RNeasy MiniKit (Qiagen, #74104, Hilden, Germany). The RNA concentration was determined by OD260/280 measurement using the Tecan Spark NanoQuant Plate. A total of 1 µg of RNA was reverse transcribed using the QuatiTect Reverse Transcription Kit (Qiagen, #205311). Quantitative real-time PCR (qPCR) reactions were performed for 50 ng cDNA in triplicate for each sample on a qTower3 G (Analytikjena, Jena, Germany), using Luna Universal qPCR Master Mix (NEB, #M3003L, Ipswich, MA, USA). The specific primers used were GAPDH (forward, 5 -TGCACCACCAACTGCTTAGC-3; reverse, 5-GGCATGGACTGTGGTCATGAG-3) and IL-12p40 (forward, 5-TGTCGTAGAATTGGATTGGTATC-3; reverse, 5-AACCT GCCTCCTTTGTG-3). After amplification, a threshold was set for each gene and Ct values were calculated for all samples.

Statistical Analysis

Statistical analysis was performed using GraphPad Prism version 8.4.3 (GraphPad Software, Inc., San Diego, CA, USA). Statistical significance was determined using two- way ANOVA, Sidak's multiple comparisons test or Tukey's multiple comparisons test. Significance was defined as * = $p \leq 0.05$; ** = $p \leq 0.01$; *** = $p \leq 0.001$; **** = $p \leq 0.0001$.

Author Contributions:

Conceptualization, N.T.; methodology, J.M.H.; software, J.M.H.; validation, J.M.H.; formal analysis, J.M.H.; investigation, J.M.H.; resources, N.T.; data curation, J.M.H.; writing— original draft preparation, J.M.H.; writing—review and editing, N.T. and J.M.H.; visualization, J.M.H.; supervision, N.T. project administration, N.T.; funding acquisition, N.T. All authors have read and agreed to the published version of the manuscript.

Funding:

This research was funded by a grant to N.T. by the Bundesministerium für Ernährung und Landwirtschaft (BMEL), funding number: 281A308C18.

Institutional Review Board Statement:

Not applicable.

Informed Consent Statement:

Not applicable.

Data Availability Statement:

Not applicable.

Acknowledgments:

The authors would like to thank Ursula Engels for sharing her profound knowledge regarding the h-CLAT assay and Kira Ludwig for her technical assistance.

Conflicts of Interest:

The authors declare no conflict of interest. The funders had no role in the design of the study; in the collection, analyses, or interpretation of data; in the writing of the manuscript; or in the decision to publish the results.

References

1. Eidsmo, L.; Allan, R.; Caminschi, I.; van Rooijen, N.; Heath, W.R.; Carbone, F.R. Differential migration of epidermal and dermal dendritic cells during skin infection. *The Journal of Immunology* 2009, *182*, 3165-3172.
2. e Sousa, C.R. Dendritic cells as sensors of infection. *Immunity* 2001, *14*, 495-498.
3. Liu, J.; Zhang, X.; Cheng, Y.; Cao, X. Dendritic cell migration in inflammation and immunity. *Cellular & Molecular Immunology* 2021, *18*, 2461-2471.
4. Hardonnière, K.; Szely, N.; El Ali, Z.; Pallardy, M.; Kerdine-Römer, S. Models of Dendritic Cells to Assess Skin Sensitization. *Front Toxicol* 2022, *4*, 851017, doi:10.3389/ftox.2022.851017.
5. LIU, L.; WATANABE, M.; MINAMI, N.; YUNIZAR, M.F.; ICHIKAWA, T. Dendritic Cells Directly Recognize Nickel Ions as an Antigen during the Development of Nickel Allergy. *Journal of Oral Health and Biosciences* 2022, *34*, 40-52.
6. Vella, J.L.; Molodtsov, A.; Angeles, C.V.; Branchini, B.R.; Turk, M.J.; Huang, Y.H. Dendritic cells maintain anti-tumor immunity by positioning CD8 skin-resident memory T cells. *Life science alliance* 2021, *4*.
7. Zhou, L.; Jiang, A.; Veenstra, J.; Ozog, D.M.; Mi, Q.-S. The Roles of Skin Langerhans Cells in Immune Tolerance and Cancer Immunity. *Vaccines* 2022, *10*, 1380.

8. Hölken, J.M.; Teusch, N.E. Recent developments of 3D models of the tumor microenvironment for cutaneous melanoma: Bridging the gap between the bench and the bedside? *Journal of Translational Science* 2020, *7*, 1-7.
9. Steinman, R.M.; Banchereau, J. Taking dendritic cells into medicine. *Nature* 2007, *449*, 419-426, doi:10.1038/nature06175.
10. Collin, M.; Bigley, V. Human dendritic cell subsets: an update. *Immunology* 2018, *154*, 3-20, doi:https://doi.org/10.1111/imm.12888.
11. Guilliams, M.; Ginhoux, F.; Jakubzick, C.; Naik, S.H.; Onai, N.; Schraml, B.U.; Segura, E.; Tussiwand, R.; Yona, S. Dendritic cells, monocytes and macrophages: a unified nomenclature based on ontogeny. *Nature Reviews Immunology* 2014, *14*, 571-578, doi:10.1038/nri3712.
12. Liu, Z.; Roche, P.A. Macropinocytosis in phagocytes: regulation of MHC class-II-restricted antigen presentation in dendritic cells. *Frontiers in physiology* 2015, *6*, 1.
13. Wilson, N.S.; El-Sukkari, D.; Villadangos, J.A. Dendritic cells constitutively present self antigens in their immature state in vivo and regulate antigen presentation by controlling the rates of MHC class II synthesis and endocytosis. *Blood* 2004, *103*, 2187-2195, doi:10.1182/blood-2003-08-2729.
14. Neefjes, J.; Jongsma, M.L.M.; Paul, P.; Bakke, O. Towards a systems understanding of MHC class I and MHC class II antigen presentation. *Nature Reviews Immunology* 2011, *11*, 823-836, doi:10.1038/nri3084.
15. Roche, P.A.; Furuta, K. The ins and outs of MHC class II-mediated antigen processing and presentation. *Nature Reviews Immunology* 2015, *15*, 203-216, doi:10.1038/nri3818.
16. Klein, J.; Sato, A. The HLA system. *New Engl. J. Med.* 2000, *343*, 702-709.
17. Embgenbroich, M.; Burgdorf, S. Current Concepts of Antigen Cross-Presentation. *Frontiers in Immunology* 2018, *9*, doi:10.3389/fimmu.2018.01643.
18. Joffre, O.P.; Segura, E.; Savina, A.; Amigorena, S. Cross-presentation by dendritic cells. *Nature Reviews Immunology* 2012, *12*, 557-569, doi:10.1038/nri3254.
19. Granucci, F.; Ferrero, E.; Foti, M.; Aggujaro, D.; Vettoretto, K.; Ricciardi-Castagnoli, P. Early events in dendritic cell maturation induced by LPS. *Microb. Infect.* 1999, *1*, 1079-1084.
20. Toebak, M.J.; Gibbs, S.; Bruynzeel, D.P.; Scheper, R.J.; Rustemeyer, T. Dendritic cells: biology of the skin. *Contact Dermatitis* 2009, *60*, 2-20.
21. Sallusto, F.; Schaerli, P.; Loetscher, P.; Schaniel, C.; Lenig, D.; Mackay, C.R.; Qin, S.; Lanzavecchia, A. Rapid and coordinated switch in chemokine receptor expression during dendritic cell maturation. *Eur. J. Immunol.* 1998, *28*, 2760-2769, doi:10.1002/(sici)1521-4141(199809)28:09<2760::Aid-immu2760>3.0.Co;2-n.
22. Tiberio, L.; Del Prete, A.; Schioppa, T.; Sozio, F.; Bosisio, D.; Sozzani, S. Chemokine and chemotactic signals in dendritic cell migration. *Cell Mol Immunol* 2018, *15*, 346-352, doi:10.1038/s41423-018-0005-3.
23. Kabashima, K.; Shiraishi, N.; Sugita, K.; Mori, T.; Onoue, A.; Kobayashi, M.; Sakabe, J.; Yoshiki, R.; Tamamura, H.; Fujii, N.; et al. CXCL12-CXCR4 engagement is required for migration of cutaneous dendritic cells. *Am J Pathol* 2007, *171*, 1249-1257, doi:10.2353/ajpath.2007.070225.
24. Ouwehand, K.; Santegoets, S.J.; Bruynzeel, D.P.; Scheper, R.J.; de Gruijl, T.D.; Gibbs, S. CXCL12 is essential for migration of activated Langerhans cells from epidermis to dermis. *Eur. J. Immunol.* 2008, *38*, 3050-3059, doi:10.1002/eji.200838384.
25. Förster, R.; Schubel, A.; Breitfeld, D.; Kremmer, E.; Renner-Müller, I.; Wolf, E.; Lipp, M. CCR7 coordinates the primary immune response by establishing functional microenvironments in secondary lymphoid organs. *Cell* 1999, *99*, 23-33.
26. Saeki, H.; Moore, A.M.; Brown, M.J.; Hwang, S.T. Cutting edge: secondary lymphoid-tissue chemokine (SLC) and CC chemokine receptor 7 (CCR7) participate in the

emigration pathway of mature dendritic cells from the skin to regional lymph nodes. *The Journal of Immunology* 1999, *162*, 2472-2475.

27. Braun, A.; Worbs, T.; Moschovakis, G.L.; Halle, S.; Hoffmann, K.; Bölter, J.; Münk, A.; Förster, R. Afferent lymph–derived T cells and DCs use different chemokine receptor CCR7–dependent routes for entry into the lymph node and intranodal migration. *Nat. Immunol.* 2011, *12*, 879-887, doi:10.1038/ni.2085.
28. La Gruta, N.L.; Gras, S.; Daley, S.R.; Thomas, P.G.; Rossjohn, J. Understanding the drivers of MHC restriction of T cell receptors. *Nature Reviews Immunology* 2018, *18*, 467-478, doi:10.1038/s41577-018-0007-5.
29. Tai, Y.; Wang, Q.; Korner, H.; Zhang, L.; Wei, W. Molecular mechanisms of T cells activation by dendritic cells in autoimmune diseases. *Frontiers in pharmacology* 2018, *9*, 642.
30. Lim, T.S.; Goh, J.K.H.; Mortellaro, A.; Lim, C.T.; Hämmerling, G.J.; Ricciardi-Castagnoli, P. CD80 and CD86 Differentially Regulate Mechanical Interactions of T-Cells with Antigen-Presenting Dendritic Cells and B-Cells. *PLOS ONE* 2012, *7*, e45185, doi:10.1371/journal.pone.0045185.
31. Parameswaran, N.; Suresh, R.; Bal, V.; Rath, S.; George, A. Lack of ICAM-1 on APCs during T Cell Priming Leads to Poor Generation of Central Memory Cells. *The Journal of Immunology* 2005, *175*, 2201, doi:10.4049/jimmunol.175.4.2201.
32. Dustin, M.L.; Tseng, S.-Y.; Varma, R.; Campi, G. T cell–dendritic cell immunological synapses. *Curr. Opin. Immunol.* 2006, *18*, 512-516, doi:https://doi.org/10.1016/j.coi.2006.05.017.
33. Leithner, A.; Altenburger, L.M.; Hauschild, R.; Assen, F.P.; Rottner, K.; Stradal, T.E.B.; Diz-Muñoz, A.; Stein, J.V.; Sixt, M. Dendritic cell actin dynamics control contact duration and priming efficiency at the immunological synapse. *J. Cell Biol.* 2021, *220*, doi:10.1083/jcb.202006081.
34. Dolatkhah, K.; Alizadeh, N.; Mohajjel-Shoja, H.; Abdoli Shadbad, M.; Hajiasgharzadeh, K.; Aghebati-Maleki, L.; Baghbanzadeh, A.; Hosseinkhani, N.; Karim Ahangar, N.; Baradaran, B. B7 immune checkpoint family members as putative therapeutics in autoimmune disease: An updated overview. *International Journal of Rheumatic Diseases* 2022, *25*, 259-271, doi:https://doi.org/10.1111/1756-185X.14273.
35. Sharpe, A.H.; Freeman, G.J. The B7–CD28 superfamily. *Nature Reviews Immunology* 2002, *2*, 116-126, doi:10.1038/nri727.
36. Lanzavecchia, A.; Sallusto, F. Regulation of T cell immunity by dendritic cells. *Cell* 2001, *106*, 263-266.
37. Klein, E.; Koch, S.; Borm, B.; Neumann, J.; Herzog, V.; Koch, N.; Bieber, T. CD83 localization in a recycling compartment of immature human monocyte-derived dendritic cells. *Int. Immunol.* 2005, *17*, 477-487.
38. Cao, W.; Lee, S.H.; Lu, J. CD83 is preformed inside monocytes, macrophages and dendritic cells, but it is only stably expressed on activated dendritic cells. *Biochem. J.* 2005, *385*, 85-93.
39. Fujimoto, Y.; Tu, L.; Miller, A.S.; Bock, C.; Fujimoto, M.; Doyle, C.; Steeber, D.A.; Tedder, T.F. CD83 expression influences CD4+ T cell development in the thymus. *Cell* 2002, *108*, 755-767, doi:10.1016/s0092-8674(02)00673-6.
40. Doebbeler, M.; Koenig, C.; Krzyzak, L.; Seitz, C.; Wild, A.; Ulas, T.; Baßler, K.; Kopelyanskiy, D.; Butterhof, A.; Kuhnt, C.; et al. CD83 expression is essential for Treg cell differentiation and stability. *JCI Insight* 2018, *3*, doi:10.1172/jci.insight.99712.
41. von Rohrscheidt, J.; Petrozziello, E.; Nedjic, J.; Federle, C.; Krzyzak, L.; Ploegh, H.L.; Ishido, S.; Steinkasserer, A.; Klein, L. Thymic CD4 T cell selection requires attenuation of March8-mediated MHCII turnover in cortical epithelial cells through CD83. *J. Exp. Med.* 2016, *213*, 1685-1694.

42. Walseng, E.; Bandola-Simon, J.; Roche, P. The role of transmembrane domains in the March-I-mediated downregulation of MHC-II and CD86. *The Journal of Immunology* 2017, *198*, 146.124.
43. Tze, L.E.; Horikawa, K.; Domaschenz, H.; Howard, D.R.; Roots, C.M.; Rigby, R.J.; Way, D.A.; Ohmura-Hoshino, M.; Ishido, S.; Andoniou, C.E.; et al. CD83 increases MHC II and CD86 on dendritic cells by opposing IL-10-driven MARCH1-mediated ubiquitination and degradation. *J. Exp. Med.* 2011, *208*, 149-165, doi:10.1084/jem.20092203.
44. Bousso, P. T-cell activation by dendritic cells in the lymph node: lessons from the movies. *Nature Reviews Immunology* 2008, *8*, 675-684, doi:10.1038/nri2379.
45. Pasparakis, M.; Haase, I.; Nestle, F.O. Mechanisms regulating skin immunity and inflammation. *Nat. Rev. Immunol.* 2014, *14*, 289-301, doi:10.1038/nri3646.
46. Basketter, D.A.; Kimber, I. Skin sensitization, false positives and false negatives: experience with guinea pig assays. *J. Appl. Toxicol.* 2010, *30*, 381-386, doi:https://doi.org/10.1002/jat.1545.
47. Coutant, K.D.; de Fraissinette, A.B.; Cordier, A.; Ulrich, P. Modulation of the activity of human monocyte-derived dendritic cells by chemical haptens, a metal allergen, and a staphylococcal superantigen. *Toxicol. Sci.* 1999, *52*, 189-198, doi:10.1093/toxsci/52.2.189.
48. Kiertscher, S.M.; Roth, M.D. Human CD14+ leukocytes acquire the phenotype and function of antigen-presenting dendritic cells when cultured in GM-CSF and IL-4. *J. Leukocyte Biol.* 1996, *59*, 208-218.
49. Palucka, K.A.; Taquet, N.; Sanchez-Chapuis, F.; Gluckman, J.C. Dendritic cells as the terminal stage of monocyte differentiation. *The Journal of Immunology* 1998, *160*, 4587-4595.
50. Chapuis, F.; Rosenzwajg, M.; Yagello, M.; Ekman, M.; Biberfeld, P.; Gluckman, J.C. Differentiation of human dendritic cells from monocytes in vitro. *Eur. J. Immunol.* 1997, *27*, 431-441.
51. Chanput, W.; Mes, J.J.; Wichers, H.J. THP-1 cell line: An in vitro cell model for immune modulation approach. *Int. Immunopharmacol.* 2014, *23*, 37-45, doi:https://doi.org/10.1016/j.intimp.2014.08.002.
52. Aiba, S.; Terunuma, A.; Manome, H.; Tagami, H. Dendritic cells differently respond to haptens and irritants by their production of cytokines and expression of co-stimulatory molecules. *Eur. J. Immunol.* 1997, *27*, 3031-3038, doi:https://doi.org/10.1002/eji.1830271141.
53. Ashikaga, T.; Yoshida, Y.; Hirota, M.; Yoneyama, K.; Itagaki, H.; Sakaguchi, H.; Miyazawa, M.; Ito, Y.; Suzuki, H.; Toyoda, H. Development of an in vitro skin sensitization test using human cell lines: The human Cell Line Activation Test (h-CLAT): I. Optimization of the h-CLAT protocol. *Toxicol. In Vitro* 2006, *20*, 767-773, doi:https://doi.org/10.1016/j.tiv.2005.10.012.
54. Ashikaga, T.; Sakaguchi, H.; Sono, S.; Kosaka, N.; Ishikawa, M.; Nukada, Y.; Miyazawa, M.; Ito, Y.; Nishiyama, N.; Itagaki, H. A Comparative Evaluation of In Vitro Skin Sensitisation Tests: The Human Cell-line Activation Test (h-CLAT) versus the Local Lymph Node Assay (LLNA). *Alternatives to Laboratory Animals* 2010, *38*, 275-284, doi:10.1177/026119291003800403.
55. Tsuchiya, S.; Yamabe, M.; Yamaguchi, Y.; Kobayashi, Y.; Konno, T.; Tada, K. Establishment and characterization of a human acute monocytic leukemia cell line (THP-1). *Int J Cancer* 1980, *26*, 171-176, doi:10.1002/ijc.2910260208.
56. Sakaguchi, H.; Ashikaga, T.; Miyazawa, M.; Kosaka, N.; Ito, Y.; Yoneyama, K.; Sono, S.; Itagaki, H.; Toyoda, H.; Suzuki, H. The relationship between CD86/CD54 expression and THP-1 cell viability in an in vitro skin sensitization test--human cell line activation test (h-CLAT). *Cell Biol Toxicol* 2009, *25*, 109-126, doi:10.1007/s10565-008-9059-9.

57. Sakaguchi, H.; Ashikaga, T.; Miyazawa, M.; Yoshida, Y.; Ito, Y.; Yoneyama, K.; Hirota, M.; Itagaki, H.; Toyoda, H.; Suzuki, H. Development of an in vitro skin sensitization test using human cell lines; human Cell Line Activation Test (h-CLAT) II. An inter-laboratory study of the h-CLAT. *Toxicol. In Vitro* 2006, *20*, 774-784, doi:https://doi.org/10.1016/j.tiv.2005.10.014.
58. Centre, J.R.; Health, I.f.; Protection, C. EURL ECVAM recommendation on the human Cell Line Activation Test (h-CLAT) for skin sensitisation testing. , EUR27022. Luxembourg (Luxembourg) Publications Office of the European Union, 2015, doi/10.2788/29986.
59. OECD. Test No. 442E: In Vitro Skin Sensitisation assays addressing the Key Event on activation of dendritic cells on the Adverse Outcome Pathway for Skin Sensitisation, OECD Guidelines for the Testing of Chemicals, Section 4, OECD Publishing, Paris, France . 2022, doi:https://doi.org/10.1787/9789264264359-en.
60. Chary, A.; Serchi, T.; Moschini, E.; Hennen, J.; Cambier, S.; Ezendam, J.; Blömeke, B.; Gutleb, A.C. An in vitro coculture system for the detection of sensitization following aerosol exposure. *ALTEX-Alternatives to animal experimentation* 2019, *36*, 403-418.
61. Scheurlen, K.M.; Snook, D.L.; Gardner, S.A.; Eichenberger, M.R.; Galandiuk, S. Macrophage differentiation and polarization into an M2-like phenotype using a human monocyte-like THP-1 leukemia cell line. *JoVE (Journal of Visualized Experiments)* 2021, e62652. doi: 10.3791/62652
62. Berges, C.; Naujokat, C.; Tinapp, S.; Wieczorek, H.; Höh, A.; Sadeghi, M.; Opelz, G.; Daniel, V. A cell line model for the differentiation of human dendritic cells. *Biochem. Biophys. Res. Commun.* 2005, *333*, 896-907, doi:10.1016/j.bbrc.2005.05.171.
63. Larsson, K.; Lindstedt, M.; Borrebaeck, C.A.K. Functional and transcriptional profiling of MUTZ-3, a myeloid cell line acting as a model for dendritic cells. *Immunology* 2006, *117*, 156-166, doi:https://doi.org/10.1111/j.1365-2567.2005.02274.x.
64. Czernek, L.; Chworos, A.; Duechler, M. The Uptake of Extracellular Vesicles is Affected by the Differentiation Status of Myeloid Cells. *Scand. J. Immunol.* 2015, *82*, 506-514, doi:https://doi.org/10.1111/sji.12371.
65. Galbiati, V.; Marinovich, M.; Corsini, E. Mechanistic understanding of dendritic cell activation in skin sensitization: additional evidences to support potency classification. *Toxicol. Lett.* 2020, *322*, 50-57, doi:https://doi.org/10.1016/j.toxlet.2020.01.014.
66. Ogasawara, N.; Kojima, T.; Go, M.; Fuchimoto, J.; Kamekura, R.; Koizumi, J.-i.; Ohkuni, T.; Masaki, T.; Murata, M.; Tanaka, S.; et al. Induction of JAM-A during differentiation of human THP-1 dendritic cells. *Biochem. Biophys. Res. Commun.* 2009, *389*, 543-549, doi:https://doi.org/10.1016/j.bbrc.2009.09.024.
67. Yang, Z.; Xiong, H.-R. Culture conditions and types of growth media for mammalian cells. *Biomedical Tissue Culture* 2012, *1*, 3-18.
68. Wu, X.; Lin, M.; Li, Y.; Zhao, X.; Yan, F. Effects of DMEM and RPMI 1640 on the biological behavior of dog periosteum-derived cells. *Cytotechnology* 2009, *59*, 103-111, doi:10.1007/s10616-009-9200-5.
69. Arora, M. Cell culture media: a review. *Mater methods* 2013, *3*, 24.
70. Yao, T.; Asayama, Y. Animal-cell culture media: History, characteristics, and current issues. *Reproductive medicine and biology* 2017, *16*, 99-117.
71. Chometon, T.Q.; Siqueira, M.d.S.; Sant´ anna, J.C.; Almeida, M.R.; Gandini, M.; Martins de Almeida Nogueira, A.C.; Antas, P.R.Z. A protocol for rapid monocyte isolation and generation of singular human monocyte-derived dendritic cells. *PLoS One* 2020, *15*, e0231132.
72. Lenschow, D.J.; and, T.L.W.; Bluestone, J.A. CD28/B7 SYSTEM OF T CELL COSTIMULATION. *Annu. Rev. Immunol.* 1996, *14*, 233-258, doi:10.1146/annurev.immunol.14.1.233.

73. Chen, J.; Namiki, S.; Toma-Hirano, M.; Miyatake, S.; Ishida, K.; Shibata, Y.; Arai, N.; Arai, K.; Kamogawa-Schifter, Y. The role of CD11b in phagocytosis and dendritic cell development. *Immunol. Lett.* 2008, *120*, 42-48, doi:10.1016/j.imlet.2008.06.010.
74. Pinet, V.; Vergelli, M.; Martini, R.; Bakke, O.; Long, E.O. Antigen presentation mediated by recycling of surface HLA-DR molecules. *Nature* 1995, *375*, 603-606.
75. Lechmann, M.; Berchtold, S.; Steinkasserer, A.; Hauber, J. CD83 on dendritic cells: more than just a marker for maturation. *Trends Immunol.* 2002, *23*, 273-275.
76. Zou, Y.-R.; Kottmann, A.H.; Kuroda, M.; Taniuchi, I.; Littman, D.R. Function of the chemokine receptor CXCR4 in haematopoiesis and in cerebellar development. *Nature* 1998, *393*, 595-599, doi:10.1038/31269.
77. Ratajczak, M.Z.; Kucia, M.; Reca, R.; Majka, M.; Janowska-Wieczorek, A.; Ratajczak, J. Stem cell plasticity revisited: CXCR4-positive cells expressing mRNA for early muscle, liver and neural cells 'hide out' in the bone marrow. *Leukemia* 2004, *18*, 29-40, doi:10.1038/sj.leu.2403184.
78. Pituch-Noworolska, A.; Majka, M.; Janowska-Wieczorek, A.; Baj-Krzyworzeka, M.; Urbanowicz, B.; Malec, E.; Ratajczak, M.Z. Circulating CXCR4-positive stem/progenitor cells compete for SDF-1-positive niches in bone marrow, muscle and neural tissues: an alternative hypothesis to stem cell plasticity. *Folia histochemica et cytobiologica* 2003, *41*, 13-21.
79. Pablos, J.L.; Amara, A.; Bouloc, A.; Santiago, B.; Caruz, A.; Galindo, M.; Delaunay, T.; Virelizier, J.L.; Arenzana-Seisdedos, F. Stromal-Cell Derived Factor Is Expressed by Dendritic Cells and Endothelium in Human Skin. *The American Journal of Pathology* 1999, *155*, 1577-1586, doi:https://doi.org/10.1016/S0002-9440(10)65474-0.
80. Ceradini, D.J.; Kulkarni, A.R.; Callaghan, M.J.; Tepper, O.M.; Bastidas, N.; Kleinman, M.E.; Capla, J.M.; Galiano, R.D.; Levine, J.P.; Gurtner, G.C. Progenitor cell trafficking is regulated by hypoxic gradients through HIF-1 induction of SDF-1. *Nat. Med.* 2004, *10*, 858-864, doi:10.1038/nm1075.
81. Minami, H.; Nagaharu, K.; Nakamori, Y.; Ohishi, K.; Shimojo, N.; Kageyama, Y.; Matsumoto, T.; Sugimoto, Y.; Tawara, I.; Masuya, M.; et al. CXCL12–CXCR4 Axis Is Required for Contact-Mediated Human B Lymphoid and Plasmacytoid Dendritic Cell Differentiation but Not T Lymphoid Generation. *The Journal of Immunology* 2017, *199*, 2343-2355, doi:10.4049/jimmunol.1700054.
82. Umemoto, E.; Otani, K.; Ikeno, T.; Verjan Garcia, N.; Hayasaka, H.; Bai, Z.; Jang, M.H.; Tanaka, T.; Nagasawa, T.; Ueda, K.; et al. Constitutive Plasmacytoid Dendritic Cell Migration to the Splenic White Pulp Is Cooperatively Regulated by CCR7- and CXCR4-Mediated Signaling. *The Journal of Immunology* 2012, *189*, 191-199, doi:10.4049/jimmunol.1200802.
83. Delgado, E.; Finkel, V.; Baggiolini, M.; Mackay, C.R.; Steinman, R.M.; Granelli-Piperno, A. Mature Dendritic Cells Respond to SDF-1, but not to Several β-Chemokines. *Immunobiology* 1998, *198*, 490-500, doi:https://doi.org/10.1016/S0171-2985(98)80073-9.
84. Ricart, B.G.; John, B.; Lee, D.; Hunter, C.A.; Hammer, D.A. Dendritic Cells Distinguish Individual Chemokine Signals through CCR7 and CXCR4. *The Journal of Immunology* 2011, *186*, 53-61, doi:10.4049/jimmunol.1002358.
85. Bleul, C.C.; Wu, L.; Hoxie, J.A.; Springer, T.A.; Mackay, C.R. The HIV coreceptors CXCR4 and CCR5 are differentially expressed and regulated on human T lymphocytes. *Proc Natl Acad Sci U S A* 1997, *94*, 1925-1930, doi:10.1073/pnas.94.5.1925.
86. Nukada, Y.; Ashikaga, T.; Sakaguchi, H.; Sono, S.; Mugita, N.; Hirota, M.; Miyazawa, M.; Ito, Y.; Sasa, H.; Nishiyama, N. Predictive performance for human skin sensitizing potential of the human cell line activation test (h-CLAT). *Contact dermatitis* 2011, *65*, 343-353.
87. Takenouchi, O.; Miyazawa, M.; Saito, K.; Ashikaga, T.; Sakaguchi, H. Predictive performance of the human Cell Line Activation Test (h-CLAT) for lipophilic chemicals

with high octanol-water partition coefficients. *J Toxicol Sci* 2013, *38*, 599-609, doi:10.2131/jts.38.599.

88. Alloatti, A.; Kotsias, F.; Magalhaes, J.G.; Amigorena, S. Dendritic cell maturation and cross-presentation: timing matters! *Immunol. Rev.* 2016, *272*, 97-108.
89. Takahashi, M.; Kobayashi, Y. Cytokine production in association with phagocytosis of apoptotic cells by immature dendritic cells. *Cell. Immunol.* 2003, *226*, 105-115, doi:https://doi.org/10.1016/j.cellimm.2003.11.008.
90. Xia, H.; Wang, Y.; Dai, J.; Zhang, X.; Zhou, J.; Zeng, Z.; Jia, Y. Selenoprotein K Is Essential for the Migration and Phagocytosis of Immature Dendritic Cells. *Antioxidants* 2022, *11*, 1264.
91. Kiama, S.; Cochand, L.; Karlsson, L.; Nicod, L.; Gehr, P. Evaluation of phagocytic activity in human monocyte-derived dendritic cells. *Journal of aerosol medicine* 2001, *14*, 289-299.
92. Tait Wojno, E.D.; Hunter, C.A.; Stumhofer, J.S. The Immunobiology of the Interleukin-12 Family: Room for Discovery. *Immunity* 2019, *50*, 851-870, doi:https://doi.org/10.1016/j.immuni.2019.03.011.
93. Riemann, H.; Schwarz, A.; Grabbe, S.; Aragane, Y.; Luger, T.A.; Wysocka, M.; Kubin, M.; Trinchieri, G.; Schwarz, T. Neutralization of IL-12 in vivo prevents induction of contact hypersensitivity and induces hapten-specific tolerance. *J. Immunol.* 1996, *156*, 1799-1803.
94. Ade, N.; Antonios, D.; Kerdine-Romer, S.; Boisleve, F.; Rousset, F.; Pallardy, M. NF-κB Plays a Major Role in the Maturation of Human Dendritic Cells Induced by NiSO4 but not by DNCB. *Toxicol. Sci.* 2007, *99*, 488-501, doi:10.1093/toxsci/kfm178.
95. Antonios, D.; Rousseau, P.; Larangé, A.; Kerdine-Römer, S.; Pallardy, M. Mechanisms of IL-12 Synthesis by Human Dendritic Cells Treated with the Chemical Sensitizer NiSO4. *The Journal of Immunology* 2010, *185*, 89-98, doi:10.4049/jimmunol.0901992.
96. Aiba, S.; Manome, H.; Nakagawa, S.; Mollah, Z.U.A.; Mizuashi, M.; Ohtani, T.; Yoshino, Y.; Tagami, H. p38 Mitogen-activated Protein Kinase and Extracellular Signal-regulated Kinases Play Distinct Roles in the Activation of Dendritic Cells by Two Representative Haptens, NiCl2 and 2,4-dinitrochlorobenzene. *Journal of Investigative Dermatology* 2003, *120*, 390-399, doi:https://doi.org/10.1046/j.1523-1747.2003.12065.x.
97. Hayashi, M.; Higashi, K.; Kato, H.; Kaneko, H. Assessment of Preferential Th1 or Th2 Induction by Low-Molecular-Weight Compounds Using a Reverse Transcription–Polymerase Chain Reaction Method: Comparison of Two Mouse Strains, C57BL/6 and Balb/c. *Toxicol. Appl. Pharmacol.* 2001, *177*, 38-45, doi:https://doi.org/10.1006/taap.2001.9286.
98. Warbrick, E.V.; Dearman, R.J.; Basketter, D.A.; Kimber, I. Analysis of interleukin 12 protein production and mRNA expression in mice exposed topically to chemical allergens. *Toxicology* 1999, *132*, 57-66, doi:https://doi.org/10.1016/S0300-483X(98)00137-1.
99. Xu, B.; Aoyama, K.; Kitani, A.; Matsuyama, T.; Matsushita, T. RT-PCR analysis of in vivo cytokine profiles in murine allergic contact dermatitis to DNCB. *Toxicology Methods* 1996, *6*, 23-31.
100. Sándor, N.; Kristóf, K.; Paréj, K.; Pap, D.; Erdei, A.; Bajtay, Z. CR3 is the dominant phagocytotic complement receptor on human dendritic cells. *Immunobiology* 2013, *218*, 652-663.
101. Li, Z.; Ju, X.; Silveira, P.A.; Abadir, E.; Hsu, W.-H.; Hart, D.N.; Clark, G.J. CD83: activation marker for antigen presenting cells and its therapeutic potential. *Frontiers in immunology* 2019, *10*, 1312.
102. Zgraggen, S.; Huggenberger, R.; Kerl, K.; Detmar, M. An important role of the SDF-1/CXCR4 axis in chronic skin inflammation. *PloS one* 2014, *9*, e93665.

103. Gallego, C.; Vétillard, M.; Calmette, J.; Roriz, M.; Marin-Esteban, V.; Evrard, M.; Aknin, M.-L.; Pionnier, N.; Lefrançois, M.; Mercier-Nomé, F. CXCR4 signaling controls dendritic cell location and activation at steady state and in inflammation. *Blood* 2021, *137*, 2770-2784.
104. Enk, A.H.; Jonuleit, H.; Saloga, J.; Knop, J. Dendritic cells as mediators of tumor-induced tolerance in metastatic melanoma. *Int. J. Cancer* 1997, *73*, 309-316.
105. Kim, C.W.; Kim, K.-D.; Lee, H.K. The role of dendritic cells in tumor microenvironments and their uses as therapeutic targets. *BMB reports* 2021, *54*, 31

2.2 A human 3D immune competent full-thickness skin model mimicking dermal dendritic cell activation

Johanna Maria Hölken[1], Katja Friedrich[1], Marion Merkel[2], Nelli Blasius[2], Ursula Engels[2], Timo Buhl[3], Karsten Rüdiger Mewes[2], Lars Vierkotten[2] and Nicole Elisabeth Teusch[1]

[1]Institute of Pharmaceutical Biology and Biotechnology, Heinrich-Heine University Düsseldorf, Düsseldorf, Germany

[2]Alternative Methods and Tissue Engineering, Henkel AG & Co. KGaA, Düsseldorf, Germany

[3]Department of Dermatology, Venereology and Allergology, University Medical Center Göttingen, Göttingen, Germany

Published in: *Frontiers in Immunology*
Hölken, J.M.; Friedrich, K.; Merkel, M.; Blasius, N.; Engels, U.; Buhl T.; Mewes, K.R.; Vierkotten, L. and Teusch, N.E. A human 3D immune competent full-thickness skin model mimicking dermal dendritic cell activation. Front. Immunol. 2023, 14:1276151.
doi: 10.3389/fimmu.2023.1276151

Keywords: full-thickness skin model, dermal dendritic cell, nickel, DNCB, CD86, p38 MAPK, NF-κB

Own contributions to the manuscript: 80%

- Conceptualization of the experiments (50%) together with Nicole Teusch
- Methodology (100%), Investigation (85%), Validation (100%), Data curation (100%), Formal analysis (100%) and Visualization (98%)
- Investigation of the following experiments:
    - Surface marker characterization of DDCs +/- sensitizer/drug treatment (100%)
    - Western Blots to determine the sensitizer-induced activation of the NF-κB and p38 MAPK pathway (100%)
    - qPCR and to determine the sensitizer-induced mRNA levels of (pro-) inflammatory cytokines (70%) together with Katja Friedrich
    - BCA assay to determine the sensitizer-induced (+/- Dex) cytokine secretion of (pro)-inflammatory cytokines (100%)
    - Engineering of the DDC models (80%) together with Katja Friedrich
    - Cryosectioning and IF-staining of the skin models (70%) together with Katja Friedrich
    - Imaging of the immunofluorescent stained tissue slides (100%)
    - IF-staining and imaging of the DDCs (100%)
    - Enzymatic dissociation of the skin models (50%) together with Katja Friedrich,
    - Surface marker characterization before and after topical sensitizer/drug treatment of the DDC models (100%)
- Writing and drafting the manuscript (100%)

Abstract

We have integrated dermal dendritic cell surrogates originally generated from the cell line THP-1 as central mediators of the immune reaction in a human full- thickness skin model. Accordingly, sensitizer treatment of THP-1-derived $CD14^-$, $CD11c^+$ immature dendritic cells (iDCs) resulted in the phosphorylation of p38 MAPK in the presence of 1-chloro-2,4-dinitrobenzene (DNCB) (2.6-fold) as well as in degradation of the inhibitor protein kappa B alpha (IκBα) upon incubation with $NiSO_4$ (1.6-fold). Furthermore, $NiSO_4$ led to an increase in mRNA levels of IL-6 (2.4-fold), TNF-α (2-fold) and of IL-8 (15-fold). These results were confirmed on the protein level, with even stronger effects on cytokine release in the presence of $NiSO_4$: Cytokine secretion was significantly increased for IL-8 (147-fold), IL-6 (11.8-fold) and IL-1β (28.8-fold). Notably, DNCB treatment revealed an increase for IL-8 (28.6-fold) and IL-1β (5.6-fold). Importantly, $NiSO_4$ treatment of isolated iDCs as well as of iDCs integrated as dermal dendritic cell surrogates into our full-thickness skin model (SM) induced the upregulation of the adhesion molecule clusters of differentiation (CD)54 (iDCs: 1.2-fold; SM: 1.3-fold) and the co-stimulatory molecule and DC maturation marker CD86 (iDCs: ~1.4-fold; SM: ~1.5-fold) surface marker expression. Noteworthy, the expression of CD54 and CD86 could be suppressed by dexamethasone treatment on isolated iDCs (CD54: 1.3-fold; CD86: 2.1-fold) as well as on the tissue-integrated iDCs (CD54: 1.4-fold; CD86: 1.6-fold). In conclusion, we were able to integrate THP-1-derived iDCs as functional dermal dendritic cell surrogates allowing the qualitative identification of potential sensitizers on the one hand, and drug candidates that potentially suppress sensitization on the other hand in a 3D human skin model corresponding to the 3R principles (“replace”, “reduce” and “refine”)

Introduction

Immune responses in the skin are mediated by antigen-presenting cells (APCs) such as macrophages, monocytes and most importantly dendritic cells [1]. Cutaneous dendritic cells include epidermal Langerhans cells (LCs) and dermal dendritic cells (DDCs), located beneath the epidermal-dermal junction and throughout the dermis [2]. While Langerhans cells are characterized by the expression of Langerin [3], to date, no specific marker exclusively expressed on all dermal dendritic subsets has been reported. However, dermal dendritic cells can be identified and distinguished from dermal monocytes and macrophages by a low CD14 expression and a high CD11c expression [4, 5]. Yet, the primary and common function of all cutaneous dendritic cell subsets includes endocytosis/phagocytosis, processing and presenting antigens to naïve T cells [6].

The activation of cutaneous dendritic cells can be divided into different central events (Figure 2.2-1): Upon exposure to inflammatory stimuli like interleukin (IL)-1β, lipopolysaccharide (LPS) or sensitizing agents such as 1 chloro-2,4-dinitrobenzene (DNCB) or nickel sulfate ($NiSO_4$), keratinocytes start to secrete a variety of cytokines including IL-1, TNF-α or IL-18 [79]. Consequently, cutaneous dendritic cells such as Langerhans cells and dermal dendritic cells become activated and start to phagocytose the hapten accompanied by cell maturation and the upregulation of adhesion molecules, such as clusters of differentiation (CD)54 and co-stimulatory molecules including CD80 and CD86 [10, 11]. Upregulation of the intracellular adhesion molecule (ICAM-1)/ CD54 is required to form a stable signaling structure, the so-called immunological synapse (IS) with the leukocyte function-associated antigen 1 (LFA-1) alpha (CD11a) and beta-2 (CD18) in naïve $CD4^+$ T cells [12]. High expressions of CD80 (B71) and CD86 (B7-2) finally ensure the co-stimulation of naïve $CD4^+$ T cells via their CD28 and cytotoxic T-lymphocyte-associated protein 4 (CTLA-4)/(CD152) receptors [13].

Regarding the underlying intracellular signal transduction, different studies with cord blood derived DCs as well as PBMC derived DCs were able to prove the central role of the mitogen-activated protein kinases (MAPK) pathway and the nuclear factor (NF)-κB pathway in skin sensitization and dendritic cell activation [14–16]. Inhibition of the p38 MAPK pathway inhibited the upregulation of the DC maturation markers CD80, CD86 and CD83 in PBMC derived DCs [16]. In addition, the up-regulation and secretion of IL-1, IL-8 and tumor necrosis factor (TNF)-α was suppressed [15, 16]. Inhibition of the NF-κB pathway resulted in a downregulation of CD86 and CD83 and abolished the secretion of IL-8, IL-6 and IL-12p40 in cord blood derived DCs [14]. While IL-8 functions as a chemotactic for neutrophils and T cells (17, 18), IL-6 is considered as a pleiotropic cytokine involved in DC maturation, T cell differentiation and proliferation as well as in B cell activation [19]. TNF-α induces the expression of adhesion molecules such as vascular endothelial cell adhesion molecule (VCAM)-1 and ICAM-1 as well as T cell infiltration into the skin [20]. IL-1 induces the expression of adhesion molecules on endothelial cells, promotes T cell priming, causes vasodilatation and hypotension [21, 22]. Finally, secretion of IL-12 leads to upregulation of the transcription factor T-box expressed in T cells (T-bet) promoting T cell differentiation into interferon-γ producing T helper 1 cells (Th1) [23, 24].

In the past decades, dendritic cell activation, toxicological assessment studies, as well as studies investigating pathophysiological pathways of inflammatory skin diseases have been conducted almost exclusively in animal models, mostly in mice. However, when compared to the situation in humans, species-specific differences in the anatomy, immune cell populations, especially in DC subsets, and pathophysiology are tremendous [25]. Furthermore, humans and mice have only ~ 30% of skin-associated genes in common [26], which impairs the translation from mouse models to human skin diseases. Admittedly, human *ex vivo* skin explants are a valuable tool for research; however, they are limited by ethical approval, logistics and high donor and

anatomic site variation [27–29]. Hence, there is an urgent need for alternative predictive human *in vitro* models.

Immune competent skin models reported to date focus mostly on the integration of Langerhans cell surrogates either derived from the human myeloid leukemia-derived cell line Mutz-3 [30, 35], originated from cord-blood derived $CD34^+$ hematopoietic progenitor [36, 37] or generated from $CD14^+$ peripheral blood mononuclear cells [32]. Notably, only one full-thickness skin equivalent has been described containing LC and DDC surrogates derived from $CD14^+$ monocytes isolated from peripheral blood mononuclear cells aiming at analyzing the impact of ultraviolet (UV) stress on skin immune cells [38]. However, no immune competent human full-thickness model with integrated functional dermal dendritic cells for sensitizer or drug analysis has been described so far. This is surprising as several studies have indicated the crucial role of DDC for antigen presentation in the skin. For instance, after sensitizer treatment dermal dendritic cells might migrate and activate T cells faster and outnumber LCs by 10:1 in draining lymph nodes [39, 40]. Furthermore, DDCs might be able to induce a stronger T cell proliferation than LCs [39].

Our previously published results showed that the human monocytic cell line THP-1 can be differentiated into immature dendritic cells (iDCs), displaying a sufficient ability and sensitivity to robustly identify classified proficiency chemicals and model sensitizers such as DNCB and $NiSO_4$ *in vitro*. Furthermore, as expected from antigen presenting cells, THP-1-originated iDCs have proven to phagocytose membrane components derived from pathogens such as zymosan and, finally, iDCs might be able to induce T cell activation via upregulation of IL-12p40 upon sensitizer treatment [41]. Since THP-1-derived iDCs fulfill all required *in vitro* criteria, we aim to demonstrate in this study the functionality of stably integrated iDCs as dermal dendritic cell surrogates within a human full-thickness skin model and their subsequent molecular characterization before and after sensitizer treatment.

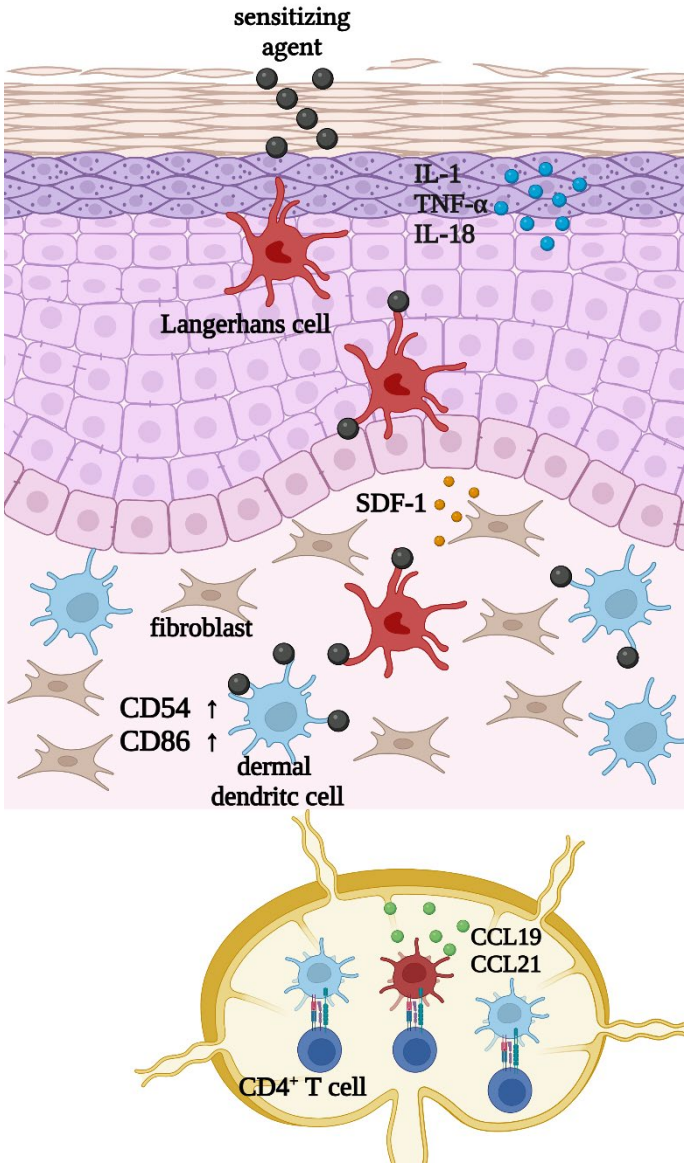

Figure 2.2-1 Upon exposure to inflammatory stimuli such as LPS, or sensitizing chemicals such as 1 chloro-2,4-dinitrobenzene (DNCB) or nickel sulfate ($NiSO_4$), keratinocytes start to secrete inflammatory cytokines such as IL-1, TNF-α and IL-18. Subsequently cutaneous dendritic cells such as Langerhans cells and dermal dendritic cells become activated and start to phagocytose haptens or exogenous particles, which is accompanied by cell maturation and the upregulation of CD54 and CD86. Finally, DCs migrate to draining lymph nodes to present the processed antigen in order to activate $CD4^+$ T cells. Created with BioRender.com.

Results

When compared to original THP-1 cells our recent study confirmed the expected pronounced ability of THP-1-derived iDCs to phagocytose pathogen membrane particles such as zymosan. Furthermore, iDCs, but not undifferentiated THP-1 cells, are able to induce T cell activation via upregulation of IL-12p40 upon sensitizer treatment [41]. Thus, a logical subsequent step is to prove whether the iDCs might be suitable surrogates for dermal dendritic cells. Firstly, the expression of CD11c, which is known to be highly expressed on dermal dendritic cells, and the absence of CD14, a marker for monocytic cells and often used to distinguish DCs from

monocytes and macrophages, was investigated. While undifferentiated THP-1 cells, as well as THP-1-derived iDCs express almost no CD14, both express CD11c. However, the expression of CD11c is significantly higher (~1.3-fold) on THP-1-derived iDCs compared to THP-1 cells (Figures 2.2-2A, C). Hence, our iDCs might be suitable $CD14^-$, $CD11c^+$ dermal dendritic cell surrogates for the integration into a full-thickness skin model.

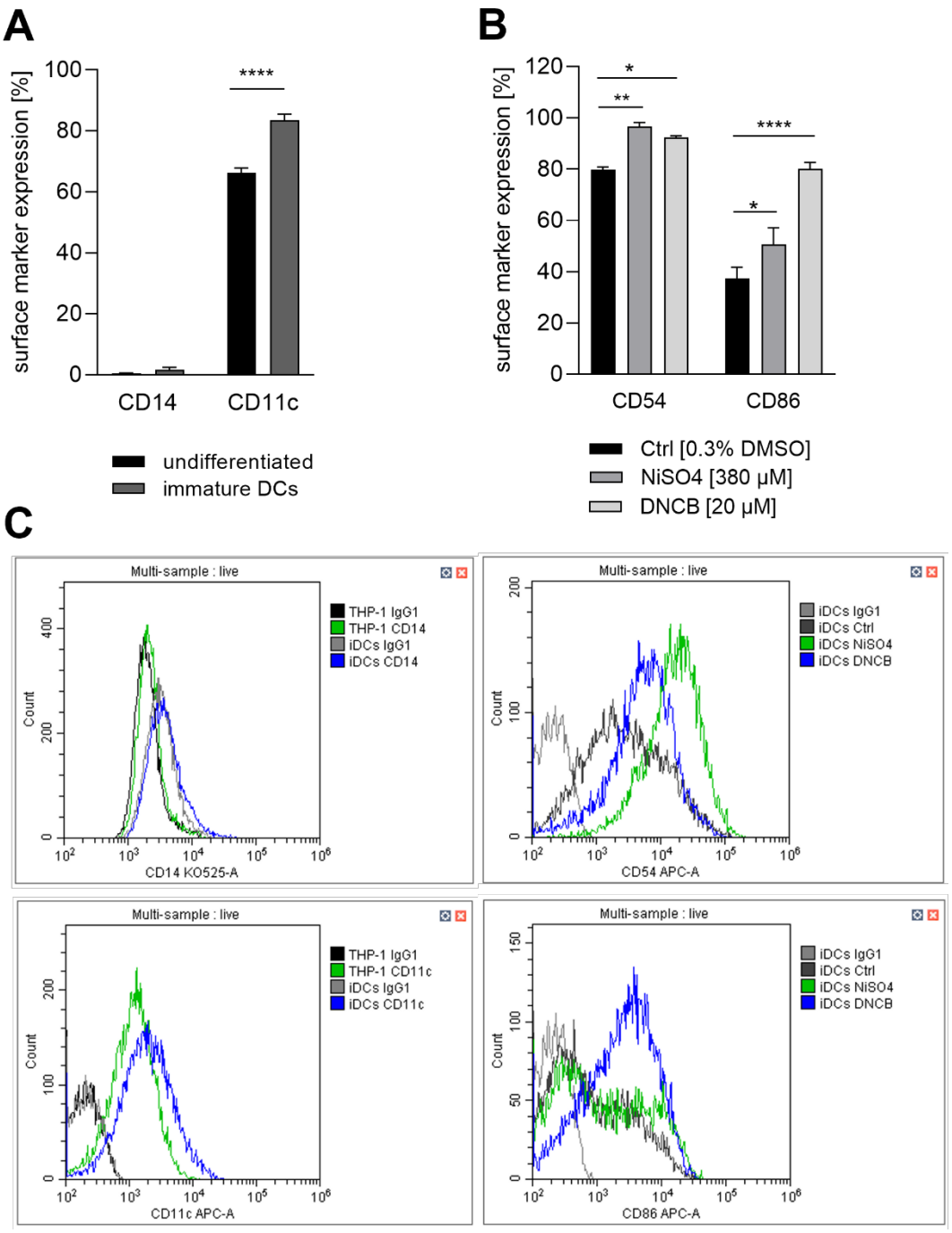

Figure 2.2-2 (A) CD14 and CD11c surface marker expression of the undifferentiated THP-1 cell line and THP-1-derived iDCs. Here, THP-1 cells were differentiated with 1500 U/ml GM-CSF and 1500 U/ml IL-4 for 5 days, with medium exchange on day 3. **(B)** iDCs were treated with $NiSO_4$ [380 µM] and DNCB [20 µM] for 23 h. **(C)** Gating strategy. Surface marker expression (depicted as percentage of positive cells) of at least 10,000 viable cells was analyzed via flow cytometry. Error bars indicate the standard errors of the mean (n = 3 independent experiments with *p ≤ 0.05 and ****p ≤ 0.0001).

Dendritic cell activation and maturation is characterized by the upregulation of adhesion molecules like CD54 and co-stimulatory molecules and DC maturation markers such as CD86, which are both required for the stimulation of T cells. As expected, treatment of iDCs with $NiSO_4$ led to a significantly higher expression of CD54 (~97%) and CD86 (~51%) while DNCB also resulted in a significantly upregulation of CD54 (~93%) and an even higher expression of CD86 (~80%) compared to the solvent control (CD54: ~80%, CD86: ~37%) (Figures 2.2-2B,C). Furthermore, a few studies demonstrated the activation of the NF-κB pathway in the presence of nickel salts [14, 15]. In contrast, for DNCB a phosphorylation of p38 MAPK in DC surrogates was shown [14–16]. Moreover, it was proven that both pathways are required for the upregulation of DC activation markers and the subsequent secretion of inflammatory cytokines such as IL-8, IL-6, IL-1 or TNF-α [14–16]. We therefore investigated the activation of these pathways as well as the expression of inflammatory cytokines. Treatment of iDCs with 500 µM $NiSO_4$ led to significant reduction (1.6-fold) of the inhibitor protein kappa B alpha (IκBα) expression, but (according to previously reported studies) no significant phosphorylation of p38 MAPK could be detected. Contrary, DNCB [25 µM] treatment led to a significant phosphorylation of p38 MAPK (2.6-fold), but no degradation of IκBα (Figure 2.2-3).

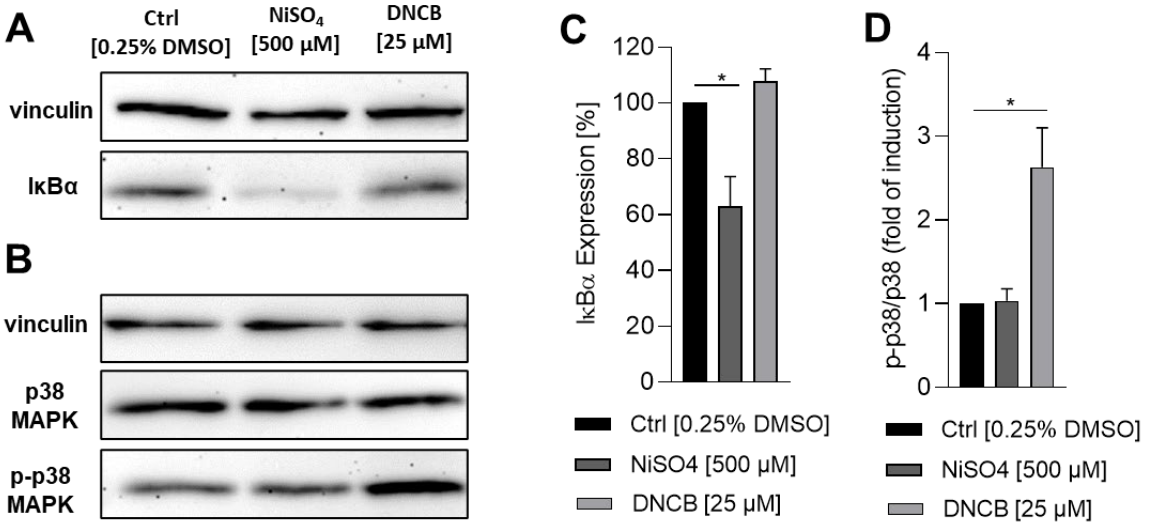

Figure 2.2-3 Activation of inflammatory pathways in iDCs after sensitizer treatment. **(A, C)** Degradation of IκBα after $NiSO_4$ [500 µM] and DNCB [25 µM] treatment for 1 h, respectively. **(B, D)** Phosphorylation of p38 MAPK after $NiSO_4$ [500 µM] and DNCB [25 µM] treatment for 30 min. **(A, B)** Depict one representative blot of three independent experiments. The housekeeping gene vinculin serves as a loading control. **(C, D)** Show the quantification of image bands normalized to the solvent control. Error bars indicate the standard errors of the mean (n = 3 independent experiments with *$p \leq 0.05$).

In order to prove whether our iDCs are able to up-regulate the expression and to secrete inflammatory cytokines after sensitizer treatment similar to previously reported DC surrogates from various sources, mRNA levels of the inflammatory cytokines IL-8, IL-6 and TNF-α were analyzed. Treatment of iDCs with $NiSO_4$ [380 µM] for 6 h induced significant upregulation of

mRNA levels for IL- 8 (~15-fold), IL-6 (~2.4-fold) and TNF-α (~2-fold). DNCB [20 µM] treatment led to significantly higher IL-8 mRNA levels (17-fold), but no significant upregulation of IL-6 and contrary to $NiSO_4$ treatment, significant reduction of TNF-α mRNA levels (0.2-fold) (Figure 2.2-4).

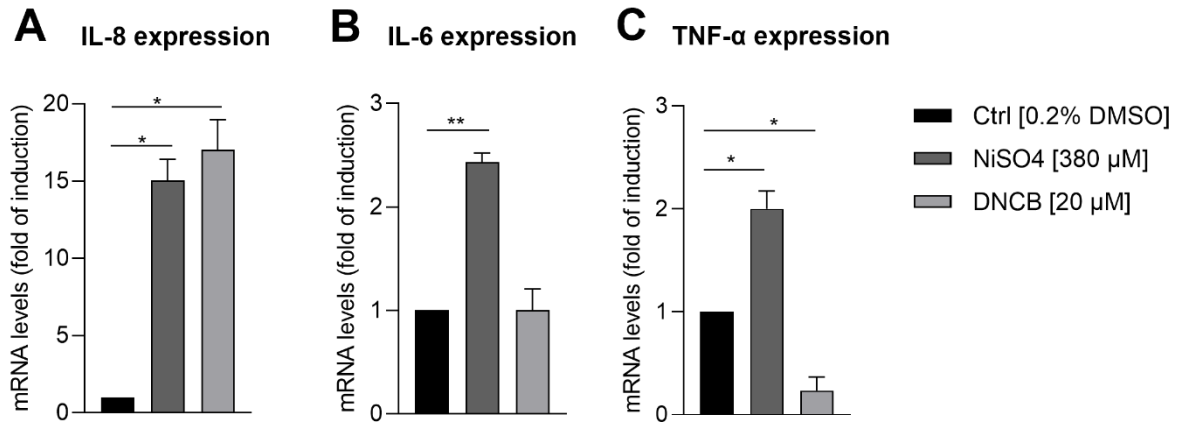

Figure 2.2-4 mRNA levels of inflammatory cytokine expression by iDCs: (A) IL-8, (B) IL-6, (C) TNF-α, after $NiSO_4$ [380 µM] and DNCB treatment [20 µM] for 6 h. Results are depicted as fold of induction compared to the solvent control [0.2% DMSO] and normalized to the expression of the housekeeping gene [GAPDH]. Error bars indicate the standard errors of the mean (n = 3 independent experiments with *p ≤ 0.05, **p ≤ 0.01).

To confirm the mRNA results on the protein level, iDCs were treated for 24 h with 380 µM $NiSO_4$ or 20 µM DNCB and the absolute cytokine concentration was determined via a Multiplexing Cytometric Bead Array Assay. Treatment of iDCs with $NiSO_4$ induced the secretion of ~17,000 pg/ml IL-8, ~20 pg/ml IL-6, ~30 pg/ml IL-1β and ~7 pg/ml TNF-α, respectively, while DNCB treatment induced the secretion of ~3376 pg/ml IL-8 and ~5.8 pg/ml IL-1β. Secretion of IL-6 and TNF-α could not be detected after DNCB treatment (Figure 2.2-5). Overall, upon sensitizer treatment THP-1-derived iDCs are able to secrete inflammatory cytokines relevant for the activation and recruitment of T cells in the skin, although in different patterns depending on the applied sensitizers.

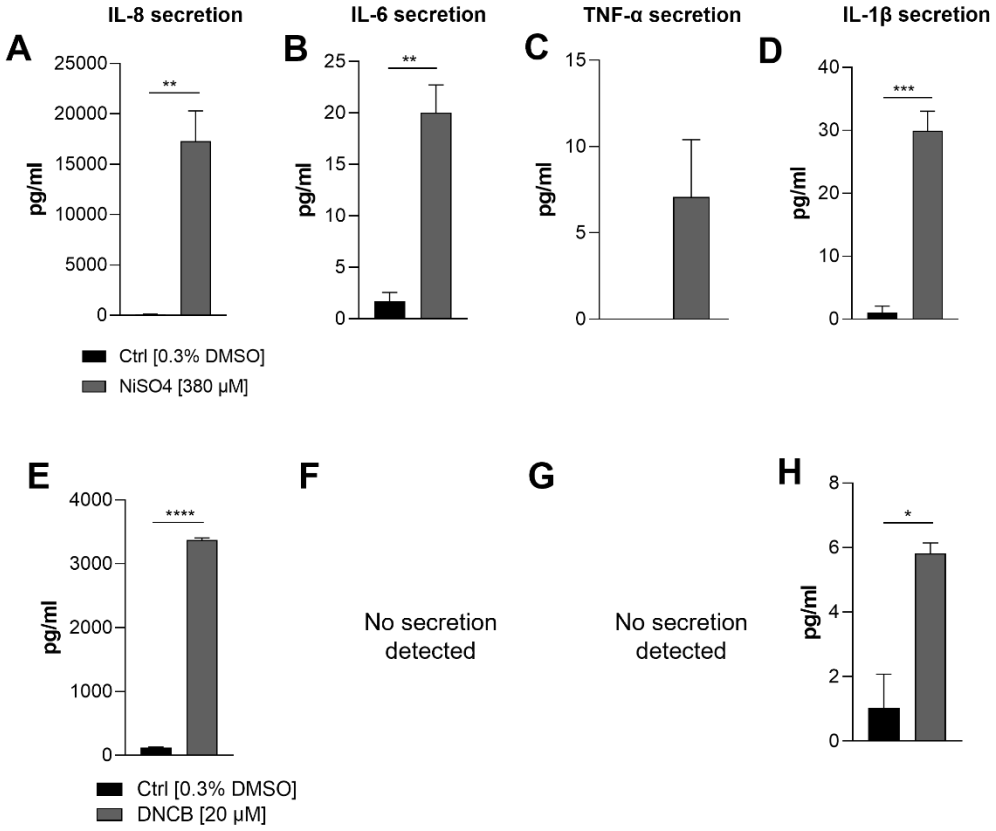

Figure 2.2-5 Secretion of inflammatory cytokines: IL-8 **(A, E)**, IL-6 **(B, F)**, TNF-a **(C, G)** IL-1β **(D, H)** by iDCs after $NiSO_4$ [380 µM] **(A-D)** and DNCB [20 µM] **(E-H)** treatment. Supernatants were harvested after 24 h and cytokine concentrations were detected using a Cytometric Bead Array Assay. Error bars indicate the standard errors of the mean (n = 3 independent experiments with *p ≤ 0.05, **p ≤ 0.01, ***p ≤ 0.001, and ****p ≤ 0.0001).

Next, we aimed to integrate the iDCs into a full-thickness skin model as potential dermal DC surrogates and to prove their functionality *in vitro*. Therefore, iDCs were integrated into the well-established and commercially available Phenion® Full-Thickness Skin Model [44, 46]. The Phenion® Full-Thickness Skin Model comprises a fully stratified epidermis including a stratum basale, stratum spinosum, stratum granulosum and stratum corneum as well as a mechanically stable dermis. The rigid porous structure allows the fibroblasts to migrate into the scaffold and to synthesize and secrete extracellular matrix components such as elastin and fibrillin-1, mimicking the elastic network of native human skin [44, 47] and thereby potentially providing the organ-specific environment for DDCs.

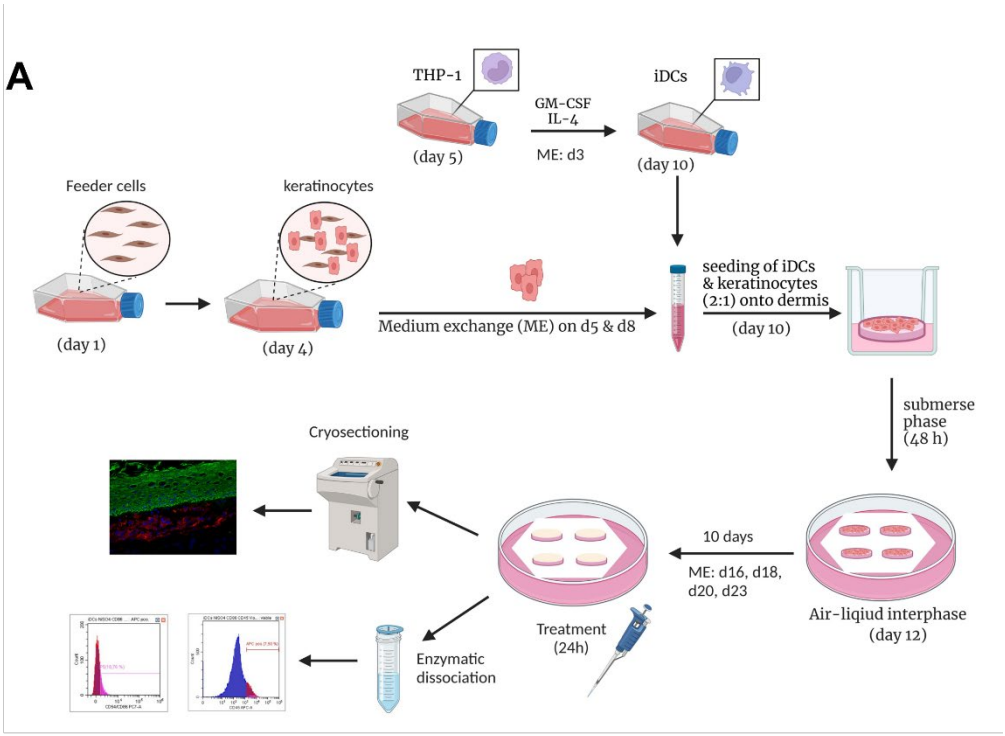

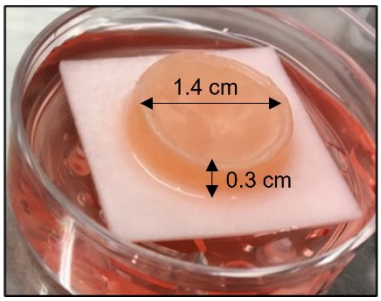

Figure 2.2-6 Engineering of human 3D immune competent full-thickness skin models. **(A)** Primary human foreskin keratinocytes are seeded onto feeder cells and harvested after six days of cultivation and seeded together with THP-1-derived iDCs (ratio 1:2) onto dermis models based on a solid collagen matrix and primary fibroblasts. After 48 h of cultivation in a submerse phase, the skin models are lifted into an air-liquid interphase. After 10 days, the skin models are cryosectioned for histological analysis or treated with sensitizers for 24 h and enzymatically dissociated. Created with BioRender.com. **(B)** The full-thickness skin model is characterized by a diameter of 1.4 cm and a height of 0.3 cm. The photo was taken on ALI d10 and depicts our immune competent skin model with a fully differentiated epidermis.

To develop an immune competent skin model, iDCs, were seeded together with primary human keratinocytes onto matured dermis equivalents. After 10 days of air-liquid interphase (ALI) cultivation, allowing the complete differentiation of all epidermal layers, the skin models were either cryo-sectioned for histological analysis or treated with a sensitizer ($NiSO_4$ or DNCB) for 24 h and subsequently proceeded towards enzymatic dissociation and DC surface marker analysis (Figure 2.2-6A). On ALI day 10, the skin model is fully differentiated displaying all epidermal layers typical for native human skin including a stratum corneum, and a dermal compartment enriched with newly synthesized ECM proteins (Figures 2.2-6, 2.2-7A, C). Histological analysis of the full-thickness skin models reveals the integration of iDCs in the dermis, mostly located underneath the epidermis, which proves the integration as dermal

dendritic cells. Compared to the control model, the overall histology of the epidermis is not impaired by the integration of our iDCs and the epidermis remains fully stratified (Figure 2.2-7).

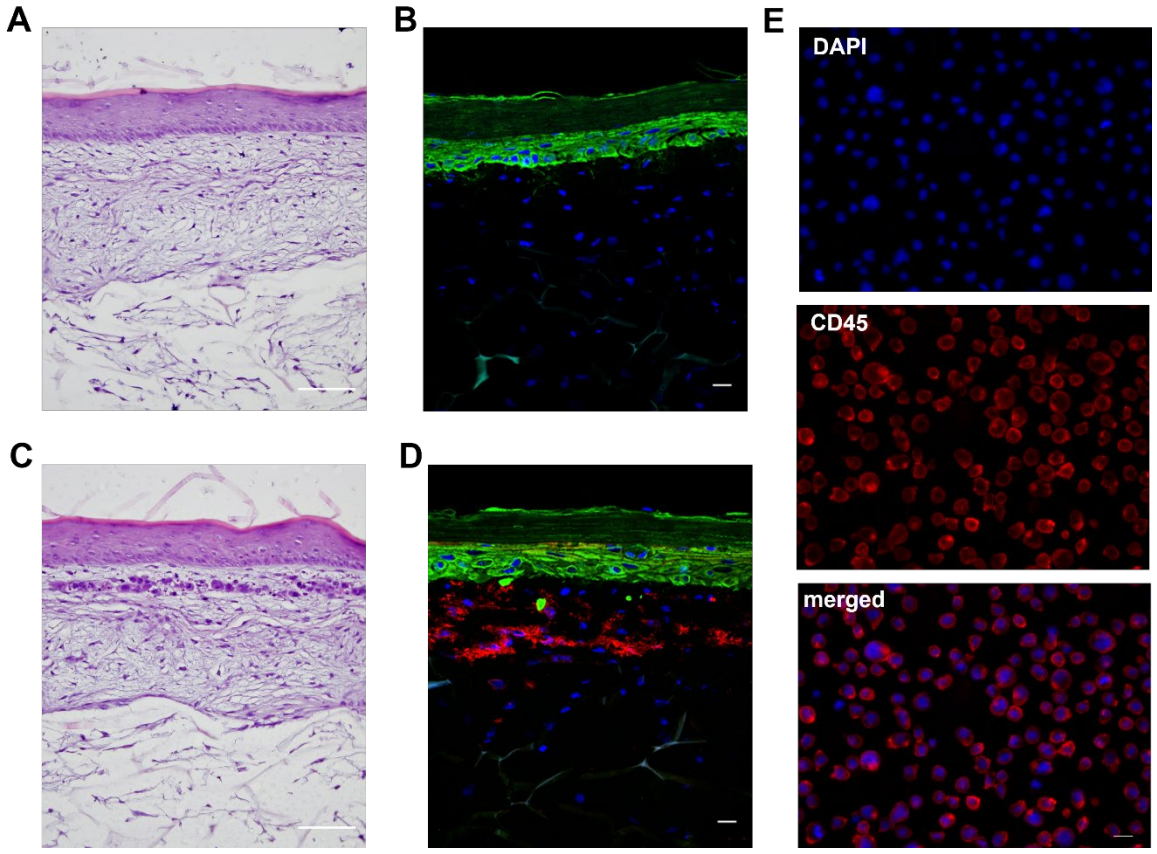

Figure 2.2-7 Histological analysis of the full-thickness skin models. **(A, C)**: H&E staining of the regular model without immune cells **(A)** and the skin model including DDC surrogates **(C)**. Scale bar = 100 µm. **(B, D)**: Immunofluorescent staining of the regular model without immune cells **(B)** and skin model including DDC surrogates **(D)**. Keratinocytes were stained with cytokeratin 5 (green signal). DDC surrogates were stained with CD45 (red signal). Nuclei were stained with DAPI (blue signal). Scale bar = 20 µm. **(E)** Immunofluorescent staining of DDC surrogates before integration into the skin models. DDC surrogates were stained with CD45 (red signal). Nuclei were stained with DAPI (blue signal). Scale bar = 20 µm.

To prove whether iDCs are applicable to a qualitative characterization of sensitizers and perspectively of drug candidates, iDCs were pre-treated for 1 h with dexamethasone, an anti-inflammatory, anti-allergic synthetic glucocorticoid [48], before applying $NiSO_4$ [380 µM] for 23 h. Treatment of isolated iDCs with $NiSO_4$ alone induced the upregulation of CD54 (~1.2-fold) and a significant upregulation of CD86 (~1.4-fold). The pre-treatment with dexamethasone led to the reduction of the $NiSO_4$ induced CD54 (~1.3-fold) expression and a significant reduction of the $NiSO_4$ induced CD86 expression (~2.1-fold) (Figure 2.2-8A) as well as a significant reduction of the IL-8 (23.5-fold), IL-6 (~20-fold) and IL-1β (~30-fold) secretion (Figure 2.2-8C).

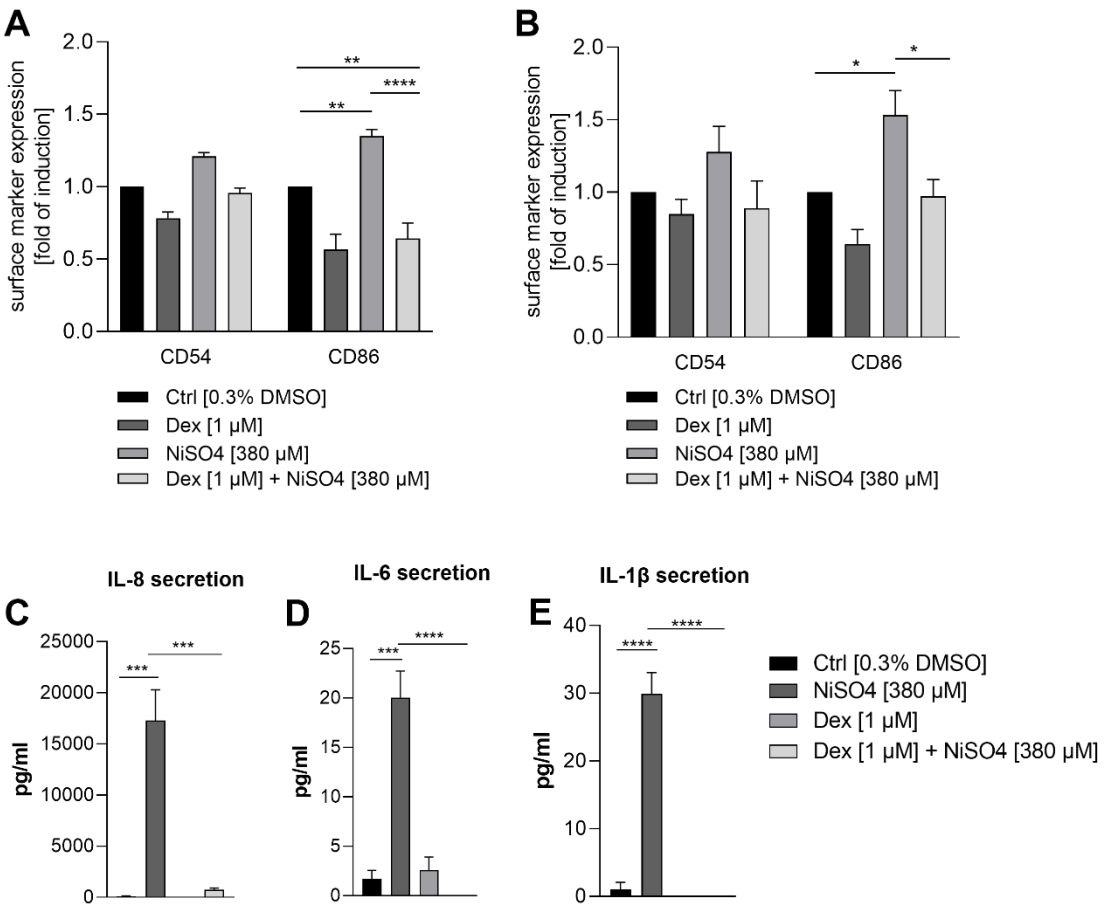

Figure 2.2-8 Surface marker expression of CD54 and CD86 (depicted as fold of induction of the percentage of all positive cells) after **(A)** pre-treatment of THP-1-derived iDCs and **(B)** topical treatment of the immune competent skin model with dexamethasone for 1 h, followed by $NiSO_4$ treatment for 23 h. Results were depicted as fold of induction compared to the solvent control [0.3% DMSO]. **(C–E)** Cytokine secretion of iDCs after 1 h dexamethasone pre-treatment, followed by 23 h of $NiSO_4$ exposure. Error bars indicate the standard errors of the mean (n = 3 independent experiments for **(A, C)** and n=4 independent experiments for **(B)** with *p ≤ 0.05, **p ≤ 0.01, ***p ≤ 0.001, and ****p ≤ 0.0001).

To validate the functionality and immune competence of the DDC surrogate skin model, a topical administration of dexamethasone [1 µM] for 1 h was followed by a topical exposure of $NiSO_4$ [380 µM] for 23 h. Afterwards, the skin models were dissociated enzymatically into single cell suspensions and CD45 positive cells were gated for the analysis of the CD54 and CD86 expression on the tissue-integrated iDCs. Topical treatment of the immune competent skin model with $NiSO_4$ alone induced a proven upregulation of CD54 (~1.3-fold) and CD86 (~1.5-fold) on the iDCs dissociated from the dermal layer (Figure 2.2-8B), demonstrating the robust functionality of our dermal DC surrogates *in vitro.* Furthermore, pre-treatment with dexamethasone led to the reduction of the CD54 (~1.4-fold) and a significant reduction of the CD86 (~1.6-fold) expression on iDCs after topical treatment of the immune competent skin model (Figure 2.2-8B). In conclusion, we were able to engineer a skin model with fully functional dermal dendritic cell surrogates derived from the monocytic cell line THP-1. Furthermore, our

immune competent skin model allows the qualitative identification of potential sensitizers and perspectively the evaluation of novel drug candidates potentially suppressing skin sensitization

Discussion

The aim of this study was to explore and validate immature dendritic cells (iDCs) derived from the monocytic cell line THP-1 as suitable surrogates for dermal dendritic cells upon integration into a human full-thickness skin model. The ability of THP-1-derived iDCs to identify sensitizers such as $NiSO_4$ and DNCB and to upregulate the DC activation markers CD54 and CD86 has been recently shown [41]. Furthermore, the capability to phagocytose pathogen-derived membrane components and to potentially induce T cell activation via upregulation of IL-12p40 upon sensitizer treatment has been proven [41]. Subsequently, the next logically step was to prove whether our iDCs might be suitable surrogates for dermal dendritic cells.

Dermal dendritic cells can be identified and distinguished from dermal monocytes and macrophages by a low CD14 expression and a high CD11c expression [4, 5]. However, in contrast to Langerhans cells, no exclusive cell-specific marker expressed on all dermal dendritic subsets has been reported so far. A commonly described low CD14 expression and a high CD11c expression could be confirmed on the THP-1-derived iDCs. In addition, the significant up-regulation of the DC activation markers CD54 and CD86 after $NiSO_4$ and DNCB treatment was verified, confirming the expected ability to respond to sensitizers as a required prerequisite for DC activation and subsequent maturation. Since several studies elucidated the necessity of the activation of the NF-κB pathway and the p38 MAPK pathway for the process of DC activation and maturation marker upregulation [14–16], we studied the impact of the two model sensitizers, $NiSO_4$ and DNCB on both pathways in the THP-1-derived iDCs. In line with the published studies, we were able to confirm a significant degradation of IκBα after $NiSO_4$ treatment and an induction of phosphorylation of p38 MAPK after DNCB treatment. Treatment of DCs derived from human cord blood with $NiSO_4$ led to maximal degradation of IκBα after 1 h and recovery after 4 h, while treatment with DNCB could not induce the degradation of IκBα [14]. Similarly, $NiCl_2$, but not DNCB treatment of PBMC-derived DCs for 1 h led to the phosphorylation and degradation of IκBα. In addition, the $NiCl_2$- induced activation of NF-κB could be proven via NF-κB p65 transcriptional factor assay kit [15]. Conversely, DNCB treatment of human cord blood-derived DCs induced a strong phosphorylation of p38 MAPK after 30 min, while $NiSO_4$ treatment could only induce minor phosphorylation of p38 MAPK after 30 min [14]. Furthermore, treatment of PBMC derived DCs with DNCB induced a strong dose-dependent phosphorylation of p38 MAPK [15]. However, treatment of a fetal mouse skin-derived skin line with $NiSO_4$ induced only a weak phosphorylation of p38 MAPK after 2 h of treatment and no degradation of IκBα [49]. In fact, sensitization to nickel in mice

cannot be achieved without an additional adjuvant to induce the expansion of nickel reactive T cells, while in humans nickel functions as its own adjuvant via the Toll like receptor (TLR)4, which was identified as receptor for Ni^{2+} in human, but not in mice [50]. These results clearly underline the species-specific differences and the necessity to study the skin immunity in human-derived systems. Furthermore, it needs to be mentioned that the TLR4 mediated nickel skin sensitization is most likely guided by dermal dendritic cells, since TLR4 is not expressed on human LCs [51, 52]. Next to the sensitizer induced upregulation of DC activation and maturation markers such as CD54 and CD86 and the activation of the NF-κB as well as the p38 MAPK pathways, the up-regulation and secretion of inflammatory cytokines such as IL-8, IL-6, IL-1 and TNF-α has been described for various DC surrogates [14–16, 53]. Thus, we were intrigued to prove the sensitizer- induced expression and secretion of those interleukins in our iDCs as well. Treatment of iDCs with $NiSO_4$ resulted in a significant upregulation of mRNA levels for IL-8, IL-6 and TNF-α. These results were confirmed on the protein level, by significant higher cytokine secretion for IL-8, IL-6 and additionally IL-1β. The secretion of IL-8 and IL-6 after $NiSO_4$ treatment has been shown for cord blood- derived iDCs as well [14]. Furthermore, enhanced mRNA levels as well as cytokine secretion of IL-1β, IL-6, IL-8, TNF-α could be detected after treatment of PBMC derived DCs with $NiCl_2$ [15, 53]. Treatment of iDCs with DNCB led to a significant upregulation of mRNA levels for IL-8 and IL-6 and significant cytokine secretion for IL-8 and IL-1β. Treatment of PBMC derived iDCs with DNCB resulted in enhanced mRNA levels for IL-8, IL-1β and TNF-α, but only in a significant increased secretion of IL-8 [15]. However, treatment of PBMC derived DCs from a different study could prove in line with our results the DNCB induced secretion of IL-1β and no secretion of IL-6 and TNF-α [53]. Taken together, our results mirror the results published for other DC surrogates in regard of the p38 MAPK pathway, the NF-κB pathway and inflammatory cytokine induction, suggesting distinct activation mechanisms, different targets and signaling pathways for DNCB compared to nickel salts. Investigating those differences, Ade et al. were able to show that the inhibition of NF-κB with BAY 11-7085 suppressed the $NiSO_4$ induced increase of CD86 and CD83 and abolished the $NiSO_4$ induced secretion of IL-8, IL-6 and IL-12p40 in cord blood derived DCs [14]. However, inhibition of p38 MAPK in PBMC derived DCs with PD98059 suppressed the $NiCl_2$ induced IL-1β, IL- 8, and TNF-α secretion [15]. Inhibition of p38 MAPK in PBMC derived iDCs with SB203580 led to suppressed DNCB induced augmentation of CD86 as well as a suppressed secretion of IL-8 [15]. Furthermore, it was shown that DNCB treatment inhibits TNF-α induced activation of the NF-κB pathway in cord blood derived DCs [14]. One hypothesis for the distinct mechanisms of action for $NiSO_4$ and DNCB could underly their lipophilicity. While DNCB as a lipophilic hapten is able to penetrate directly into the DCs, it can be processed endogenously and presented via MHC class I molecules, hydrophilic nickel ions are more likely processed exogenously and presented via the MHC class II molecules [54,

56]. In order to elucidate the distinct activation of iDCs upon sensitizer treatment, the molecular mechanism of the haptenization, including the (covalent) binding and modification of proteins followed by the individual, sensitizer or hapten specific DC activation, needs to be addressed in future studies. Although the binding capacity of migratory DCs in skin-draining lymph nodes was proven [57], unfortunately, to date, the precise mechanism of the DNCB and $NiSO_4$ DC activation has not been fully established. Furthermore, it has been reported that metal ions such as nickel are bound and presented via different ways to $CD4^+$ T cells. While classic allergens such as DNCB tend to form covalent bonds with MHC-bound proteins, metal ions can interact via several molecular mechanisms with T cells [58].

By proving low CD14 and high CD11c expression, the activation of the p38 MAPK and the NF-κB pathway as well as the secretion of inflammatory cytokines after sensitizer treatment in addition to their capability to phagocytose pathogen-derived membrane particles, our THP-1-derived iDCs could be identified as potential dermal dendritic cell surrogates.

For compound characterization, a robust and relatively easily accessible human tissue platform would be desirable as an alternative to animal experiments or highly variable and time- consuming transplants from human skin. Hence, the overall aim was to integrate the iDCs into a human skin model. For this the Phenion® Full-Thickness Skin Model was chosen due its unique porous matrix, which allows the fibroblasts to adhere to and migrate into the collagen and to secrete extracellular matrix components such as elastin and fibrillin-1 [44, 47], mimicking the elastic network of native human skin and thereby potentially providing the inevitable environment for DDCs. Histological analysis of the skin tissue revealed the integration iDCs in the dermis, predominantly underneath the epidermis. This location is in line with the observation for CD11c positive dendritic cells in normal human skin, which have been found to be located in the superior dermis [59]. Contrary, cells expressing monocyte/macrophage markers such as CD14 or CD163 are largely located in the superior papillary and reticular dermis [59]. Noteworthy, the integration of the iDCs as DDCs did not impair the stratification of the epidermis.

To prove the immune competence of the newly developed iDC containing full-thickness skin model, the skin models were treated topically with 380 µM $NiSO_4$ and 20 µM DNCB for 23 h and subsequently dissociated enzymatically into single cell suspensions for the analysis of the surface marker expression of CD54 and CD86 on the DDC surrogates (identified via CD45 expression). While treatment of iDCs with $NiSO_4$ only resulted in a 1.2-fold upregulation of CD54 and a 1.4-fold upregulation of CD86, topical sensitizer administration resulted in a 1.3-fold upregulation of CD54 and a 1.5-fold upregulation of CD86 on tissue-integrated iDCs. Thus, we were able to prove the functionality and thereby the immune competence of our DDC surrogate model 12 days after the integration of iDCs. Noteworthy, despite the vigorous enzymatic dissociation, the expression of both surface markers was still detectable on tissue -

integrated iDCs and the upregulation could be detected in a similar manner (fold of induction) compared to the isolated iDCs. In fact, this is not self-evidently, as on one hand the protein expression pattern could change due to the complex three- dimensional co-cultivation with keratinocytes and fibroblasts and on the other hand the enzymatic tissue dissociation has been proven to alter or even diminish the cell surface antigen expression on distinct immune cell populations [60–63].

In order to initially assess the potential of our engineered skin tissue for drug discovery applications, we aimed to prove that our immune competent skin model is amenable for the qualitative characterization of putative anti-inflammatory compounds. Therefore, isolated iDCs as well as the immune competent skin model were treated with dexamethasone, an anti-inflammatory, anti-allergic synthetic glucocorticoid [48], for 1 h followed by 23 h of $NiSO_4$ exposure. Indeed, pre-treatment with dexamethasone significantly reduced the $NiSO_4$ induced secretion of IL-8, IL-6 and IL-1β and could suppress the expression of CD54 and CD86 on isolated as well as on the tissue-integrated iDCs. In line with our results, the expression of CD54 and CD86 on murine bone marrow derived DC surrogates was downregulated by dexamethasone treatment in a dose-dependent manner and the secretion of IL-1β was decreased significantly [64]. Furthermore, the presence of dexamethasone during the differentiation of PBMC into DC surrogates decreased the basal expression of CD86 as well as the TNF-α induced upregulation of CD86 and the LPS-induced secretion of TNF-α and IL1β [65]. By suppressing the expression of CD54 and CD86, as well as the secretion of IL-8, IL-6 and IL-1, which are required for the activation, stimulation and recruitment of T cells, dexamethasone might contribute to T cell inhibitory effects and thereby suppressing the immune response.

Altogether, the THP-1 derived iDCs are profoundly characterized by a low CD14 and high CD11c expression, the ability phagocytose membrane components derived from pathogens [41] and to identify sensitizers such as DNCB and $NiSO_4$, which is subsequently followed by the upregulation of adhesion molecules, such as CD54 and co- stimulatory molecules such as CD86 required for the co-stimulation of naïve $CD4^+$ T cells. In addition, T cell activation might be supported via upregulation of IL-12p40 upon sensitizer treatment [41]. Our findings may contribute to the understanding of the crucial role of DDC for antigen presentation in the skin and the potential to migrate and activate T cells faster and outnumber LCs by 10:1 in draining lymph nodes [39, 40]. Furthermore, the sensitizer induced activation of the NF-κB and the p38 MAPK pathway and the secretion of inflammatory cytokines such as IL-8, IL-6, IL-1β and TNF-α as it was stated for other DC surrogates could be validated. Thus, our THP-1-derived iDCs fulfill all required *in vitro* criteria for dermal dendric cell surrogates. By integrating those iDCs into a full- thickness skin model, we are the first to engineer a human immune competent full-thickness skin model containing THP-1-derived iDCs as dermal dendritic cell surrogates,

which serve as an easily accessible tool to identify sensitizers and to qualitatively analyze putative anti- inflammatory compounds according to the 3R principles. Prospectively, our immune competent DDC model might be suitable for the research and understanding of inflammatory skin conditions such as psoriasis or diabetic skin manifestations often accompanied with recurring fungal or bacterial infections [66, 67]

Materials and Methods

Generation of immature dendritic cells

Immature dendritic cells were generated according to the protocol described by Hölken and Teusch [41]. In total, 1 × 10^6 THP-1 cells were seeded in 5 mL RPMI-1640 (Gibco, #22400089) containing 10% FBS (Gibco, #10270-106), 50 U/mL Pen-Strep (Gibco, #15140122) and 50 µM 2-mercaptoethanol (Gibco, #21985023) into a T25 flask. For the differentiation 1500 IU/mL rhGM-CSF (ImmunoTools, #11343125) and 1500 IU/ml rhIL-4 (ImmunoTools, #11340045) were added with a medium exchange on day 3. The cells were incubated in total for 5 days at 37°C, 5% CO_2

Sensitization assays

1 × 10^6 THP-1-derived iDCs were seeded into a 24-well plate in 1 mL RPMI-1640 containing 10% FBS, 50 U/ml Pen-Strep, and 50 µM 2-mercaptoethanol. Cells were pre-treated with 1 µM dexamethasone (Peprotech, #5000222) for 1 h. Afterwards cells were treated with 1-chloro-2,4-dinitrobenzene (DNCB) [20 µM] (Sigma-Aldrich, #237329, Darmstadt, Germany), nickel sulfate ($NiSO_4$) [380 µM] (Sigma-Aldrich, #227676) or their respective solvent control dimethyl sulfoxide (DMSO). After 24 h, the cells were harvested for the analysis of surface marker expression via flow cytometry.

Flow cytometry

The cells were harvested after differentiation, treatment or skin model dissociation and washed in Automacs Running Buffer (Miltenyi, #130-091-221). At least 2 × 10^5 cells for each antibody panel were transferred to 96-well u-bottom plates. For staining the cells were incubated in Automacs Running Buffer with the following antibodies (1:50): REA Control (S)-VioGreen (Miltenyi, #130-113- 444), REA Control (S)-PE (Miltenyi, #130-113-438), REA Control (S)-APC (Miltenyi, #130-113-434); REA Control (S)-PE-Vio770, (Miltenyi, #130-113-440); CD54-APC (Miltenyi, #130-121-342); CD86-APC (Miltenyi, #130-116-161), CD14-VioGreen (Miltenyi, #130-110-525), CD11c-APC (Miltenyi, #130-113-584) for 10 minutes in the dark. For single cells from the dissociates skin models the following antibodies were used (1:50): CD45-VioBright R667 (Miltenyi #130-110-779), CD54-PE-Vio770 (Miltenyi, #130-127-992), CD86-PE-

Vio770 (Miltenyi, #130-116-265). The cells were washed twice with automacs running buffer. To determine the cell viability, cells were stained with DAPI (Sigma, #D9542). Flow cytometry analysis was performed using the CytoFlex (B5-R3-V5) from Beckman Coulter.

Western Blot analysis

THP-1-derived iDCs were seeded with 1 × 10^6 cells into a 24-well plate in 1 mL RPMI-1640 containing 10% FBS, 50 U/mL Pen-Strep, and 50 µM 2-mercaptoethanol. Cells were treated with DNCB [25 µM] (Sigma-Aldrich, #237329) and $NiSO_4$ [500 µM] (Sigma-Aldrich, #227676) for 30 min or 1 h. Cells were harvested, washed once in 1x PBS and lysed with radioimmunoprecipitation assay (RIPA) buffer containing a protease inhibitor (Roche, #11836170001) and a phosphatase inhibitor (Roche, #04906845001). Protein concentration was determined using a BCA protein assay kit (Thermo Scientific, 23227). For western blot analysis, Laemmli buffer (Bio-Rad Laboratories, Inc., #1610747) was added to 20 µg protein lysate. Proteins were denaturated for 10 min at 95 °C and separated on 10% SDS-Gels using a Biometra Eco-Mini Buffer Tank system (Analytik Jena, #846-017-103/017-170). Protein transfer to a PVDF membrane (BioRad Laboratories, Inc., #1620177) was performed with the Biometra Fastblot system (Analytik Jena, #846-015-299). The membrane was blocked in 5% BSA (Roth, #8076.2) and then incubated with the respective primary antibodies, p38 MAPK (Cell Signaling Technology, #8690T), phospho-p38 MAPK (Thr180/ Tyr182) (Cell Signaling Technology, #4511T), IκBα (Cell Signaling Technology, #9242S) or vinculin (Cell Signaling Technology, #13901S) over night at 4° C. After washing with 1x TBS-T the membrane was incubated with the respective horseradish peroxidase-coupled secondary antibody (Goat anti-Rabbit (H+L), Thermo Fisher Scientific, #31460) for 1 h at room temperature. Antibody binding was detected with the SuperSignal West Pico Plus substrate kit (Thermo Fisher Scientific, #34577). For imaging we used a ChemStudio Imager (Analytik Jena, #849-97-0928-04).

Cytokine sekretion

THP-1-derived iDCs were seeded with 1 × 10^6 cells into a 24-well plate in 1 mL RPMI-1640 containing 10% FBS, 50 U/mL Pen-Strep, and 50 µM 2-mercaptoethanol. Cells were treated with DNCB [20 µM] (Sigma-Aldrich, #237329) and $NiSO_4$ [380 µM] (Sigma-Aldrich, #227676) or their respective solvent control dimethyl sulfoxide (DMSO). Supernatants were collected after 24 h for cytokine analysis. Secretion of the inflammatory cytokines was detected according to the manufacturer's instructions of the Cytometric Bead Array Human Inflammatory Cytokines Kit (BD, #551811) and the CytoFlex (B5-R3-V5) from Beckman Coulter. Analysis was performed using the CBA Analysis Software (BD Biosciences).

3D immune competent skin model generation

Feeder cells (Phenion, #hFeeder) were seeded with 5 × 10^5 cells in 23 mL keratinocyte medium (Phenion, #K CM-250) into a T175 flask. After three days 5 × 10^5 primary human foreskin keratinocytes from juvenile donors (Phenion, #hK P1) were seeded onto the feeder cells. After 6 days of cultivation, feeder cells were detached by incubation with 0.05% trypsin (Gibco, #25300054) for 2 min at 37 °C, 5% CO and keratinocytes were harvested using 0.05% trypsin for 6 min, 37° C, 5% CO_2. 5 × 10^5 Keratinocytes in P2 were seeded together with 1 × 10^6 THP-1-derived iDCs (ratio 1:2) in 1 mL keratinocyte medium (Phenion, #K CM-250) onto dermis models based on a solid and porous collagen matrix [42, 43] and primary human foreskin fibroblasts (kindly provided by Henkel AG & Co. KGaA, Düsseldorf, Germany). After 24 h of incubation at 37° C, 5% CO the medium was exchanged. After 24 h submerse phase, the skin models were lifted into the Air-liquid Interface and cultivated with Air-liquid Interface Culture Medium (Phenion, #ALI CM HC-250, w/o hydrocortisone) for 10 to 14 days.

Cryosectioning and immunofluorescence staining

Skin models were embedded and frozen in Tissue-Tek (Sakura, #4583), cut into 7 µm slices and transferred to Microscope slides (expredia, #J1800AMNZ). The tissue slides were fixed in ice- cold acetone for 10 minutes and blocked in 10% normal goat serum (Invitrogen, #50062Z), for 1 h at room temperature. Primary antibodies were diluted in DAKO antibody diluent (Dako, #S0809) and Cytokeratin 5 (OriGene, DM361) (1:75) and CD45-VioBright R667 (Miltenyi, #130-110-779) (1:50) were applied for staining at 4° C overnight. Secondary antibody staining with Alexa Flour 488 (Invitrogen, #A11017) (1:200) combined with DAPI staining (10 µg/ml) (Sigma, ##D9542) was performed for 1 h at room temperature (RT). The stained tissue slides were imbedded with Tissue Fluorescence mounting medium (Agilent, S3023) to avoid bleaching and imaged using confocal spinning disc microscopy (CQ1, Yokogawa). For immunofluorescent staining of the isolated iDCs, cells were transferred into a 96 well plate and fixed with 4% paraformaldehyde (PFA) (Roth, #0964.1) for 10 min. The cells were blocked and permeabilized in 0.1% BSA (Roth, #8076.2), 0.01% Tween20 (Sigma, #P7949) and 0.1% Triton X100 (Sigma, #T9284) in 1x PBS for 30 min. The primary antibody CD45-VioBright R667 was diluted 1:50 in DAKO antibody diluent and applied over night at 4°C. DAPI staining (10 µg/ml) was performed the next day for 1 h at RT. Washing steps were performed each 3x with 1 x PBS at 200 xg for 3 min. Immunofluorescent staining of the cells was analyzed using fluorescence microscopy (Keyence, #BZ-X800L/BZ-X810).

Hematoxylin and eosin staining

Skin models were fixed in 4% formaldehyde solution (Roth, #P087.5) for at least 24 h before dehydration was conducted in the automated tissue processor (Sakura Finetek USA, Inc.,

#Tissue-Tek VIP 5 Jr.). For paraffin embedding, samples were processed on Histo Core Arcadia C/H (Leica) and cut into 5 µm sections with the rotary microtome (Leica, #RM2145). Transferred sections on object slides were dried overnight at 37° C in a heating cabinet (Memmert) followed by automated hematoxylin and eosin staining procedure (Thermo Scientific, #Gemini AS). Images were taken with Olympus microscope (BX51, Camera Olympus DP7).

Skin model dissociation

The immune competent skin models were digested on ALI day 11, 24 h after sensitizer treatment. The tissue was minced via scalpel and tissue scissors and transferred to 1.5 ml tubes. For enzymatic dissociation 1 mL RPMI-1640 containing 10% FBS, 50 U/mL Pen- Strep, 50 µM 2-mercaptoethanol, 100 µg/mL liberase (Roche, #05401119001) and 40 µg/mL DNAse (Roche, #10104159001) was added and the tissue was incubated for 90 min at 37° C, 400 RPM on a thermoshaker (Eppendorf, #PMCT). After 90 minutes, the dissociated cell suspension was filtered through a 70 µm cell strainer (VWR, #732-2758) to obtain single cell suspensions. The cells were washed with PBS and stained for flow cytometry analysis.

Statistical evaluation

Analysis of the data was conducted with GraphPad Prism version 8.4.3 (GraphPad Software, Inc., San Diego, CA, USA). Statistical significance was calculated using an unpaired t-test, one-way ANOVA or two-way ANOVA. Significance was defined and referred to as * = $p \leq 0.05$; ** = $p \leq 0.01$; *** = $p \leq 0.001$; **** = $p \leq 0.0001$.

Data availability statement

The raw data supporting the conclusions of this article will be made available by the authors, without undue reservation.

Ethics statement

Ethical approval was not required for the studies on humans in accordance with the local legislation and institutional requirements because only commercially available established cell lines were used.

Author contributions

NT: Conceptualization, Funding acquisition, Project administration, Resources, Supervision, Writing – review & editing. JH: Data curation, Investigation, Methodology, Visualization, Writing – original draft. KF: Data curation, Investigation, Validation, Visualization, Writing – review & editing. MM: Validation, Data curation, Investigation, Visualization, Writing – review & editing.

NB: Investigation, Data curation, Methodology, Validation, Visualization, Writing – review & editing. UE: Methodology, Validation, Investigation, Visualization, Writing – review & editing. TB: Conceptualization, Funding acquisition, Supervision, Project administration, Resources, Writing – review & editing. KM: Funding acquisition, Methodology, Project administration, Supervision, Resources, Investigation, Writing – review & editing. LV: Data curation, Methodology, Resources, Supervision, Validation, Investigation, Visualization, Writing – review & editing.

Funding

The author(s) declare financial support was received for the research, authorship, and/or publication of this article. This research was funded by a grant to NT, TB and KM by the Bundesministerium für Ernährung und Landwirtschaft (BMEL), funding number: 281A308C18.

Acknowledgments

We would like to thank Prof. Dr. Eckhard Lammert for his profound support throughout this work.

Conflict of interest

Authors MM, NB, UE, KM, LV are employed by the company Henkel AG & Co. KGaA. The remaining authors declare that the research was conducted in the absence of any commercial or financial relationships that could be construed as a potential conflict of interest

References

1. Kabashima K, Honda T, Ginhoux F, Egawa G. The immunological anatomy of the skin. Nature Reviews Immunology. 2019;19(1):19-30.
2. Matejuk A. Skin Immunity. Archivum Immunologiae et Therapiae Experimentalis. 2018;66(1):45-54.
3. Valladeau J, Ravel O, Dezutter-Dambuyant C, Moore K, Kleijmeer M, Liu Y, et al. Langerin, a novel C-type lectin specific to Langerhans cells, is an endocytic receptor that induces the formation of Birbeck granules. Immunity. 2000;12(1):71-81.
4. Zaba LC, Fuentes-Duculan J, Steinman RM, Krueger JG, Lowes MA. Normal human dermis contains distinct populations of CD11c+BDCA-1+ dendritic cells and CD163+FXIIIA+ macrophages. J Clin Invest. 2007;117(9):2517-25.
5. Zaba LC, Krueger JG, Lowes MA. Resident and “Inflammatory” Dendritic Cells in Human Skin. Journal of Investigative Dermatology. 2009;129(2):302-8.
6. Sumpter TL, Balmert SC, Kaplan DH. Cutaneous immune responses mediated by dendritic cells and mast cells. JCI Insight. 2019;4(1).
7. Naik SM, Cannon G, Burbach GJ, Singh SR, Swerlick RA, Wilcox JN, et al. Human keratinocytes constitutively express interleukin-18 and secrete biologically active interleukin-18 after treatment with pro-inflammatory mediators and dinitrochlorobenzene. J Invest Dermatol. 1999;113(5):766-72.

8. Lisby S, Müller KM, Jongeneel CV, Saurat J-H, Hauser C. Nickel and skin irritants up-regulate tumor necrosis factor-α mRNA in keratinocytes by different but potentially synergistic mechanisms. International immunology. 1995;7(3):343-52.
9. Gueniche A, Viac J, Lizard G, Charveron M, Schmitt D. Effect of nickel on the activation state of normal human keratinocytes through interleukin 1 and intercellular adhesion molecule 1 expression. British Journal of Dermatology. 1994;131(2):250-6.
10. Tuschl H, Kovac R. Langerhans cells and immature dendritic cells as model systems for screening of skin sensitizers. Toxicology in Vitro. 2001;15(4):327-31.
11. Xu H, Guan H, Zu G, Bullard D, Hanson J, Slater M, et al. The role of ICAM-1 molecule in the migration of Langerhans cells in the skin and regional lymph node. European journal of immunology. 2001;31(10):3085-93.
12. Dustin ML, Tseng S-Y, Varma R, Campi G. T cell–dendritic cell immunological synapses. Current opinion in immunology. 2006;18(4):512-6.
13. Sharpe AH, Freeman GJ. The B7–CD28 superfamily. Nature Reviews Immunology. 2002;2(2):116-26.
14. Ade N, Antonios D, Kerdine-Romer S, Boisleve F, Rousset F, Pallardy M. NF-kappaB plays a major role in the maturation of human dendritic cells induced by NiSO(4) but not by DNCB. Toxicol Sci. 2007;99(2):488-501.
15. Aiba S, Manome H, Nakagawa S, Mollah ZUA, Mizuashi M, Ohtani T, et al. p38 Mitogen-activated Protein Kinase and Extracellular Signal-regulated Kinases Play Distinct Roles in the Activation of Dendritic Cells by Two Representative Haptens, NiCl2 and 2,4-dinitrochlorobenzene. Journal of Investigative Dermatology. 2003;120(3):390-9.
16. Arrighi J-Fo, Rebsamen M, Rousset Fo, Kindler V, Hauser C. A Critical Role for p38 Mitogen-Activated Protein Kinase in the Maturation of Human Blood-Derived Dendritic Cells Induced by Lipopolysaccharide, TNF-α, and Contact Sensitizers. The Journal of Immunology. 2001;166(6):3837-45.
17. Casilli F, Bianchini A, Gloaguen I, Biordi L, Alesse E, Festuccia C, et al. Inhibition of interleukin-8 (CXCL8/IL-8) responses by repertaxin, a new inhibitor of the chemokine receptors CXCR1 and CXCR2. Biochemical Pharmacology. 2005;69(3):385-94.
18. Harada A, Sekido N, Akahoshi T, Wada T, Mukaida N, Matsushima K. Essential involvement of interleukin-8 (IL-8) in acute inflammation. Journal of leukocyte biology. 1994;56(5):559-64.
19. Xu Y-D, Cheng M, Shang P-P, Yang Y-Q. Role of IL-6 in dendritic cell functions. Journal of Leukocyte Biology. 2022;111(3):695-709.
20. Briscoe D, Cotran R, Pober J. Effects of tumor necrosis factor, lipopolysaccharide, and IL-4 on the expression of vascular cell adhesion molecule-1 in vivo. Correlation with CD3+ T cell infiltration. Journal of immunology (Baltimore, Md: 1950). 1992;149(9):2954-60.
21. Feldmeyer L, Werner S, French LE, Beer H-D. Interleukin-1, inflammasomes and the skin. European Journal of Cell Biology. 2010;89(9):638-44.
22. Nakae S, Asano M, Horai R, Sakaguchi N, Iwakura Y. IL-1 enhances T cell-dependent antibody production through induction of CD40 ligand and OX40 on T cells. The Journal of Immunology. 2001;167(1):90-7.
23. Riemann H, Schwarz A, Grabbe S, Aragane Y, Luger TA, Wysocka M, et al. Neutralization of IL-12 in vivo prevents induction of contact hypersensitivity and induces hapten-specific tolerance. The Journal of Immunology. 1996;156(5):1799-803.
24. Tait Wojno ED, Hunter CA, Stumhofer JS. The Immunobiology of the Interleukin-12 Family: Room for Discovery. Immunity. 2019;50(4):851-70.
25. Pasparakis M, Haase I, Nestle FO. Mechanisms regulating skin immunity and inflammation. Nature Reviews Immunology. 2014;14(5):289-301.

26. Gerber PA, Buhren BA, Schrumpf H, Homey B, Zlotnik A, Hevezi P. The top skin-associated genes: a comparative analysis of human and mouse skin transcriptomes. Biological Chemistry. 2014;395(6):577-91.
27. Rougier A, Lotte C, Maibach HI. In vivo percutaneous penetration of some organic compounds related to anatomic site in humans: predictive assessment by the stripping method. J Pharm Sci. 1987;76(6):451-4.
28. Abd E, Yousef SA, Pastore MN, Telaprolu K, Mohammed YH, Namjoshi S, et al. Skin models for the testing of transdermal drugs. Clin Pharmacol. 2016;8:163-76.
29. Van Gele M, Geusens B, Brochez L, Speeckaert R, Lambert J. Three-dimensional skin models as tools for transdermal drug delivery: challenges and limitations. Expert Opinion on Drug Delivery. 2011;8(6):705-20.
30. Laubach V, Zöller N, Rossberg M, Görg K, Kippenberger S, Bereiter-Hahn J, et al. Integration of Langerhans-like cells into a human skin equivalent. Arch Dermatol Res. 2011;303(2):135-9.
31. Ouwehand K, Spiekstra SW, Waaijman T, Scheper RJ, de Gruijl TD, Gibbs S. Technical advance: Langerhans cells derived from a human cell line in a full-thickness skin equivalent undergo allergen-induced maturation and migration. J Leukoc Biol. 2011;90(5):1027-33.
32. Bock S, Said A, Müller G, Schäfer-Korting M, Zoschke C, Weindl G. Characterization of reconstructed human skin containing Langerhans cells to monitor molecular events in skin sensitization. Toxicol In Vitro. 2018; 46:77-85.
33. Kosten IJ, Spiekstra SW, de Gruijl TD, Gibbs S. MUTZ-3 derived Langerhans cells in human skin equivalents show differential migration and phenotypic plasticity after allergen or irritant exposure. Toxicology and applied pharmacology. 2015;287(1):35-42.
34. Rodrigues Neves CT, Spiekstra SW, de Graaf NP, Rustemeyer T, Feilzer AJ, Kleverlaan CJ, et al. Titanium salts tested in reconstructed human skin with integrated MUTZ-3-derived Langerhans cells show an irritant rather than a sensitizing potential. Contact Dermatitis. 2020;83(5):337-46.
35. Koning JJ, Rodrigues Neves CT, Schimek K, Thon M, Spiekstra SW, Waaijman T, et al. A multi-organ-on-chip approach to investigate how oral exposure to metals can cause systemic toxicity leading to Langerhans cell activation in skin. Frontiers in toxicology. 2022; 3:824825.
36. Régnier M, Staquet MJ, Schmitt D, Schmidt R. Integration of Langerhans cells into a pigmented reconstructed human epidermis. J Invest Dermatol. 1997;109(4):510-2.
37. Régnier M, Patwardhan A, Scheynius A, Schmidt R. Reconstructed human epidermis composed of keratinocytes, melanocytes and Langerhans cells. Med Biol Eng Comput. 1998;36(6):821-4.
38. Bechetoille N, Dezutter-Dambuyant C, Damour O, André V, Orly I, Perrier E. Effects of solar ultraviolet radiation on engineered human skin equivalent containing both Langerhans cells and dermal dendritic cells. Tissue Eng. 2007;13(11):2667-79.
39. Fukunaga A, Khaskhely NM, Sreevidya CS, Byrne SN, Ullrich SE. Dermal dendritic cells, and not Langerhans cells, play an essential role in inducing an immune response. J Immunol. 2008;180(5):3057-64.
40. Kissenpfennig A, Henri S, Dubois B, Laplace-Builhé C, Perrin P, Romani N, et al. Dynamics and function of Langerhans cells in vivo: dermal dendritic cells colonize lymph node areas distinct from slower migrating Langerhans cells. Immunity. 2005;22(5):643-54.
41. Hölken JM, Teusch N. The Monocytic Cell Line THP-1 as a Validated and Robust Surrogate Model for Human Dendritic Cells. Int J Mol Sci. 2023;24(2).

42. Bernd A, Friess W, Mewes KR, Raus M, Bendz H, Kippenberger S, inventors Cross-linked collagen matrix for producing a skin equivalent. Germany patent WO 2006/018147 A3. 23.02.2006.
43. Escherich D, Graf R., Mewes RM, Raus M, inventors Hautmodell mit dendritischen Zellen. Germany patent DE 10 2006 006 461 A1 2007.08.23. 23.08.2007.
44. Mewes KR, Raus M, Bernd A, Zöller NN, Sättler A, Graf R. Elastin Expression in a Newly Developed Full-Thickness Skin Equivalent. Skin Pharmacology and Physiology. 2006;20(2):85-95.
45. Vierkotten L, Petersohn D, Förster T, Mewes KR. The importance of being three-dimensional in biology.
46. Reisinger K, Pfuhler S. 3D Skin Comet Assay. Alternatives for Dermal Toxicity Testing. 2017:527-39.
47. Mewes KR, Zöller NN, Bernd A, Prießner A, DeWever B, Graf R, et al., editors. Expression of Dermal Extracellular Matrix Proteins in a Newly Developed Full-Thickness Skin Model. Cells and Culture; 2010 2010//; Dordrecht: Springer Netherlands.
48. Cohen DE, Heidary N. Treatment of irritant and allergic contact dermatitis. Dermatol Ther. 2004;17(4):334-40.
49. Neves BM, Rosa SC, Martins JD, Silva A, Gonçalo M, Lopes MC, et al. Development of an in vitro dendritic cell-based test for skin sensitizer identification. Chemical Research in Toxicology. 2013;26(3):368-78.
50. Schmidt M, Raghavan B, Müller V, Vogl T, Fejer G, Tchaptchet S, et al. Crucial role for human Toll-like receptor 4 in the development of contact allergy to nickel. Nat Immunol. 2010;11(9):814-9.
51. van der Aar AMG, Sylva-Steenland RMR, Bos JD, Kapsenberg ML, de Jong EC, Teunissen MBM. Cutting Edge: Loss of TLR2, TLR4, and TLR5 on Langerhans Cells Abolishes Bacterial Recognition1. The Journal of Immunology. 2007;178(4):1986-90.
52. Takeuchi J, Watari E, Shinya E, Norose Y, Matsumoto M, Seya T, et al. Down-regulation of Toll-like receptor expression in monocyte-derived Langerhans cell-like cells: implications of low-responsiveness to bacterial components in the epidermal Langerhans cells. Biochemical and Biophysical Research Communications. 2003;306(3):674-9.
53. Aiba S, Terunuma A, Manome H, Tagami H. Dendritic cells differently respond to haptens and irritants by their production of cytokines and expression of co-stimulatory molecules. Eur J Immunol. 1997;27(11):3031-8.
54. Czarnobilska E, Obtułowicz K, Wsołek K, Pietowska J, Spiewak R. Mechanisms of nickel allergy. Przeglad lekarski. 2007;64(7-8):502-5.
55. Chipinda I, Hettick JM, Siegel PD. Haptenation: chemical reactivity and protein binding. Journal of allergy. 2011;2011.
56. Rustemeyer T, Van Hoogstraten IM, Von Blomberg BME, Scheper RJ. Mechanisms of allergic contact dermatitis. Kanerva's occupational dermatology. 2020:151-90.
57. Kuroishi T, Bando K, Bakti RK, Ouchi G, Tanaka Y, Sugawara S. Migratory dendritic cells in skin-draining lymph nodes have nickel-binding capabilities. Scientific Reports. 2020;10(1):5050.
58. Thierse H-J, Gamerdinger K, Junkes C, Guerreiro N, Weltzien HU. T cell receptor (TCR) interaction with haptens: metal ions as non-classical haptens. Toxicology. 2005;209(2):101-7.
59. Ochoa MT, Loncaric A, Krutzik SR, Becker TC, Modlin RL. "Dermal Dendritic Cells" Comprise Two Distinct Populations: CD1+ Dendritic Cells and CD209+ Macrophages. Journal of Investigative Dermatology. 2008;128(9):2225-31.

60. Hagman DK, Kuzma JN, Larson I, Foster-Schubert KE, Kuan LY, Cignarella A, et al. Characterizing and quantifying leukocyte populations in human adipose tissue: impact of enzymatic tissue processing. J Immunol Methods. 2012;386(1-2):50-9.
61. Ford AL, Foulcher E, Goodsall AL, Sedgwick JD. Tissue digestion with dispase substantially reduces lymphocyte and macrophage cell-surface antigen expression. Journal of Immunological Methods. 1996;194(1):71-5.
62. Autengruber A, Gereke M, Hansen G, Hennig C, Bruder D. Impact of enzymatic tissue disintegration on the level of surface molecule expression and immune cell function. European Journal of Microbiology and Immunology. 2012;2(2):112-20.
63. Abuzakouk M, Feighery C, O'Farrelly C. Collagenase and Dispase enzymes disrupt lymphocyte surface molecules. J Immunol Methods. 1996;194(2):211-6.
64. Pan J, Ju D, Wang Q, Zhang M, Xia D, Zhang L, et al. Dexamethasone inhibits the antigen presentation of dendritic cells in MHC class II pathway. Immunology Letters. 2001;76(3):153-61.
65. Piemonti L, Monti P, Allavena P, Sironi M, Soldini L, Leone BE, et al. Glucocorticoids Affect Human Dendritic Cell Differentiation and Maturation1. The Journal of Immunology. 1999;162(11):6473-81.
66. Popoviciu MS, Kaka N, Sethi Y, Patel N, Chopra H, Cavalu S. Type 1 Diabetes Mellitus and Autoimmune Diseases: A Critical Review of the Association and the Application of Personalized Medicine. Journal of Personalized Medicine. 2023;13(3):422.
67. Kamata M, Tada Y. Dendritic Cells and Macrophages in the Pathogenesis of Psoriasis. Frontiers in Immunology. 2022;13.

2.3 Incorporating immune cell surrogates into a full-thickness tissue equivalent of human skin to characterize dendritic cell activation

Johanna Maria Hölken[1], Anna-Lena Wurz[1], Katja Friedrich[1], Patricia Böttcher[2], Dounia Asskali[1], Holger Stark[3], Jörg Breitkreutz[4], Timo Buhl[5], Lars Vierkotten[2], Karsten Rüdiger Mewes[2], Nicole Teusch[1]

[1]Institute of Pharmaceutical Biology and Biotechnology, Heinrich Heine University Düsseldorf, Universitätsstr.1, 40225 Düsseldorf, Germany

[2]Henkel AG & Co. KGaA, Henkelstr. 67, 40589 Düsseldorf, Germany

[3]Institute of Pharmaceutical and Medicinal Chemistry, Heinrich Heine University Düsseldorf, Universitätsstr.1, 40225 Düsseldorf, Germany

[4]Institute of Pharmaceutics and Biopharmaceutics, Heinrich Heine University Düsseldorf, Universitätsstr.1, 40225 Düsseldorf, Germany

[5]Department of Dermatology, Venereology and Allergology, University Medical Center Göttingen, Robert-Koch-Straße 40, 37099 Göttingen, Germany

Submitted to: *Scientific reports*

Keywords: Full-thickness skin model, skin equivalent, Langerhans cells, dermal dendritic cells, CD1a, CD207

Own contributions to the manuscript: **65%**

- Conceptualization of the experiments (70%) together with Nicole Teusch
- Methodology (70%), Investigation (50%), Validation (100%), Data curation (100%), Formal analysis (100%) and Visualization (98%)
- Investigation of the following experiments:
    - Surface marker characterization of Mutz-LCs (70%) together with Anna-Lena
    - Western Blots to determine the sensitizer induced activation of the NF-κB and p38 MAPK pathway (60%), together with Anna-Lena
    - qPCR to determine the sensitizer-induced mRNA levels of (pro)-inflammatory cytokines/chemokines (100%)
    - Engineering of the LC/ LC+DDC models (60%) together with Anna-Lena
    - Cryosectioning and IF-staining of the skin models (30%) together with Anna-Lena and Katja Friedrich
    - Enzymatic dissociation of the skin models (20%) together with Katja Friedrich, Anna-Lena and Dounia Asskali
    - qPCR to determine the mRNA levels in the LC-models before and after sensitizer/drug treatment (30%) together with Anna-Lena
    - whole slide imaging and quantification (60%) together with Anna-Lena and Dounia Asskali
- Writing and drafting the manuscript (100%)

Abstract

Background: In the past decades studies investigating the dendritic cell (DC) activation have been conducted almost exclusively in animal models. However, due to species-specific differences in the DC subsets, there is an urgent need for alternative *in vitro* models allowing the investigation of Langerhans cell (LC) and dermal dendritic cell (DDC) activation in human tissue. Methods: We have engineered a full-thickness (FT) human skin tissue equivalent with incorporated LC surrogates derived from the human myeloid leukemia-derived cell line Mutz-3, and DDC surrogates generated from the human leukemia monocytic cell line THP-1. **Results:** Topical treatment of the skin models encompassing Mutz-LCs only with nickel sulfate ($NiSO_4$) or 1-chloro-2,4-dinitrobenzene (DNCB) for 24 h resulted in significant higher numbers of CD1a positive cells in the dermal compartment, suggesting a sensitizer-induced migration of LCs. Remarkably, exposure of the skin models encompassing both, LC and DDC surrogates, revealed an early sensitizer-induced response reflected by increased numbers of CD1a positive cells in the epidermis and dermis after 8 h of treatment. **Conclusion:** Our human skin tissue equivalent encompassing incorporated LC and DDC surrogates allows the investigation of DC activation, subsequent sensitizer identification and drug discovery according to the principles of 3R.

Introduction

The key players of the cutaneous immune response include epidermal and dermal dendritic cells [1]. Epidermal dendritic cells, known as Langerhans cells (LCs), are located predominantly suprabasal in the stratum spinosum with extended cell protrusions reaching into the stratum corneum [2, 3]. Dermal dendritic cells (DDCs) are located throughout the dermis, but mostly underneath the epidermal-dermal junction [4]. In fact, due to their epidermal location, Langerhans cells were considered for a long time to function as the exclusive key regulators of the cutaneous immune response. However, contact hypersensitivity studies (CHS) in LC-deficient mouse models led to the concept of three different outcomes, varying from a diminished sensitization [5] to an enhanced sensitization [6] and an unchanged response, proposing LCs to be dispensable for CHS [7]. Furthermore, a central role for dermal dendritic cells in contact hypersensitivity was suggested as dermal dendritic cells were found to colonize in distinct areas of the lymph node. Studies indicate that DDCs might migrate faster and significantly outnumber LCs in lymph nodes [7]. However, these studies were exclusively conducted in mice and therefore limited in terms of prediction. Noteworthy, an overlap of only ~30% of skin associated genes was identified comparing the mouse and the human genome [8].

The genetic discrepancy as well as fundamental differences in skin anatomy and in cutaneous immune cell populations, particularly in dendritic cell subsets, might explain translation failures from murine models to the human system [9]. As species-specific differences lead to controversial discussions regarding the precise roles and molecular events of both dermal dendritic cell types in human skin immunity and contact hypersensitivity, there is an urgent need for alternative *in vitro* models allowing the investigation of the human immune response according to the criteria of the 3R principles ("replace", "reduce", "refine"). In the past years, skin equivalents containing Langerhans cell surrogates derived from $CD14^+$ peripheral blood mononuclear cells (PBMCs) [10, 11], from cord-blood-derived $CD34^+$ hematopoietic progenitor cells [12, 13] or from the human myeloid leukemia-derived cell line Mutz-3 [11, 14-16] have been reported. Accordingly, in our recent study we were able to generate a human immune competent full-thickness (FT) skin model by incorporating functional dermal dendritic cell surrogates derived from the monocytic cell line THP-1 allowing the qualitative identification of potential sensitizers or drug candidates [17]. However, to date, only one human FT skin model including LC as well as DDC surrogates, both derived from $CD14^+$ PBMCs, has been described for analyzing the impact of ultraviolet (UV) stress on cutaneous immune cells [10]. According to our knowledge, no human FT skin model comprising functional LC and DDC surrogates aiming at exploring skin sensitization or inflammation has been reported yet although both DC cell types are considered to be crucial mediators regulating skin immunity and homeostasis.

Upon cutaneous infectious, inflammatory or sensitizing stimuli, such as nickel sulfate ($NiSO_4$) or 1-chloro-2,4-dinitrobenzene (DNCB), LCs as well as DDCs capture and phagocytose the hapten-protein complex, undergo a maturation process, which is accompanied by the induction of several molecular pathways, and migrate to skin draining lymph nodes to subsequently activate T cells [1, 18]. LCs are mainly characterized by a distinctively high expression of Cluster of Differentiation (CD)1a and CD207 (also named Langerin) [19, 20]. While the function of CD1a and CD207 surface marker expression on LCs still remains elusive, several studies indicate antigen presenting roles for both surface markers [21-26]. CD207/ Langerin is not only expressed on the cell surface but has been identified as the main molecular component of Birbeck granules, which are formed as subdomains of endosomal recycling compartments upon langerin accumulation [27], suggesting the role in antigen uptake and degradation. So far, the potential to recognize, uptake and degrade viral particles, glycoproteins and glycolipid antigens has been described [21-23]. Furthermore, a CD1a mediated antigen presentation of lipid antigens to T cells, promoting skin inflammation, was shown in various studies [24-26]. In steady state conditions, it is presumed that the adhesion of Langerhans cells to keratinocytes is mediated by E-cadherin [28]. Upon LC differentiation and maturation, the E-cadherin expression is proposed to become downregulated [29, 30] and the expression of CXC chemokine receptor type 4 (CXCR4) is induced for a stromal cell-derived factor 1 (SDF-1)

(secreted by fibroblasts) mediated migration to the dermis [31, 32]. In LCs and DDCs, phagocytosis of hapten-protein complexes is accompanied by the upregulation of the major histocompatibility complex (MHC) class II, such as the Human Leukocyte Antigen–DR isotype (HLA-DR), required for the presentation of antigens to $CD4^+$ T cells [33]. Furthermore, high expressions of the maturation markers Cluster of Differentiation (CD)80 and CD86 are induced and essential for the co-stimulation of naïve $CD4^+$ T cells via their CD28 and cytotoxic T-lymphocyte-associated protein 4 (CTLA-4)/(CD152) receptors [34]. In addition, high expression of CD83 stimulates the CD86 surface marker expression and stabilizes the MHC II surface expression on activated DCs, thereby promoting the stimulation, proliferation, and maturation of naïve $CD4^+$ T cells [35, 36].

In summary, we have engineered a human immune competent full-thickness skin model encompassing incorporated and functional DDC surrogates, described earlier as THP-1-derived $CD14^-$, $CD11c^+$ immature dendritic cells (iDCs) [17, 37] on one hand, and containing $CD1a^+$, $CD207^+$ LC surrogates derived from the human myeloid leukemia-derived cell line Mutz-3 on the other hand, allowing the molecular characterization of human DC activation *in vitro* upon compound treatment according to the 3R criteria.

Results

Langerhans cells are primarily distinguished from other dendritic cell subtypes by their pronounced CD207/Langerin and CD1a expression [19, 20].

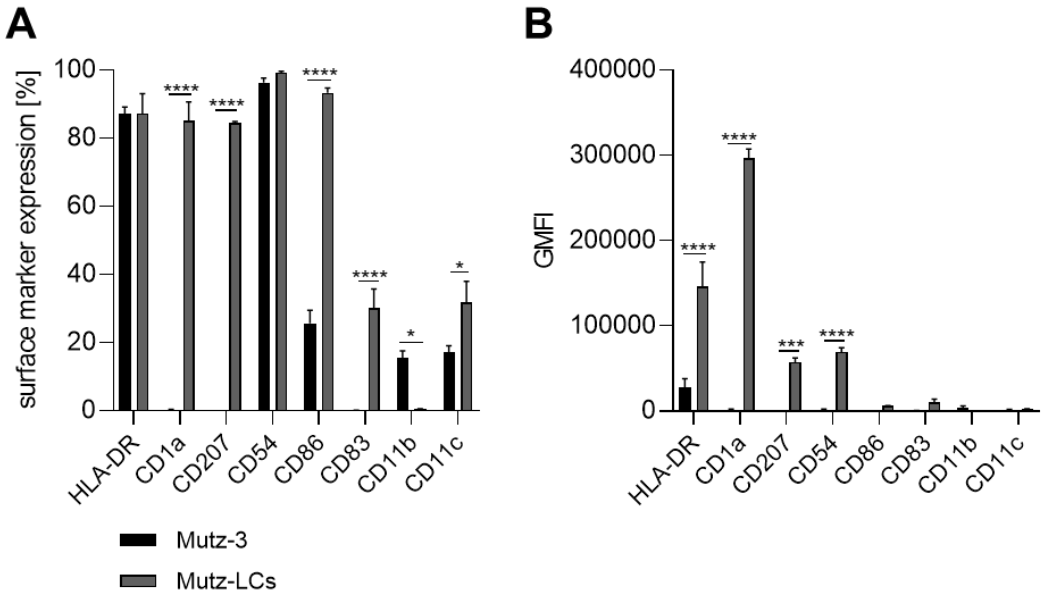

Figure 2.3-1 Surface marker expression of undifferentiated Mutz-3 cells and Mutz-LCs. **(A)** Surface marker expression depicted as percentage of positive cells **(B)** Surface marker expression depicted as geometric mean fluorescence intensity (GMFI). Here, Mutz3 cells were differentiated into Mutz-LCs with 1000 U/mL GM-CSF, 400 U/mL TGF-β and 100 U/mL TNF-α for 9 days. Surface marker expression of at least 10,000 viable cells was analyzed via flow cytometry. Error bars indicate the standard errors of the mean (n = 3 independent experiments with * = $p \leq 0.05$, *** = $p \leq 0.001$, and **** = $p \leq 0.0001$).

The successful differentiation of Mutz-3 cells into LC surrogates in the presence of GM-CSF, TGF-β and TNF-α was proven by the induction of CD1a (~85%) and CD207 (~84.5%) surface marker expression compared to control. In addition, the expression of CD86 (~3.6-fold), CD83 (~158-fold) and CD11c (~1.9-fold) could also be significantly increased (Figure 2.3-1A). Moreover, the geometric mean fluorescence intensity (GMFI), depicting the brightness and relative measure of antigen abundance, was significantly enhanced for HLADR (~5.2-fold), CD1a (~221-fold), CD207 (157~fold) and CD54 (~41-fold) (Figure 2.3-1B). In line with previously published marker expression patterns for LC surrogates after treatment with skin sensitizers [38], we were able to induce a significant increase in the number of CD83 positive cells (~3.0-fold) and a significant increase of the GMFI for HLA-DR (~3.2-fold) after $NiSO_4$ treatment [380 µM] for 24 h. However, DNCB [20 µM] treatment led only to minor increase in the number of CD83 positive cells (~1.5-fold) and a minor increase of the GMFI for HLA-DR (~1.3-fold). In contrast, compared to the solvent control, the GMFI for CD1a was significantly decreased 24 h after exposure to $NiSO_4$ [380 µM] (~1.8-fold) or DNCB [20 µM] (~2.0-fold) (Supplementary Figure 2.3-1).

Alongside the mentioned changes in the LC-specific and DC-specific activation and maturation markers, it is known for DCs that sensitization and activation is accompanied by sensitizer-specific activation of distinct inflammatory pathways such as the nuclear factor (NF)-κB and the p38 mitogen activated protein kinase (MAPK) pathways [17, 39-41]. Moreover, loss of function studies revealed, that the activation of the NF-κB pathway via IκBα degradation upon treatment with nickel salts and the phosphorylation of p 38 MAPK upon DNCB exposure is crucial for the upregulation of CD80, CD86 and CD83 and therefore fundamentally involved in the maturation of DCs [39, 41]. However, this was proven for various DC surrogates, including DDCs [17, 38-41], but not for Mutz-LCs yet. To confirm the activation of the signaling pathways mentioned, Mutz-LCs were treated with either $NiSO_4$ [500 µM] for 1 h or DNCB [25 µM] for 30 min. Compared to the control, treatment of Mutz-LCs with $NiSO_4$, but not with DNCB, resulted in a significant degradation of IκBα (~1.6-fold). In contrast, while treatment with DNCB led to a significant phosphorylation of p38 MAPK (~3.8-fold) in Mutz-LCs, treatment with $NiSO_4$ resulted only in a minor phosphorylation induction of p38 MAPK (~1.4-fold) (Figure 2.3-2). Hence, Mutz-3 derived LC surrogates reveal a similar sensitizer-specific induced activation pattern of intracellular inflammatory pathways, namely NF-κB and p38 MAPK, as published for DCs, including DDC surrogates [17, 38-41], suggesting a fundamental role of both pathways in the maturation of LCs as well.

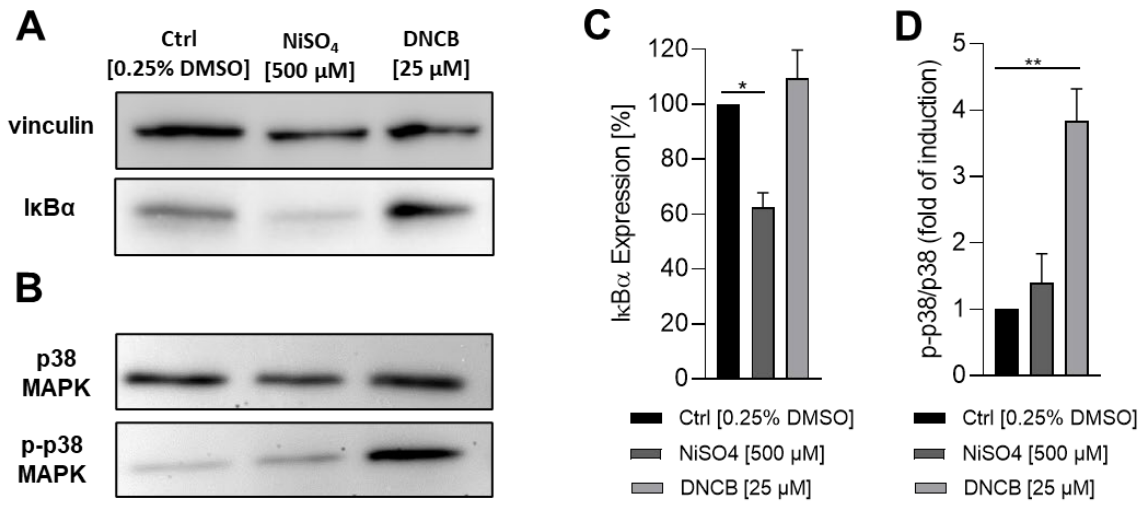

Figure 2.3-2 Degradation of IκBα after $NiSO_4$ [500 µM] and DNCB [25 µM] treatment for 1 h **(A & C)** and phosphorylation of p38 MAPK after $NiSO_4$ [500 µM] and DNCB [25 µM] treatment for 30 min **(B & D)**. **(A)** and **(B)** depict one representative blot of three independent experiments. **(C)** and **(D)** Quantification of image bands normalized to the solvent control. Error bars indicate the standard errors of the mean (n = 3 independent experiments with * = $p \leq 0.05$ and ** = $p \leq 0.01$).

Furthermore, loss of function studies for the NF-κB and the p38 MAPK pathway in PBMC as well as in cord-blood derived DCs, revealed the central role of both pathways in the secretion of inflammatory cytokines such as interleukin (IL)-1, IL-8 or IL-12p40 [39-41], required for T cell activation in cutaneous CHS [42-44]. In line, former studies confirmed the sensitizer induced upregulation of IL-8, IL-6 and IL-12p40 in dermal dendritic cell surrogates [17, 37]. To prove whether Mutz-LCs are capable to upregulate inflammatory cytokines after sensitizer treatment, mRNA levels of IL-6, IL-8, TNF-α, IL-1α and IL-1β and IL-12p40 were analyzed (Figure 2.3-3). Treatment of Mutz-LCs with $NiSO_4$ [380 µM] resulted in significant higher mRNA levels of IL-8 (~11.5-fold), IL-1α (~5.6-fold) and IL-1-β (~6.6-fold), but only in a minor induction for IL-6 (~2.5-fold). Treatment with DNCB [25 µM] revealed significant higher mRNA levels of IL-6 (~14.7-fold) and IL-8 (~13.7-fold), but only a minor induction of IL-1α (~2.2-fold) and no significant change for IL-1β mRNA levels. Furthermore, both DNCB and $NiSO_4$ treatment of Mutz-LCs lowered mRNA levels for TNF-α ($NiSO_4$: 2.7-fold; DNCB: ~6-fold). Comparable to dermal dendritic cell surrogates [37], Mutz-LCs treated with DNCB upregulated mRNA levels of IL-12p40 significantly, while treatment with $NiSO_4$ led only to a minor induction of IL-12p40 ($NiSO_4$: ~1.7-fold; DNCB: ~13-fold) (Figure 2.3-3). Overall, depending on the applied sensitizer, Mutz-LCs might be able to secrete inflammatory cytokines essential for the activation and recruitment of T cells in the skin.

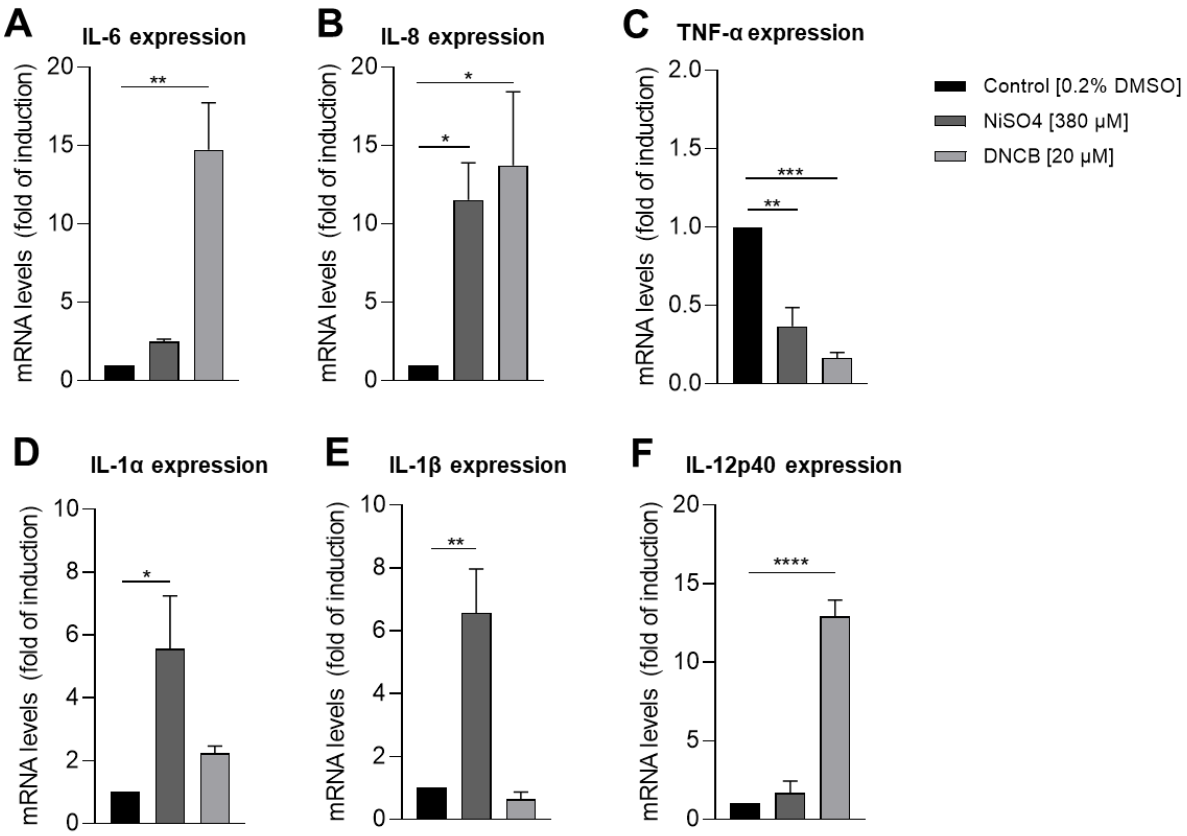

Figure 2.3-3 mRNA levels of inflammatory cytokine expression by Mutz-LCs: **(A)** IL-6, **(B)** IL-8, **(C)** TNF-α **(D)** IL-1α, **(E)** IL-1β and **(F)** IL-12p40, after $NiSO_4$ [380 µM] and DNCB treatment [25 µM] for 6 h. Results are depicted as fold of induction compared to the solvent control [0.2% DMSO] and normalized to the expression of the housekeeping gene [GAPDH]. Error bars indicate the standard errors of the mean (n = 3 independent experiments with * = $p \leq 0.05$, ** = $p \leq 0.01$, *** = $p \leq 0.001$, and **** = $p \leq 0.0001$).

After confirming the ability of isolated Mutz-LCs to demonstrate a molecular Langerhans cell response in the presence of common sensitizers such as $NiSO_4$ and DNCB in 2D, we integrated the Mutz-LCs into the engineered skin equivalent. In line with published data [11, 14, 15], we were able to integrate Mutz-3 derived LC surrogates into the epidermis of the skin model. Integration of Mutz-LCs did not impair the epidermis (Figure 2.3-4A). The integrated Mutz-LCs were identified and visualized via immunofluorescence staining with CD1a. (Figure 2.3-4B). When compared to the regular skin models, integration of Mutz-LCs resulted in a significant upregulation of mRNA levels for CD1a, CD207, CD86, CD83 and IL-1β in the epidermis. mRNA levels of E-cadherin, IL-8 and CXCR4 were only slightly increased after the integration of Mutz-LCs. CCR7 mRNA levels could not be detected in the epidermis, even after incorporating Mutz-LCs (Figure 2.3-4C). Similar to the epidermis, integration of Mutz-LCs significantly increased mRNA levels of CD1a, CD207 and CD86 in the dermis, but there was no influence on the mRNA levels of CD83, CXCR4, CCR7, IL-1β and IL-8 (Figure 2.3-4D). Hence, integration of Mutz-LC surrogates did not change the epidermal differentiation. Most importantly, the LC integration did not lead to an increase of the pro-inflammatory IL-8, related

to the severity of skin inflammation [45] and therefore often used as a biomarker for sensitizer identification [46, 47].

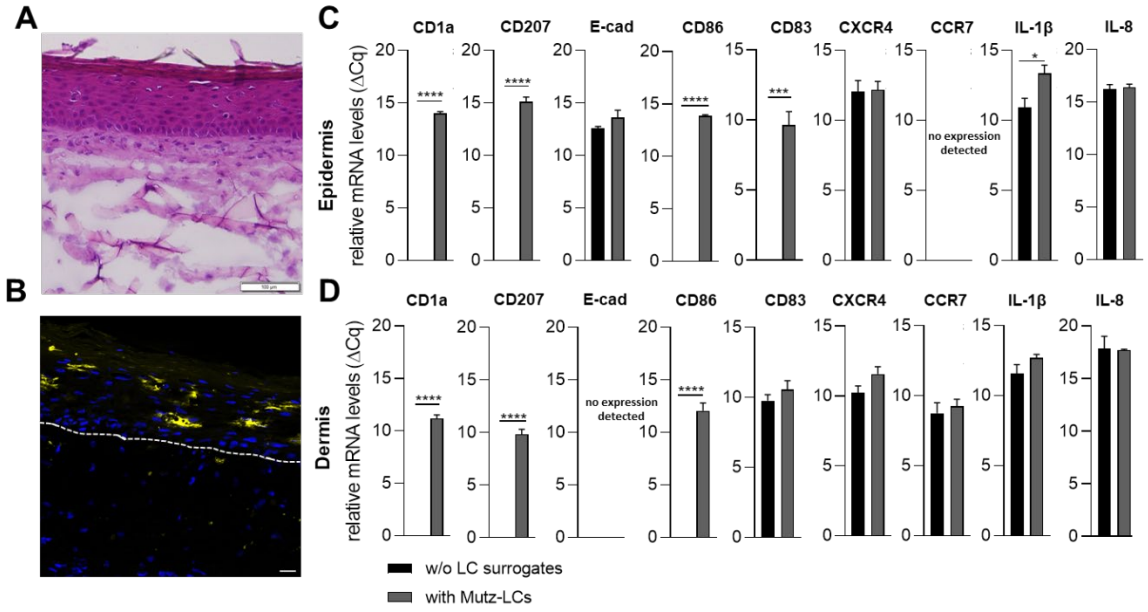

Figure 2.3-4 Integration of Mutz-LCs into a full-thickness skin model. **(A)** H&E staining of the full-thickness skin model including LC surrogates. Scale Bar = 100 µm. **(B)**: Immunofluorescent staining skin model including LC surrogates. LC surrogates were stained with CD1a (yellow signal) and nuclei were stained with DAPI (Blue signal). Scale bar = 20 µm. **(C-D)** Analysis of the relative mRNA levels (ΔCq) of LC markers, maturation and migration markers and cytokines expressed by the epidermal **(C)** and dermal **(D)** compartment in the regular full-thickness skin model vs. the full-thickness skin model with incorporated LC surrogates. Epidermis and dermis of the full-thickness model without and with incorporated LC surrogates were separated and dissociated enzymatically and RNA was extracted for cDNA synthesis for RT-qPCR. Error bars indicate the standard errors of the mean (n=3 independent experiments with * = $p \leq 0.05$, *** = $p \leq 0.001$ and **** = $p \leq 0.0001$)

To prove the functionality and immune competence of the LC surrogates in the tissue equivalent, the skin models were treated topically with either $NiSO_4$ [380 µM], DNCB [20 µM] or the solvent control DMSO for 24 h. In line with reported studies, but to our knowledge the first to quantify whole slide images, we were able to prove significant lower numbers of CD1a positive cells in the epidermis (~1.7-fold) and a pronounced higher number of CD1a positive cells in the dermal compartment (~1.3-fold) after $NiSO_4$ treatment compared to the solvent control (Figures 2.3-5A, B). Furthermore, a comparable trend of a lower number of CD1a positive cells in the epidermis (~1.1-fold) and higher numbers of CD1a positive cells in the dermis (~1.2-fold) was found after DNCB treatment (Figures 2.3-5 A, B). Notably, whole slide image quantification of the CD1a signal revealed significant higher numbers of CD1a positive cells in the dermis compared to the respective epidermal compartment after $NiSO_4$ (~2.4-fold) as well as after DNCB (~1.6-fold) treatment (Figures 2.3-5 C), suggesting a sensitizer-induced migration of CD1a positive LC-surrogates.

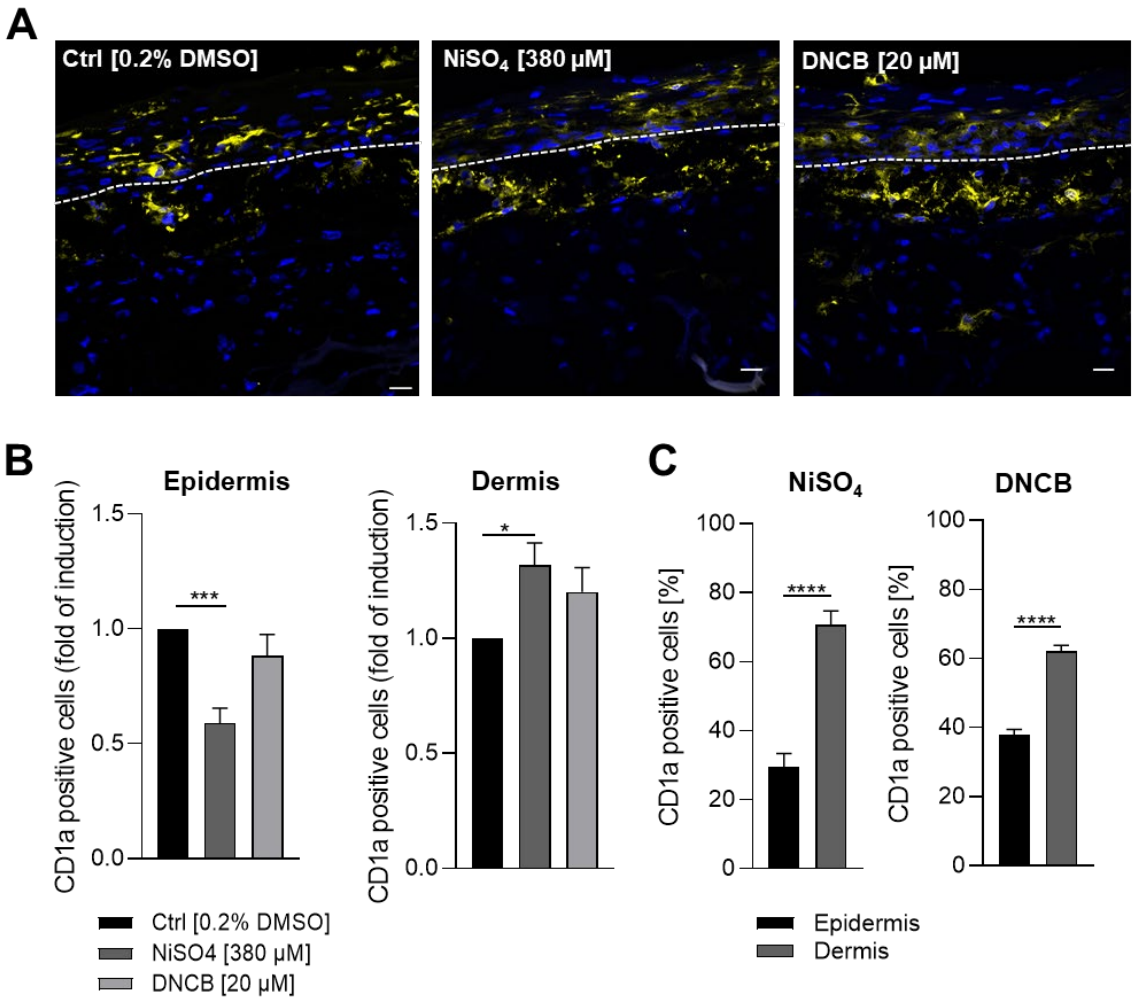

Figure 2.3-5 Histological analysis of the full thickness skin model with incorporated LC surrogates. Skin models were topically treated with $NiSO_4$ [380 µM] and DNCB [20 µM] for 24 h. **(A)** Immunofluorescent staining of the full-thickness skin model tissue including LC surrogates after treatment with solvent control or sensitizers. LC surrogates were stained with CD1a (yellow signal). Nuclei were stained with DAPI (blue signal). Scale bar = 20 µm. Sensitizer induced migration of the LC surrogates from the epidermis to the dermal compartment was quantified via whole slide image analysis and depicted as fold of induction for CD1a positive cells in the epidermis and dermis compared to the solvent control **(B)** and as distribution in percentage **(C)**. Error bars indicate the standard errors of the mean (n=3 independent experiments with * = $p \leq 0.05$, ** = $p \leq 0.01$ and *** = $p \leq 0.001$)

So far, the presumed molecular events of LC activation, maturation and migration were mostly concluded from *in vivo* experiments in mice, which do not represent the cutaneous anatomy and immune cell population of human skin [9]. To investigate these molecular events in the engineered skin tissue equivalent after incorporating LC surrogates, we analyzed the mRNA levels in the epidermal versus the dermal compartment of LC specific markers (CD1a, CD07), of maturation markers (CD83, CD86), of markers assumed to be involved in migration (E-cadherin, CXCR4 and CCR7) and of inflammatory cytokines (IL-1β, IL-8) 24 h after topical treatment with $NiSO_4$ [380 µM] or DNCB [20 µM]. Results of the ΔΔCt values are indicated as fold of induction compared to the solvent control and normalized to the housekeeping gene (GAPDH) (Figures 2.3-6A, C). The proportional changes for each marker analyzed, was calculated as the Log2 fold change, outlining the upregulation (+1) and downregulation (-1) of

the mRNA levels for each specific marker compared to the solvent control, and illustrated in the form of a heatmap (Figures 2.3-6B, D). First of all, topical DNCB treatment of the skin model with incorporated LC surrogates led to significant lower CD1a (~1.5-fold) and CD207 (~1.6-fold) mRNA levels in the epidermis and 1.2-fold induced mRNA levels in the dermis for CD1a and CD207 compared to the solvent control. Similarly, treatment with $NiSO_4$ resulted in a significant decrease of mRNA levels for CD1a (~2.2-fold) and CD207 (~2.5-fold) in the epidermis and a in a significant increase in the dermis (CD1a: ~1.5-fold, CD207: ~1.6fold) (Figure 2.3-6), thereby confirming the results of the whole slide image analysis (Figure 2.3-5), suggesting a sensitizer-induced migration of our LC-surrogates. Furthermore, mRNA levels for E-cadherin, which is expressed by keratinocytes and required for the selective adhesion of epidermal cells [48] and presumed to be involved in the localization and mobilization of LCs in the epidermis [29], were significantly decreased after $NiSO_4$ (~2.3-fold) and DNCB (~2-fold) treatment. While treatment of the FT skin model with $NiSO_4$ induced a significant decrease of CD86 (~1.9-fold) and a significant increase of CD83 (~1.5-fold), mRNA levels in the epidermis, DNCB treatment caused a 1.5-fold decrease of CD86 and a 1.1-fold increase of CD83 mRNA levels in the epidermis. However, treatment with both sensitizers was accompanied by significant decreased mRNA levels of CD83 (~1.7-fold) in the dermis. Notably, after treatment with $NiSO_4$ as well as with DNCB the mRNA levels for the migration markers CXCR4 ($NiSO_4$: ~2.4-fold, DNCB: ~3.5fold) and CCR7 ($NiSO_4$: ~1.8-fold, DNCB: ~2fold) are decreased significantly in the dermal compartment. Furthermore, mRNA levels for IL-8, which is known to play a crucial role in skin sensitization and inflammation [45], were significantly increased after DNCB treatment in the epidermal (~2.1-fold) and dermal (~2.6-fold) compartment and after $NiSO_4$ treatment in the dermal (~1.5-fold), but not in the epidermal compartment (Figures 6A, C). Treatment of the LC surrogate skin models with sensitizers for 24 h led to a noticeable decrease of mRNA levels for IL-1β (~1.5-fold), which is proposed to be one of the first cytokine secreted in response to topical allergens (~15 min after exposure) [49].

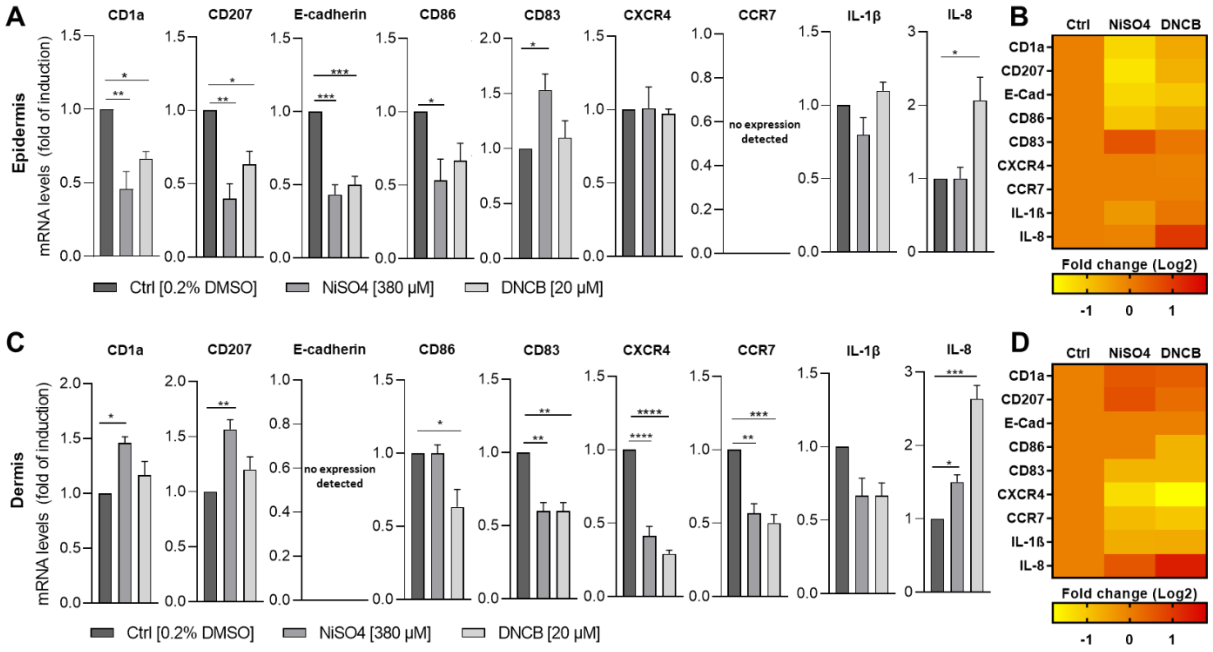

Figure 2.3-6 Analysis of the mRNA levels of LC markers, maturation and migration markers and cytokines expressed by the epidermal **(A-B)** and dermal **(C-D)** compartment in the regular full-thickness skin model vs. the full-thickness skin model with incorporated LC surrogates after topical application of sensitizers. 24 h after application of $NiSO_4$ [380 µM] or DNCB [20 µM] the regular full-thickness skin models and the full-thickness skin models with incorporated LC surrogates were separated into epidermis and dermis and mechanically and enzymatically dissociated. RNA was extracted for cDNA synthesis for RT-qPCR. **(A & B)** Results are depicted as fold of induction/ fold change compared to the solvent control [0.2% DMSO] and normalized to the expression of the housekeeping gene [GAPDH]. **(C & D)** Heatmap of the RT-qPCR analysis as fold change (Log2). Error bars indicate the standard errors of the mean (n=3 independent experiments with * = $p \leq 0.05$, *** = $p \leq 0.001$ and **** = $p \leq 0.0001$).

Finally, to model immune cell surrogates in the epidermis and the dermis, we incorporated both, LC surrogates and DDC surrogates into the skin. Immunofluorescence staining (Figure 2.3-7A) revealed the successful integration of Mutz-3 derived LC surrogates in the epidermis and the integration of THP-1 derived iDCs as DDC surrogates in the dermis. However, compared to the skin model containing Mutz-LC surrogates only (Figure 2.3-5), sensitizer treatment of the skin models encompassing both, LC and DDC surrogates, did not lead to an increased number of CD1a positive cells in the epidermis or dermis after 24 h of treatment. Remarkably, whole slide image analysis revealed a significant increase of CD1a positive cells in the epidermal and dermal compartment after 8 h of treatment with 380 µM $NiSO_4$ (epidermis: ~1.7-fold; dermis: ~2.3-fold) and 20 µM DNCB (epidermis: ~3.3-fold, dermis: ~2.7-fold) (Figure 2.3-7B). However, the total number and localization of integrated LCs and therefore the quantity of migrating LCs within two biological replicates as can vary (Figure 2.3-7B). Nevertheless, computing the relative number (fold of induction) of CD1a positive cells in the epidermal and dermal compartment before and after $NiSO_4$/ DNCB treatment, the results show the same trend indicating a significant sensitizer induced migration of LCs from the epidermis to the dermis, overall. Hence, incorporation of DDC and LC surrogates leads to an early (8 h) sensitizer induced increase of CD1a positive cells in the

epidermis and dermis, which, compared to the models with Mutz-LCs only, appears to be diminished after 24 h of treatment.

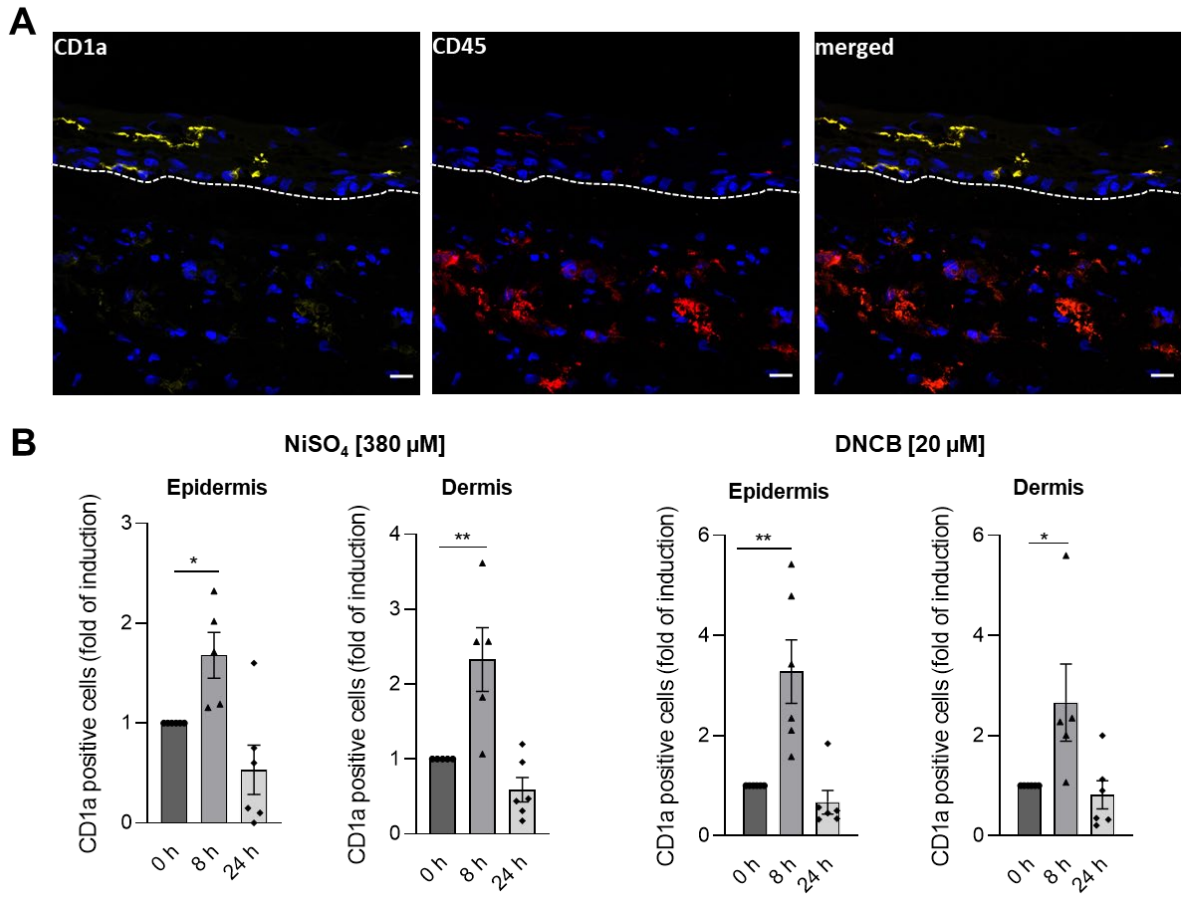

Figure 2.3-7 Histological analysis of the full-thickness skin model with incorporated LC surrogates and DDC surrogates. **(A)** Immunofluorescent staining of the immune competent full-thickness skin model including LC and DDC surrogates. LC surrogates were stained with CD1a (yellow signal). DDC surrogates were stained with CD45 (red signal) and Nuclei were stained with DAPI (Blue signal). Scale bar = 20 µm. **(B)** Quantification of the CD1a signal after topical treatment with $NiSO_4$ and DNCB for 0h, 8 h, and 24 h was achieved via whole slide image analysis and depicted as fold of induction of CD1a positive cells for the epidermal compartment and the dermal compartment. Error bars indicate the standard errors of the mean (n = 3) independent experiments with each two technical replicates and with * = $p \leq 0.05$ and ** = $p \leq 0.01$).

Discussion

The aim of this study was to integrate LC surrogates derived from the human myeloid leukemia cell line Mutz-3, and DDC surrogates derived from the human leukemia monocytic cell line THP-1 into a FT skin model. To this date, distinct protocols for the differentiation of Mutz-3 cells and the integration of Mutz-3 derived LC surrogates have been described by various sources [14, 15, 50]. In line with the published literature, we confirmed the differentiation of Mutz-3 cells into LC surrogates by a high expression (>85%) for both LC specific markers CD1a and CD207. While most of the published protocols obtain a number of CD1a positive cells between 34-89% and of CD207 positive cells between 24-73%[14, 15, 51, 52] after 7-10

days of differentiation using differentiation medium supplemented with 20% fetal bovine serum (FBS) [14-16, 51, 52], we were able to decrease the FBS concentration to 5% and yet obtaining a surface marker expression of >85% for CD1a as well as for CD207 after 9 days of differentiation without any medium exchange or additional cytokine supplementation. Thus, our differentiation protocol is favorable in terms of costs regarding the amount of FBS and cytokines used, as well as according to the 3R principle by reducing the FBS concentration considering the animal welfare concerns using FBS.

To validate the functionality *in vitro*, we exposed the Mutz-LCs to the two commonly used sensitizers $NiSO_4$ and DNCB and investigated the changes of the surface marker expression, activation of intracellular inflammatory pathways and expression of inflammatory cytokines. Similar to the results described for $CD1a^+$ and $CD207^+$ DCs derived from $CD34^+$ hematopoietic progenitor cells [38], but not yet for Mutz-LCs, treatment of our Mutz-LCs with $NiSO_4$ and DNCB resulted in an increased MFI for HLA-DR, but decreased MFI for CD1a and CD207. Due to the initially high expression of CD54 and CD86 (~99% and ~93%), the surface marker expression could only be increased marginally. However, in line with the published literature [53] a significant increase in the number of cells expressing the maturation marker CD83 was observed after $NiSO_4$ (3.0-fold) exposure. Furthermore, we could demonstrate a 1.5-fold induction in the number of CD83 positive cells after DNCB treatment, which was observed in a similar manner for $CD1a^+$ and $CD207^+$ DCs generated from cord blood derived $CD34^+$ cells [38]. Intriguingly, various studies demonstrated for DC surrogates derived from distinct cell types a fundamental role of the inflammatory pathways NF-κB and p38 MAPK in the sensitizer-induced upregulation of CD80, CD86 and CD83, as well as for the secretion of inflammatory cytokines such as IL-1, IL-6, IL-8 or IL-12 by DCs [17, 38-41]. We were able to prove the $NiSO_4$ induced activation of the NF-κB pathway via IκBα-degradation and the phosphorylation of p38 MAPK upon $NiSO_4$ as well as DNCB treatment in our Mutz-LCs, suggesting a similar activation manner for LCs as published for DCs, including DDCs, and confirming the expected ability to respond to sensitizers as required for DC activation.

Furthermore, we were interested in the sensitizer-induced responsiveness of Mutz-LCs via inflammatory cytokines. In fact, we could prove significantly increased mRNA levels for IL-6, IL-8 and IL-12p40 and minor increased mRNA levels for IL-1α upon DNCB exposure. Furthermore, treatment with $NiSO_4$ resulted in significantly increased mRNA levels for IL-8, IL-1α and IL-1β and minor increased mRNA levels for IL-6 and IL-12p40. Thus, in terms of inflammatory cytokines LCs respond again in a similar manner to $NiSO_4$ and DNCB exposure as published for various DC surrogates [17, 37, 39-41].

The integration of Mutz-3 derived LC surrogates into tissue-equivalents of the skin has been published previously [11, 14-16]. Furthermore, the migration of integrated Mutz-LCs upon $NiSO_4$ exposure was demonstrated, but the concentrations chosen for topical treatment with a

range from 6.5 mM to 19 mM are quite high [15, 16] and concentrations of 10-19 mM were required to induce a significant migration of $CD1a^+$ cells [15, 16]. Contrary, we were able to induce a significant reduction of $CD1a^+$ cells in the epidermis and a significant increase in the dermis after topical exposure of only 380 µM $NiSO_4$. While the mentioned LC-models were exposed to $NiSO_4$ for 16 h [15, 16], our LC-models were treated for 24 h. However, it seems unlikely, that additional 4 h of treatment result in such tremendous differences regarding the LC migration upon sensitizer treatment. Moreover, differences in the treatment concentrations required to induce a significant migration of $CD1a^+$ LC surrogates could be caused by various technical and biological aspects, due to the complexity that comes along with engineered tissue comprising multiple distinct cell types. In fact, it needs to be considered that the immune response is not alone mediated by the immune cells, but also by the keratinocytes and fibroblasts, secreting important cytokines and chemokines such thymic stromal lymphopoietin (TLSP) or CXCL12 [32, 54, 55]. Even though keratinocytes (KCs) and fibroblasts (FBs) from neonatal/ juvenile foreskin were used for all tissue equivalents [15, 16], donor variations leading to different epidermal thickness, number of epidermal layers or dermo-epidermal adhesion [56], may impact the immune response. Furthermore, despite the chosen cytokines (GM-CSF, TGF-β and TNF-α) for the differentiation were the same for all LC-models, differences in in the differentiation protocols, including the serum concentration (20% [11, 15, 16] vs. 5%), differentiation time (e.g., 7 days [15, 16] vs. 9 days). Furthermore, the seeding protocol for the tissue equivalents varies in the number of integrated LC surrogates (0.5×10^6 [15]-1 x 10^6 cells), the KC:LC ratio (1:2[16] vs. 1:1[15]) the matrix and collagen source (rat [15, 16] vs. bovine) of the dermis as well as in the media composition (+ serum (substitute) [15, 16] vs. no serum; + hydrocortisone [15, 16] vs. no hydrocortisone) of the ALI-medium. Indeed, crucial differences between the chosen dermis constructs can be identified. While for the published LC-models a simple hydrated collagen was used as matrix for the dermal compartment [11, 15, 16], our dermis is characterized by a solid, porous collagen matrix, which allows the fibroblasts to migrate into the scaffold and to synthesize and secrete extracellular matrix components such as elastin and fibrillin-1, mimicking the elastic network of native human skin [57, 58] and thereby potentially providing the required environment for LCs. However, the composition of the ALI medium, in particular the supplementation with hydrocortisone is most likely to be one of the major factors for the reported lower sensitivity and higher treatment concentration up to (10-19 mM [15, 16] vs. 380 µM $NiSO_4$) needed for the sensitization and induction of LC migration. In the cell culture hydrocortisone is utilized to support the growth and differentiation of keratinocytes and therefore commonly used for keratinocyte medium and engineering of skin models [58, 59]. However, hydrocortisone is a synthetic glucocorticoid, with anti-inflammatory properties frequently prescribed for inflammatory skin diseases such as CHS [60]. Moreover, DCs exposed to glucocorticoids

showed lower expression levels of CD80, CD83 and CD86 and IL-12, resulting in suppressed DC activation and maturation [61, 62].

Since in the past decades, studies investigating DC activation, including LCs and DDCs activation, have been conducted almost exclusively in animal models, mostly in mice, which do not display the human anatomy and LC/ DC subsets [9], we aimed to mimic and monitor the sensitizer-induced LC activation in our engineered immune competent tissue of the skin. Thus, after topical exposure to $NiSO_4$ or DNCB, the epidermis and dermis were separated and mRNA levels of LC specific markers, maturation and migration markers were determined. First of all, the migration of LC surrogates induced by the exposure of $NiSO_4$ and DNCB could be confirmed by significant lower mRNA levels of CD1a and CD207 in the epidermis and enhanced levels in the dermis. Furthermore, after topical application of both sensitizers, significant lower numbers of E-cadherin could be observed, contributing to the hypothesis that E-cadherin is involved in the retention and migration of LCs [48]. Even though we could confirm the sensitizer-induced LC migration from the epidermis to the dermis on protein and mRNA levels for CD1a, mRNA levels of the migration markers CXCR4 and CCR7 were significantly reduced in the dermal compartment after 24 h of exposure to $NiSO_4$ or DNCB. While Bock et al. could demonstrate a minor increase of CXCR4 mRNA levels in the dermal compartment upon DNCB treatment, they could not observe any significant induction of CXCR4 upon DNCB exposure of skin models with integrated LCs derived from Mutz-3 cells or from PBMCs [11]. However, analysis of the CXCR4 mRNA levels in the regular skin model without immune cells indicate that CXCR4 is highly expressed by keratinocytes and fibroblasts, and epidermal mRNA levels in the skin model with integrated Mutz-LCs are only marginally higher. Hence, the CXR4 expression of keratinocytes and fibroblasts could also be affected, making it difficult to formulate hypotheses that relate to LCs only. Notably, in line with the observed sensitizer-induced secretion of IL-8 by isolated LC surrogates [50], we could determine a significant increase of IL-8 mRNA levels in the dermal compartment upon $NiSO_4$ and DNCB exposure. In conclusion, we could elucidate that sensitization of Mutz-LCs is accompanied by similar molecular events observed in DC activation, including the activation of p38 MAPK and NF-κB as well as the increase in mRNA levels of IL-6, IL-8, IL-1 and IL-12p40. Furthermore, we could prove that our Mutz-3 derived LC surrogates can be integrated as functional LC surrogates, displaying the sensitizer-induced molecular events of maturation and migration not only in 2D, but also in a 3D tissue equivalent. Hence, our model can be used to study the molecular events of LC activation and maturation *in vitro* and potentially for sensitizer identification and drug discovery.

In a final step, we were able to integrate functional LC surrogates and DDC surrogates into the FT skin model. However, compared to the Mutz-LC model, exposure of the of the skin models comprising LC and DDC surrogates to $NiSO_4$ or DNCB for 24 h, did not lead to an increased

number of CD1a positive cells in the epidermis or dermis. Remarkably, after 8 h of treatment with $NiSO_4$ or DNCB, a significant increase of CD1a positive cells in the epidermal and dermal compartment could be observed. One vague hypothesis could be that due to the presence of DDCs, which have been proposed to migrate faster and in a larger number than LCs to the lymph nodes [7], some sort of crosstalk and transfer of the captured antigens by LCs to DDCs might occur, followed by LC apoptosis. In fact, Langerin mediated LC-DDC crosstalk and antigen transfer of HIV-1 has been reported [63]. In addition, it was proposed that LCs might transfer targeted antigens to DDCs [64]. In line with our results, *in vivo* sensitization studies conducted in guinea pigs, revealed an increase of LCs in the epidermis and dermis within 4-6 h after DNCB exposure, but first ultrastructural signs of cell damage in LCs 6-12 h after exposure and between 19-24 h a notably decrease in LC numbers [65]. Furthermore, exposure of human skin with nonanoic acid led to a significant decrease in Langerhans cells and induction of apoptosis after 24 h of treatment [66]. However, the precise molecular events, including the potential crosstalk between LCs and DDCs remains elusive.

Materials and Methods

Langerhans cell (LC) surrogates

Mutz-3 cells (DSMZ, #ACC 295, Braunschweig, Germany) were maintained at a cell density of 2 × 10^5 cells/mL in 12 well plates in MEM α (Gibco, # 12561056, Grand Island, NY, USA) supplemented with 20% FBS (Gibco, #22400089), 1% P/S (Gibco, #15140122), 0.05 mM 2-mercaptoethanol (Gibco, #21985023) and 200 U/mL rhGM CSF (ImmunoTools, #11343125, Friesoythe, Germany).

For the generation of LC surrogates 2 × 10^5 Mutz-3 cells/mL were seeded in 2 mL MEM α (Gibco, # 12561056) supplemented with 5% FBS (Gibco, #22400089), 1% P/S (Gibco, #15140122) and 0.05 mM 2-mercaptoethanol (Gibco, #21985023) into a 12-well plate. For differentiation, the following cytokines were added: 1000 U/mL rhGM-CSF (ImmunoTools, #11343125), 400 U/mL TGF-β (ImmunoTools, #11343160) and 100 U/mL TNF-α (PeproTech, #300-01A, Rocky Hill, NJ, USA). The cells were incubated for 9 days at 37 °C, 5% CO_2 without medium exchange.

Immature dendritic cell (iDC) surrogates

iDC were generated according to our previous protocol [37]. Briefly 2 × 10^5 THP-1 cells/ mL were differentiated with 1500 U/mL rhGM-CSF (ImmunoTools, #11343125) and 1500 U/ml IL-4 (ImmunoTools, #11340045) over 5 days with medium exchange on day 3.

Incorporation of Mutz-LCs and iDCs into full-thickness skin models

Feeder cells (Phenion, #hFeeder, Henkel AG & Co. KGaA, Düsseldorf, Germany) were seeded with 2.5 × 10^5 in 11 mL keratinocyte medium (Phenion, #K CM-250, Henkel AG & Co. KGaA) into a T75 flask. After three days 2.5 × 10^5 primary human foreskin keratinocytes from juvenile donors (Phenion, #hK P1, Henkel AG & Co. KGaA) were seeded onto the feeder cells. After 6 days of cultivation, feeder cells were detached by incubation with 0.05% trypsin (Gibco, #25300054) for 2 min at 37 °C, 5% CO and keratinocytes were harvested using 0.05% trypsin for 6 min, 37 °C, 5% CO_2. For Mutz-LC models, 2.5 × 10^5 keratinocytes in P2 were seeded together with 1 × 10^6 Mutz-LCs in 1 mL keratinocyte medium (Phenion, #K CM-250, Henkel AG & Co. KGaA) onto dermis models based on a solid and porous collagen matrix and primary human foreskin fibroblasts (kindly provided by Henkel AG & Co. KGaA, Düsseldorf, Germany). For Mutz LC + iDC models, 2.5 × 10^5 keratinocytes in P2 were seeded together with 5 × 10^5 Mutz-LCs and 5 × 10^5 THP-1 derived iDCs in 1 mL keratinocyte medium onto the dermis models. After 2 h of incubation at 37 °C, 5% CO_2, 2.5 × 10^5 freshly detached keratinocytes in were seeded in 1 mL keratinocyte medium on top of the Mutz-LC/ Mutz-LC + iDC models. After 24 h of incubation at 37 ° C, 5% CO the medium was exchanged. After further 24 h submerse phase, the skin models were lifted into the Air-liquid Interface (ALI) and cultivated with Air-liquid Interface Culture Medium (Phenion, #ALI CM HC-250, w/o hydrocortisone, Henkel AG & Co. KGaA) for 10 days. For treatment, sensitizers (380 µM $NiSO_4$ and 20 µM DNCB) or the respective solvent control (0.2% DMSO in PBS) were applied topically, by carefully pipetting 30 µl of the test substances onto the skin models.

Surface marker detection via flow cytometry

Cells were harvested after differentiation or treatment and washed in autoMacs Running Buffer (Miltenyi Biotec, #130-091-221, Gladbach, Germany). At least 1 × 10^5 cells for each antibody panel were transferred to 96-well u-bottom plates and incubated in Automacs Running Buffer with the following antibodies (1:50): REA Control (S)-VioGreen (Miltenyi Biotec, #130-113-444), REA Control (S)-PE (Miltenyi Biotec, #130-113-438), REA Control (S)-APC (Miltenyi Biotec, #130-113-434); REA Control (S)-PE-Vio770, (Miltenyi Biotec, #130-113-440); HLA-DR-VioGreen (Miltenyi Biotec, #130-111-948), CD1a-PE (Miltenyi Biotec, #130-112-022); CD207-PE-Vio770 (Miltenyi Biotec, #130-112-370), CD54-APC (Miltenyi Biotec, #130-121-342); CD86-APC (Miltenyi Biotec, #130-116-161), CD83-PE (Miltenyi Biotec, #130-110-561), CD11b-VioGreen (Miltenyi Biotec, #130-110-617), CD11c-APC (Miltenyi Biotec, #130-113-584) for 10 minutes in the dark. The cells were washed twice with autoMacs Running Buffer. To determine the cell viability, cells were stained with DAPI (10 µg/mL) (Sigma-Aldrich, #D9542, Darmstadt, Germany). Flow cytometry analysis was performed using the CytoFlex (B5-R3-V5) from Beckman Coulter (Brea, CA, USA).

Western blot analysis

2×10^5 Mutz-LCs/ mL were seeded in 4 mL MEM α supplemented with 5% FBS, 1% P/S and 0.05 mM 2-mercaptoethanol into a 12-well plate and treated with DNCB [25 µM] (Sigma-Aldrich, #237329) or $NiSO_4$ [500 µM] (Sigma-Aldrich, #227676) for 30 min or 1 h, respectively. Sample preparation, determination of protein concentrations, SDS-Page and western blotting was performed as published previously [17]. The following primary antibodies were used: phospho-p38 MAPK (Thr180/Tyr182) (Cell Signaling Technology, #4511T, Danvers, MA, USA), p38 MAPK (Cell Signaling Technology, #8690T), IκBα (Cell Signaling Technology, #9242S) and vinculin (Cell Signaling Technology, #13901S). Secondary antibody incubation was performed using the respective horseradish peroxidase-coupled secondary antibody (Goat anti-Rabbit (H+L), Thermo Fisher Scientific, #31460, Waltham, MA, USA). Antibody binding was detected with the SuperSignal West Pico Plus substrate kit (Thermo Fisher Scientific, #34577) in a ChemStudio Imager (Analytik Jena, #849-97-0928-04, Jena, Germany).

Skin model dissociation and RNA isolation

For qPCR analysis epidermis and dermis were separated by incubation in thermolysin (0.5 mg/mL) (#T7902, Sigma-Aldrich) for 2 h at 4 °C. The separated epidermis and dermis were minced into small pieces. RNA isolation was performed using the RNeasy Mini Kit (Qiagen, #74104, Düsseldorf, Germany), the DNase Kit (Qiagen, #79254) and proteinase K (Qiagen, #19133). Enzymatic dissociation was achieved by incubation with the RLT buffer from the RNeasy Kit at 20 °C for 45 min followed by an incubation step with proteinase K for 30 min at 55 °C, 400 RPM. After centrifugation, the supernatant was mixed with 0.7x of the volume of 98% ethanol and spinned through a RNeasy spin column. One washing step with RW1 buffer was performed before applying RNase/RDD solution (10 µl + 70 µl) from the DNase Kit for at least 15 minutes. The following steps were performed according to the manufacturer's instructions of the RNeasy Mini Kit.

Real-time quantitative PCR (RT-qPCR)

Mutz-LCs were seeded as described for Western blot analysis and treated with DNCB [20 µM] (Sigma-Aldrich, #237329) or $NiSO_4$ [380 µM] (Sigma-Aldrich, #227676) for 6 h. RNA extraction, cDNA synthesis and qPCR was performed as published in former studies [17, 37]. The specific primers used are listed in Table 1. After amplification, a threshold was set for each gene and Ct values were calculated for all samples.

Table 2.3-1 Primer sequences used for RT-qPCR

	Forward (5′→3′)	Reverse (5′→3′)
GAPDH	TGCACCACCAACTGCTTAGC	GGCATGGACTGTGGTCATGAG
IL-6	GGCACTGGCAGAAAACAACC	GCAAGTCTCCTCATTGAATCC
IL-8	ACTGAGAGTGATTGAGAGTGGAC	AACCCTCTGCACCCAGTTTTC
IL-1α	TGTATGTGACTGCCCAAGATGAAG	AGAGGAGGTTGGTCTCACTACC
IL-1β	GCACGATGCACCTGTACGAT	CACCAAGCTTTTTTGCTGTGAGT
IL-12p40	TGTCGTAGAATTGGATTGGTATC	AACCT GCCTCCTTTGTG
TNF-α	CCCTGCTGCACTTTGGAGTG	TCGGGGTTCGAGAAGATGAT
CD1a	CGCACCATTCGGTCATTTGAGG	TCCTGAGACCTTTCCAGAGTGC
CD207	TAATCTGCCTGACGCTGGTCCT	GGTGCTGATGTTGTCCACACGA
CD86	CCATCAGCTTGTCTGTTTCATTCC	GCTGTAATCCAAGGAATGTGGTC
CD83	TCCTGAGCTGCGCCTACAG	GCAGGGCAAGTCCACATCTT
CXCR4	CTCCTCTTTGTCATCACGCTTCC	GGATGAGGACACTGCTGTAGAG
CCR7	CAACATCACCAGTAGCACCTGTG	TGCGGAACTTGACGCCGATGAA
E-cad	CGAGAGCTACACGTTCACGG	GGGTGTCGAGGGAAAAATAGG

Cryosectioning and immunofluorescence staining

Cryosectioning and immunofluorescence staining were performed as described previously [17]. Briefly, skin models were cryosectioned into 7 µm slices and blocked in 10% goat serum (Invitrogen, #50062Z, Waltham, MA, USA). Primary antibody incubation was conducted using: Cytokeratin 5 (OriGene, DM361, Rockville, MD, USA) (1:75), CD1a (Santa Cruz Biotechnology, #sc-18885, Dallas, TX, USA) (1:50) and CD45-VioBright R667 (Miltenyi Biotec, #130-110-779) (1:50). Secondary antibody staining was performed using Alexa Flour 488 (Invitrogen, #A11017) (1:200) and Alexa Flour 546 (Invitrogen, #A11018) (1:200) combined with DAPI staining (10 µg/ml) (Sigma, ##D9542).

Haematoxylin and eosin staining

Haematoxylin and eosin staining's were performed according to our previous protocol [17]. Briefly, skin models were fixed in formaldehyde, dehydrated, paraffin embedded and cut into 5 µm sections. The hematoxylin and eosin staining was conducted using an automated procedure (Thermo Scientific, #Gemini AS). Imaging was performed using an Olympus microscope (BX51, Camera Olympus DP7).

Whole slide imaging and quantification

Imaging of the whole skin tissue slices was performed using a confocal spinning disc imaging system (CQ1, Yokogawa, Ratingen, Germany). To obtain focused images, the 40x objective was chosen and a region with at least four sections and a total of 70-80 field of views (FOVs) (≙ 4-6 sections with 6-10 × 2 FOVs) were defined for each slide depending on the length and

alignment of the tissue slice. The whole slide image quantification of CD1a positive cells was carried out with the help of the analysis software CellPathfinder (Yokogawa). First, the single FOVs were aligned and threshold values (grey level) were defined to identify the epidermal compartment and the integrated LC surrogates. In a final step the range of the size filter for LCs was set to >10.7 µm to exclude cell debris, representing putative false positive counts.

Statistical evaluation

Statistical evaluation was performed using GraphPad Prism version 8.4.3 (GraphPad Software, Inc., San Diego, CA, USA). Statistical significances were calculated using an unpaired t-test, one-way ANOVA with Dunnett's multiple comparisons test or two-way ANOVA with Sidak's multiple comparisons test. The significance levels were defined and referred to as * = $p \leq 0.05$; ** = $p \leq 0.01$; *** = $p \leq 0.001$; **** = $p \leq 0.0001$.

Disclosure

The authors report no conflicts of interest in this work.

Funding Sources

This research was funded by a grant to NT, KRM and TB by the Bundesministerium für Ernährung und Landwirtschaft (BMEL), funding number: 281A308C18.

Author Contributions

Conceptualization: JMH and NT; Methodology: JMH, AW, KF, PB, NT, LV; Validation: JMH, AW; Formal analysis: JMH; Investigation: JMH, AW, KF, DA, PB; Resources: NT, KRM, LV; Data curation: JMH; Supervision: NT, TB, KRM, HS; JB, Writing – Original Draft: JMH; Project administration: NT; Funding acquisition: NT, TB, KRM

Data Availability Statement

Datasets are available on request.

Acknowledgements

We would like to thank Nelli Blasius, Marion Merkel and Laura Steinmeyer for their technical support. We thank Michael Schell for his assistance and valuable support in developing and generating the whole slide image analysis.

References

1. Toebak, MJ, Gibbs, S, Bruynzeel, DP, Scheper, RJ, and Rustemeyer, T. Dendritic Cells: Biology of the Skin. Contact dermatitis. 2009, 60, 1: 2-20.
2. Deckers, J, Hammad, H, and Hoste, E. Langerhans Cells: Sensing the Environment in Health and Disease. Front Immunol. 2018, 993.
3. Jaitley, S, and Saraswathi, T. Pathophysiology of Langerhans Cells. J Oral Maxillofac Pathol. 2012, 16, 2: 239-44.
4. Matejuk, A. Skin Immunity. Archivum Immunologiae et Therapiae Experimentalis. 2018, 66, 1: 45-54.
5. Bennett, CL, Van Rijn, E, Jung, S, Inaba, K, Steinman, RM, Kapsenberg, ML, and Clausen, BrE. Inducible Ablation of Mouse Langerhans Cells Diminishes but Fails to Abrogate Contact Hypersensitivity. The Journal of cell biology. 2005, 169, 4: 569-76.
6. Kaplan, DH, Jenison, MC, Saeland, S, Shlomchik, WD, and Shlomchik, MJ. Epidermal Langerhans Cell-Deficient Mice Develop Enhanced Contact Hypersensitivity. Immunity. 2005, 23, 6: 611-20.
7. Kissenpfennig, A, Henri, S, Dubois, B, Laplace-Builhé, C, Perrin, P, Romani, N, Tripp, CH, Douillard, P, Leserman, L, and Kaiserlian, D. Dynamics and Function of Langerhans Cells in Vivo: Dermal Dendritic Cells Colonize Lymph Node Areasdistinct from Slower Migrating Langerhans Cells. Immunity. 2005, 22, 5: 643-54.
8. Gerber, PA, Buhren, BA, Schrumpf, H, Homey, B, Zlotnik, A, and Hevezi, P. The Top Skin-Associated Genes: A Comparative Analysis of Human and Mouse Skin Transcriptomes. Biol Chem. 2014, 395, 6: 577-91.
9. Pasparakis, M, Haase, I, and Nestle, FO. Mechanisms Regulating Skin Immunity and Inflammation. Nature Reviews Immunology. 2014, 14, 5: 289-301.
10. Bechetoille, N, Dezutter-Dambuyant, C, Damour, O, André, V, Orly, I, and Perrier, E. Effects of Solar Ultraviolet Radiation on Engineered Human Skin Equivalent Containing Both Langerhans Cells and Dermal Dendritic Cells. Tissue Eng. 2007, 13, 11: 2667-79.
11. Bock, S, Said, A, Müller, G, Schäfer-Korting, M, Zoschke, C, and Weindl, G. Characterization of Reconstructed Human Skin Containing Langerhans Cells to Monitor Molecular Events in Skin Sensitization. Toxicology in Vitro. 2018, 4677-85.
12. Régnier, M, Staquet, MJ, Schmitt, D, and Schmidt, R. Integration of Langerhans Cells into a Pigmented Reconstructed Human Epidermis. J Invest Dermatol. 1997, 109, 4: 510-2.
13. Régnier, M, Patwardhan, A, Scheynius, A, and Schmidt, R. Reconstructed Human Epidermis Composed of Keratinocytes, Melanocytes and Langerhans Cells. Med Biol Eng Comput. 1998, 36, 6: 821-4.
14. Laubach, V, Zöller, N, Rossberg, M, Görg, K, Kippenberger, S, Bereiter-Hahn, J, Kaufmann, R, and Bernd, A. Integration of Langerhans-Like Cells into a Human Skin Equivalent. Archives of Dermatological Research. 2011, 303, 2: 135-39.
15. Ouwehand, K, Spiekstra, SW, Waaijman, T, Scheper, RJ, de Gruijl, TD, and Gibbs, S. Technical Advance: Langerhans Cells Derived from a Human Cell Line in a Full-Thickness Skin Equivalent Undergo Allergen-Induced Maturation and Migration. Journal of Leukocyte Biology. 2011, 90, 5: 1027-33.
16. Kosten, IJ, Spiekstra, SW, de Gruijl, TD, and Gibbs, S. Mutz-3 Derived Langerhans Cells in Human Skin Equivalents Show Differential Migration and Phenotypic Plasticity after Allergen or Irritant Exposure. Toxicol Appl Pharmacol. 2015, 287, 1: 35-42.
17. Hölken, JM, Friedrich, K, Merkel, M, Blasius, N, Engels, U, Buhl, T, Mewes, KR, Vierkotten, L, and Teusch, NE. A Human 3d Immune Competent Full-Thickness Skin Model Mimicking Dermal Dendritic Cell Activation. Frontiers in Immunology. 2023, 14.

18. Yamaguchi, HL, Yamaguchi, Y, and Peeva, E. Role of Innate Immunity in Allergic Contact Dermatitis: An Update. International Journal of Molecular Sciences. 2023, 24, 16: 12975.
19. Valladeau, J, Ravel, O, Dezutter-Dambuyant, C, Moore, K, Kleijmeer, M, Liu, Y, Duvert-Frances, V, Vincent, C, Schmitt, D, Davoust, J, Caux, C, Lebecque, S, and Saeland, S. Langerin, a Novel C-Type Lectin Specific to Langerhans Cells, Is an Endocytic Receptor That Induces the Formation of Birbeck Granules. Immunity. 2000, 12, 1: 71-81.
20. Kim, JH, Hu, Y, Yongqing, T, Kim, J, Hughes, VA, Le Nours, J, Marquez, EA, Purcell, AW, Wan, Q, Sugita, M, Rossjohn, J, and Winau, F. Cd1a on Langerhans Cells Controls Inflammatory Skin Disease. Nature Immunology. 2016, 17, 10: 1159-66.
21. de Witte, L, Nabatov, A, Pion, M, Fluitsma, D, De Jong, MA, de Gruijl, T, Piguet, V, van Kooyk, Y, and Geijtenbeek, TB. Langerin Is a Natural Barrier to Hiv-1 Transmission by Langerhans Cells. Nature medicine. 2007, 13, 3: 367-71.
22. Stambach, NS, and Taylor, ME. Characterization of Carbohydrate Recognition by Langerin, a C-Type Lectin of Langerhans Cells. Glycobiology. 2003, 13, 5: 401-10.
23. Hunger, RE, Sieling, PA, Ochoa, MT, Sugaya, M, Burdick, AE, Rea, TH, Brennan, PJ, Belisle, JT, Blauvelt, A, and Porcelli, SA. Langerhans Cells Utilize Cd1a and Langerin to Efficiently Present Nonpeptide Antigens to T Cells. The Journal of clinical investigation. 2004, 113, 5: 701-08.
24. Birkinshaw, RW, Pellicci, DG, Cheng, T-Y, Keller, AN, Sandoval-Romero, M, Gras, S, De Jong, A, Uldrich, AP, Moody, DB, and Godfrey, DI. Aβ T Cell Antigen Receptor Recognition of Cd1a Presenting Self Lipid Ligands. Nature Immunology. 2015, 16, 3: 258-66.
25. De Jong, A, Cheng, T-Y, Huang, S, Gras, S, Birkinshaw, RW, Kasmar, AG, Van Rhijn, I, Peña-Cruz, V, Ruan, DT, and Altman, JD. Cd1a-Autoreactive T Cells Recognize Natural Skin Oils That Function as Headless Antigens. Nature Immunology. 2014, 15, 2: 177-85.
26. Peña-Cruz, V, Ito, S, Dascher, CC, Brenner, MB, and Sugita, M. Epidermal Langerhans Cells Efficiently Mediate Cd1a-Dependent Presentation of Microbial Lipid Antigens to T Cells. Journal of Investigative Dermatology. 2003, 121, 3: 517-21.
27. Mc Dermott, R, Ziylan, U, Spehner, D, Bausinger, H, Lipsker, D, Mommaas, M, Cazenave, J-P, Raposo, G, Goud, B, and de la Salle, H. Birbeck Granules Are Subdomains of Endosomal Recycling Compartment in Human Epidermal Langerhans Cells, Which Form Where Langerin Accumulates. Molecular biology of the cell. 2002, 13, 1: 317-35.
28. Tang, A, Amagai, M, Granger, LG, Stanley, JR, and Uddy, MC. Adhesion of Epidermal Langerhans Cells to Keratinocytes Mediated by E-Cadherin. Nature. 1993, 361, 6407: 82-85.
29. Jakob, T, Udey, MC, and Brown, MJ. Characterization of E-Cadherin-Containing Junctions Involving Skin-Derived Dendritic Cells. Journal of Investigative Dermatology. 1999, 112, 1: 102-08.
30. Udey, MC. Cadherins and Langerhans Cell Immunobiology. Clin Exp Immunol. 1997, 107 Suppl 16-8.
31. Kabashima, K, Shiraishi, N, Sugita, K, Mori, T, Onoue, A, Kobayashi, M, Sakabe, J-i, Yoshiki, R, Tamamura, H, and Fujii, N. Cxcl12-Cxcr4 Engagement Is Required for Migration of Cutaneous Dendritic Cells. The American journal of pathology. 2007, 171, 4: 1249-57.
32. Ouwehand, K, Santegoets, SJ, Bruynzeel, DP, Scheper, RJ, de Gruijl, TD, and Gibbs, S. Cxcl12 Is Essential for Migration of Activated Langerhans Cells from Epidermis to Dermis. European journal of immunology. 2008, 38, 11: 3050-59.

33. Villadangos, JA, Schnorrer, P, and Wilson, NS. Control of Mhc Class Ii Antigen Presentation in Dendritic Cells: A Balance between Creative and Destructive Forces. Immunological reviews. 2005, 207, 1: 191-205.
34. Sharpe, AH, and Freeman, GJ. The B7–Cd28 Superfamily. Nature Reviews Immunology. 2002, 2, 2: 116-26.
35. Tze, LE, Horikawa, K, Domaschenz, H, Howard, DR, Roots, CM, Rigby, RJ, Way, DA, Ohmura-Hoshino, M, Ishido, S, and Andoniou, CE. Cd83 Increases Mhc Ii and Cd86 on Dendritic Cells by Opposing Il-10–Driven March1-Mediated Ubiquitination and Degradation. Journal of Experimental Medicine. 2011, 208, 1: 149-65.
36. Riaz, B, Islam, SMS, Ryu, HM, and Sohn, S. CD83 Regulates the Immune Responses in Inflammatory Disorders. International Journal of Molecular Sciences. 2023, 24, 3: 2831.
37. Hölken, JM, and Teusch, N. The Monocytic Cell Line Thp-1 as a Validated and Robust Surrogate Model for Human Dendritic Cells. Int J Mol Sci. 2023, 24, 2.
38. Boislève, F, Kerdine-Römer, S, Rougier-Larzat, N, and Pallardy, M. Nickel and Dncb Induce Ccr7 Expression on Human Dendritic Cells through Different Signalling Pathways: Role of Tnf-A and Mapk. Journal of investigative dermatology. 2004, 123, 3: 494-502.
39. Ade, N, Antonios, D, Kerdine-Romer, S, Boisleve, F, Rousset, F, and Pallardy, M. Nf-Kappab Plays a Major Role in the Maturation of Human Dendritic Cells Induced by Niso(4) but Not by Dncb. Toxicol Sci. 2007, 99, 2: 488-501.
40. Aiba, S, Manome, H, Nakagawa, S, Mollah, ZU, Mizuashi, M, Ohtani, T, Yoshino, Y, and Tagami, H. P38 Mitogen-Activated Protein Kinase and Extracellular Signal-Regulated Kinases Play Distinct Roles in the Activation of Dendritic Cells by Two Representative Haptens, Nicl2 and 2,4-Dinitrochlorobenzene. J Invest Dermatol. 2003, 120, 3: 390-9.
41. Arrighi, JF, Rebsamen, M, Rousset, F, Kindler, V, and Hauser, C. A Critical Role for P38 Mitogen-Activated Protein Kinase in the Maturation of Human Blood-Derived Dendritic Cells Induced by Lipopolysaccharide, Tnf-Alpha, and Contact Sensitizers. J Immunol. 2001, 166, 6: 3837-45.
42. Taub, DD, Anver, M, Oppenheim, JJ, Longo, DL, and Murphy, WJ. T Lymphocyte Recruitment by Interleukin-8 (Il-8). Il-8-Induced Degranulation of Neutrophils Releases Potent Chemoattractants for Human T Lymphocytes Both in Vitro and in Vivo. J Clin Invest. 1996, 97, 8: 1931-41.
43. Nakae, S, Asano, M, Horai, R, Sakaguchi, N, and Iwakura, Y. Il-1 Enhances T Cell-Dependent Antibody Production through Induction of Cd40 Ligand and Ox40 on T Cells. J Immunol. 2001, 167, 1: 90-7.
44. Riemann, H, Schwarz, A, Grabbe, S, Aragane, Y, Luger, TA, Wysocka, M, Kubin, M, Trinchieri, G, and Schwarz, T. Neutralization of Il-12 in Vivo Prevents Induction of Contact Hypersensitivity and Induces Hapten-Specific Tolerance. J Immunol. 1996, 156, 5: 1799-803.
45. Murata, S, Kaneko, S, and Morita, E. Interleukin-8 Levels in the Stratum Corneum as a Biomarker for Monitoring Therapeutic Effect in Atopic Dermatitis Patients. International Archives of Allergy and Immunology. 2021, 182, 7: 592-606.
46. Takahashi, T, Kimura, Y, Saito, R, Nakajima, Y, Ohmiya, Y, Yamasaki, K, and Aiba, S. An in Vitro Test to Screen Skin Sensitizers Using a Stable Thp-1–Derived Il-8 Reporter Cell Line, Thp-G8. Toxicological Sciences. 2011, 124, 2: 359-69.
47. Coquette, A, Berna, N, Vandenbosch, A, Rosdy, M, De Wever, B, and Poumay, Y. Analysis of Interleukin-1α (Il-1α) and Interleukin-8 (Il-8) Expression and Release in in Vitro Reconstructed Human Epidermis for the Prediction of in Vivo Skin Irritation and/or Sensitization. Toxicology in Vitro. 2003, 17, 3: 311-21.

48. Furukawa, F, Fujii, K, Horiguchi, Y, Matsuyoshi, N, Fujita, M, Toda, K, Imamura, S, Wakita, H, Shirahama, S, and Takigawa, M. Roles of E- and P-Cadherin in the Human Skin. Microsc Res Tech. 1997, 38, 4: 343-52.

49. Enk, AH, and Katz, SI. Early Events in the Induction Phase of Contact Sensitivity. Journal of Investigative Dermatology. 1992, 99, 5, Supplement: S39-S41.

50. Ouwehand, K, Spiekstra, SW, Waaijman, T, Breetveld, M, Scheper, RJ, de Gruijl, TD, and Gibbs, S. Ccl5 and Ccl20 Mediate Immigration of Langerhans Cells into the Epidermis of Full Thickness Human Skin Equivalents. Eur J Cell Biol. 2012, 91, 10: 765-73.

51. Masterson, AJ, Sombroek, CC, de Gruijl, TD, Graus, YMF, van der Vliet, HJJ, Lougheed, SM, van den Eertwegh, AJM, Pinedo, HM, and Scheper, RJ. Mutz-3, a Human Cell Line Model for the Cytokine-Induced Differentiation of Dendritic Cells from Cd34+Precursors. Blood. 2002, 100, 2: 701-03.

52. Bock, S, Murgueitio, MS, Wolber, G, and Weindl, G. Acute Myeloid Leukaemia-Derived Langerhans-Like Cells Enhance Th1 Polarization Upon Tlr2 Engagement. Pharmacological Research. 2016, 10544-53.

53. Rodrigues Neves, CT, Spiekstra, SW, de Graaf, NP, Rustemeyer, T, Feilzer, AJ, Kleverlaan, CJ, and Gibbs, S. Titanium Salts Tested in Reconstructed Human Skin with Integrated Mutz-3-Derived Langerhans Cells Show an Irritant Rather Than a Sensitizing Potential. Contact dermatitis. 2020, 83, 5: 337-46.

54. Jiang, Y, Tsoi, LC, Billi, AC, Ward, NL, Harms, PW, Zeng, C, Maverakis, E, Kahlenberg, JM, and Gudjonsson, JE. Cytokinocytes: The Diverse Contribution of Keratinocytes to Immune Responses in Skin. JCI insight. 2020, 5, 20.

55. Ni, X, and Lai, Y. Crosstalk between Keratinocytes and Immune Cells in Inflammatory Skin Diseases. Exploration of Immunology. 2021, 1, 5: 418-31.

56. Lange, J, Weil, F, Riegler, C, Groeber, F, Rebhan, S, Kurdyn, S, Alb, M, Kneitz, H, Gelbrich, G, Walles, H, and Mielke, S. Interactions of Donor Sources and Media Influence the Histo-Morphological Quality of Full-Thickness Skin Models. Biotechnology Journal. 2016, 11, 10: 1352-61.

57. Mewes, KR, Raus, M, Bernd, A, Zöller, NN, Sättler, A, and Graf, R. Elastin Expression in a Newly Developed Full-Thickness Skin Equivalent. Skin Pharmacology and Physiology. 2007, 20, 2: 85-95.

58. Mewes, KR, Zöller, NN, Bernd, A, Prießner, A, DeWever, B, Graf, R, and Schröder, KR. Expression of Dermal Extracellular Matrix Proteins in a Newly Developed Full-Thickness Skin Model. Paper presented at the Cells and Culture, Dordrecht, 2010// 2010.

59. Rheinwald, JG, and Green, H. Serial Cultivation of Strains of Human Epidermal Keratinocytes: The Formation of Keratinizing Colonies from Single Cells. Cell. 1975, 6, 3: 331-43.

60. Cohen, DE, and Heidary, N. Treatment of Irritant and Allergic Contact Dermatitis. Dermatologic Therapy. 2004, 17, 4: 334-40.

61. Toebak, MJ, De Rooij, J, Moed, H, Stoof, TJ, Von Blomberg, BME, Bruynzeel, DP, Scheper, RJ, Gibbs, S, and Rustemeyer, T. Differential Suppression of Dendritic Cell Cytokine Production by Anti-Inflammatory Drugs. British Journal of Dermatology. 2008, 158, 2: 225-33.

62. Mainali, ES, Kikuchi, T, and Tew, JG. Dexamethasone Inhibits Maturation and Alters Function of Monocyte-Derived Dendritic Cells from Cord Blood. Pediatric Research. 2005, 58, 1: 125-31.

63. van den Berg, LM, Cardinaud, S, van der Aar, AMG, Sprokholt, JK, de Jong, MAWP, Zijlstra-Willems, EM, Moris, A, and Geijtenbeek, TBH. Langerhans Cell–Dendritic Cell Cross-Talk Via Langerin and Hyaluronic Acid Mediates Antigen Transfer and Cross-Presentation of Hiv-1. The Journal of Immunology. 2015, 195, 4: 1763-73.

64. Yao, C, and Kaplan, DH. Langerhans Cells Transfer Targeted Antigen to Dermal Dendritic Cells and Acquire Major Histocompatibility Complex Ii In vivo. J Invest Dermatol. 2018, 138, 7: 1665-68.

65. Silberberg-Sinakin, I, and Thorbecke, J. Contact Hypersensitivity and Langerhans Cells. Journal of Investigative Dermatology. 1980, 75, 1: 61-67.

66. Forsey, Shahidullah, Sands, Mcvittie, Aldridge, Hunter, and Howie. Epidermal Langerhans Cell Apoptosis Is Induced in Vivo by Nonanoic Acid but Not by Sodium Lauryl Sulphate. British Journal of Dermatology. 1998, 139, 3: 453-61.

Supplementary Information

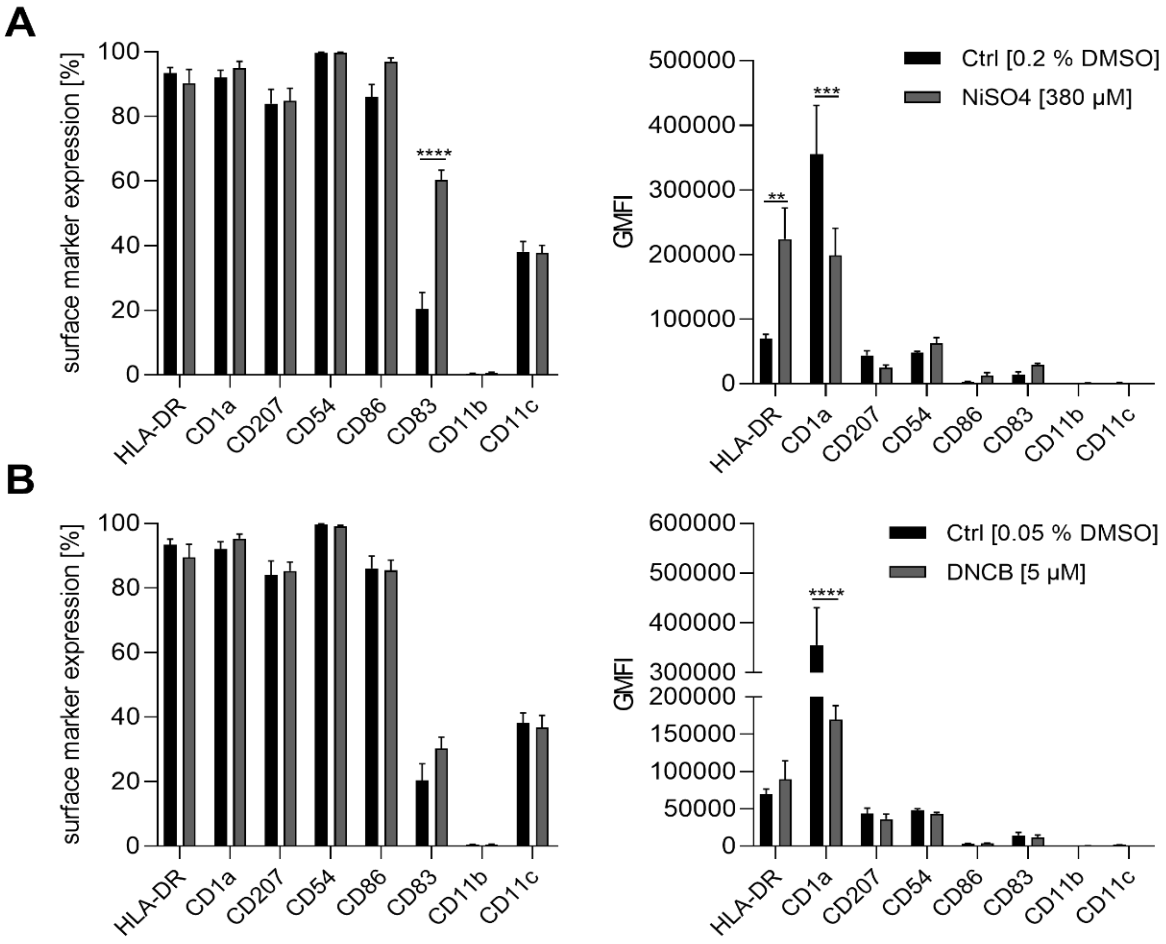

Supplementary Figure 2.3-1 Surface marker expression of Mutz-3 derived LCs after sensitization, depicted as percentage of positive cells and as geometric mean fluorescence intensity (GMFI). 2 × 10^5 Mutz-LCs/ mL were seeded in 4 mL MEM α supplemented with 5% FBS, 1% P/S and 0.05 mM 2-mercaptoethanol into a 12-well plate and exposed to **(A)** $NiSO_4$ [380 µM] or **(B)** DNCB [20 µM] for 24 h. Surface marker expression of at least 10,000 viable cells was analyzed via flow cytometry. Error bars indicate the standard errors of the mean (n = 3 independent experiments with ** = $p \leq 0.01$, *** = $p \leq 0.001$, and **** = $p \leq 0.0001$).

3 Unpublished data

The following chapters contain additional unpublished datasets, which were generated as part of this dissertation in the process of developing an immune competent skin model (Chapter 3.1), as well as for the initial characterization of the natural compound of pseudopterosin as potential anti-inflammatory drug candidate in skin sensitization (Chapter 3.2).

3.1 Exploring potential DC surrogates and readouts

3.1.1 Phenotypical characterization of potential DC surrogates

The activation of cutaneous DCs is a crucial event in skin sensitization. Thus, distinct methods based on DC surrogates have been developed to distinguish between sensitizers and non-sensitizers. Notably, two out of four OECD-approved test systems (at the start of this project two out of three[1]) are based on the human monocytic leukemia cell line THP-1, specifically the h-CLAT and the IL-8 Luc assay [151]. Subsequently, the most logical step was to explore whether THP-1 cells could be suitable DC surrogates for integration into full-thickness skin models. Hence, our first aim was to characterize the cell surface marker phenotype of different THP-1 derivatives and following the sensitizer-induced changes in the surface marker expression profile. In fact, the h-CLAT is based on the quantification of the sensitizer-induced surface marker expression of the intercellular adhesion molecule CD54 and the co-stimulatory molecule CD86. More specifically, a chemical is classified by the h-CLAT as a sensitizer when the relative fluorescence intensity (RFI) exceeds a defined threshold for CD54 ≥ 200 or CD86 ≥ 150 in at least two out of three independent measurements [151, 152]. Thus, I characterized the change in the surface marker expression of THP cells upon exposure to the two model sensitizers, $NiSO_4$ and DNCB (Figure 3.1-1). Beyond the two h-CLAT markers CD54 and CD86, I examined the surface marker expression of CD11b, which is associated with phagocytosis [210] and HLA-DR, a MHC class II complex involved in antigen presentation [211]. In addition, I examined the surface marker expression of CD1a and CD207 as characteristic markers for LCs and the expression of CD83 as an indicator for DC maturation. Furthermore, the surface marker expression of the migration markers CXCR4 and CCR7 was determined.

[1] At the start of this project (in 2020), only the h-CLAT, U-SENS and IL-8 Luc assays were approved by the OECD (in 2018) to investigate the third KE of the AOP [136]. The GARD assay was approved by the OECD in 2022 [151].

Exposure of THP-1 cells to $NiSO_4$ (Figure 3.1-1A) resulted in significantly higher numbers of THP-1 cells expressing the surface marker CD54 ($NiSO_4$: ~1.7-fold). Treatment of THP-1 cells with DNCB (Figure 3.1-1B) induced a significantly higher surface marker expression of CD54 (~1.5-fold) and CD86 (~2.7-fold). Thus, THP-1 cells could successfully identify $NiSO_4$ and DNCB as sensitizers according to the guidelines of the h-CLAT. Furthermore, exposure of THP-1 cells to $NiSO_4$ but not DNCB led to a significantly high number of THP-1 cells expressing the maturation marker CD83 (Ctrl: ~0.88%; $NiSO_4$: ~38%; DNCB: ~0.76%). The surface marker expression of HLA-DR was increased by ~1.85-fold upon exposure to $NiSO_4$ and by ~1.13-fold upon exposure to DNCB. Importantly, treatment with $NiSO_4$ or DNCB significantly decreased the numbers of THP-1 cells expressing CXCR4 ($NiSO_4$: ~1.13-fold; DNCB: ~2.9-fold), which is associated with the migration of LCs from the epidermis to the dermis. However, minor increases were observed in the number of THP-1 cells expressing CCR7 ($NiSO_4$: 4.2-fold (9,6%); DNCB: 2.-fold (~12%)), which is required for migration to local lymph nodes. It is noteworthy that THP-1 cells did not express the characteristic LC surface markers CD1a or CD207 before or after exposure to $NiSO_4$ or DNCB.

Furthermore, I investigated the response of the THP1-Blue™ NF-κB reporter cell line to sensitizers (Figures 3.1-1C, D) as the NF-κB pathway has been reported to be involved in the sensitizer-induced activation of DC surrogates [111, 113]. Similar to the response in original THP-1 cells, exposure of THP1-Blue™ NF-κB cells to $NiSO_4$ induced a significant increase in the number of cells expressing CD54 and CD86 ($NiSO_4$: ~1.14-fold: DNCB: ~1.4-fold). Analog to original THP-1 cells, THP1-Blue™ NF-κB cells did not express CD1a or CD207, and the expression of both surface markers could not be induced upon exposure to $NiSO_4$ or DNCB. However, CD207/ Langerin in particular is considered as one of the phenotypic hallmarks of LCs [72], which are the only DC subtype located in the epidermis. Although some studies reported antigen-presenting functions for CD207, the precise role of CD207 remains elusive [212, 213]. Thus, we sought to explore whether the surface marker expression of CD207 could influence the location of LC surrogates in the epidermis. I therefore characterized THP-Langerin cells (kindly provided by Prof. Dr. Theo Geijtenbeek) and their sensitizer-induced surface marker expression profile as well (Figures 3.1-1E, F). However, the surface marker expression of CD54 on untreated THP-Langerin cells was over 99% and could not be induced upon exposure to $NiSO_4$ or DNCB. Exposure of THP-Langerin cells to $NiSO_4$ resulted in significantly higher numbers of cells expressing CD86 (~1.34-fold) and CD83 (31-fold; Ctrl: ~0.69%; $NiSO_4$: ~21.8%). Exposure of THP-Langerin cells to DNCB induced only a significant reduction in cells expressing CXCR4 (~1.35-fold), in a similar manner to that observed upon $NiSO_4$ (~1.35-fold) exposure. The surface marker expression of CD207 (> 85%) was not affected upon treatment with $NiSO_4$ or DNCB.

Contemplating the sensitizer-induced alterations of surface marker expression, it seems that the native THP-1 cells tend to be more sensitive towards sensitizers than the stably transfected THP1-Blue™ NF-κB reporter cell line or the THP-Langerin cell line.

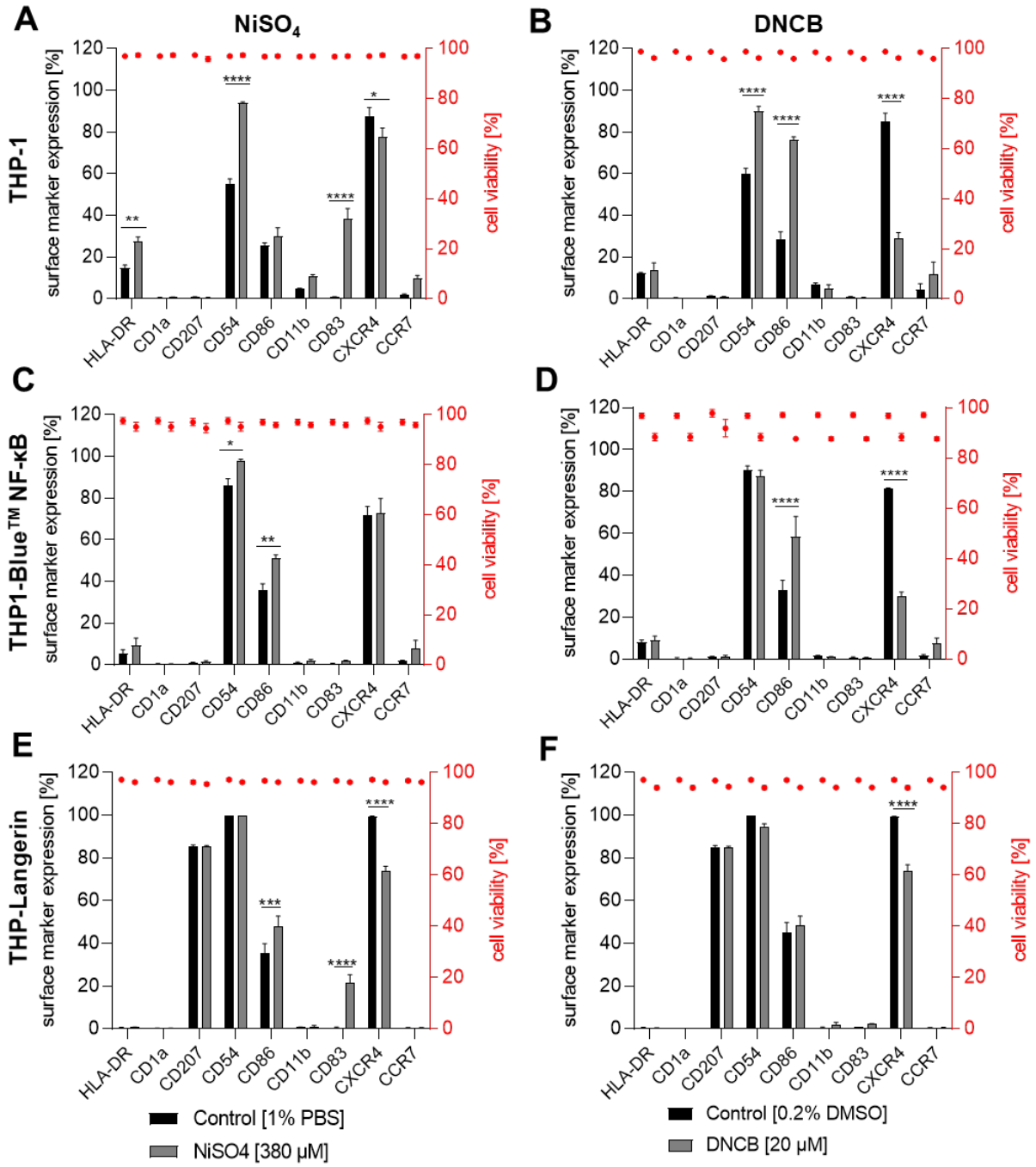

Figure 3.1-1 Surface marker expression of THP-1 cells **(A & B),** THP1-Blue™ NF-κB cells **(C & D)** or THP-Langerin cells **(E & F)** after sensitization according to the h-CLAT assay. THP-derivates were seeded with 1 × 10^6 cells/mL in 1 mL RPMI supplemented with 10% FBS, 1% PenStrep, and 0.05 mM 2 mercaptoethanol into a 24-well plate. Cells were treated with 380 µM $NiSO_4$, 20 µM DNCB, or their respective solvent control, namely PBS or DMSO. Surface marker expression of at least 10,000 viable cells was analyzed via flow cytometry. Error bars indicate the standard errors of the mean (n = 3 independent experiments with * = p ≤ 0.05, ** = p ≤ 0.01, *** = p ≤ 0.001, and **** = p ≤ 0.0001).

In the native human skin and therefore after integration into epidermal or full-thickness skin models, dendritic cells are in close proximity and have frequent intercellular contact with keratinocytes. Thus, I investigated whether the co-cultivation of THP-1 or THP-Langerin cells with keratinocytes has an impact on the basal surface marker expression pattern or on the sensitizer-induced changes in the surface marker expression of THP-1 or THP-Langerin cells (Figure 3.1-2).

Significantly, co-cultivation of THP-1 cells with primary human keratinocytes (KCs) from a juvenile or an adult donor (without exposure to a sensitizer) resulted in a substantially higher surface marker expression of the intracellular adhesion molecule CD54 (juvenile KCs: ~2.0-fold; adult KCs: ~1.9-fold) and a minor upregulation in the surface marker expression of the co-stimulatory molecule CD86 (juvenile KCs: ~1.2-fold; adult KCs: ~1.4-fold). While co-cultivation of THP-1 cells with adult KCs significantly decreased the number of cells expressing CXCR4 on their surface (~1.3-fold), only a minor reduction (~1.1-fold) of the CXCR4 surface marker expression on THP-1 cells was observed after co-cultivation with KCs from a juvenile donor. Furthermore, an increase in the surface marker expression of CD11b (up to 17%) was detected after co-cultivation of THP-1 cells with KCs from a juvenile (3.3-fold) or an adult donor (~1.7-fold) (Figures 3.1-2A, B). Contrary, co-cultivation with keratinocytes from juvenile or adult KCs did not change the surface marker expression of any of the investigated markers on THP-Langerin cells (Figures 3.1-2C, D).

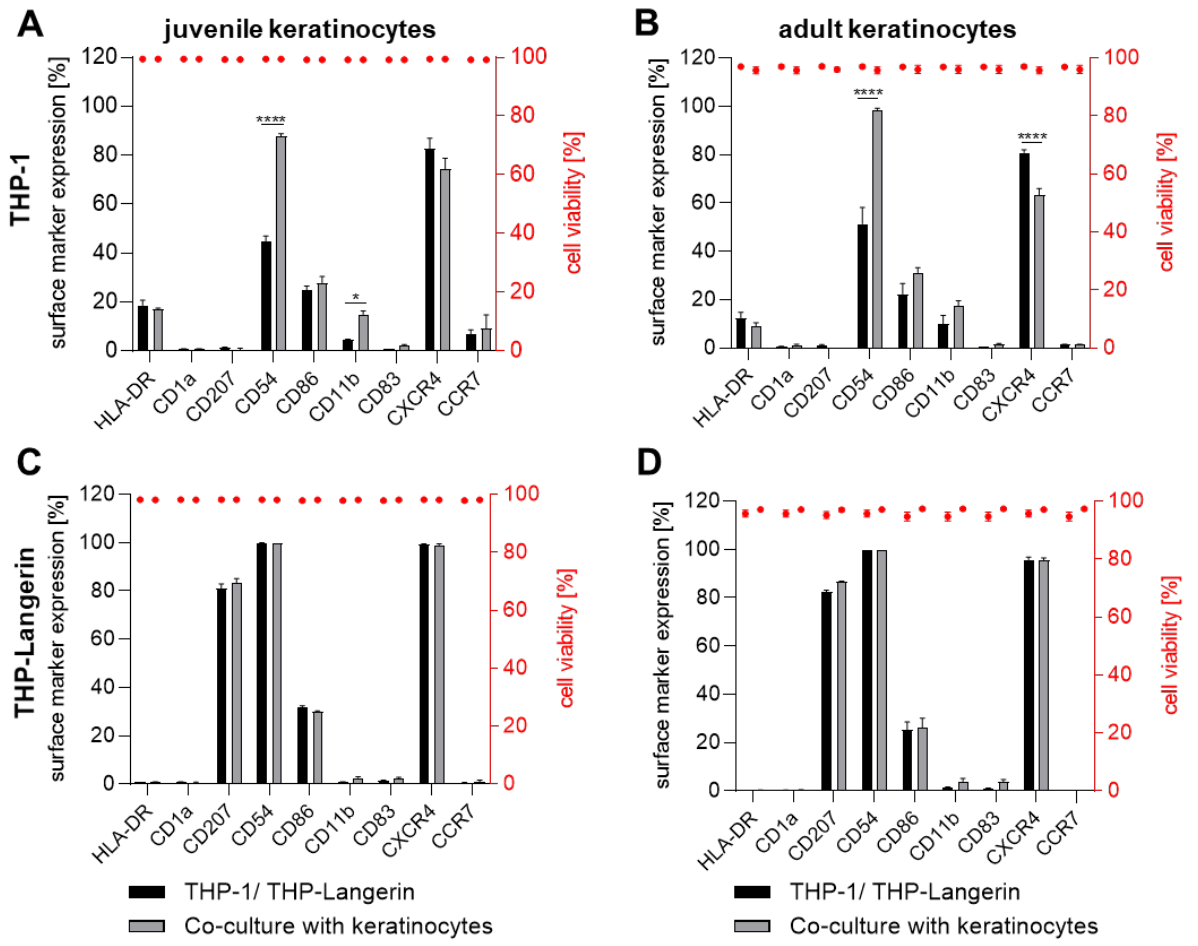

Figure 3.1-2 Surface marker expression of THP-1 **(A & B)** or THP-Langerin **(C & D)** cells before and after co-culture with keratinocytes from a juvenile donor **(A & C)** or an adult donor **(B &D)**. Here, 6 x 10^5 THP-1 or THP-Langerin cells in 1 mL THP-1 medium were added to keratinocytes, which were previously seeded, and allowed to adhere to 24-well plates. After 24 h of co-cultivation, THP-1 or THP-Langerin cells were harvested, and the surface marker expression of at least 10,000 viable cells was analyzed via flow cytometry. Error bars indicate the standard errors of the mean (n = 3 independent experiments with * = $p \leq 0.05$ and **** = $p \leq 0.0001$).

Furthermore, I investigated which impact the co-cultivation of THP-1 and THP-Langerin cells with KCs from juvenile and adult donors might have on the sensitizer-induced surface marker expression pattern of THP-1 or THP-Langerin cells (Figures 3.1-3 and 3.1-4).

Due to the high surface marker expression of CD54 on THP-Langerin cells itself (> 99%) and on THP-1 cells after co-cultivation with keratinocytes (> 88%–98%) (Figure 3.1-2), treatment of the co-culture with $NiSO_4$ or DNCB induced only minor increases in the number of THP-1 cells expressing CD54 ($NiSO_4$: ~1.23-fold; DNCB: ~1.08-fold), but no increases were observed in the number of THP-Langerin cells (Figure 3.1-3). In contrast, the number of cells positive for the surface marker CD86 were significantly increased in THP-1 and THP-Langerin cells upon exposure to $NiSO_4$ (THP-1: ~1.7-fold; THP-Langerin: ~1.3-fold) or DNCB (THP-1: ~2.9-fold; THP-Langerin: ~1.4fold). Surface marker expression of CD83 after co-cultivation with juvenile KCs could be induced after $NiSO_4$ exposure by ~8.7-fold on THP-1 cells and by ~3.6-fold on THP-Langerin cells. The number of cells expressing the migration marker CXCR4 was

significantly reduced after co-culturing with juvenile KCs and simultaneous exposure to DNCB on THP-1 (~2.1-fold) and THP-Langerin cells (~1.4-fold). Upon co-cultivation with juvenile KCs and exposure to $NiSO_4$, the number of cells expressing CXCR4 was decreased by ~1.06-fold for THP-1 cells and ~1.4-fold for THP-Langerin cells. Surface marker expression of CCR7 was increased on with juvenile KC co-cultivated and $NiSO_4$- or DNCB-exposed THP-1 cells ($NiSO_4$: ~2.8-fold; DNCB: ~1.7-fold), but not on THP-Langerin cells (Figure 3.1-3).

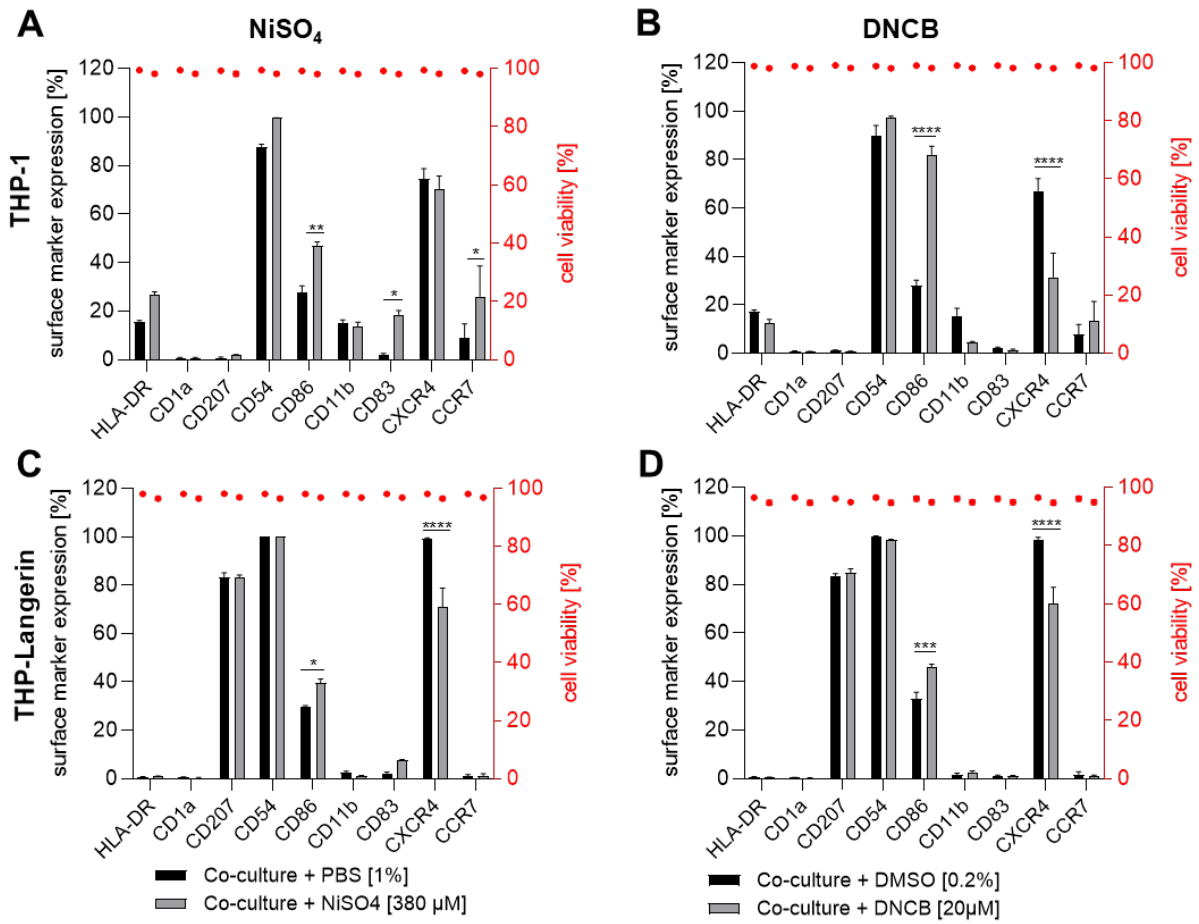

Figure 3.1-3 Surface marker expression of THP-1 cells **(A & B)** and THP-Langerin cells **(C & D)** after co-cultivation with keratinocytes derived from a juvenile donor ± sensitization with $NiSO_4$ or DNCB. Here, 6 x 10^5 THP-1 or THP-Langerin cells in 1 mL THP-1 medium were added to keratinocytes, which were previously seeded, and allowed to adhere to 24-well plates. Cells were treated with $NiSO_4$ [380 µM] or DNCB [20 µM] or their respective solvent control, namely PBS or DMSO. After 24 h of co-cultivation and treatment, THP-1 or THP-Langerin cells were harvested, and the surface marker expression of at least 10,000 viable cells was analyzed via flow cytometry. Error bars indicate the standard errors of the mean (n = 3 independent experiments with * = $p \leq 0.05$, ** = $p \leq 0.01$, *** = $p \leq 0.001$, and **** = $p \leq 0.0001$).

Similar to the co-cultivation of THP-1 and THP-Langerin cells with juvenile KCs, co-cultivation with adult KCs resulted in such high surface marker expression of CD54 on THP-1 (98.5%) and THP-Langerin cells (99.9%) that a further increase in the number of cells positive for CD54 upon exposure to sensitizers was not possible. Conversely, treatment of the co-culture of THP-1 cells with adult KCs resulted in a 1.3-fold decrease in the number of cells positive for CD54. This striking observation might be explained by the slightly decreased (~1.1-fold) viability of THP-1 cells upon treatment of the co-culture. In line with the results from the co-

cultivation and simultaneous sensitization of THP-1 or THP-Langerin cells and juvenile KCs, the number of cells positive for the surface marker CD86 was significantly increased on THP-1 and THP-Langerin cells upon exposure of the co-culture with adult KCs to $NiSO_4$ (THP-1: ~1.6-fold; THP-Langerin: ~1.3-fold) or DNCB (THP-1: ~1.6-fold; THP-Langerin: ~1.5-fold). Surface marker expression of CD83 after co-cultivation with adult KCs could be induced after $NiSO_4$ exposure on THP-1 cells by ~5.4-fold, and by ~2.4-fold on THP-Langerin cells. Congruent with the data from the THP-1/ THP-Langerin co-culture with juvenile KCs, DNCB treatment of the THP-1/ THP-Langerin co-culture with adult KCs resulted in significantly reduced numbers of cells expressing CXCR4 (THP-1: ~2.4-fold; THP-Langerin cells ~1.8-fold). Upon exposure to $NiSO_4$, the number of cells expressing CXCR4 was slightly increased (~1.06-fold) for THP-1 cells but significantly decreased (~1.9-fold) for THP-Langerin cells. Expression of the surface marker CCR7 was increased on with adult KC co-cultivated and to DNCB exposed THP-1 cells (~8.8-fold), but not on THP-Langerin cells (Figure 3.1-4).

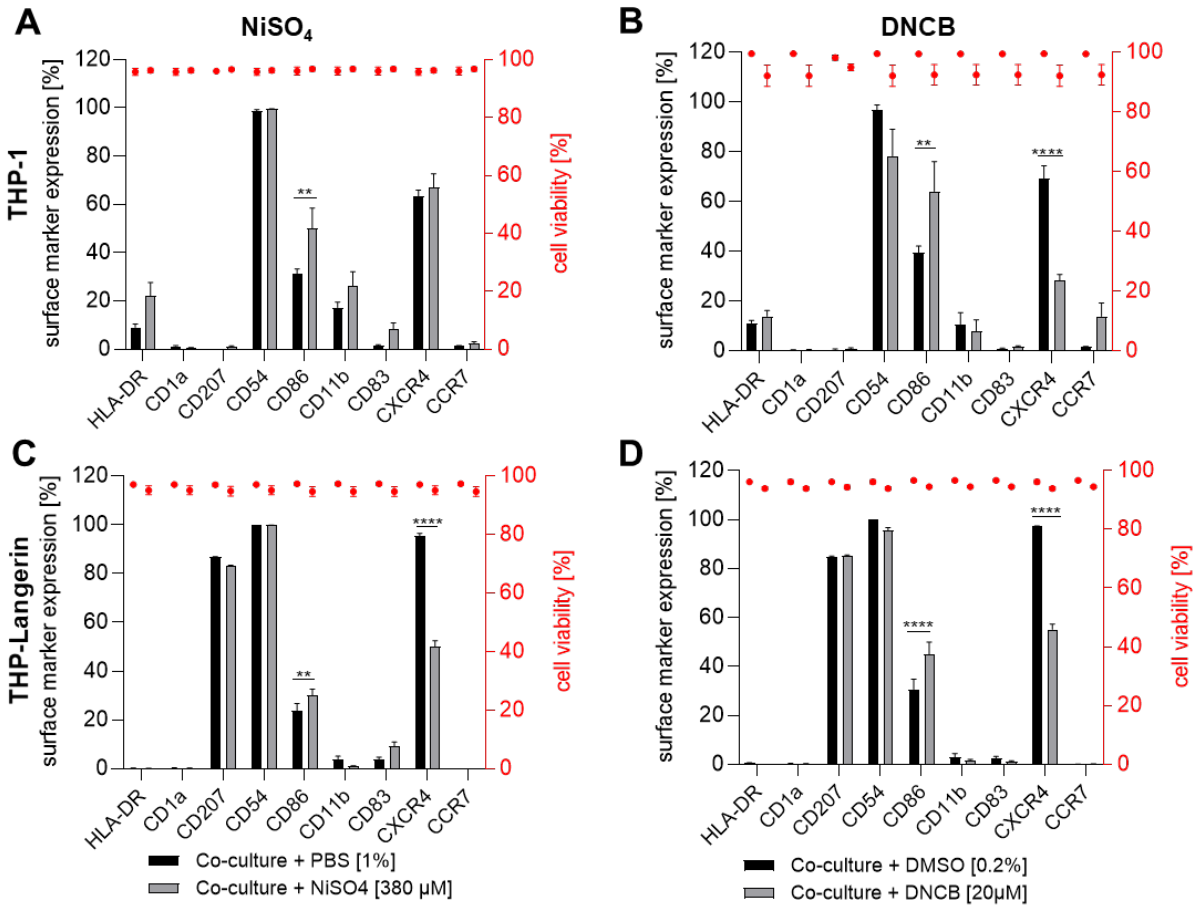

Figure 3.1-4 Surface marker expression of THP-1 cells **(A & B)** and THP-Langerin cells **(C & D)** after co-cultivation with keratinocytes derived from an adult donor ± sensitization with $NiSO_4$ or DNCB. Here, 6 x 10^5 THP-1 or THP-Langerin cells in 1 mL THP-1 medium were added to keratinocytes, which were previously seeded, and allowed to adhere to 24-well plates. Cells were treated with $NiSO_4$ [380 µM] or DNCB [20 µM] or their respective solvent control, namely PBS or DMSO. After 24 h of co-cultivation and treatment, THP-1 or THP-Langerin cells were harvested, and the surface marker expression of at least 10,000 viable cells was analyzed via flow cytometry. Error bars indicate the standard errors of the mean (n = 3 independent experiments with ** = $p \leq 0.01$ and **** = $p \leq 0.0001$).

3.1.2 Migration capabilities of potential DC surrogates

To present antigens to naïve T cells, DCs must migrate to local lymph nodes. While DDCs migrate from the dermis, LCs must first migrate from the epidermis into the dermis. Migration of LCs from the epidermis to the dermis is mediated through the secretion of SDF-1 by dermal fibroblasts and lymphatic endothelial cells [120-122]. Thus, I investigated the migratory capability of THP-1 cells, THP1-Blue™ NF-κB, and THP-Langerin cells towards SDF-1 (Figure 3.1-5). When compared to the respective controls with medium only, ~188% of THP-1 cells, ~196% of THP1-Blue™ NF-κB cells, and ~263% of THP-Langerin cells migrated towards SDF-1 (Figure 3.1-5). Hence, in terms of the migratory potential towards SDF-1, all three cell lines might be suitable LC surrogates.

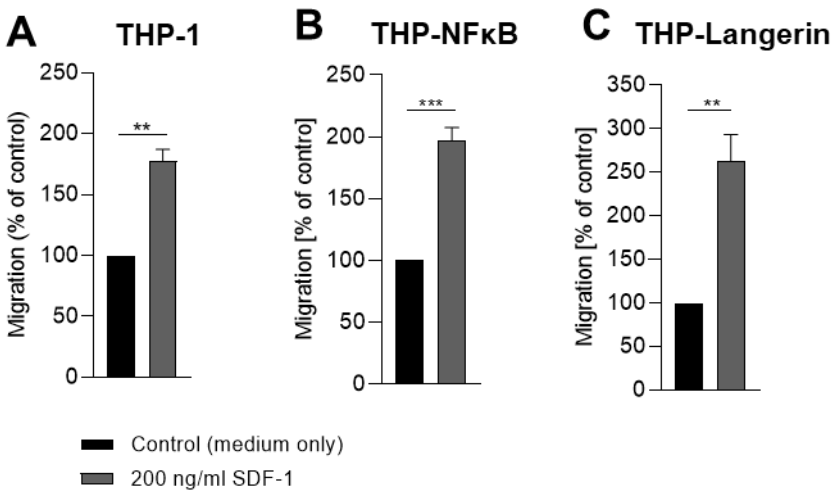

Figure 3.1-5 Transwell Migration Assay (TMA) of **(A)** THP-1 cells, **(B)** THP1-Blue™ NF-κB, and **(C)** THP-Langerin cells towards SDF-1. THP-derivatives were seeded with 1 x 10^5 cells in 100 µl RPMI + 2.5% FBS onto the membrane (5.0 µm) of the upper transwell inserts. The lower chamber was filled with 600 µl RPMI + 2.5% FBS containing 200 ng/mL SDF-1. Migration towards SDF-1 compared to the medium only (control) was determined after 16

3.1.3 Identification of potential readout parameters

Beyond integrating functional DC surrogates into a FTSE, this project also sought to further characterize the sensitizer-induced activation of cutaneous DCs as well as to identify potential readout parameters for the identification and characterization of sensitizers and prospectively anti-sensitizing compounds. Thus, in addition to the sensitizer-induced activation of surface markers such as CD54, CD86, and CD83 or the migratory capabilities of our potential cutaneous DC surrogates, we were interested in the underlying molecular signaling pathways involved in skin sensitization and DC activation. I first investigated whether the two model sensitizers $NiSO_4$ and DNCB could induce the NF-κB or p38 MAPK pathway in THP-1 cells. For this, the optimal treatment concentration and time points had to be determined. Notably,

treatment of THP-1 cells with $NiSO_4$ for 1 h revealed a significant degradation of IκBα after exposure to 380 µM $NiSO_4$ (~1.8-fold) and 500 µM $NiSO_4$ (~2.5-fold) (Figure 3.1-6).

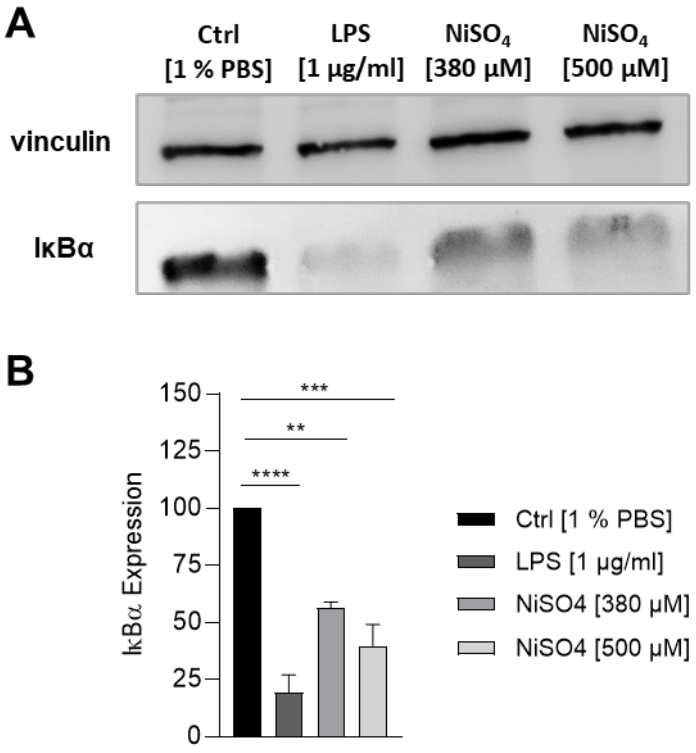

Figure 3.1-6 Degradation of IκBα after treatment of THP-1 cells with $NiSO_4$. Here, THP-1 cells were seeded with 1 x 10^6 cells in 1 mL THP-1 medium into a 24-well plate. Cells were treated with 380 µM or 500 µM $NiSO_4$ for 1 h. Treatment with LPS [1 µg/mL] served as positive control and PBS as solvent control. **(A)** depicts one representative blot of three independent experiments. **(B)** depicts the quantification of image bands normalized to the solvent control.

Furthermore, treatment of THP-1 cells with $NiSO_4$ resulted in a minor phosphorylation of p38 MAPK after 30 min (~1.3-fold) and 60 min (~1.4-fold). However, exposure of THP-1 cells to DNCB led to a significant phosphorylation of p38 MAPK after 15 min (~2.9-fold), 30 min (~4.2-fold) and 60 min (~5.7 fold) (Figure 3.1-7).

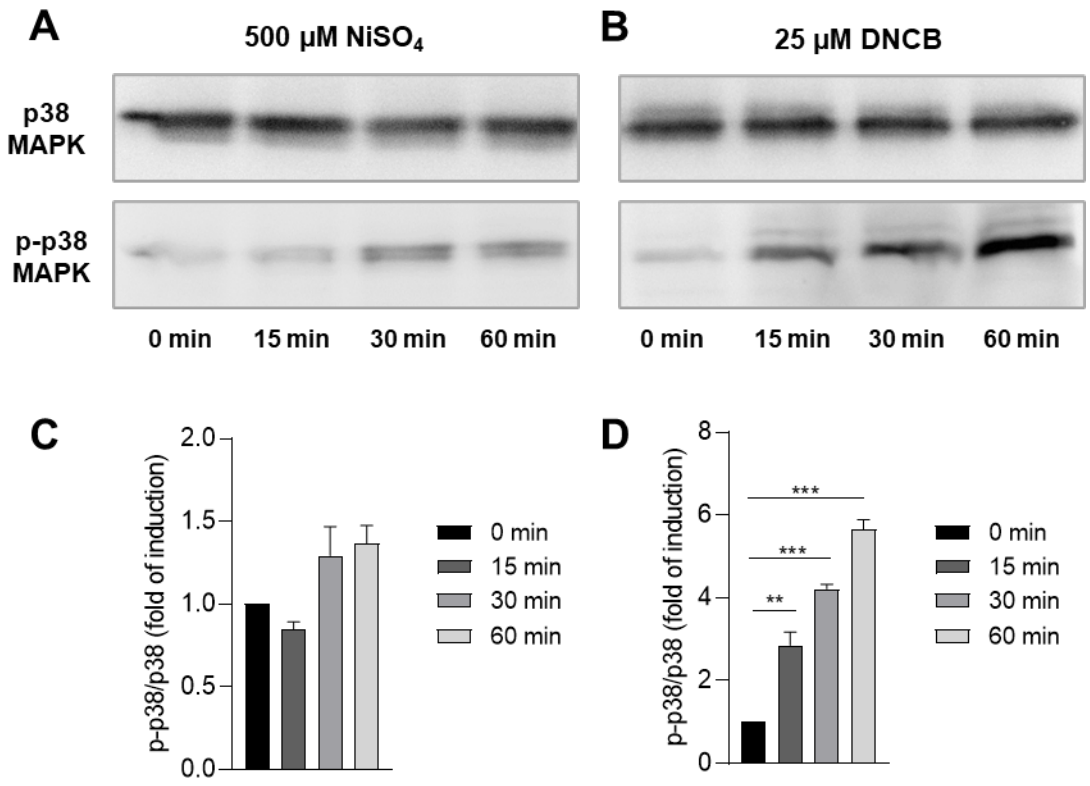

Figure 3.1-7 Timeline (0–60 min) for the phosphorylation of p38 MAPK in THP-1 cells after **(A)** $NiSO_4$ [500 µM] and **(B)** DNCB [25 µM] treatment. Here, THP-1 cells were seeded with 1 x 10^6 cells in 1 mL THP-1 medium into a 24-well plate. Cells were treated with $NiSO_4$ [500 µM] or DNCB [25 µM] for 0 min, 15 min, 30 min, and 60 min. **(A)** depicts one representative blot of three independent experiments. **(B)** depicts one representative blot of two independent experiments. **(C)** and **(D)** depict the quantification of image bands normalized to the solvent control.

Next, I investigated the mRNA levels of inflammatory cytokines after exposure of THP-1 cells to $NiSO_4$ and DNCB (Figure 3.1-8). While both sensitizers induced a significant upregulation of the mRNA levels for IL-8 in THP-1 cells ($NiSO_4$: ~11-fold; DNCB: ~51-fold), only $NiSO_4$ could induce significantly higher mRNA levels for TNF-α (~10-fold) in THP-1 cells. In contrast, exposure of THP-1 cells to DNCB resulted in a minor reduction in mRNA levels for TNF-α (~1.3-fold). Treatment of THP-1 cells with $NiSO_4$ or DNCB led to a minor decrease in the mRNA levels for IL-6 ($NiSO_4$: ~1.4-fold; DNCB: ~1.6-fold) compared to the solvent control.

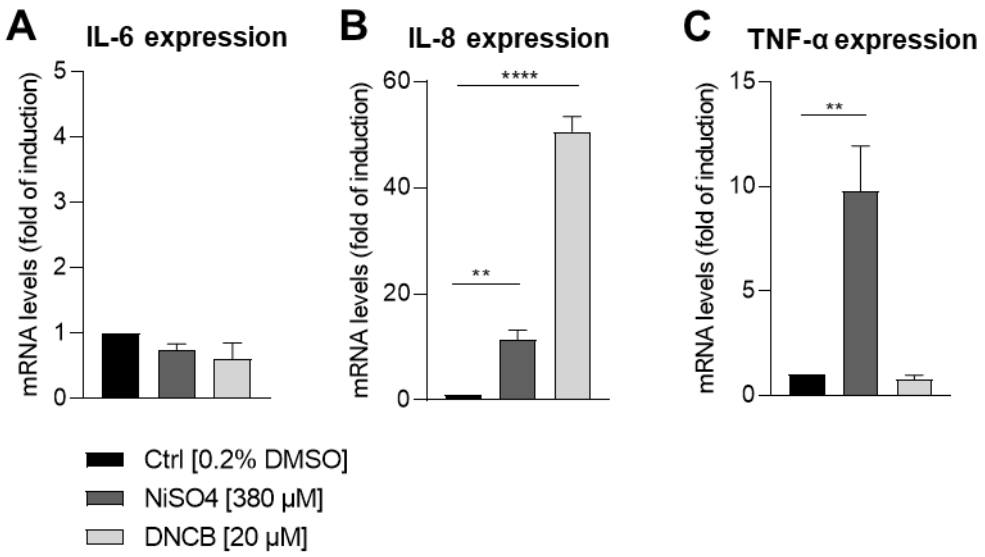

Figure 3.1-8 mRNA levels of inflammatory cytokine expression by THP-1 cells: **(A)** IL-6, **(B)** IL-8, and **(C)** TNF-α after $NiSO_4$ [380 µM] and DNCB treatment [20 µM] for 6 h. Results are depicted as folds of induction compared to the solvent control [0.2% DMSO] and normalized to the expression of the housekeeping gene [GAPDH]. Error bars indicate the standard errors of the mean (n = 3 independent experiments with ** = $p \leq 0.01$ and

The sensitizer-induced secretion of inflammatory cytokines by keratinocytes has been reported as crucial in the mediation of DC activation [100, 101]. Thus, I investigated the mRNA levels of inflammatory cytokines after exposure of KCs from juvenile and adult donors to the two model sensitizers $NiSO_4$ and DNCB (Figure 3.1-9). Treatment of KCs from a juvenile donor with DNCB resulted in a minor upregulation of the mRNA levels for IL-6 (~1.4-fold), IL-8 (~1.7-fold) and TNF-α (~1.3-fold). Conversely, treatment of KCs derived from an adult donor with DNCB induced significantly higher mRNA levels for IL-6 (~5.3-fold), IL-8 (~3.7-fold) and TNF-α (~12-fold) compared to the solvent control. mRNA levels for IL-1α and IL-1β were slightly reduced in juvenile and adult KCs upon exposure to $NiSO_4$ or DNCB (~1.12-fold). Furthermore, exposure of keratinocytes from juvenile or adult donors to $NiSO_4$ did not induce any significant changes in mRNA levels.

Notably, the results give the impression that keratinocytes derived from an adult donor might be more sensitive towards sensitizers, in particular DNCB, than keratinocytes from a juvenile donor. However, it bears mentioning that both primary cell types were cultivated in their customized keratinocyte medium manufactured by their supplier. When comparing the cultivation media, it became evident that both media are supplemented with the anti-inflammatory compound hydrocortisone. Moreover, according to the manufacturer (Henkel AG & Co. KGaA), the keratinocyte medium for KCs derived from a juvenile donor comprises 4 µg/ml hydrocortisone, while the medium for KCs derived from an adult donor contains, according to the manufacturer (Lonza), hydrocortisone at a concentration between 0 .1–3 µg/ml. Hence, the lower hydrocortisone concentration could be one factor in the higher mRNA levels in adult KCs upon sensitization. Thus, we concluded that for the characterization of

sensitizers and potential anti-inflammatory compounds, a medium with low concentrations or preferably no hydrocortisone at all should be used.

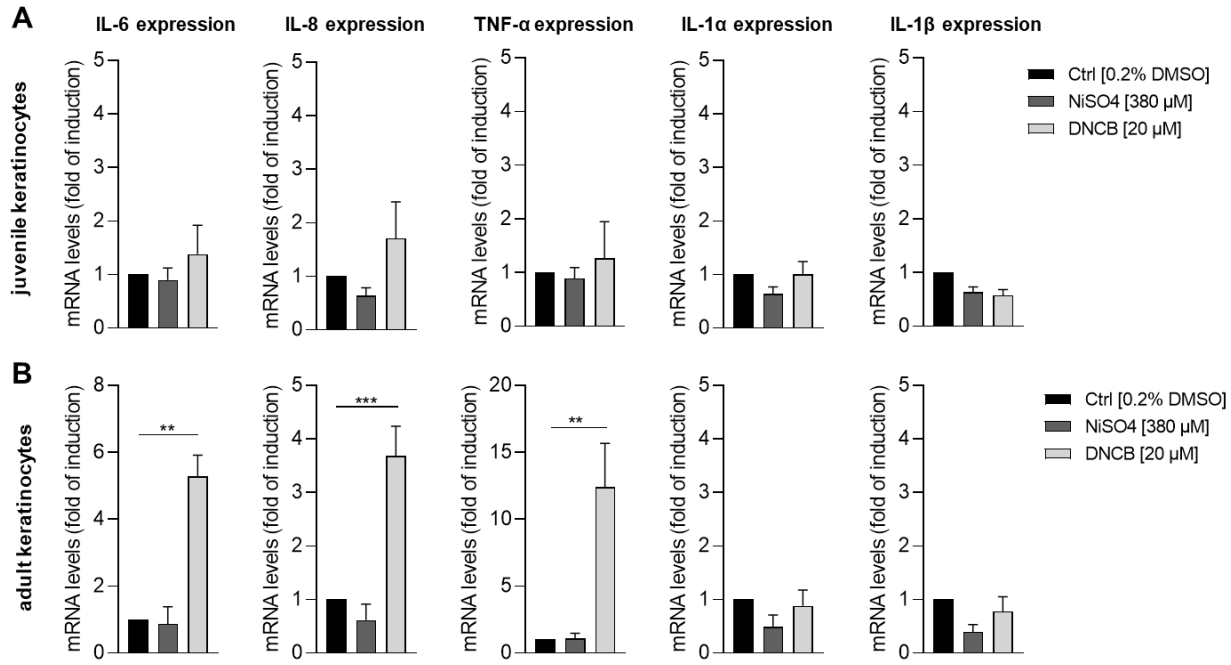

Figure 3.1-9 mRNA levels of inflammatory cytokine expression by **(A)** juvenile keratinocytes and **(B)** adult keratinocytes after $NiSO_4$ [380 µM] and DNCB treatment [20 µM] for 6 h. Results are depicted as folds of induction compared to the solvent control [0.2% DMSO] and normalized to the expression of the housekeeping gene [GAPDH]. Error bars indicate the standard errors of the mean (n = 3 independent experiments with ** = $p \leq 0.01$ and

3.2 Integration of THP-1 and THP-Langerin cells as potential LC surrogates into skin equivalents

Next, we aimed to integrate the THP-1 and THP-Langerin cell lines as potential LC surrogates into 3D human skin equivalents. To this end, I utilized the well-established dermis construct of the commercially available Phenion® Full-Thickness Skin models. The Phenion® dermis construct is based on primary human foreskin fibroblasts and a solid, porous collagen matrix, which allows the fibroblasts to migrate into the scaffold and to synthesize and secrete extracellular matrix components such as elastin and fibrillin-1, mimicking an *in vivo*-like elastic network of the native human skin [214, 215]. Briefly, THP-1 or THP-Langerin cells were seeded together with keratinocytes from a juvenile donor or from an adult donor at a 2:1 ratio onto the dermis constructs. After 10 days of air-liquid interphase (ALI) cultivation, the skin models were cryosectioned for histological analysis. Immunofluorescence staining of the tissue slides reveals that FTSE generated with keratinocytes from a juvenile donor with or without incorporated THP-1 or THP-Langerin cells were fully differentiated, displaying all epidermal

layers (Figure 3.2-1). In contrast, FTSE generated with keratinocytes from an adult donor comprised noticeably fewer layers, resulting in a thinner epidermis, particularly upon integration of immune cell surrogates. Nonetheless, THP-1 or THP-Langerin cells were integrated into the dermis, regardless of the keratinocyte donor cell type (juvenile vs. adult) (Figure 3.2-1). In conclusion, keratinocytes from juvenile donors seemed to be more suitable for generating a physiological FTSE. Furthermore, THP-1 cells, as well as THP-Langerin cells, could not be integrated as LC surrogates into the epidermal compartment of the FTSE. Indeed, multiple attempts to integrate THP-Langerin cells or THP-1 cells (including THP-1-derived iDCs and mDCs) into the epidermis failed.

The following seeding protocols were tested:
(1): seeding of THP-1/ THP-Langerin/ iDCs/ mDCs and KCs together
(2): seeding of THP-1/ THP-Langerin/ iDCs/ mDCs first, then keratinocytes (after 2 h)
(3): seeding of THP-1/ THP-Langerin/ iDCs/ mDCs together with ½ of the KCs and the other ½ KCs after 2 h
(4): seeding THP-1/ THP-Langerin cells together with ½ of the KCs first and the other ½ KCs after 24 h or 2 days of ALI Phase

Furthermore, the following compositions of ALI medium were tested:
(a) ALI medium with hydrocortisone
(b) ALI medium without hydrocortisone
(c) ALI medium (+/- HC) + distinct cytokine cocktails including GM-CSF, IL-4 or TGF-β

Nevertheless, all seeding protocols and ALI media compositions did not allow the integration of THP-1 cells, THP-Langerin cells, iDCs or mDCs into the epidermis.

To investigate how and at which time point THP-1 or THP-Langerin cells start to integrate into the dermis, I monitored integration over time (Figure 3.1-2). Significantly, by ALI d3, THP-1 and THP-Langerin cells could be detected in the dermal compartment. However, not all THP-1 or THP-Langerin cells were integrated in the dermal compartment as some of the cells appeared to be located on top of the differentiating epidermis on ALI day 3, day 5 and day 7. These results suggest that the keratinocytes might form a tight intercellular network that does not allow the integration of THP-1 or THP-Langerin cells, therefore potentially “driving” or “forcing” those cells out.

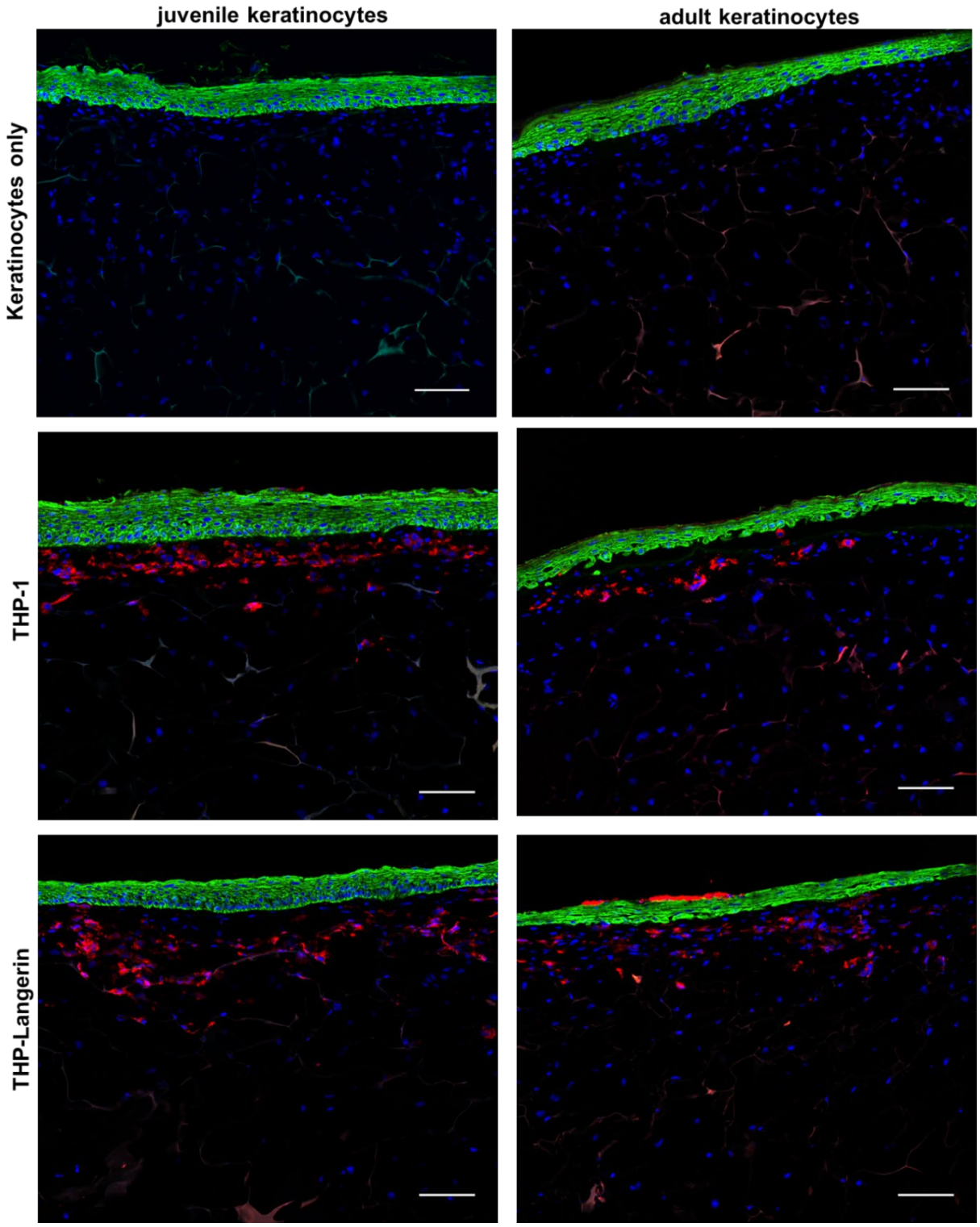

Figure 3.2-1 Histological analysis of the full-thickness skin equivalents with keratinocytes derived from a juvenile or an adult donor with and without integrated THP-1 or THP-Langerin cells. Skin models were cultivated in an air-liquid interphase (ALI) for 10 days and histologically processed via cryosectioning into 7µm tissue slides for immunofluorescence staining. Keratinocytes were stained with cytokeratin 5 (green signal). THP-1 or THP-Langerin cells were stained with CD45 (red signal). Nuclei were stained with DAPI (blue signal). Immunofluorescent imaging was conducted via spinning disk confocal microscopy on the CQ1. Scale bar = 100 µm.

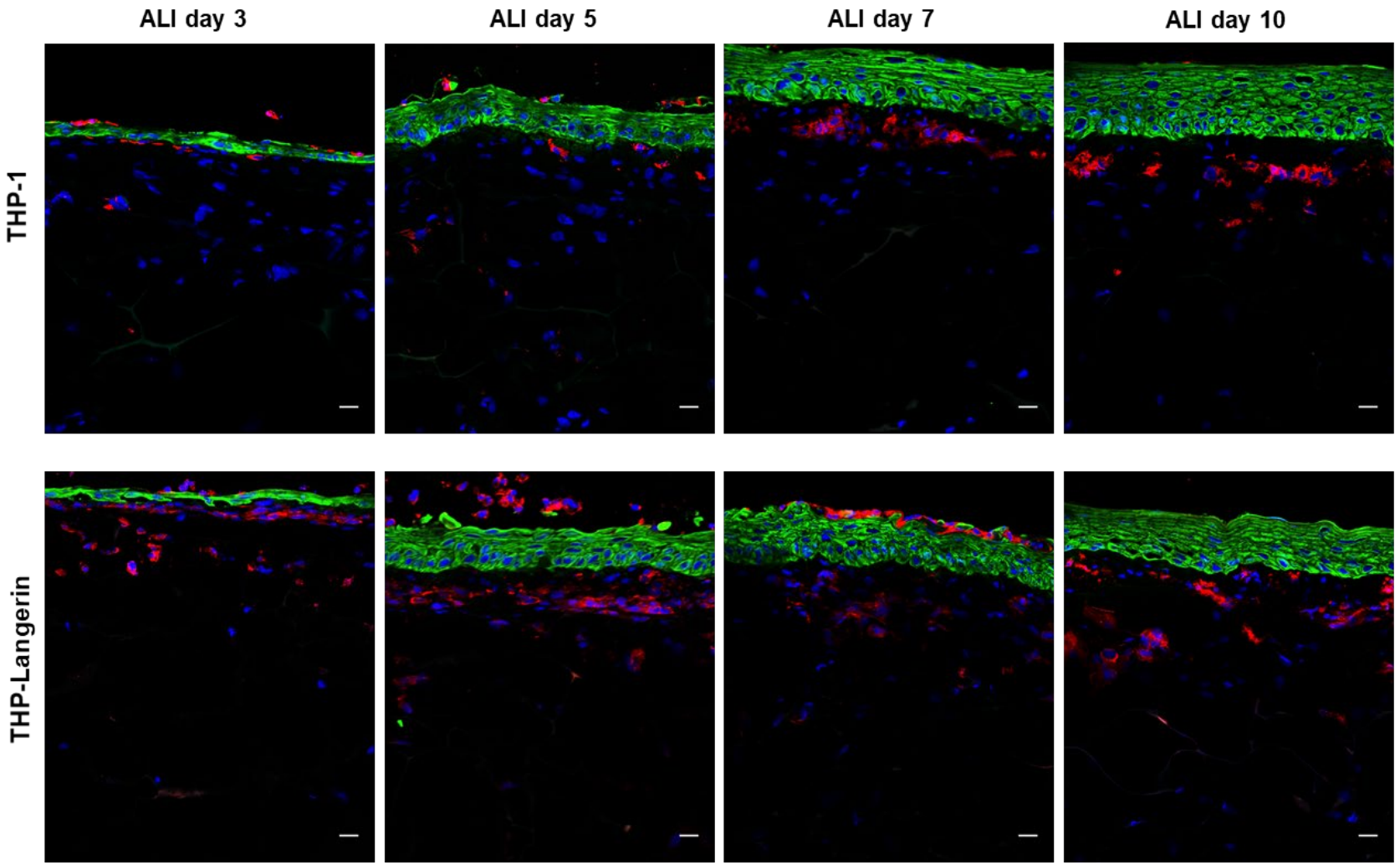

Figure 3.2-2 Time course for the integration of THP-1 and THP-Langerin cells into full-thickness skin equivalents. THP-1/THP-Langerin cells were seeded together with keratinocytes from juvenile donors onto the dermis models provided by Phenion. Skin models were cultivated in an air-liquid interphase (ALI) and histologically processed via cryosectioning on ALI d3, d5, d7, and d10 to monitor the integration of THP-1/THP-Langerin cells over time. Keratinocytes were stained with cytokeratin 5 (green signal). THP-1 or THP-Langerin cells were stained with CD45 (red signal). Nuclei were stained with DAPI (blue signal). Immunofluorescent imaging was conducted via spinning disk confocal microscopy on the CQ1. Scale bar = 20 µm

Furthermore, we were interested in whether primary human fibroblasts, located in the dermis construct, also impacted the integration of THP-1 or THP-Langerin cells into the dermis. Thus, I investigated the migratory capabilities of THP-1 and THP-Langerin cells towards isolated primary human fibroblasts and towards conditioned medium derived from the Phenion dermis (Figure 3.2-3). In fact, THP-1 cells actively migrated within 16 h towards conditioned medium from the dermis constructs (~146%) as well as towards primary human fibroblasts (~204%). Notably, when compared to the control (unconditioned medium), the number of THP-Langerin cells migrating to the conditioned dermal medium was significantly reduced (~3.7-fold). Furthermore, when compared to the control (medium only), the number of migrated THP-Langerin cells towards isolated fibroblasts was lower (~1.1-fold), indicating that THP-Langerin cells do not actively migrate towards primary human fibroblasts.

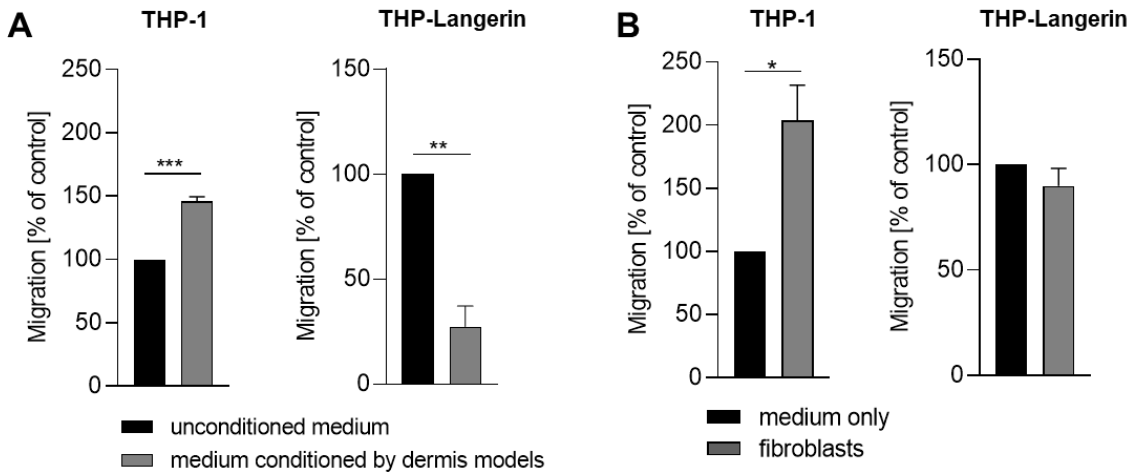

Figure 3.2-3 Transwell Migration Assay (TMA) of THP-1 or THP-Langerin cells towards **(A)** conditioned medium derived from Phenion dermis models or **(B)** primary human fibroblasts from a juvenile donor. Here, THP-1 cells or THP-Langerin cells were seeded with 1 x 10^5 cells in 100 µL fibroblast medium onto the membrane (5.0 µm) of the upper transwell inserts. Migration of THP-1/THP-Langerin cells towards **(A)** conditioned medium (48 h) from dermis models or **(B)** 4 x 10^4 primary human fibroblasts from a juvenile donor was determined after 16 h of incubation via flow cytometry (n = 3 independent experiments with * = $p \leq 0.05$, ** = $p \leq 0.01$ and *** = $p \leq 0.001$).

In conclusion, THP-1 cells seem to actively migrate towards the dermis and the primary human fibroblasts, but they also seem to be partially forced out of the epidermis. Contrary, THP-Langerin cells do not actively migrate towards the dermal compartment, including primary human fibroblasts. However, when compared to the time course of the THP-1 incorporation, THP-Langerin cells seem to be forced out of the dermis to a greater extent.

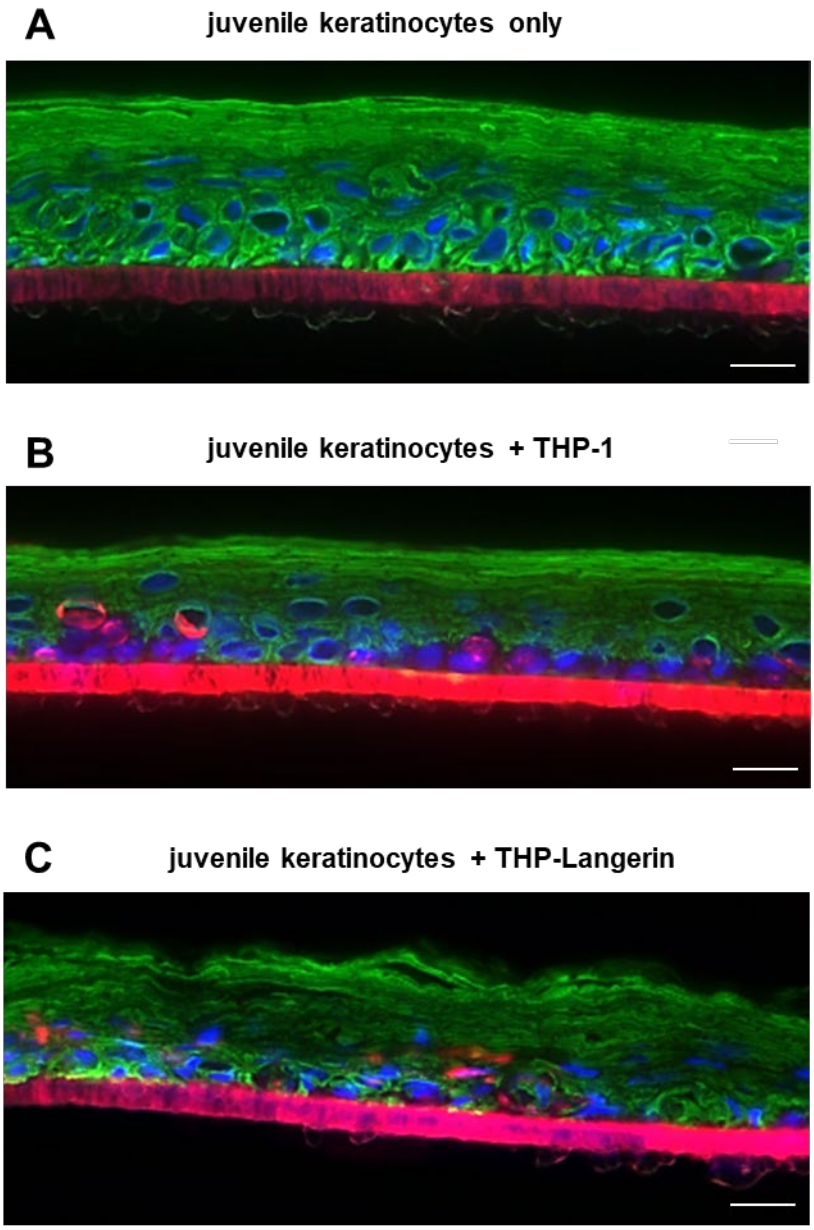

Figure 3.2-4 Integration of THP-1 or THP-Langerin cells into epidermal models. Keratinocytes from a juvenile donor (3.1 x 10^5 cells) were **(A)** seeded alone or together with **(B)** THP-1 or **(C)** THP-Langerin cells (4.7 x 10^5 cells) onto the polycarbonate membrane of transwell inserts (0.47 cm^2, 0.4 µm pore size). To enhance the adherence of the keratinocytes, the cell culture inserts were coated with 5 µg/cm^2 collagen before seeding the cells. After seeding, the epidermal models were cultivated for 48 h in a submerse phase and then transferred into an air-liquid interphase for 20 days until histological processing via cryosectioning (7 µm tissue slides). Keratinocytes were stained with cytokeratin 5 (green signal). THP-1 or THP-Langerin cells were stained with CD45 (red signal). Nuclei were stained with DAPI (blue signal). Immunofluorescent imaging was conducted using the high-resolution fluorescence microscope Keyence BZ-X800 Scale bar = 20 µm.

Furthermore, we were interested in whether THP-1 or THP-Langerin cells could be integrated into an epidermal model, thereby eliminating the impact of the dermal compartment and fibroblasts. Remarkably, THP-1 as well as THP-Langerin cells could be integrated into epidermal models and detected 22 days after integration. However, the membrane of the

inserts was coated with collagen to enhance cell adherence, which may have had an impact on the integration of THP-1 or THP-Langerin cells (Figure 3.2-4).

In conclusion, THP-1 and THP-Langerin cells can be successfully integrated into the epidermis of epidermal models, but not into the epidermis of a FTSE. Hence, we investigated undifferentiated THP-1 cells and immature DCs differentiated from THP-1 cells as potential dermal dendritic cell surrogates for the identification and characterization of sensitizers and drug discovery (Chapter 2.1 and 2.2).

3.3 Pseudopterosin A-D as a potential natural anti-inflammatory drug candidate in skin sensitization

Pseudopterosins have been described as potent anti-inflammatory and wound-healing agents [191, 198, 203, 205]. However, to our knowledge, the anti-inflammatory effects of pseudopterosins on skin sensitization have not been reported yet. Thus, we aimed to investigate the potential of pseudopterosin to attenuate or suppress the sensitizer-induced activation of DC surrogates. For this, I used a mixture of four different pseudopterosin derivates (PsA-D) (PsA:B:C:D ≙ 85:5:5:5), which were isolated from the octocoral sea whip *A. elisabethae* collected from the Bahamas (South Bimini Island).

To establish the optimal treatment concentrations, we determined the cytotoxicity and half maximal inhibitory concentration (IC_{50}) of PsA-D on THP-1 cells and keratinocytes (Figure 3.3-1). The IC_{50} of PsA-D upon 24-hour exposure was calculated based on three independent experiments, yielding the following IC_{50} values: 39.8 µM ± 1.5 µM for THP-1 cells, 12. µM ± 0.6 µM for keratinocytes, and 28.2 µM ± 1.1 µM for the co-culture encompassing keratinocytes and THP-1 cells. Furthermore, a significant decrease in cell viability for THP-1 cells after 24 h of treatment with PsA-D was detected at concentrations higher than 35 µM (Figure 3.3-1 B). Hence, treatment concentrations ≤ 20 µM were chosen for treatment times equal to or higher than 24 h.

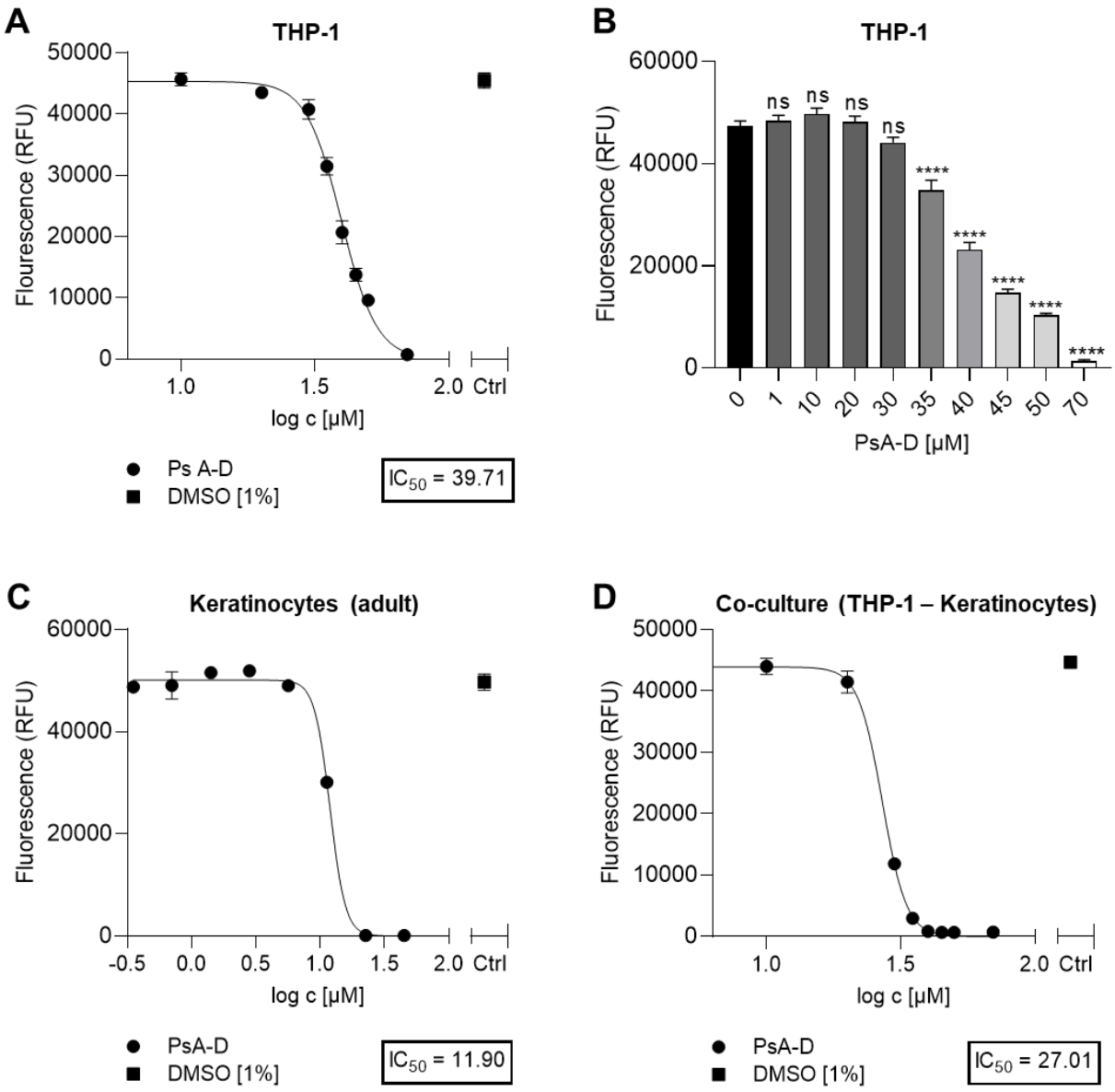

Figure 3.3-1 Determination of the cytotoxicity and half maximal inhibitory concentration (IC_{50}) of Pseudopterosin A-D (PsA-D) on (**A & B**) THP-1 cells, **(C)** primary human keratinocytes (from an adult donor), and **(D)** a co-culture of THP-1 cells and keratinocytes. Cells were seeded in triplicate for each treatment concentration as well as for the solvent control (1% DMSO). PsA-D was applied in decreasing concentrations [70 µM, 50 µM, 45 µM, 40 µM, 35 µM, 30 µM, 20 µM, 10 µM, 1 µM] for 24 h. Cell viability was determined according to the PrestoBlue assay and is depicted in relative fluorescence units (RFUs). **(A, C, and D)** depict one experiment (with three technical replicates) out of three independent experiments. **(B)** depicts n = 3 independent experiments (each with three technical replicates). Error bars indicate the standard errors of the mean. Statistical significance was defined as

Since one of the hallmarks of DC activation and maturation is the upregulation of distinct surface markers such as CD54, CD86, or CD83, we investigated whether PsA-D could reduce the sensitizer-induced upregulation of those markers on THP-1 cells or THP-1-derived iDCs. First of all, I examined the impact of PsA-D treatment alone on THP-1 cells and iDCs. In fact, treatment of THP-1 cells for 24 h significantly reduced the basal surface marker expression of CD54 (5 µM: ~1.1fold; 10 µM: ~1.3-fold, 20 µM: ~1.7-fold), CD86 (5 µM: ~1.15-fold; 10 µM: ~1.6-fold; 20 µM: ~2.4fold) and CXCR4 (5 µM: ~1.1-fold; 10 µM: ~1.2-fold; 20 µM:

~1.4fold) in a dose-dependent manner (Figure 3.3-2A). Comparable dose-dependent trends in the reduction of cells expressing the surface markers CD54 (10 µM: ~1.1-fold; 20 µM: ~1.4-fold), CD86 (10 µM: ~1.2fold; 20 µM: ~1.7-fold), and CD11b (10 µM: ~1.5-fold; 20 µM: ~1.9-fold) could be observed for iDCs upon exposure to PsA-D.

In a second step, I investigated the anti-inflammatory potential of PsA-D on the $NiSO_4$-/DNCB-induced upregulation of surface markers such as CD54, CD86, CD83, and CD11b on THP-1 and THP-1-derived iDCs. Pre-treatment of THP-1 cells and iDCs with PsA-D for 1 h before applying $NiSO_4$ for 23 h resulted in a significant dose-dependent decrease of the $NiSO_4$-induced upregulation of the surface markers CD54 (THP-1 cells: 10 µM: ~1.2-fold; 20 µM: ~1.3-fold **I** iDCs: 10 µM: 1.1-fold; 20 µM: ~1.2-fold), CD86 (THP-1 cells: 10 µM: ~1.7-fold; 20 µM: ~2.7-fold **I** iDCs: 10 µM: ~1.3-fold; 20 µM: ~1.6-fold) and CD11b (THP-1 cells: 10 µM: ~1.9-fold; 20 µM: ~2.7-fold **I** iDCs: 10 µM: ~1.7-fold; 20 µM: ~2.2-fold). In addition, pre-treatment of THP-1 cells with PsA-D reduced the $NiSO_4$-induced surface marker expression of HLA-DR (10 µM: ~1.5-fold; 20 µM: ~1.9-fold) and CD83 (10 µM: ~3-fold; 20 µM: ~5.5-fold) in a dose-dependent manner.

Furthermore, pre-treatment of THP-1 cells with PsA-D led to a significant, dose-dependent decrease in the DNCB-induced upregulation of the surface markers CD54 (10 µM: ~1.1-fold; 20 µM: ~1.3-fold), CD86 (10 µM: ~1.2-fold; 20 µM: ~1.6-fold), and CCR7 (10 µM: ~3.2-fold; 20 µM: ~4.8-fold). However, pre-treatment of iDCs with 10 µM PsA-D could only induce a minor decrease in the DNCB-induced upregulation of CD54 (10 µM: ~1.03-fold), CD86 (10 µM: ~1.07-fold), and pre-treatment with 20 µM PsA-D was required to significantly reduce the DNCB-induced upregulation of CD54 (20 µM: ~1.1-fold) and CD86 (20 µM: ~1.4-fold). The DNCB-induced upregulation of CD11b on iDCs was reduced by PsA-D pre-treatment in a dose-dependent manner (10 µM: ~1.6-fold; 20 µM: ~2.6-fold) (Figure 3.3-2).

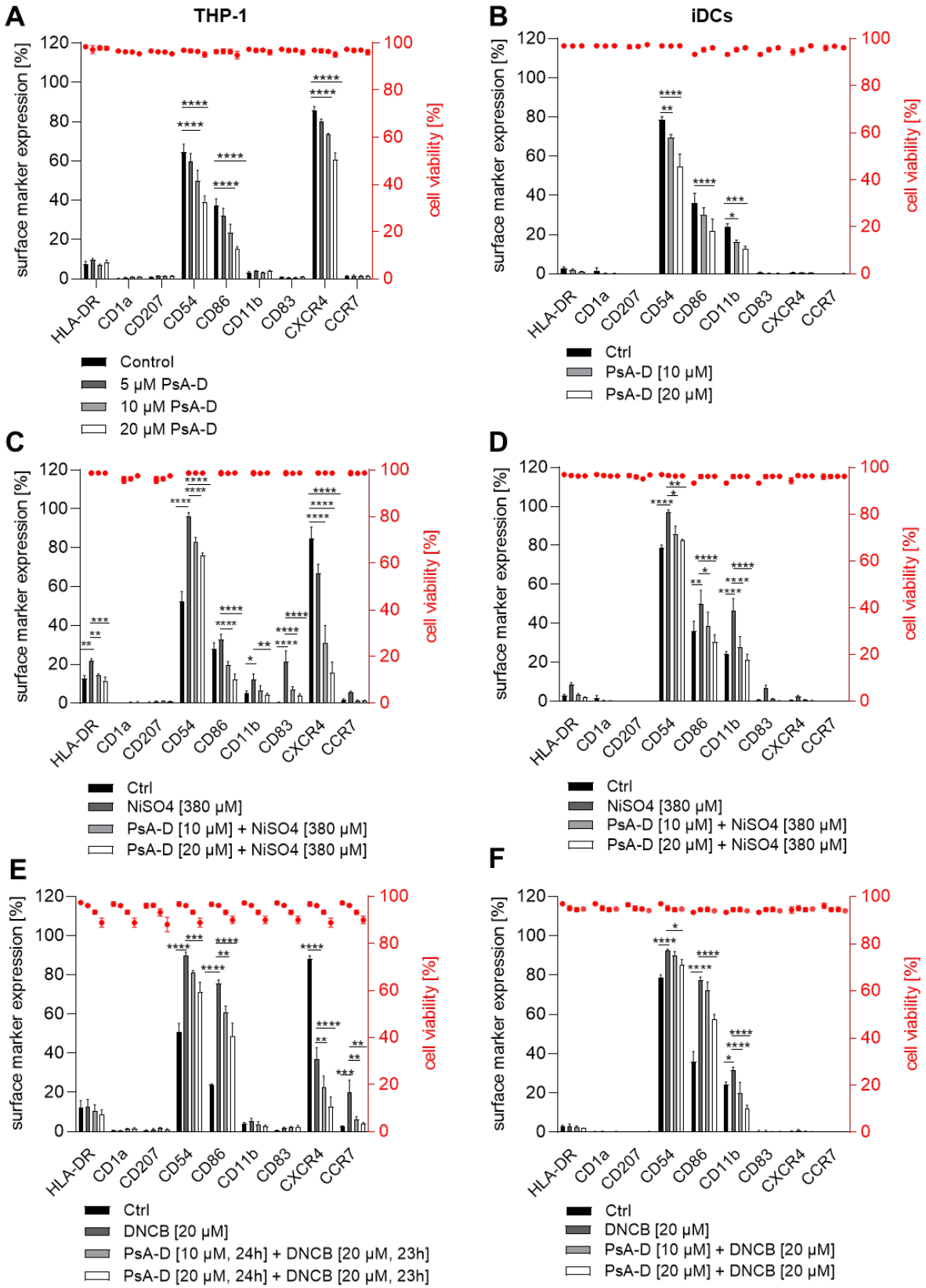

Figure 3.3-2 Anti-inflammatory properties of Pseudopterosin (Ps) A-D on sensitizer-induced surface marker expression by THP-1 cells and THP-1-derived iDCs. Here, THP-1 cells **(A, C, E)** or iDCs **(B, D, F)** were seeded with 1 × 10^6 cells/mL in 1 mL THP-1 medium into 24-well plates. To determine the potential of PsA-D to block the sensitizer-induced upregulation of surface markers, cells were pre-treated with PsA-D for 1 h before applying sensitizers, namely $NiSO_4$ [380 µM] and DNCB [20 µM] for 23 h. Surface marker expression of at least 10,000 viable cells was analyzed via flow cytometry. Error bars indicate the standard errors of the mean (n = 3 independent experiments with * = $p \leq 0.05$, ** = $p \leq 0.01$, *** = $p \leq 0.001$, and **** = $p \leq 0.0001$).

To assess the anti-inflammatory impact of PsA-D on the sensitizer-induced activation of the NF-κB and p38 MAPK pathways, western blot analysis was performed. While treatment of THP-1 cells with 30 µM PsA-D alone did not affect the expression of IκBα, treatment with higher concentrations of PsA-D [40 µM and 50 µM] slightly induced the degradation of IκBα (~1.2–1.3-fold). However, pre-treatment of THP-1 cells with 30 µM or 40 µM PsAD before applying $NiSO_4$ [380 µM] for 1 h resulted in a significant blockade of the IκBα-degradation (30 µM: ~98%; 40 µM: ~92% expression) (Figure 3.3-3).

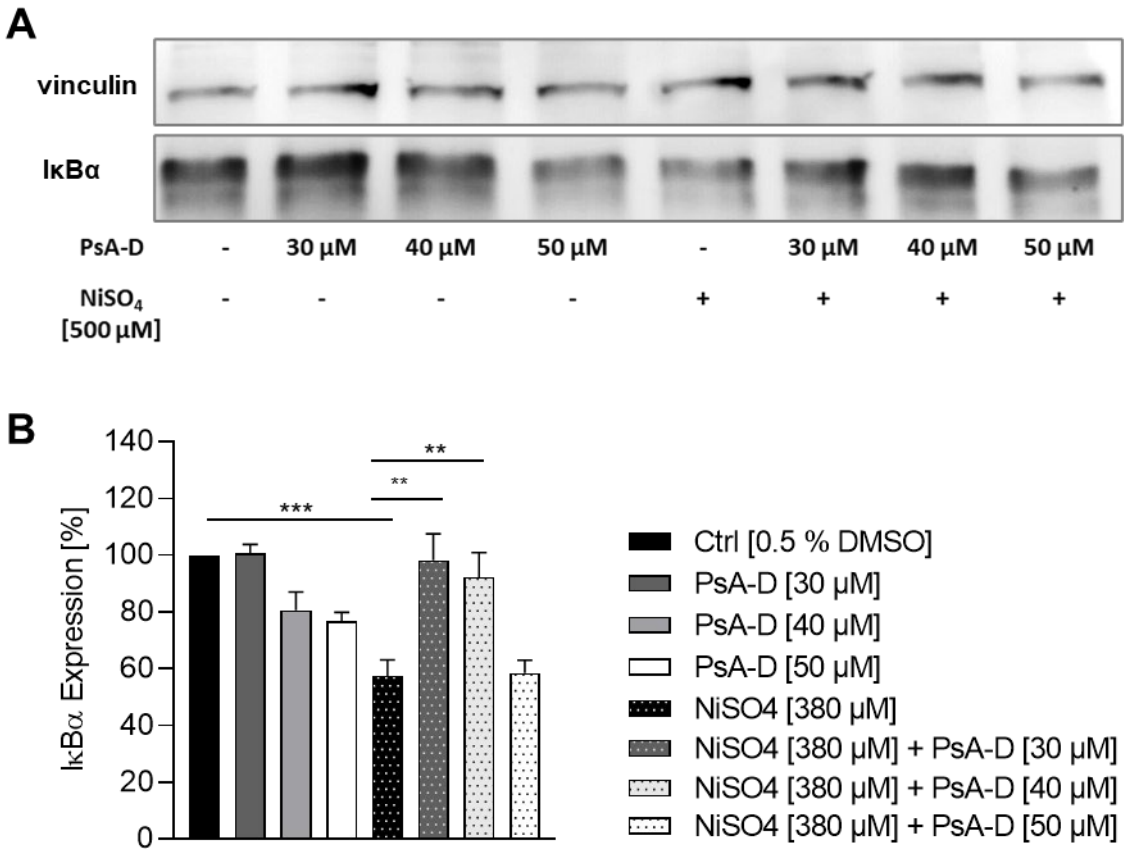

Figure 3.3-3 Pseudopterosin A-D blocks the $NiSO_4$-induced degradation of IκBα. Here, THP-1 cells were seeded with 1 x 10^6 cells in 1 mL THP-1 medium into a 24-well plate. Cells were re-treated with different concentrations of PsA-D [30 µM, 40 µM, 50 µM] for 1 h before applying $NiSO_4$ [380 µM] for 1 h. **(A)** depicts one representative blot of three independent experiments. **(B)** depicts the quantification of image bands normalized to the solvent control [0.5% DMSO].

Furthermore, we investigated the anti-inflammatory potential of PsA-D for the sensitizer-induced phosphorylation of p38 MAPK. Pre-treatment of THP-1 cells with PsA-D did not reduce the minor (~1.3-fold) $NiSO_4$-induced phosphorylation of p38 MAPK in THP-1 cells. However, pre-treatment of THP-1 cells with PsA-D could reduce the DNCB-induced 3.8-fold phosphorylation of p38 MAPK to a 1.48-fold phosphorylation compared to the solvent control (Figure 3.3-4).

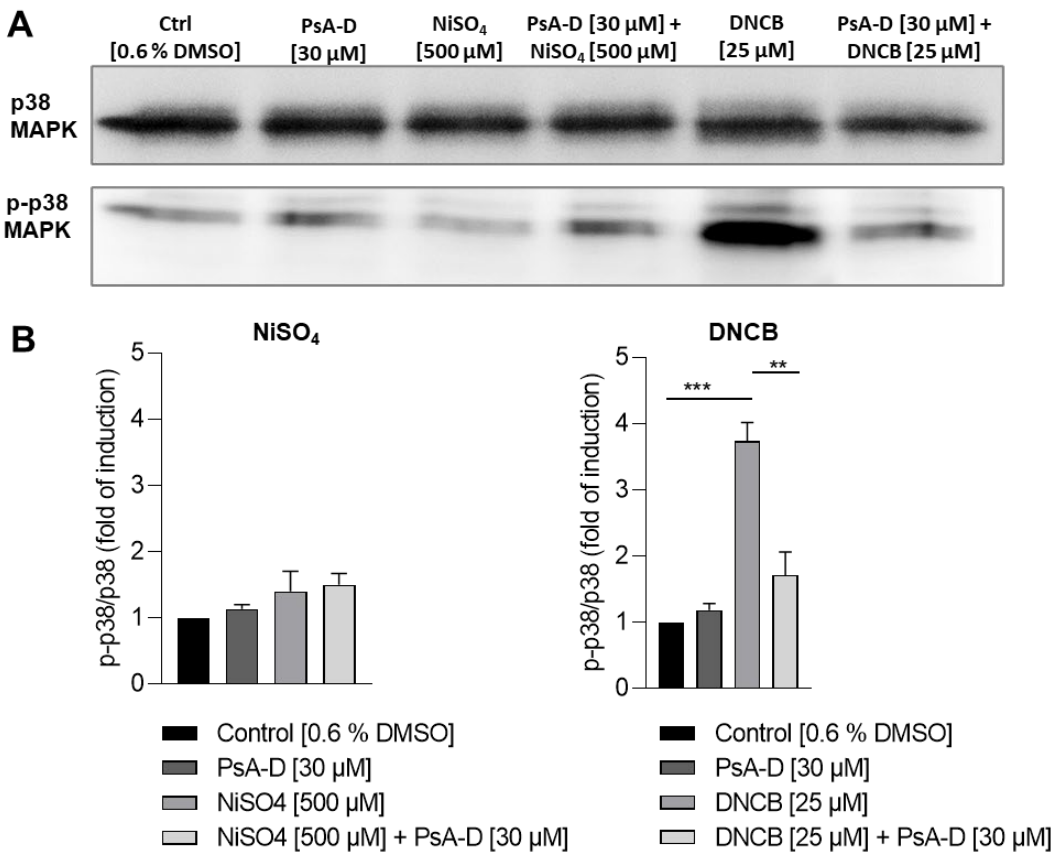

Figure 3.3-4 Pseudopterosin A-D blocks the DNCB-induced phosphorylation of p38 MAPK. Here, THP-1 cells were seeded with 1 x 10^6 cells in 1 mL THP-1 medium into a 24-well plate. Cells were re-treated with PsA-D [30 µM] for 1 h before applying $NiSO_4$ [500 µM] or DNCB [25 µM] for 30 min. **(A)** depicts one representative blot of three independent experiments. **(B)** depicts the quantification of image bands normalized to the solvent control [0.6% DMSO].

To examine the anti-inflammatory characteristics of PsA-D on the sensitizer-induced secretion of inflammatory cytokines, the supernatants of THP-1-derived iDCs pre-treated with PsA-D [20 µM] for 1 h, followed by a 23 h exposure to $NiSO_4$ [380 µM] or DNCB [25 µM], were collected and analyzed using a cytometric bead array assay. Pre-treatment of iDCs with PsA-D significantly reduced the $NiSO_4$-induced secretion of IL-8 (~9-fold), IL-6 (~6.5-fold), and blocked the $NiSO_4$-induced secretion of IL-1β (Figures 3.2-5A, B, C). In addition, PsA-D could decrease the DNCB-induced secretion of IL-8 (~2.9-fold) and IL-1β (~7.8-fold) (Figures 3.3-5E, F, G).

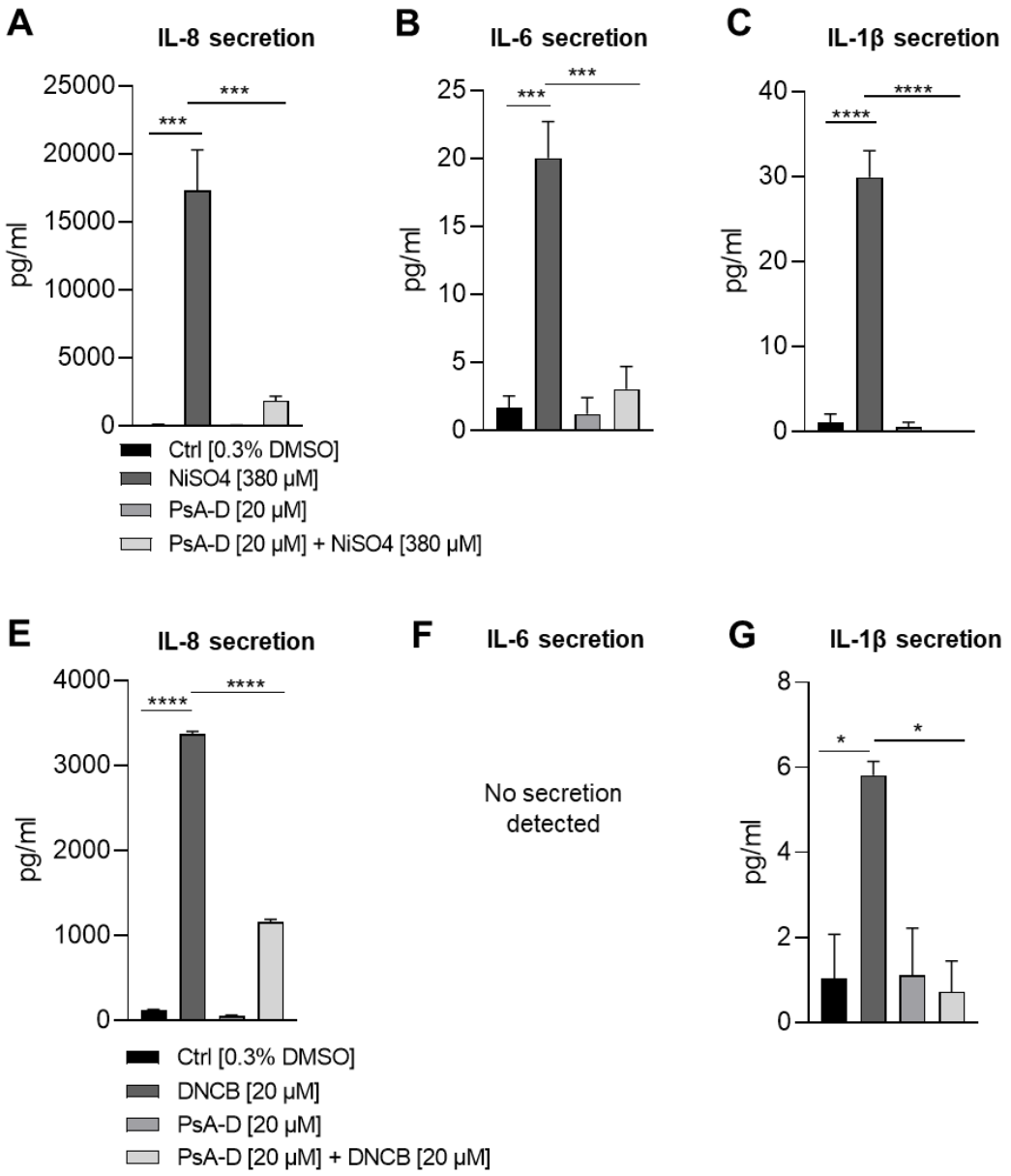

Figure 3.3-5 Pseudopterosin A-D diminishes the sensitizer-induced secretion of inflammatory cytokines such as IL-8 (A & E), IL-6 (B), and IL-1β (C & G) by iDCs. Here, iDCs were seeded with 1 x 10^6 cells in 1 mL THP-1 medium into a 24-well plate. Cells were pre-treated with PsA-D [20 µM] for 1 h before applying $NiSO_4$ [380 µM] or DNCB [20 µM] for 23 h. Supernatants were harvested, and cytokine concentrations were detected using a cytometric bead array assay. Error bars indicate the standard errors of the mean (n = 3 independent experiments with *p ≤ 0.05, ***p ≤ 0.001, and ****p ≤ 0.0001).

Since PsA-D significantly reduced the number of cells expressing CXCR4 on their surface, we were interested in examining whether PsA-D might also impact the migratory capabilities of THP-1 cells towards SDF-1 (a CXCR4-ligand). When compared to the solvent-treated control (DMSO [0.2%] + medium only), treatment of THP-1 cells with 10 µM PsA-D for 24 h blocked the migration of THP-1 cells towards SDF-1 completely. Notably, treatment of THP-1 cells with PsA-D also reduced the basal migratory capability of THP-1 cells (towards the medium only) by 1.7-fold) (Figure 3.3-6). However, Figure 3.3-6 depicts only one dataset, and further independent replicates need to be conducted to confirm these preliminary results.

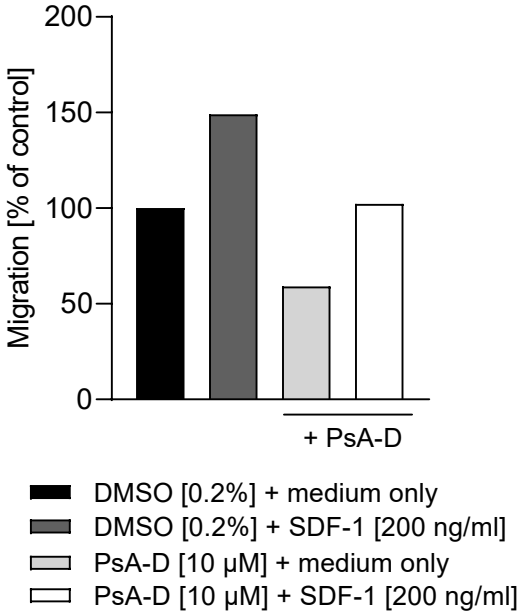

Figure 3.3-6 Pseudopterosin reduces the migratory capabilities of THP-1 cells. Here, 1 x 10^6 THP-1 cells were seeded in 1 mL of THP-1 medium into a 24-well plate. Cells were treated with 10 µM of PsA-D for 24 h. For the TMA assay, treated or untreated THP-1 cells were seeded with 1 x 10^5 cells in 100 µl THP-1 medium onto the membrane (5.0 µm) of the upper transwell inserts. Migration of THP-1/ THP-Langerin cells towards medium only (controls) or 200 ng/ml SDF-1 was determined after 16 h of incubation via flow cytometry. This graphic shows one preliminary dataset.

In summary, we proved that pre-treatment with PsA-D decreases the sensitizer-induced up-regulation of surface markers, including CD54, CD86, CD11b, CD83, and CCR7. Furthermore, PsA-D pre-treatment blocked the $NiSO_4$-induced degradation of IκBα and the DNCB-induced phosphorylation of p38 MAPK. In addition, PsA-D reduced the sensitizer-induced secretion of IL-6, IL-8, TNF-α and IL-1β. The first preliminary data indicated a PsA-D mediated inhibition of of THP-1 cell migration towards SDF1. Overall, these data suggest strong anti-inflammatory properties for PsA-D on skin sensitization.

3.4 Material and Methods

3.4.1.1 Suppliers and their locations

Table 3.3-1 Suppliers and their locations

Supplier	Headquarter
Agilent Dako	Santa Clara, California, USA
Agilent Technologies	Santa Clara, California, USA
ATCC	Manassas, Virginia, USA
Beckman Coulter	Brea, California, USA
Becton Dickinson	Franklin Lakes, New Jersey, USA
BioCat GmbH	Heidelberg, Germany
Bio-Rad Laboratories, Inc.	Hercules, California, USA
BMG Labtech	Ortenberg, Germany
Carl Roth GmbH + Co.KG	Karlsruhe, Germany
Carlo Erba Reagents GmbH	Emmendingen, Germany
Cell Signaling Technology	Danvers, Massachusetts, USA
Corning	Corning, New York, USA
Epredia	Portsmouth, New Hampshire, USA
Eurofins Scientific	Luxemburg, Luxemburg
Fisher Scientific	Hampton, New Hampshire, USA
Gibco	Grand Island, New York, USA
GraphPad Software, Inc.	San Diego, California, USA
Greiner	Frickenhausen, Germany
ImmunoTools	Friesoythe, Germany
Invitrogen™	Waltham, Massachusetts, USA
InvivoGen	San Diego, California, USA
Lonza	Basel, Switzerland
Miltenyi Biotec	Gladbach, Germany
New England BioLabs (NEB)	Frankfurt, Germany
OriGene Technologies	Rockville, Maryland, USA
PAN-Biotech GmbH	Aidenbach, Germany
Phenion	Düsseldorf, Germany
Promega	Madison, Wisconsin, USA
Roche	Basel, Switzerland
Sakura Finetek	Torrance, California, USA
Santa Cruz Biotechnology	Dallas, Texas, USA
Sarstedt	Hildesheim, Germany
Sigma-Aldrich	Darnstadt, Germany
Thermo Fisher Scientific	Waltham, Massachusetts, USA

VWR	Radnor, Pennsylvania, USA
Yokogawa	Musashino, Japan

3.4.2 Materials

3.4.2.1 Chemicals

Table 3.3-2 Chemicals

Chemicals	Supplier	Catalog number
10% normal goat serum	Invitrogen	50062Z
10X ThermoPol® Reaction Buffer	NEB	B9004S
4‘,6-diamidino-2-phenylidole (DAPI)	Sigma	D9542
Aceton	Carlo Erba Reagents GmbH	V2B071252B
Agarose Standard	Roth	3810.3
Ammonium persulfate (APS)	Roth	271299378
Bovine serum albumin (BSA)	Roth	8076.2
Calcium chloride ($CaCl_2$)	Sigma-Aldrich	C5670
Deoxynucleotide (dNTP) Solution Mix	NEB	N0447S
Dimethyl sulfoxide (DMSO)	Roth	A994.1
Gel Loading Dye Purple (6X)	NEB	B7024S
Glycine	Roth	HN07.2
Methanol	Fisher Scientific	M/4000/17
Phosphatase Inhibitor	Roche	04906845001
Precision Plus Protein Dual Color Standards	Bio-Rad	1610374
Proteinase inhibitor	Roche	11836170001
Quick-Load® Low Molecular Weight DN	NEB	N0557S
Rhodamine/Rotiphorese	Roth	3043.1
Sodium chloride (NaCl)	Roth	9265.2
Sodium dodecyl sulfate (SDS)	Roth	072318806
Sodium-deocycholate	Roth	D6750
Taq DNA Polymerase	NEB	M0267S
Tetramethylethylenediamine (TEMED)	Roth	2367.1
Tissue Fluorescence mounting medium	Agilent	S3023
Tissue-Tek	Sakura	4583
Tris	Roth	A411.4
Triton X-100	Sigma-Aldrich	T9284
Trypan Blue Stain (0.4%)	Gibco	15250061
Tween 20	Roth	9127.1

3.4.2.2 Buffers and Solutions

The following buffers and solutions listed in the table below were solved or diluted in demineralized water

Table 3.3-3 Buffers and solutions

Buffer or solution	Components
RIPA Buffer (stock)	50 mM Tris, pH 8 150 mM NaCl 1% Triton X-100 0.5% sodium deoxycholate 0.1% sodium dodecyl sulfate (SDS)
RIPA ++	RIPA Buffer (stock) Protease inhibitor (1 pill) Phosphatase inhibitor (1 pill)
SDS-Running Buffer (10x)	250 mM Tris 1.9 M Glycine 1% SDS
TBS-T (10x)	200 mM Tris, pH 7.5 1.5 M NaCl 1% Tween
Transfer/Blotting Buffer (10x)	250 mM Tris, pH 8.3 1.9 M Glycine

Table 3.3-4 Commercially available buffers

Buffer	Supplier	Catalog number
4x Laemmli buffer	Bio-Rad Laboratories, Inc.	1610747
AutoMACs running buffer	Miltenyi Biotec	130-091-221
DAKO antibody diluent	Agilent Dako	S0809
Dulbecco's phosphate buffered saline (DPBS) (1x)	PAN Biotec	P04-36500
PrestoBlue™ HS Cell Viability Reagent	Invitrogen	P50201
Restore™ Western Blot Stripping Buffer	Thermo Scientific	21059

3.4.2.3 Cell culture medium, supplements and reagents

Table 3.3-5 Basic cell culture medium, supplements and reagents

Media/ reagent/ supplement	Supplier	Catalog number
2-Mercaptoethanol	Gibco	21985023
Blasticidin	InvivoGen	ant-bl-1
EpiLife™	Gibco	MEPI500CA
FBS	Gibco	10270-106
HEPES buffered saline solution	Lonza	CC-5022
HKGS	Gibco	S0015
Normocin	InvivoGen	ant-nr-1
Pen-Strep	Gibco	15140122
RPMI	Gibco	22400-089
Trypsin neutralizing solution	Lonza	CC-5002
Trypsin/EDTA	Lonza	CC-5012
Trypsin-EDTA 0.05%	Gibco	25300054

Table 3.3-6 Commercially available and “ready to use” cell culture medium

Media	Supplier	Catalog number
Fibroblast medium	Phenion	FB CM-250
Keratinocyte medium (for KCs from juvenile donors, Phenion)	Phenion	K CM-250
KGM Gold Bulletkit: KBM Gold Keratinocyte Growth Basal Medium + KGM Gold Keratinocyte Growth Medium SingleQuots (for KCs from adult donors, Phenion)	Lonza	00192060 (00192152 + 00192151)
Air liquid interphase medium (full-thickness skin model)	Phenion	ALI CM HC-250

Table 3.3-7 Cell culture medium compositions

Media composition for	Media composition
THP-1 and THP-Langerin	RPMI FBS (10%) Pen-Strep (1%) 2-Mercaptoethanol (0.05 mM)
THP1-Blue™ NF-κB	RPMI FBS (10%) Pen-Strep (1%) 2-Mercaptoethanol (0.05 mM) Blasticidin (10 µg/mL)

	Normocin (100 µg/mL)
Keratinocyte medium for epidermal models	EpiLife™ HKGS (1%) Pen-Strep (1%)
Submerse medium for epidermal models	EpiLife™ HKGS (1%) Pen-Strep (1%) $CaCl_2$ (1.5mM)
Air-liquid interface medium (epidermal models)	EpiLife™ HKGS (1%) Pen-Strep (1%) $CaCl_2$ (1.5mM) L-ascorbic acid 2-phosphate (73 µg/mL) KGF (10 ng/mL)

3.4.2.4 Cytokines, growth factors and treating compounds

Table 3.3-8 Cytokines, chemokines and growth factors

Agent	Dissolved in	Supplier	Catalog number
rhGM-CSF	$_{dd}H_2O$	ImmunoTools	11343125
rhIL-4	$_{dd}H_2O$	ImmunoTools	11340045
rhKGF	$_{dd}H_2O$	ImmunoTools	11343653
SDF-1	$_{dd}H_2O$	R&D Systems	6448-SD-025/CF

Table 3.3-9 Treating compounds

Compound	Dissolved in	Supplier	Catalog number
1-chloro-2,4-dinitrobenzene (DNCB)	DMSO	Sigma-Aldrich	237329
Lipopolysaccharide (LPS) from E. coli O111:B4	PBS	Sigma-Aldrich	L2630
Nickel sulfate ($NiSO_4$)	PBS	Sigma-Aldrich	227676
Pseudopterosin A-D (PsA-D)	DMSO	-	-

3.4.2.5 Antibodies

Table 3.3-10 Primary antibodies

Antibody	Conjugate	Species	Application	Supplier	Catalog no.
CCR7 (CD197)	PE-Vio770	recombinant	Flow cytometry (1:50)	Miltenyi Biotec	130-117-545
CD11b	VioGreen	recombinant	Flow cytometry (1:50)	Miltenyi Biotec	130-110-559
CD1a	PE	recombinant	Flow cytometry (1:50)	Miltenyi Biotec	130-111-870
CD207 (Langerin)	PE-Vio770	recombinant	Flow cytometry (1:50)	Miltenyi Biotec	130-112-213
CD54 (ICAM-1)	APC	recombinant	Flow cytometry (1:50)	Miltenyi Biotec	130-121-342
CD83	PE	recombinant	Flow cytometry (1:50)	Miltenyi Biotec	130-110-503
CD86	APC	recombinant	Flow cytometry (1:50)	Miltenyi Biotec	130-116-161
CXCR4 (CD184)	PE-Vio770	recombinant	Flow cytometry (1:50)	Miltenyi Biotec	130-120-728
HLA-DR	VioGreen	recombinant	Flow cytometry (1:50)	Miltenyi Biotec	130-111-795
REA Control (S)-APC	APC	recombinant	Flow cytometry (1:50)	Miltenyi Biotec	130-113-434
REA Control (S)-PE	PE	recombinant	Flow cytometry (1:50)	Miltenyi Biotec	130-113-438
REA Control (S)-PE Vio770	PE-Vio770	recombinant	Flow cytometry (1:50)	Miltenyi Biotec	130-113-440
REA Control (S)-VioGreen	VioGreen	recombinant	Flow cytometry (1:50)	Miltenyi Biotec	130-113-444
REA Control (S)-VioBright R667	VioBright R667	recombinant	Flow cytometry (1:50)	Miltenyi Biotec	130-118-217
CD45	VioBright R667	recombinant	IF-staining (1:50)	Miltenyi Biotec	130-110-779
CD1a	-	mouse	IF-staining (1:50)	Santa Cruz Biotechnology	Sc-18885
Cytokeratin 5 (CK5)	-	rabbit	IF-staining (1:75)	OriGene	TA327666
IκBα	-	rabbit	Western blot (1:1000)	Cell Signaling Technology	9242S

P38 MAPK	-	rabbit	Western blot (1:1000)	Cell Signaling Technology	8690T
Phopho-p38 MAPK (Thr180/Tyr182)	-	rabbit	Western blot (1:1000)	Cell Signaling Technology	4511T
Vinculin	-	rabbit	Western blot (1:1000)	Cell Signaling Technology	13901S

Table 3.3-11 Secondary antibodies

Antibody	Conjugate	Species	Application	Supplier	Catalog no.
Alexa Fluor 488 F(ab´) 2 fragment goat anti-mouse IgG (H+L)	Alexa Flour 488	Goat	IF staining (1:200)	Invitrogen	A11017
Goat anti-rabbit IgG (H+L) Secondary Antibody, HRP	HRP	Goat	Western Blot (1:5000)	Thermo Fisher Scientific	31460

3.4.2.6 Oligonucleotides

All primers used were purchased from Eurofins. Forward and reverse primers are listed in the table below.

Table 3.3-12 PCR Primers

	Forward (5′→3′)	Reverse (5′→3′)
GAPDH	TGCACCACCAACTGCTTAGC	GGCATGGACTGTGGTCATGAG
IL-6	GGCACTGGCAGAAAACAACC	GCAAGTCTCCTCATTGAATCC
IL-8	ACTGAGAGTGATTGAGAGTGGAC	AACCCTCTGCACCCAGTTTTC
IL-1α	TGTATGTGACTGCCCAAGATGAAG	AGAGGAGGTTGGTCTCACTACC
IL-1β	GCACGATGCACCTGTACGAT	CACCAAGCTTTTTTGCTGTGAGT
TNF-α	CCCTGCTGCACTTTGGAGTG	TCGGGGTTCGAGAAGATGAT

3.4.2.7 Eukaryotic cells and cell lines

Table 3.3-13 Eukaryotic cells and cell lines

Eukaryotic cells/ cell lines	Species	Supplier	Catalog number/ reference
Fibroblasts	derived from primary human foreskin from juvenile donors (male, <7 years)	Phenion®	hFB P1
Feeder cells	derived from primary human foreskin fibroblasts from juvenile donors (male, <7 years), growth inhibited upon mitomycin C treatment	Phenion®	hFeeder
Keratinocytes (juvenile)	derived from primary human foreskin from juvenile donors (male, <7 years)	Phenion®	hK P1
Keratinocytes (adult)	derived from primary human skin from an adult donor (female, 33 years)	Lonza	00192627 (LOT: 18TL180364)
THP-1	derived from peripheral blood from an acute monocytic leukemia patient (male, 1 year)	American Type Culture Collection (ATCC)	TIB-202 (LOT:70025047)
THP-Langerin	derived from the human THP-1 monocyte cell line by stable integration (via lentiviral transduction) of Langerin [216]	Kindly provided by Prof. Dr. Theo Geijtenbeek	[216]
THP1-Blue™ NF-κB Cells	derived from the human THP-1 monocyte cell line by stable integration of an NF-κB-inducible SEAP reporter construct	InvivoGen	Thp-nfkbv2

3.4.2.8 Commercial Kits

Table 3.3-14 Commercial Kits

Kit	Supplier	Catalog number
BD CBA Human Inflammatory Cytokines Kit	BD Biosciences	551811
Coomassie protein assay	Thermo Fisher Scientific	1856209
iScript cDNA Synthesis Kit	Bio-Rad Laboratories Inc.	1708891
ITaq™ SYBR® Green Supermix	Bio-Rad Laboratories Inc.	1725121
ReliaPrep™ RNA Miniprep	Promega	Z6011
SuperSignal™ West Pico substrate	Thermo Scientific	34577

3.4.2.9 Consumables

Table 3.3-15 Consumables

Consumables	Supplier	Catalog number
1.5 mL tube	Sarstedt	72.690.001
2 mL tube	Sarstedt	72.691
96-well plate u-bottom	Thermo Fisher Scientific	353910
Cell counting slides	BioCat (LUNA 2-channel)	L12001
CELLSTAR® T75 Flask	Greiner	658195
Dako Fat Pen	Dako	S2002
Microscope slides	Epredia™ (Superfrost™Plus Adhesion)	J1800AMNZ
Microtome Blade	Epredia™ (MX35 Premier™)	3052835
Multiply®-µStrip Pro 8-strip	Sarstedt	72.991.002
Nunc™ Polycarbonat - cell culture inserts in multi-well plates	Thermo Fisher Scientific	140620
PCR plate	Sarstedt	72.1978
Petri Dish	Sarstedt	82.1472.001
Scalpel	Paragon	6862204
TC plate 24-well, standard, F	Sarstedt	83.3922.005
TC plate 24-well, standard, F	Sarstedt	83.3924
TC plate 96-well, black, flat	Greiner	655090
TC-Flask T175	Sarstedt	83.3912.002
TC-Flask T25	Sarstedt	83.3910.002
TC-Flask T75	Sarstedt	83.3911.002
Transwell inserts	Corning	CLS3415
Tubes 15 ml	Sarstedt	62.547.254
Tubes 50 ml	Sarstedt	62.554.502

3.4.2.10 Laboratory devices

Table 3.3-16 Laboratory device**s**

Devices	Supplier
Cell Counter, Luna II™ (automated)	Logos biosystems
Centrifuge (1.5 mL tubes): Heraeus™ Fresco21	ThermoFisher Scientific
Centrifuge (15 & 50 mL tubes): Heraeus™	ThermoFisher Scientific
Centrifuge (Plates): 3-30KS	Sigma-Aldrich
CFX96 Real-Time PCR Detection System	Bio-Rad Laboratories, Inc.
CO_2 Incubator Heracell 150i	ThermoFisher Scientific
Confocal spinning disc microscopy (CQ1)	Yokogawa

Cryostat	Leica
Flow Cytometer, CytoFLEX (B5-R3-V5)	Beckman Coulter
Fluorescence Microscope BZ-X810	Keyence
Fusion Pulse^{TS} Imager	Vilber
Keyence BZ-X800	Keyence
Microplate Reader Fluostar OPTIMA	BMG Labtech
Mini-Protean Tetra Cell tank system	Bio-Rad Laboratories, Inc.
Multichannel Pipettes	Eppendorf
NanoDrop^{TM} Lite	Thermo Scientific
PowerPac Basic Power Supply	Bio-Rad Laboratories, Inc.
Rocking Platform	IKA
Thermo cycler peqSTAR	peQlab
Thermoshaker	Eppendorf (Grant-bio #PMCT)
Trans-Blot® SD Semi-Dry transfer cell system	Bio-Rad Laboratories, Inc.
Vortex	Scientific Industries
Water bath	Memmert

3.4.2.11 Software

Table 3.3-17 Software

Software (Version)	Application	Developer
BZ-800 Viewer	Microscopic imaging	Keyence
CBA Analysis Software (1.1.14)	CBA-Assay	Becton Dickinson
CFX Manager^{TM} (3.1)	qPCR analysis	Bio-Rad Laboratories, Inc.
CQ1 Measurement	Microscopic imaging	Yokogawa
CytExpert (2.4)	Flow cytometry analysis	Beckman Coulter
EndNote (20.2)	Citation	Clarivate Analytics
EvolutionCapt	Western Blot analysis - (imaging & quantification)	VILBER
GraphPad Prism (8.4.3)	Data visualization, statistics	GraphPad Software, Inc.
Microsoft Office LTSC Professional Plus 2021	Raw data processing, writing	Microsoft
Optima	Fluorescence measurement, plate reader	BMG Labtech

3.4.3 Methods

3.4.3.1 Cell line cultivation

THP-1 and THP-Langerin cells were maintained in T75 flasks for suspension cells (Greiner, #658195) in 20 mL RPMI supplemented with 10% FBS, 1% penicillin–streptomycin (PenStrep), and 0.05 mM 2-mercaptoethanol in a humidified incubator at 37 °C and 5% CO_2. Cell density was maintained between 1 × 10^5 cells/mL and 5 × 10^5 cells/mL and cells were passaged every 2–3 days.

THP1-Blue™ NF-κB cells were maintained in T75 flasks for suspension cells (Greiner, #658195) in 15 mL RPMI supplemented with 10% FBS, 1% Pen-Strep, 100 µg/mL Normocin and 10 µg/mL Blasticidin in a humidified incubator at 37 °C and 5% CO_2. Cell density was maintained between 5 × 10^5 cells/mL and 1 × 10^6 cells/mL and cells were passaged every 3 days.

3.4.3.2 Cultivation of primary human cells

Primary human fibroblasts were thawed and seeded into T175 flasks with a seeding density of 5 x 10^5 cells and 15 mL of fibroblast medium. The cells were cultivated in a humidified incubator at 37 °C and 5% CO_2 for 4-5 days. When reaching 80% confluency, the cells were passaged or harvested for distinct analysis. For this, the medium was aspirated, and the cells were washed with 1 x PBS. To detach the cells, 0.05% trypsin-EDTA was applied for 2-5 minutes at room temperature. Afterwards, fibroblast medium was added, and the detached cells were transferred to 50 mL tubes and centrifuged at 200 x g for 3 min. The cell pellet was resuspended in fresh fibroblast medium, counted, and either reseeded for passaging or used for assays.

Primary human keratinocytes from juvenile donors were cultivated via feeder cell-supported culture. For this, mitomycin C-treated and therefore growth-inhibited primary human fibroblasts were used as feeder cells to enrich the cultivation medium for keratinocytes with secreted cytokines, supporting the attachment and growth of keratinocytes [217]. Thus, feeder cells were seeded with 5 x 10^5 cells in 23 mL keratinocyte medium into a T175 flask. After three days, 5 x 10^5 primary human keratinocytes from juvenile donors were seeded onto the feeder cells and cultivated in a humidified incubator at 37 °C and 5% CO_2. Medium was exchanged after 24 hours and 4 days of cultivation. After at least 6 days of cultivation and the appropriate confluency, cells were washed with 1 x PBS, and feeder cells were detached by adding 0.05% trypsin for 2 min at 37°C. Afterwards, keratinocytes were detached by applying 0.05% trypsin for 6 min at 37 °C. The keratinocytes were harvested by adding fresh keratinocyte medium, transferred to a 50 mL tube, and centrifuged for 5 min at 200 x g. The cell pellet was

resuspended in fresh keratinocyte medium, counted, and either used for the generation of skin models or 2D cell culture assays.

Primary human keratinocytes from an adult donor were thawed and seeded with a density of 3.500 cells/cm^2 into a T25 or T75 flask with 5 mL or 15 mL of keratinocyte medium, respectively. Cells were incubated in a humidified incubator at 37 °C and 5% CO_2 until reaching a confluency of 70–80%. Medium was exchanged every 2-3 days. For subculturing or harvesting, medium was aspirated, and cells were washed with HEPES-BSS. Following cells were incubated with a trypsin/EDTA solution for 2-6 minutes at 37°C, until 90% of the cells detached. The trypsinization process was neutralized by rinsing the flask with trypsin neutralizing solution (TNS). The detached keratinocytes were transferred to 15 mL tubes and centrifuged at 200 x g for 5 min. Cells were resuspended in fresh keratinocyte medium, counted, and either subcultured or used for the generation of skin models or 2D cell culture assays.

3.4.3.3 Cell counting

Cell suspensions (10 µl) were diluted 1:1 with Trypan Blue to exclude dead cells and were counted using an automated cell counter. For each cell type, including primary cells and cell lines, a customized protocol according to the cell shape (roundness), clustering, and minimal and maximal size was programmed. The determined number of viable cells was used to calculate the cell density for seeding.

3.4.3.4 Cell viability studies

Cell viability was determined using the PrestoBlue™ reagent, which depends on the reduction of the dark blue oxidized fluorescent dye resazurin into the reduced red-fluorescent form by viable cells. For this, THP-1 cells (6 x 10^4 cells) or adult keratinocytes (8 x 10^3) were seeded in 90 µl of their respective cultivation medium into the wells of a 96-well plate. Cells were seeded in triplicate for each treatment concentration as well as for the solvent control. While THP-1 cells were treated immediately after seeding, adult keratinocytes were allowed to detach and grow for 72 h at 37°C and 5% CO_2. Treatment compounds in decreasing concentrations or serial dilutions were applied to the seeded cells with 10 µl/well. The treated cells were incubated in a humidified incubator at 37°C and 5% CO_2 for 24 h. To determine the cell viability, PrestoBlue™ reagent (10 µl/well) was added, and a blank control was prepared. After 1 h of incubation at 37°C, 5% CO_2, the cell viability was determined by measuring the fluorescence (Exc.: 560 nm; Em.: 590 nm) with a Fluostar Optima BMG Labtech plate reader. To determine the cell viability in keratinocyte-THP-1 co-cultures, keratinocytes were seeded with 8 x 10^3 cells/ well in 90 µl/well into a 96-well plate and incubated for 72 h at 37°C and 5%

CO_2. Following, the keratinocyte medium was aspirated, and the keratinocytes were washed twice with 90 µl THP-1 medium. Afterwards, 6 x 10^4 THP-1 cells per well were seeded in 180 µl THP-1 medium onto the keratinocytes. The cells were treated immediately with 20 µl/ well of the respective compounds. After 24 h, 22 µl/well PrestoBlue™ reagent was added after 24 h of treatment. Cell viability was determined as described above.

3.4.3.5 Differentiation of THP-1 cells into iDCs

For the generation of THP-1-derived immature dendritic cells (iDCs), 2 × 10^5 THP-1 cells/mL were seeded into T25 flasks with 5 mL THP-1 medium, supplemented with 1500 IU/mL rhGM-CSF and 1500 IU/mL rhIL-4. The cells were incubated for 5 days in a humidified incubator at 37 °C and 5% CO_2. Medium was exchange, and fresh cytokines were added on day 3.

3.4.3.6 Sensitization assays

The THP-1 cells, THP-Langerin cells, or THP-derived iDCs were seeded and treated according to the h-CLAT assay. Briefly, 1 × 10^6 cells/mL were seeded in 1 mL RPMI supplemented with 10% FBS, 1% PenStrep, and 0.05 mM 2-mercaptoethanol into a 24-well plate and treated with 380 µM $NiSO_4$, 20 µM DNCB, or their respective solvent control for 24 h. To determine the anti-sensitizing potential of pseudopterosin A-D, cells were pre-treated with PsA-D for 1 h before applying sensitizers, namely $NiSO_4$ [380 µM] and DNCB [20 µM] for 23 h. To determine the surface marker expression, the cells were transferred to a 1.5 ml tube, centrifuged at 200 x g for 3 min, The supernatant was aspirated, and the cell pellet was resuspended in autoMACS running buffer and prepared for flow cytometry analysis (Section 3.4.3.8).

3.4.3.7 Co-culture Studies

Co-culture studies were conducted for THP-1 or THP-Langerin cells and keratinocytes from juvenile or adult donors. For co-cultivation with juvenile KCs, 4 x 10^4 feeder cells were seeded into a 24-well plate in 1 mL keratinocyte medium and incubated in a humidified incubator at 37 °C, 5% CO_2. After 72 h, 4 x 10^4 primary human keratinocytes from juvenile donors were seeded on top of feeder cells in a volume < 50 µl. Medium was exchanged after 24 h and 4 days of cultivation. On day 5, medium was aspirated, and cells were washed with PBS and incubated with 0.05% trypsin for 2 min at RT until feeder cells were detached. The remaining keratinocytes were washed with PBS, 1 mL of keratinocyte medium was added, and cells were incubated at 37°C, 5% CO_2. After 24 h, the juvenile keratinocytes were washed twice with THP-1 medium, and 6 x 10^5 THP-1 cells, or THP-Langerin cells, were seeded in 1 mL of THP-1 medium on top of the keratinocytes. The co-culture was exposed to 380 µM $NiSO_4$, 20 µM

DNCB, or the respective solvent control for 24 h. Surface marker expression was determined via flow cytometry analysis (Section 3.4.3.8).
For co-cultivation with adult KCs, 4 x 10^4 keratinocytes from an adult donor were seeded into a 24-well plate in 1 mL keratinocyte medium and incubated in a humidified incubator at 37 °C, 5% CO2. After 72 h, the keratinocytes were washed twice with THP-1 medium, and THP-1 or THP-Langerin cells were seeded and treated as stated in the paragraph above.

3.4.3.8 Surface marker analysis via flow cytometry

To determine the surface marker expression, THP-1 or THP-Langerin cells, were harvested and washed in autoMACS running buffer. Cells were transferred to a 96-well u-bottom plate with at least 2 x 10^5 cells per well and antibody panel. Cells were stained with the following antibodies, diluted 1:50 in autoMACS running buffer: HLA-DR-VioGreen, CD1a-PE, CD207-PE-Vio770, CD54-APC, CD11b-VioGreen, CD83-PE, CXCR4-PE-Vio770, CD86-APC, CXCR4-PE-Vio770, and CCR7-PE-Vio770 for 10 min at 4°C in the dark. The following IgG1 controls were used for gating: REA Control (S)-VioGreen, REA Control (S)-PE, REA Control (S)-APC; REA Control (S)-PE-Vio770 (all from Miltenyi Biotec). After staining, the cells were washed with autoMACS running buffer and stained with DAPI to determine cell viability and exclude dead cells.

3.4.3.9 Transwell migration assays

For transwell migration assays, 1 x 10^5 THP-1 or THP-Langerin cells were seeded in 100 µl THP-1 medium onto the membrane (5.0 µm) of the upper transwell inserts of a 24-well plate system. To investigate the migratory potential to the chemoattractant SDF1, the bottom chamber was filled with 600 µl THP-1 medium containing 200 ng/mL of SDF-1. The plate was incubated in a humidified incubator at 37°C and 5% CO_2 for 16 h. To determine the number of migrated cells, the cell suspension from the bottom chamber (600 µl) was transferred to 1.5 mL tubes, centrifuged at 200 x g for 5 min, and resuspended in 200 µl autoMACS running buffer and 1 µg/mL DAPI. Cell counting of viable cells was performed via flow cytometry.
To investigate the migratory potential of THP-1/THP-Langerin cells towards the utilized dermis constructs, dermis models (Phenion®) were incubated with 1 mL of fibroblast medium at 37°C, 5% CO_2. After 48 h, the dermis model-conditioned medium was harvested and used immediately for the TMA. Thus, 600 µl of the conditioned medium were placed in the bottom chamber, and 1 x 10^5 THP-1 or THP-Langerin cells were seeded in 100 µl fresh (unconditioned) fibroblast medium onto the membrane (5.0 µm) of the upper transwell inserts. The TMA was performed as described in the section above.

The migratory potential to primary human fibroblasts was examined by seeding 4 x 10^4 primary human fibroblasts from juvenile donors in 1 mL fibroblast medium into the bottom chamber of the traswell insert plate. After 24 h at 37°C and 5% CO_2, the medium was aspirated and 600 µl of fresh fibroblast medium was added. Subsequently, 1 x 10^5 THP-1 or THP-Langerin cells were seeded in 100 µl fibroblast medium onto the membrane (5.0 µm) of the upper transwell inserts. The plate was incubated in a humidified incubator at 37°C and 5% CO_2 for 16 h. The number of migrated cells was determined via flow cytometry, as described in the former sections.

3.4.3.10 Western Blot

THP-1 cells were seeded with 1 x 10^6 cells/mL into a 24-well plate in 1 mL RPMI supplemented with 10% FBS, 1% P/S and 0.05 mM 2-mercaptoethanol. Cells were treated with different concentrations for different lengths of time (0 min, 15 min 30 min, 60 min) with DNCB [2025 µM] and $NiSO_4$ [380/ 500 µM] to determine the optimal treatment time point and concentrations. To determine the optimal pre-treatment concentration for PsA-D, concentrations ranging from 30 to 50 µM were tested. different Cell lysates were obtained by lysing the harvested cells with 30 µL radioimmunoprecipitation assay (RIPA) buffer containing a protease inhibitor and a phosphatase inhibitor (RIPA++). Protein levels were quantified in duplicate for each sample using the Coomassie protein assay according to the manufacturer's instructions. Absorbance was measured at 590 nm on the BMG Labtech OPTIMA plate reader. Protein concentrations were calculated with the integrated software. Sample preparation for SDS-Page was performed as follows: 20 µg of total protein were replenished with Laemmli buffer, denaturized for 10 min at 95°C and centrifuged for 15 min at >13,000 x g. Proteins were separated on 10% SDS-Gels at 100 V for 10 min, followed by 120 V constant for 1 h in 1x running buffer, using a Mini-Protean Tetra Cell tank system. Protein transfer to a methanol-activated nitrocellulose membrane was performed via semi-dry blotting at 20 V constant for 40 min in 1x transfer/blotting buffer using the Trans-Blot® SD Semi-Dry transfer cell system. To block unspecific antibody binding, the membranes were incubated with 5% BSA in 1% TBS-T solution for at least 30 min. Incubation with the respective primary antibodies, IκBα, vinculin, p38 MAPK or phospho-p38 MAPK (Thr180/Tyr182), was performed over night at 4°C. After washing with 1x TBS-T (3 x 5 min) the membrane was incubated with the respective horseradish peroxidase-coupled secondary antibody (Goat anti-Rabbit (H+L), for 1 h at room temperature. Antibody binding was detected with the SuperSignal West Pico Plus substrate kit and imaged on the Fusion Pulse^{TS} imager from Vilber. Protein levels were quantified using the provided software, EvolutionCapt. After subtracting the background noise, protein levels were determined based on the band intensity of the protein of interest. Protein levels for the protein of interest were then normalized to the respective housekeeping gene.

3.4.3.11 CBA-Assay

In total, 1 x 10^6 THP-1-derived iDCs/ well were seeded in in 1 mL RPMI-1640 supplemented with 10% FBS, 50 U/mL Pen-Strep, and 0.05 mM 2-mercaptoethanol in a 24-well plate. Subsequently, iDCs were pre-treated with PsA-D [20 µM] for 1 h, followed by exposure to DNCB [20 µM], $NiSO_4$ [380 µM] or their respective solvent control DMSO for 23 h in a humidified incubator at 37°C and 5% CO_2. Supernatants were collected after 24 h and prepared for cytokine analysis according to the manufacturer's instructions for the Cytometric Bead Array Human Inflammatory Cytokines Kit. Briefly, the supernatants were diluted 1:2 with the provided assay diluent. The diluted samples (50 µl) and previously prepared inflammatory cytokine standard dilutions were then added to the prepared mix of the human inflammation capture bead suspension (50 µl/ well in a 96-well u-bottom plate). Subsequently, the provided PE detection reagent was added, and the plate was incubated for 3 h at room temperature in the dark. Afterwards, samples were washed with 200 µl washing buffer (provided) and the pellet was resuspended in 200 µl washing buffer. The cytometer setup and the respective positive controls were prepared according to the manufacturer's instructions. Sample acquisition and, therefore, detection of the secretion of the inflammatory cytokines were performed via flow cytometry using the CytoFlex (B5-R3-V5) from Beckman Coulter. Analysis was performed using the provided CBA Analysis Software.

3.4.3.12 Treatment for RT-qPCR

To determine the sensitizer-induced mRNA levels of THP-1 cells and juvenile and adult keratinocytes, the cells were seeded and treated as follows:
Keratinocytes derived from adult donors were seeded with 1 x 10^5 cells per well into a 6-well plate in 2 mL of their respective cultivation medium. Cells were grown in a humidified incubator at 37°C and 5% CO_2 until reaching 70% confluency.
Keratinocytes from juvenile donors were grown in a feeder-cell-supported culture. For this, 1 x 10^5 feeder cells were seeded into a 6-well plate in 2 mL keratinocyte medium and incubated in a humidified incubator at 37 °C, 5% CO_2. After 72 h, 1 x 10^5 primary human keratinocytes from juvenile donors were seeded on top of feeder cells in a volume < 100 µl. Medium was exchanged after 24 h and 4 days of cultivation. On day 5, medium was aspirated, and cells were washed with PBS and incubated with 0.05% trypsin for 2 min at RT until feeder cells were detached. The remaining keratinocytes were washed with PBS, 2 mL of keratinocyte medium was added, and the remaining keratinocytes were incubated at 37°C, 5% CO_2 for 24 h.
THP-1 cells were seeded with 1 x 10^6 cells into a 24-well plate in 1 mL of their cultivation medium and treated immediately after seeding. THP-1 cells and juvenile and adult

keratinocytes were treated with DNCB [20 µM] and $NiSO_4$ [380 µM] or their respective solvent control, dimethyl sulfoxide, for 6 h.

3.4.3.13 Quantitative real-time Polymerase-chain-reaction (RT-qPCR)

RNA-extraction was performed using the ReliaPrep Kit according to the manufacturer's instructions. DNA digestion was prolonged to 30 min. Elution was performed in 15 µl nuclease-free water. The RNA yield and concentration were determined with the spectrophotometer NanoDrop™ Lite. Reverse transcription of 1µg RNA was performed according to the iScript cDNA Synthesis Kit using the thermal cycler PeqStar (Table 3.3-16). A sample without reverse transcriptase was included as a no-reverse transcriptase (nRT) control. To assess whether any genomic DNA contamination in the RNA and following cDNA samples was left, a simple PCR for GAPDH was performed (master mix (1x): 18.875 µl $_{dd}H2O$, 2.5 µl buffer, 0.5 µl dNTPs, 0.5 µl GAPDH forward primer, 0.5 µl GAPDH reverse primer, 0.125 µl Taq-Polymerase) (Table 3.3-15). Quantitative real-time PCR (qPCR) reactions for IL-8, IL-6, TNF-α, IL-1α and IL-1β (primer sequences are listed in table 3.3-12) were performed in triplicate for 50 ng cDNA per sample using the iTaq SYBR Green Supermix kit (master mix (1x): 3.5 µl $_{dd}H2O$, 0.25 µl forward primer (10 µM), 0.25 µl reverse primer (10 µM), 5 µl iTaq SYBR Green Supermix) on a thermal cycler CFX96 from Bio-Rad (Table 3.3-18). To monitor potential nucleic acid contamination, no template controls (NTCs) containing $_{dd}H2O$ instead of cDNA were included for every gene of interest as well as the housekeeping gene.

Table 3.3-18 Protocol for cDNA synthesis

Step	Temperature [°C]	Time
Primimg	25	5 min
Reverse transcription	46	20 min
Inactivation of Reverse Transcriptase	95	1 min
Cooling	4	∞

Table 3.3-19 Protocol for PCR

Step	Temperature [°C]	Time	Cycles
Initial Denaturation	95	30 s	x1
Amplification	95	30 s	x40
	55	30 s	
	72	30 s	
Final Extension	72	5 min	x1
Cooling	4	∞	-

Table 3.3-20 Protocol for RT-qPCR

Step	Temperature [°C]	Time	Cycles
Denaturation	95	30 s	x1
Amplification	95	5 s	x37
	55	40 s	
Melt curve	65 -95 (0.5 °C increment)	5 s	x1

3.4.3.14 Generation of Full-thickness skin models

Keratinocytes from juvenile and adult donors were maintained and grown as described in Section 3.4.3.2. To generate full-thickness skin models with THP-1/THP-Langerin as potential LC surrogates, 5 x 10^5 Keratinocytes from juvenile ore adult donors were seeded together with 1 x 10^6 THP-1 or THP-Langerin cells in 1 mL of the respective keratinocyte medium onto dermis models (provided by Phenion/ Henkel AG & Co. KGaA, Düsseldorf, Germany). The skin models were cultivated for 48 h in a submerse phase at 37° C, 5% CO_2 with a complete medium exchange 24 h after seeding. The medium was exchanged. After 48 h of submerse phase, the skin models were lifted into the air-liquid interface (ALI) phase with air-liquid interface culture medium for 10 days.

3.4.3.15 Generation of epidermis models

The generation of epidermis models was established using cell culture inserts (24well system, 0.4 µm pore size) in carrier plate systems with adjustable height capabilities. To enhance the adherence of the keratinocytes, the cell culture inserts were coated with 5 µg/cm^2 collagen. For this, a coating solution with 50 µg/mL rat tail collagen diluted in 20 mM acetic acid was prepared and applied to the cell culture inserts for 2 h at 37°C. Afterwards, the collagen solution was carefully removed, and the inserts were rinsed twice with PBS. Keratinocytes from juvenile donors were grown as described in Section 3.4.3.2. To generate epidermal models with incorporated THP-1 or THP-Langerin cells, 3.1 x 10^5 keratinocytes were seeded together with 4.7 x 10^5 THP-1 or THP-Langerin cells in 500 µl of the prepared keratinocyte medium (EpiLife® medium supplemented with 1% HKGS & 1% P/S) into the upper inserts (position low). The lower compartment was filled with 500 µl keratinocyte medium, and the plate was incubated in a humidified incubator at 27°C, 5% CO_2. After 24 h the epidermal models were transferred into the submerse phase by aspirating all of the medium from the lower compartment and the cell culture insert. Subsequently, 500 µl of submerse medium (EpiLife® + 1% HKGS + 1% P/S + 1.5mM $CaCl_2$) were carefully added to the lower compartment and the upper inserts. After 24 h of submerse phase, the epidermal models were lifted into the ALI phase. For this, the

submerse medium was completely removed from the upper inserts and the lower compartments. Furthermore, the upper inserts were lifted to the middle position and left empty. The lower compartment was filled with 1 mL of ALI medium (EpiLife® + 1% HKGS + 1% P/S + 1.5 mM $CaCl_2$, + L-ascorbic acid 2-phosphate (73 µg/mL) and KGF (10 ng/mL)). Epidermal models were cultivated in the ALI phase for 20 days with medium exchanges every 3-4 days.

3.4.3.16 Cryosectioning

Full-thickness skin models and epidermal models were cut in two halves. Furthermore, the left and right edges were removed using scalpels. Subsequently, the two halves were embedded and frozen (at -20°C) onto specimen holders in upright positions next to each other using a glycerine-based embedding medium. The tissue blocks were processed and cut at -20°C and 7 µm tissue slices were transferred to SuperFrost® microscope slides.

3.4.3.17 IF-Staining

First of all, the tissue slides were fixed in ice-cold acetone for 10 minutes. Subsequently, the slides were air dried for 5 min and the tissue sections were encircled with a fat pen. To block unspecific antibody binding, 100 µl (50 µl/section) 10% normal goat serum was applied, and the slides were incubated in a humid chamber for 1 h at RT. Primary antibodies were diluted in DAKO antibody diluent, and Cytokeratin 5 (1:75) and CD45-VioBright R667 (1:50) were applied (25 µl/section) for staining at 4°C overnight in a humid chamber. Before applying the secondary antibodies, tissue slides were washed 3 x 5 min with PBS. Secondary antibody staining with Alexa Flour 488 (1:200) and DAPI staining (10 µg/ml) was performed for 1 h at RT in a humid chamber. After washing 3 x 5 min in PBS, the stained tissue slides were embedded with fluorescence mounting medium to avoid bleaching.
Immunofluorescent imaging was conducted using the CQ1 Benchtop High-Content Confocal Imaging System with exλ/emλ at 405 nm - BP447/60, 488 nm - BP525/50 and 640 nm BP685/40. The excitation power was set to 20% and the exposure time to 500 ms. The pinhole disk speed was set to 3600 rpm. The binning number was set to 1 (one camera pixel was saved as one pixel of image data).

3.4.3.18 Statistical analysis

Results are depicted as the mean ± standard error of the mean (SEM) from at least three independent biological replicates. Calculation of the half-maximal inhibitory concentration (IC_{50}) in drug-response studies and statistical evaluation was performed using GraphPad Prism version 8.4.3. Assuming a normal distribution, statistical significance was calculated

using an unpaired t-test, a one-way ANOVA with Dunnett's multiple comparisons test or two-way ANOVA with Sidak's multiple comparisons test. The confidence interval was set to 95%. The significance levels were defined and referred to as * = $p \leq 0.05$; ** = $p \leq 0.01$; *** = $p \leq 0.001$; **** = $p \leq 0.0001$.

4 Discussion

4.1 Steps towards an immune competent skin model – identifying suitable LC and DDC surrogates

Dendritic cells, including LCs and DDCs, are crucial mediators in skin sensitization and CHS [69]. In the past, toxicological testing and the predictive identification of potentially sensitizing chemicals, as well as studies investigating the molecular mechanisms of DC activation in skin sensitization and CHS, have been performed almost exclusively in animal models, primarily in mice. However, species-specific differences in the DC subtypes [33, 37, 38] and the demands for non-animal methods according to the 3R principles have encouraged research on new test systems for predicative sensitizer identification [24, 47]. To this end, the OECD developed an adverse outcome pathway with defined key events for skin sensitization and provided the basis for the development of various non-animal methods [218]. However, the resulting OECD-approved non-animal methods are mostly based on a single isolated cell type and thus represent just one or a few steps of the sensitization cascade and not the complex inter- and intracellular mechanisms of skin sensitization [162]. Furthermore, these test systems do not allow for assessment of substances with poor solubility, mixtures, or formulations; they can only be applied to mono-constituent substances and cannot provide information about the absorption, distribution, or metabolism of test substances [161, 166, 167]. As such, the existing models are insufficient to fully replace animal models [165]. To overcome these limitations, three-dimensional tissue equivalents, including epidermal and full-thickness skin models, have been developed. However, most of them lack immune cells, in particular functional DC surrogates [182]. Hence, our aim was to develop a human 3D immunocompetent FTSE with incorporated DC surrogates to enable the identification and characterization of sensitizers and drug candidates.

4.1.1 THP-1 and THP-Langerin cells cannot be integrated as LC surrogates into FTSE

To address the sensitizer-induced activation of DCs, according to KE3 of the AOP, distinct non-animal test systems such as the h-CLAT, U-SENS, IL-8 Luc, and GARD assay have been developed by various scientists and accepted by the OECD [151]. Given that the h-CLAT and the IL-8 Luc assay—and therefore two out of four OECD-approved test systems addressing the third key event—were based on the human monocytic leukemia cell line THP-1 [152, 155], we focused on the characterization of THP cells as an easy and accessible tool for potential DC surrogates for integration into full-thickness skin models and consequently the identification and characterization of sensitizers. For phenotypical surface marker characterization, THP-1

cells, THP-Langerin cells, and the THP1-Blue™ NF-κB reporter cell line were exposed to the two model sensitizers, $NiSO_4$ or DNCB, according to the guidelines of the h-CLAT. As expected, treatment with $NiSO_4$ or DNCB resulted in significantly enhanced expression of CD54 and/or CD86 on THP-1 cells. However, in naïve (non-sensitized) THP-Langerin and THP1-Blue™ NF-κB cells, the number of cells expressing CD54 was already quite high (THP1-Blue™ NF-κB > 85%; THP-Langerin > 99%) and could thus not be further induced (except for THP1-Blue™ NF-κB cells upon $NiSO_4$ exposure). Furthermore, the number of cells expressing CD83 was significantly increased upon $NiSO_4$ exposure on THP-1 and THP-Langerin cells, but not on THP1-Blue™ NF-κB cells. In addition, a significant increase in the number of cells expressing HLA-DR could only be observed on THP-1 cells upon $NiSO_4$ exposure, but not on THP1-Blue™ NF-κB or THP-Langerin cells. Thus, in terms of surface marker expression, THP-1 cells seemed more sensitive towards sensitizers than the stably transfected THP1-Blue™ NF-κB reporter cell line or the THP-Langerin cell line. However, THP-1 and THP1-Blue™ NF-κB cells did not express the typical LC marker CD207, and CD207 could not be induced upon treatment with the sensitizers DNCB or $NiSO_4$. As expected, THP-Langerin cells stably expressed CD207 (> 85%). Although antigen-presenting functions for CD207 have been assumed, the precise role of CD207 remains elusive [212, 213]. However, since LCs are the only DC subtype located in the epidermis and CD207/Langerin is considered as one of the phenotypic hallmarks of LCs [72], we cautiously deliberated whether CD207, among other factors, could be responsible for the epidermal location. Based on this consideration, the surface marker expression of CD207 by THP-Langerin cells may have been a benefit compared to the two other THP cell lines in terms of their integration into the epidermis as LC surrogates.

One central hallmark of activated DCs is their migration to local lymph nodes for antigen presentation to naïve T cells [219]. Cutaneous DC migration is mainly mediated in a chemokine-dependent manner. Upon antigen exposure, SDF-1 secretion by fibroblasts and endothelial cells is enhanced, inducing the chemotactic migration of CXCR4-expressing LCs towards lymphatic vessels in the dermis [120, 121], followed by a chemokine (C-C motif) ligand (CCL)19- and CCL21-mediated migration towards the lymph nodes [220]. Since CXCR4 was highly expressed on THP-1 and THP-Langerin cells, I investigated whether the THP cell lines could migrate towards SDF-1. In fact, both the naïve THP-1 cell line and the stably transfected langerin expressing THPs migrated towards SDF-1 (THP-1: ~188%; THP-Langerin: ~263%). In line with our results, Macanas-Pirard et al. demonstrated a similarly strong SDF-1-mediated chemotaxis of THP-1 cells (~280% migration in 16 h) [221]. Confirming these results, in another study THP-1 cells strongly migrated towards 300 ng/mL SDF-1 (~700%) [222].

After confirming the significant sensitizer-induced upregulation of CD54, CD86, and/or CD83 and therefore the expected ability to respond to sensitizers, as well as the strong migratory potential towards SDF-1, we hypothesized that THP-1 and/or THP-Langerin cells might be suitable LC surrogates for integration into FTSE. However, despite distinct variations in the seeding protocols, THP-1 and THP-Langerin cells could only be integrated into the dermis and not as LC surrogates into the epidermis of a FTSE. Monitoring the integration of THP-1 and THP-Langerin cells over time revealed that both cell lines are partially “forced” or “driven out” by keratinocytes during the epidermal formation and stratification. When comparing microscopic images depicting the time course of THP-1 cells and THP-Langerin cells, more THP-Langerin cells are located on top of the epidermis above the stratum corneum, suggesting that THP-Langerin cells are forced out by keratinocytes in a stronger manner than THP-1 cells. Furthermore, I proved that THP-1 cells are not only expelled by keratinocytes but also actively migrate towards conditioned dermis medium and unstimulated primary human fibroblasts.
On the one hand, these findings might be due to fibroblasts constitutively secreting SDF-1 [223]. On the other hand, THP-Langerin cells did not actively migrate towards the dermis-conditioned medium or fibroblasts, even though the number of THP-Langerin cells expressing CXCR4 and migrating towards isolated SDF-1 was much higher compared to THP-1 cells. Therefore, the migration of THP-1 cells towards the conditioned dermis medium and primary human fibroblasts might also have occurred in a SDF1-CXCR4-independent manner.
In conclusion, the underlying mechanism remains elusive, though integration of THP-1 and THP-Langerin cells into the epidermis of epidermal models was successful. However, epidermal models do not permit investigation of the first three key events of skin sensitization as LC migration cannot be displayed due to the missing dermal compartment. Thus, we deliberated whether undifferentiated or differentiated THP-1 cells could be integrated as functional DDC surrogates into a FTSE (reviewed in Chapter 2.1 and discussed in Chapters 4.1.2 and 4.3).

4.1.2 THP-1 cells can be differentiated into CD11c^{+} CD14^{-} DDC surrogates

Various protocols have been reported for the generation of DC/LC surrogates derived from human donor-derived peripheral blood monocytes (PBMCs) to study skin sensitization and DC activation [185, 186, 224-226]. However, the quantity, availability, and donor heterogeneity potentially leading to increased inter-experimental variation are only a few of the biological and technical restrictions that come with isolating and differentiating PBMCs [227, 228]. Therefore, the most logical step was to explore whether the well-characterized THP-1 cell line could be differentiated into functional DC surrogates. Indeed, a few protocols were published for the differentiation of THP-1 cells into DC surrogates [229-233]. However, the protocols varied in terms of basic media composition and media supplementation, including the applied cytokine

concentrations, the frequency of media exchange, the number of days for differentiation, and the utilized cell number [229-233].

Thus, Chapter 2.1 strove to develop a robust and highly reproducible protocol that would provide DC surrogates for toxicological studies and investigate the underlying mechanisms of cutaneous sensitization. The successful differentiation of THP-1 cells into iDCs and mDCs was confirmed by a high expression of the h-CLAT and DC activation markers CD54 and CD86. In the literature, maturation of THP-1-derived DCs was mainly assumed from high CD80 and CD86 expression [230-232]. However, fully matured DCs like ours are characterized by a significant induction of the maturation marker CD83 [234] and the migration marker CXCR4 [235-237]. Notably, I discovered that for CXCR4 expression, it is mandatory to differentiate the THP-1 cells for 72 h and not for 24 h or 48 h, as it has been previously reported [229, 232, 233]. Unlike mDCs, iDCs—including our THP-1-derived iDCs—do not express CD83 and CXCR4 [237]. In addition, our THP-1-derived iDCs were characterized by low CD14 expression, a marker used to distinguish DCs from monocytes and macrophages, and a high expression of CD11c, which is abundantly expressed and associated with DDCs [77, 78]. Furthermore, when compared to undifferentiated THP-1 cells, a significantly higher number of iDCs expressed CD11b, which is associated with phagocytosis [210, 238]. In line with this, a significantly higher number of our THP-1-derived iDCs were able to phagocytose zymosan, an insoluble β-1,3-glucan polysaccharide extracted from the cell wall of *Saccharomyces cerevisiae*, compared to the undifferentiated THP-1. Consequently, obtaining fully functional DC surrogates requires the differentiation of THP-1 cells into iDCs as the undifferentiated THP-1 cell line does not display the fully functional properties of DC surrogates. Subsequently, we concluded that THP-1-derived iDCs might be suitable functional surrogates for the integration of DDCs into human skin tissue equivalents. To confirm this assumption, I investigated the responsiveness of DDCs towards sensitizers, including the surface intracellular pathways, surface marker expression, and secretion of inflammatory cytokines (see Chapter 4.2).

In terms of technical aspects, the systematic comparison of the surface marker expression for iDCs and mDCs, generated according to the published cytokine concentrations in ng/mL [230, 231] vs. U/mL [229, 233], revealed tremendous differences in the expression levels for CD54, CD11b, and CD83. For reliable and reproducible results, I strongly recommend applying and indicating cytokine concentrations in U/mL as biological activity can vary between suppliers and occasionally between lots [239]. In addition, to reduce the costs by a quarter of those incurred by published protocols [229, 233], I recommend downsizing the volume from T75 flasks with 20 mL of differentiation medium to T25 flasks with 5 mL of medium.

4.1.3 Mutz-3 cells can be differentiated into CD1a$^+$ CD207$^+$ LC surrogates

For an immune competent full-thickness skin model comprising DDC and LC surrogates representative of the situation in native skin, CD1a$^+$ CD207$^+$ LC surrogates were required. Reviewing the literature for the generation of LC surrogates, multiple protocols have been published with variations in the cell source, cell numbers, basic media composition, media supplementation, the number of days for differentiation, the frequency of media exchange, and the cytokine concentrations in the differentiation cocktail [121, 183-189, 230]. Hence, in Chapter 2.3 we aimed to generate a robust and highly reproducible protocol by providing LC surrogates for integration into a full-thickness tissue equivalent of the human skin.

The successful differentiation of Mutz-3 cells into Mutz-LCs was confirmed by a high expression (> 85%) for the LC-specific markers CD1a and CD207. In comparison to existing protocols [186-188] and in accordance with the 3R principles, we were able to reduce the FBS concentration in the differentiation medium from 20% to 5%. Furthermore, high expression of CD1a and CD207, including the number of positive cells and the GMFI (associated with the relative measure of antigen abundance), could be achieved without any medium exchange or additional cytokine supplementation. Similar to the differentiation for THP-1-derived iDCs, almost all protocols for the differentiation of Mutz-3 into Mutz-LCs indicated the mass (ng/mL) of the utilized cytokine concentrations [187-189]. However, as stated in the previous chapter (Chapter 4.1.2), for reliable and reproducible results, the application and indication of cytokines according to their biological activity (U/mL) is highly recommended as the biological activity between suppliers and occasionally between lots can differ [239]. Thus, our protocol for the stable and robust generation of Mutz-LCs was based on the application of cytokines according to their specific activity (U/mL).

4.2 Sensitizer-induced activation of DC surrogates and potential readout parameters

After establishing robust and highly reproducible standard operating procedures for the generation of THP-1-derived CD11c$^+$ CD14$^-$ DDC surrogates and CD1a$^+$ CD207$^+$ LC surrogates from the Mutz-3 cell line, we aimed to prove the functionality of our DC surrogates and to further examine the underlying mechanisms of LC and DDC activation in skin sensitization.

Regarding inflammatory pathways, loss of function studies revealed that the NF-κB pathway and the p38 MAPK cascade play a crucial role in the maturation of DCs [92, 225, 226] and consequently in antigen presentation. To our knowledge, sensitizer-induced activation of the NF-κB pathway and phosphorylation of p38 MAPK have not been reported for either THP-1-

derived iDCs or for Mutz-3-derived LCs. Hence, we are the first to prove the $NiSO_4$-induced activation of the NF-κB pathway via IκBα degradation and the DNCB-induced phosphorylation of p38 MAPK in THP-1-derived iDCs and Mutz-LCs. However, in line with our results, activation of the NF-κB pathway after treatment with nickel salts was reported for undifferentiated THP-1 cells [227], macrophages [228], endothelial cells [229], and DCs derived from human cord blood $CD34^+$ hematopoietic progenitor cells [93]. In addition, activation of the p38 MAPK pathway could be induced upon DNCB treatment in undifferentiated THP-1 cells [230], in DCs derived from human cord blood $CD34^+$ hematopoietic progenitor cells [93, 94], and in PBMC-derived DCs [91].

To recruit and activate T cells, the secretion of inflammatory cytokines such as IL-6, IL-8, IL-1, and IL-12 by DCs is crucial [102]. In fact, for THP-1-derived iDCs, I demonstrated that treatment with $NiSO_4$ increased the mRNA levels for IL-8, IL-6, and TNF-α, which was confirmed on a protein level by significant increased secretion of IL-8, IL-6, TNF-α, and IL-1β in THP-1-derived iDCs. Treatment of iDCs with DNCB resulted in increased mRNA levels and secretion of IL-8 and IL-1β, but not of IL-6 or TNF-α. Similar to iDCs, treatment of Mutz-LCs with $NiSO_4$ resulted in increased mRNA levels for IL-6, IL-8, IL-1α, and IL1β. Upon exposure of Mutz-LCs to DNCB, elevated mRNA levels for IL-6, IL-8, and IL-1α but not for IL-β or TNF-α could be detected. In line with our results, enhanced mRNA levels for IL-6, IL-8, and TNF-α upon treatment with $NiCl_2$ have been previously reported for PBMC-derived DC surrogates [109, 111]. In addition, $NiSO_4$-induced secretion of IL-6 and IL-8 was shown for cord blood-derived DC surrogates [113]. In terms of DNCB treatment, increased secretion for IL-8 and IL-1β but not for TNF-α has been described for PBMC-derived DC surrogates [109], coinciding with our results. Notably, IL-12 in particular was described as a major driver of T cell activation. More precisely, IL-12 induces the upregulation of the transcription factor T-box expressed in T cells (T-bet), promoting their differentiation into interferon-γ-producing T helper 1 cells (T_H1) [240-242]. Hence, I analyzed the sensitizer-induced mRNA expression of IL-12p40 for our THP-1-derived DDC surrogates and Mutz-3-derived LC surrogates. For the THP-1-derived iDC as well as Mutz-LCs, minor mRNA levels were detected upon $NiSO_4$ exposure, and significantly higher mRNA levels of IL-12p40 were detected upon DNCB exposure (see Chapters 2.1 and 2.3). These results indicate that THP-1-derived iDCs as well as Mutz-LCs might be able to initiate sensitizer-induced activation of T cells. However, though the p40 subunit of IL-12p70 possesses the required epitopes for receptor-binding, binding to the p35 subunit or another p40 subunit is required for a proper conformation, resulting in high-affinity binding. Significantly, while the p35-p40 heteromer acts as an agonist mediating biological activity, a p40 homodimer acts as an antagonist [243].

One major challenge in identifying sensitizers is to distinguish them from irritants. While upregulation of the two h-CLAT markers CD54 and CD86 seemed to be a promising tool, more

recent studies have reported increased expression of CD54 upon treatment with irritants such as phenol or sodium lauryl sulfate [244]. While irritants have been reported to induce CD86 expression only at partially cytotoxic concentrations [245], not all sensitizers induce CD86 [246], making it difficult to rely on CD86 to distinguish between sensitizers and irritants. Notably, when compared to sensitizers, irritants were shown to fail in activating inflammatory pathways such as p38 MAPK [112] and to induce the secretion of inflammatory cytokines such as IL-8 [246, 247]. Thus, the increased upregulation of surface markers such as CD54, CD86, or CD83 can be used to identify sensitizing agents, but to distinguish them from irritants, additional investigation of inflammatory pathways and cytokines might provide more robust outcomes. However, in line with the previous reported findings for distinct DC surrogates [111, 113], our studies with DNCB and $NiSO_4$ clearly indicate that sensitizers operate via different pathways. Hence, to identify sensitizers, the screening of multiple readouts, including surface marker expression, inflammatory pathways, and cytokine secretion, is recommended.

4.3 Incorporation of LC and DDC surrogates into human skin tissue equivalents for characterization of sensitizers and drug candidates

As the first cells encountered in the skin when exposed to sensitizing substances, keratinocytes are linked to critical roles in haptenation processes and dendritic cell activation [248]. Strikingly, tissue-engineered epidermal as well as full-thickness skin models are mostly generated with keratinocytes from neonatal or juvenile donors [187-189, 249]. However, ACD affects groups of all ages [5]. Thus, prior to generating full-thickness skin models, I characterized the impact of keratinocytes derived from a juvenile donor (≤ 7 years) and an adult donor (33 years) on the surface marker expression of THP-1 and THP-Langerin cells before and after exposure to the two sensitizers $NiSO_4$ and DNCB. In addition, I investigated the sensitizer-induced secretion of inflammatory cytokines by juvenile and adult keratinocytes. While treatment of keratinocytes from an adult donor induced significantly higher mRNA levels for IL-6, IL-8, and TNF-α, treatment of juvenile keratinocytes with DNCB resulted in only a minor upregulation of the mRNA levels for L-6, IL-8, and TNF-α. However, the assay was conducted using supplier-specific and customized media for the respective cells. A comparison of the ingredients of the respective media revealed the supplementation of both media with the anti-inflammatory corticosteroid hydrocortisone. According to the manufacturer's statements, the medium for the juvenile keratinocytes was supplemented with 4 µg/mL (~11 µM) hydrocortisone, while the medium for adult keratinocytes was only supplemented with 0.1 to 3 µg/mL [~275 nM - 8.3 µM]. Thus, it is highly likely that the higher

hydrocortisone concentrations in the medium for juvenile keratinocytes suppressed the sensitizer-induced secretion of anti-inflammatory cytokines. In fact, glucocorticoids, including hydrocortisone, were shown to suppress the UV-induced secretion of IL-6 and IL-8 by keratinocytes [250]. Hence, for the characterization of sensitizers and potential anti-inflammatory compounds in cells and full-thickness skin models, a medium without hydrocortisone was chosen.

Our first attempts to develop an immune competent full-thickness skin model revealed that primary human keratinocytes from an adult donor can in principle be used to generate a full-thickness skin model; however, compared to the full-thickness skin models with keratinocytes from juvenile donors, the epidermis was thinner, especially after the integration of potential immune cell surrogates. Consistent with our results, age-related variations have been reported in the epidermal thickness of skin equivalents engineered by seeding human foreskin keratinocytes from neonatal (2–3 days), juvenile (4–10 years), or adult donors (15–26 years) onto a fibroblast-populated collagen gel [251]. While seeding of neonatal keratinocytes resulted in 6–8 KC layers after one week of cultivation, SE with juvenile keratinocytes comprised 4–5 KC layers, and SE with adult KCs formed a thin epithelium with only 1–2 layers of KCs, suggesting greater proliferation potential for neonatal and juvenile keratinocytes [251]. Indeed, distinct studies have revealed higher proliferation potential [252] and a longer culture lifespan for neonatal keratinocytes versus adult keratinocytes in plastic cultures [253, 254]. In addition, skin equivalents with keratinocytes derived from neonatal or juvenile donors exhibited a greater number of cutaneous stem cells than SE with keratinocytes derived from adult donors [251]. This aligns with observations that neonatal keratinocytes exhibit significantly faster rates of healing experimental wounds than adult keratinocytes [255] because the re-epithelialization of wounds is mediated by stem/progenitor cells [256, 257]. Therefore, we concluded that keratinocytes from juvenile donors are the more suitable choice for the generation of an immune competent full-thickness skin model.

For the dermal construct, we chose the matrix from the Phenion® Full-Thickness Skin Model because of its unique porous nature, which enables fibroblasts to adhere to and migrate into the collagen. Remarkably, the Phenion® dermis constructs mimic the elastic network of native human skin, including the secretion of extracellular matrix components like elastin and fibrillin-1.[214, 215], which might provide the necessary environment for DDC surrogates. In fact, I was able to integrate THP-1-derived iDCs as $CD11c^+$ $CD14^-$ DDCs into the dermal construct without impairing the stratification of the epidermis. Furthermore, upon topical exposure to $NiSO_4$, the surface marker expression of CD54 and CD86 on the tissue-integrated DDC surrogates was increased, which could be suppressed by pre-treatment with dexamethasone, thus demonstrating the immune competence of our DDC model and the applicability to study drug candidates.

However, skin sensitization is not only mediated by DDCs but also by LCs [74, 75]. Thus, to obtain a physiologically immune competent skin model close to the native human skin, we aimed to integrate our Mutz-LC surrogates as well as our DDC surrogates into the Phenion® FTSE. To study the integration of Mutz-LCs and further potential readouts, we first generated a FTSE comprising only Mutz-LCs. In line with the published studies [187-189], integration of Mutz LC into the epidermis of the FTSE did not impair the stratification of the epidermis. Topical treatment of the Mutz-LC FTSE with $NiSO_4$ or DNCB resulted in significantly decreased mRNA levels for CD1a and CD207 in the epidermis as well as increased mRNA levels in the dermal compartment for both markers, suggesting a sensitizer-induced migration of Mutz-LCs. These results were confirmed at the protein level via whole slide image quantification. Importantly, we proved a significantly induced migration of Mutz-LCs by applying 17-50-fold lower concentrations of $NiSO_4$ compared to the concentrations utilized in published literature [188, 189]. These tremendous differences are presumably based on the media supplementation of hydrocortisone. Hydrocortisone supports the growth and differentiation of keratinocytes and is therefore commonly used for keratinocyte medium and the engineering of skin models [215, 254]. As mentioned, when investigating skin sensitization or CHS, a medium without hydrocortisone is strongly recommended as hydrocortisone, amongst other glucocorticoids prescribed for CHS, exhibits anti-inflammatory effects [258].

In a final step, we incorporated the Mutz-LCs together with our THP-1-derived DDC surrogates into the Phenion® FTSE. As expected, and like the models comprising the respective isolated DC surrogates, the integration of both surrogates did not affect epidermal stratification. Nevertheless, when compared to the Mutz-LC skin model, topical treatment of the FTSE comprising LC and DDC surrogates with $NiSO_4$ or DNCB revealed an early sensitizer-induced response, reflected by increased numbers of CD1a-positive cells in the epidermis and dermis 8 hours after exposure, which was diminished 24 h after exposure. However, the impact of the co-integration of LC and DDC surrogates on the early sensitizer response compared to the models with the isolated surrogates remains to be elucidated.

Overall, to my knowledge, we are the first to report the generation of an immune competent FTSE comprising LC and DDC surrogates for the identification and characterization of sensitizers and, prospectively, drug discovery.

4.4 Pseudopterosin A-D as a potential anti-inflammatory drug candidate in skin sensitization

Proper handling of ACD is essential in preventing dermatitis from progressing into a long-term chronic issue, particularly when it occurs in significant areas like the face or hands, where it can cause a substantial impact on quality of life [259]. First-line treatment of ACD includes topical application of corticosteroids [1], which are known for their high therapeutic efficacy, including anti-inflammatory and immunosuppressive effects in various inflammatory disorders [260]. Unfortunately, corticosteroids pose various local side effects, such as atrophy; striae; steroid rosacea; perioral dermatitis; hypo- or hyperpigmentation; photosensitivity; bacterial or fungal infections; steroid acne; or, more rarely, contact hypersensitivity and allergy to topical steroids [261-263]. However, rare systemic adverse events upon topical application of glucocorticosteroids, such as glaucoma, Cushing's disease, hyperglycemia, hypertension, or osteopathy, have been reported as well [261]. In particular, long-term usage at high concentrations increases the risks of side effects and complicates their use such that the adverse effects may sometimes outweigh the therapeutic benefits. [260]. Hence, the identification of new anti-inflammatory compounds with fewer side effects is appreciated.

Pseudopterosin is a natural, marine-derived metabolite isolated from the octocoral sea whip *Antillogorgia elisabethae* [191]. To date, at least 31 chemical derivatives of pseudopterosin [192] with anti-inflammatory [190, 191, 195, 198, 199], analgesic [190, 191], anti-cancer [201, 202], antimicrobial [193, 264], neurological [265], and wound healing [203-206] activity have been described. However, to the best of our knowledge, no data has been published yet on the effects of pseudopterosin on skin sensitization or ACD. Hence, we are the first to report that PsA-D significantly reduces sensitizer-induced upregulation of the intercellular adhesion molecule CD54 and the co-stimulatory marker CD86 on THP-1-derived iDCs. In addition, pre-treatment of iDCs with PsA-D decreases the sensitizer-induced upregulation of the surface marker CD11b in a dose-dependent manner. These results are in accordance with the literature as CD11b has been associated with phagocytosis in DCs [238] and pseudopterosin A, which was the most abundant derivative in the PsA-D extract (85%), has been found to decrease phagocytosis and phagosome formation in eukaryotic *Tetrahymena thermophila* cells in a dose-dependent manner [266].

Regarding intracellular pathways, we demonstrated that PsA-D significantly decreases the DNCB-induced phosphorylation of p38 MAPK and blocks the $NiSO_4$-induced degradation of IκBα. To our knowledge, pseudoperosin-mediated inhibition of the p38 MAPK pathway has not been reported before. However, PsA-D decreases the LPS-induced activation of the NF-κB pathway in THP-1 cells as well as in MDA-MB-231 breast cancer cells [201]. In addition, PsA reduces NF-κB concentrations in the brains of Ischemia-induced brain-injured rats compared

to untreated controls [267]. Furthermore, PsA-D was shown to inhibit the LPS-induced cytokine release of IL-6, TNF-α and MCP-1 in THP-1 and MDA-MB-231 breast cancer cells [201] as well as the cytokine expression of IL-6, IL-8, and TNF-α in PBMCs induced by breast cancer cell-conditioned media [202]. We and others have shown that the release of inflammatory cytokines by DC surrogates in response to sensitizers like nickel or DNCB is an important hallmark of DC activation. Moreover, the secretion of inflammatory cytokines is required for the polarization and chemoattraction of T cells [102]. Pre-treatment of THP-1-derived iDCs with PsA-D significantly decreased the sensitizer-induced secretion of inflammatory cytokines, namely IL-8, IL-6, and IL-1β, to a similar extent as observed after pre-treatment with dexamethasone.

Notably, treatment of THP-1 cells with PsA-D led to significantly decreased surface marker expression of the migration marker CXCR4. In addition, one preliminary dataset investigating the impact of PsA-D treatment on the migratory capability of THP-1 cells towards SDF-1 indicated a complete inhibition of migration by PsA-D. Indeed, in former studies, PsA-D inhibited the migration and invasion of triple-negative breast cancer tumor spheroids into the surrounding matrix [202]. Furthermore, the migration of HUVEC cells was significantly reduced upon exposure to PsA [204]. Significantly, administration of CXCR4 antagonists during the sensitization phase substantially decreases cutaneous DC migration towards lymph nodes, ear swelling, and impaires contact hypersensitivity in mice [120]. Thus, CXCR4 could be a promising target for reducing skin sensitization. However, the impact of PsA-D on cutaneous DC migration in humans needs to be confirmed in further migration assays and in our newly developed immune competent tissue equivalent.

4.5 Conclusion, context, and future prospects

Industrialization and modern life have increased exposure to consumer products containing a variety of potential sensitizing ingredients, leading to constantly evolving trends and shifts in allergen exposure and an increasing prevalence of ACD worldwide over the last several decades [14, 268]. Thus, to ensure consumer safety, predictive hazard assessment of chemicals has become more important. Historically, toxicological testing and risk assessment were performed on animal models. However, species-specific differences resulting in limited translatability, ethical concerns, and regulatory demands have encouraged the development of non-animal test systems, including 2D single-endpoint test systems, as well as 3D tissue equivalents of the human skin [43, 159, 182]. Nonetheless, the majority of FTSEs lack the structural and immune complexity of native skin and thus the ability to identify and characterize sensitizers and drug candidates [182]. Hence, the aims of this thesis were to (I) identify, differentiate, and characterize potential LC and DDC surrogates; (II) determine readout

parameters for the identification of sensitizers and drug candidates; (III) generate an immune-competent FTSE by incorporating LC and/or DDC surrogates; and (IV) confirm the immune competence and applicability for sensitizer identification and drug discovery of the newly developed FTSE.

In this thesis, I successfully established robust and highly reproducible protocols for the differentiation of THP-1 cells into DDC surrogates and Mutz-3 cells into LC surrogates. We note that several published test systems, including the OECD-approved h-CLAT and IL-8 Luc assays, are based on undifferentiated THP-1 cells as DC surrogates to identify sensitizers according to the 3rd key event of skin sensitization, namely activation of DCs [152, 155, 269, 270]. However, my results clearly demonstrate that the differentiation of THP-1 cells into iDCs is required to obtain DC surrogates that can effectively phagocytose exogenous particles and upregulate IL-12p40—which is required for T cell activation—when exposed to sensitizers such as DNCB. Furthermore, since multiple studies have indicated that the surface markers CD54 and CD86, which are utilized to identify sensitizers in the h-CLAT and U-SENS assays [152, 153], are not sufficient to distinguish sensitizers from irritants [244-246], we aimed to identify further readout parameters. This thesis identified the following readout parameters for the identification of sensitizers by isolated Mutz-LCs and/or THP-1-derived DDC surrogates: upregulation of CD54, CD86, CD11b, CD83, and CCR7; degradation of IκBα; phosphorylation of p38 MAPK; secretion of IL-8, IL-6, and IL1β.

These findings may be used not only to identify sensitizers but also to serve as targets for drug candidates. In fact, one further aim of this thesis was to (V) investigate the natural, marine-derived compound Pseudopterosin A-D as a potential anti-inflammatory drug candidate for skin sensitization. According to the previously identified readout parameters, we determined the anti-inflammatory properties of PsA-D in skin sensitization. In particular, PsA-D significantly reduced the sensitizer-induced upregulation of CD54, CD86, CD11b, CD83, and CCR7. Furthermore, PsA-D inhibited the release of the inflammatory cytokines IL-8, IL-6, and IL-1β to a similar extent as dexamethasone and blocked the $NiSO_4$-induced-activation of the NF-κB pathway via degradation of IκBα and the DNCB-induced phosphorylation of p38 MAPK. However, in accordance with the previously reported results for different DC surrogates [111, 113], our studies with DNCB and $NiSO_4$ clearly indicate that sensitizers operate via different pathways. Therefore, screening of multiple readouts, including the expression of surface markers, inflammatory pathways, and cytokine secretion, is recommended to identify and distinguish sensitizers from non-sensitizers and irritants. Since these findings are based on isolated LC and DDC surrogates, I recommend confirming the results in an immune competent FTSE.

One of the key findings of this thesis was that THP-1-derived iDCs can be integrated as functional DDC surrogates into a FTSE, resulting in an immune competent FTSE that allows

the identification of sensitizers and drug candidates via surface marker expression of CD54 and CD86 on tissue-integrated DDC surrogates. To my knowledge, no immune competent human FTSE with integrated functional DDCs for sensitizer or drug analysis has been described thus far, which is surprising as several studies have indicated the crucial role of DDC for antigen presentation in the skin [74, 75]. Another major accomplishment of this thesis is the co-incorporation of Mutz-3-derived LC surrogates and THP-1-derived DDC surrogates into a FTSE. Interestingly, sensitizer treatment of the FTSE, comprising both DC subtypes, revealed an early sensitizer-induced response 8 hours after exposure, reflected by increased numbers of CD1a-positive cells in the epidermis and dermis. Although *in vivo* studies have demonstrated an early response to sensitizers by increasing LCs in the epidermis and dermis after only 6 hours of topical exposure [271], the precise mechanism remains elusive and needs to be investigated.

In conclusion, our newly developed immune competent FTSE could serve as an easily accessible *in vitro* test system to investigate the complex inter- and intracellular mechanisms of DC activation in ACD. In addition, our FTSE might be a promising predictive tool to address the unmet need for readout parameters to identify, classify, and discriminate sensitizers from non-sensitizers and irritants, as well as to discover and characterize new drug candidates. To become a serious, standardized *in vitro* alternative to current animal models, our findings need to be confirmed, and further readout parameters determined by large-scale intra- and interlaboratory screenings with well-characterized sensitizers and anti-inflammatory drugs. Prospectively, an ideal FTSE close to the physiology of the native human skin would comprise additional immune cells such as macrophages, monocytes, mast cells, or T cells; additional skin cells such as melanocytes and Merkel cells; as well as vascularization and innervation [182]. Furthermore, to monitor intercellular interactions and mimic the exchange of immune cells, microfluidic platforms, including skin-on-chip models, would be a great advantage. Moreover, regarding pharmacological research, perfusable vascularized skin on-chip-models could allow the real-time monitoring of topically and systemically applied drugs [272-274]. In fact, the first attempts to develop skin-on-chip models have been made, but most of these models are simple, far from a complex FTSE, and lack functional immune cells [272, 275]. To improve these models in terms of immune competence, our Mutz-LCs and THP-1-derived DDCs could be integrated. Despite the progress still to be made in this area, immune competent FTSE-on-chip are expected to hold great potential for the risk assessment of potentially sensitizing substances and drug testing [272-274].

5 References

1. Nassau, S, and Fonacier, L. Allergic Contact Dermatitis. *Med Clin North Am.* 2020, 104, 1: 61-76.
2. Gell, P, and Coombs, R. Clinical Aspects of Immunology. Edited by RRAC P. G. H. Gell: 24-25, Broad Street, Oxford Blackwell Scientific Publications Ltd.
3. Yosipovitch, G, and Papoiu, AD. What Causes Itch in Atopic Dermatitis? *Current allergy and asthma reports.* 2008, 8, 4: 306-11.
4. Usatine, RP, and Riojas, M. Diagnosis and Management of Contact Dermatitis. *American family physician.* 2010, 82, 3: 249-55.
5. Li, Y, and Li, L. Contact Dermatitis: Classifications and Management. *Clinical Reviews in Allergy & Immunology.* 2021, 61, 3: 245-81.
6. Alinaghi, F, Bennike, NH, Egeberg, A, Thyssen, JP, and Johansen, JD. Prevalence of Contact Allergy in the General Population: A Systematic Review and Meta-Analysis. *Contact Dermatitis.* 2019, 80, 2: 77-85.
7. Adler, BL, and DeLeo, VA. Allergic Contact Dermatitis. *JAMA dermatology.* 2021, 157, 3: 364-64.
8. Mowad, CM, Anderson, B, Scheinman, P, Pootongkam, S, Nedorost, S, and Brod, B. Allergic Contact Dermatitis: Patient Management and Education. *Journal of the American Academy of Dermatology.* 2016, 74, 6: 1043-54.
9. Dickel, H, Kuss, O, Schmidt, A, Kretz, J, and Diepgen, TL. Importance of Irritant Contact Dermatitis in Occupational Skin Disease. *Am J Clin Dermatol.* 2002, 3, 4: 283-9.
10. Belsito, DV. Occupational Contact Dermatitis: Etiology, Prevalence, and Resultant Impairment/Disability. *Journal of the American Academy of Dermatology.* 2005, 53, 2: 303-13.
11. Kucenic, MJ, and Belsito, DV. Occupational Allergic Contact Dermatitis Is More Prevalent Than Irritant Contact Dermatitis: A 5-Year Study. *Journal of the American Academy of Dermatology.* 2002, 46, 5: 695-99.
12. Forkel, S, Cevik, N, Schill, T, Worm, M, Mahler, V, Weisshaar, E, Vieluf, D, Pfützner, W, Löffler, H, and Schön, MP. Atopic Skin Diathesis Rather Than Atopic Dermatitis Is Associated with Specific Contact Allergies. *JDDG: Journal der Deutschen Dermatologischen Gesellschaft.* 2021, 19, 2: 231-40.
13. DeKoven, JG, Silverberg, JI, Warshaw, EM, Atwater, AR, Reeder, MJ, Sasseville, D, Taylor, JS, Zug, KA, Belsito, DV, Maibach, HI, Pratt, MD, Cgt, M, DeLeo, VA, and Fowler, JF. North American Contact Dermatitis Group Patch Test Results: 2017–2018. *Dermatitis.* 2021, 32, 2: 111-23.
14. Rodriguez, O, Brod, BA, and James, WD. Impact of Trends in New and Emerging Contact Allergens. *Int J Womens Dermatol.* 2022, 8, 1: e006.
15. Kalboussi, H, Kacem, I, Aroui, H, El Maalel, O, Maoua, M, Brahem, A, El Guedri, S, Chatti, S, Ghariani, N, and Mrizak, N. Impact of Allergic Contact Dermatitis on the Quality of Life and Work Productivity. *Dermatol Res Pract.* 2019, 20193797536.
16. Kadyk, DL, McCarter, K, Achen, F, and Belsito, DV. Quality of Life in Patients with Allergic Contact Dermatitis. *Journal of the American Academy of Dermatology.* 2003, 49, 6: 1037-48.
17. Linn Holness, D. Results of a Quality of Life Questionnaire in a Patch Test Clinic Population. *Contact Dermatitis.* 2001, 44, 2: 80-84.
18. Bawany, F, Northcott, CA, Beck, LA, and Pigeon, WR. Sleep Disturbances and Atopic Dermatitis: Relationships, Methods for Assessment, and Therapies. *J Allergy Clin Immunol Pract.* 2021, 9, 4: 1488-500.
19. Dietz, JB, Menné, T, Meyer, HW, Viskum, S, Flyvholm, M-A, Ahrensbøll-Friis, U, John, SM, and Johansen, JD. Degree of Employment, Sick Leave, and Costs Following

Notification of Occupational Contact Dermatitis—a Register-Based Study. *Contact Dermatitis.* 2021, 84, 4: 224-35.

20. Cashman, MW, Reutemann, PA, and Ehrlich, A. Contact Dermatitis in the United States: Epidemiology, Economic Impact, and Workplace Prevention. *Dermatologic clinics.* 2012, 30, 1: 87-98.
21. Kleinstreuer, NC, Hoffmann, S, Alépée, N, Allen, D, Ashikaga, T, Casey, W, Clouet, E, Cluzel, M, Desprez, B, Gellatly, N, Göbel, C, Kern, PS, Klaric, M, Kühnl, J, Martinozzi-Teissier, S, Mewes, K, Miyazawa, M, Strickland, J, van Vliet, E, Zang, Q, and Petersohn, D. Non-Animal Methods to Predict Skin Sensitization (Ii): An Assessment of Defined Approaches (*). *Crit Rev Toxicol.* 2018, 48, 5: 359-74.
22. Lahl, U, and Hawxwell, KA. Reach—the New European Chemicals Law. ACS Publications, 2006.
23. Union, POotE. Regulation (Ec) No 1907/2006 – Concerning the Registration, Evaluation, Authorisation and Restriction of Chemicals and Establishing a European Chemicals Agency. edited by E Parliament, 2006.
24. Parliament, E. Regulation (Ec) No 1223/2009 of the European Parliament and of the Council of 30 November 2009 on Cosmetic Products. In *Off. J. Eur. Union. Eur. Parliam. Counc. Eur. Union.*, 59-209, 2009.
25. Foth, H, and Hayes, A. Concept of Reach and Impact on Evaluation of Chemicals. *Human & experimental toxicology.* 2008, 27, 1: 5-21.
26. Williams, ES, Panko, J, and Paustenbach, DJ. The European Union's Reach Regulation: A Review of Its History and Requirements. *Critical reviews in toxicology.* 2009, 39, 7: 553-75.
27. European Commission. Regulation (EC) No 1272/2008 of the European Parliament and of the Council of 16 December 2008 on Classification, Labelling and Packaging of Substances and Mixtures, Amending and Repealing Directives 67/548/Eec and 1999/45/EC, and Amending Regulation (EC) No 1907/2006. In *Official Journal of the European Union*, 1-1355, 2008.
28. Winder, C, Azzi, R, and Wagner, D. The Development of the Globally Harmonized System (Ghs) of Classification and Labelling of Hazardous Chemicals. *Journal of Hazardous Materials.* 2005, 125, 1: 29-44.
29. Kimber, I, Mitchell, JA, and Griffin, AC. Development of a Murine Local Lymph Node Assay for the Determination of Sensitizing Potential. *Food and Chemical Toxicology.* 1986, 24, 6: 585-86.
30. Kimber, I, and Weisenberger, C. A Murine Local Lymph Node Assay for the Identification of Contact Allergens. *Archives of Toxicology.* 1989, 63, 4: 274-82.
31. Buehler, E. Delayed Contact Hypersensitivity in the Guinea Pig. *Archives of Dermatology.* 1965, 91, 2: 171-75.
32. Magnusson, B. The Identification of Contact Allergens by Animal Assay. The Guinea Pig Maximization Test. *J Invest Dermatol.* 1969, 52268-76.
33. Pasparakis, M, Haase, I, and Nestle, FO. Mechanisms Regulating Skin Immunity and Inflammation. *Nat Rev Immunol.* 2014, 14, 5: 289-301.
34. Bronaugh, RL, Stewart, RF, and Congdon, ER. Methods for in Vitro Percutaneous Absorption Studies Ii. Animal Models for Human Skin. *Toxicology and Applied Pharmacology.* 1982, 62, 3: 481-88.
35. Bond, JR, and Barry, BW. Limitations of Hairless Mouse Skin as a Model for in Vitro Permeation Studies through Human Skin: Hydration Damage. *Journal of investigative dermatology.* 1988, 90, 4: 486-89.
36. Haniffa, M, Gunawan, M, and Jardine, L. Human Skin Dendritic Cells in Health and Disease. *Journal of Dermatological Science.* 2015, 77, 2: 85-92.

37. Brown, CC, Gudjonson, H, Pritykin, Y, Deep, D, Lavallée, V-P, Mendoza, A, Fromme, R, Mazutis, L, Ariyan, C, Leslie, C, Pe'er, D, and Rudensky, AY. Transcriptional Basis of Mouse and Human Dendritic Cell Heterogeneity. *Cell.* 2019, 179, 4: 846-63.e24.
38. Guilliams, M, Henri, S, Tamoutounour, S, Ardouin, L, Schwartz-Cornil, I, Dalod, M, and Malissen, B. From Skin Dendritic Cells to a Simplified Classification of Human and Mouse Dendritic Cell Subsets. *European journal of immunology.* 2010, 40, 8: 2089-94.
39. de Jong, A, Cheng, TY, Huang, S, Gras, S, Birkinshaw, RW, Kasmar, AG, Van Rhijn, I, Peña-Cruz, V, Ruan, DT, Altman, JD, Rossjohn, J, and Moody, DB. Cd1a-Autoreactive T Cells Recognize Natural Skin Oils That Function as Headless Antigens. *Nat Immunol.* 2014, 15, 2: 177-85.
40. Kim, JH, Hu, Y, Yongqing, T, Kim, J, Hughes, VA, Le Nours, J, Marquez, EA, Purcell, AW, Wan, Q, and Sugita, M. CD1a on Langerhans Cells Controls Inflammatory Skin Disease. *Nature Immunology.* 2016, 17, 10: 1159-66.
41. Kobayashi, C, Shiina, T, Tokioka, A, Hattori, Y, Komori, T, Kobayashi-Miura, M, Takizawa, T, Takahara, K, Inaba, K, Inoko, H, Takeya, M, Dranoff, G, and Sugita, M. GM-CSF-Independent CD1a Expression in Epidermal Langerhans Cells: Evidence from Human CD1a Genome-Transgenic Mice. *J Invest Dermatol.* 2012, 132, 1: 241-4.
42. Schmidt, M, Raghavan, B, Müller, V, Vogl, T, Fejer, G, Tchaptchet, S, Keck, S, Kalis, C, Nielsen, PJ, Galanos, C, Roth, J, Skerra, A, Martin, SF, Freudenberg, MA, and Goebeler, M. Crucial Role for Human Toll-Like Receptor 4 in the Development of Contact Allergy to Nickel. *Nature Immunology.* 2010, 11, 9: 814-19.
43. Gerber, PA, Buhren, BA, Schrumpf, H, Homey, B, Zlotnik, A, and Hevezi, P. The Top Skin-Associated Genes: A Comparative Analysis of Human and Mouse Skin Transcriptomes. *Biol Chem.* 2014, 395, 6: 577-91.
44. Haneke, KE, Tice, RR, Carson, BL, Margolin, BH, and Stokes, WS. Iccvam Evaluation of the Murine Local Lymph Node Assay: Iii. Data Analyses Completed by the National Toxicology Program Interagency Center for the Evaluation of Alternative Toxicological Methods. *Regulatory Toxicology and Pharmacology.* 2001, 34, 3: 274-86.
45. Russell, WMS, and Burch, RL. *The Principles of Humane Experimental Technique*: Methuen, 1959.
46. EUs Directive. 63/EU of the European Parliament and of the Council of 22 September 2010 on the Protection of Animals Used for Scientific Purposes. In *Off. J. Eur. Union*, 33-79, 2010.
47. European Chemicals, A. *Non-Animal Approaches – Current Status of Regulatory Applicability under the Reach, Clp and Biocidal Products Regulations*: European Chemicals Agency, 2017.
48. Zushin, P-JH, Mukherjee, S, and Wu, JC. Fda Modernization Act 2.0: Transitioning Beyond Animal Models with Human Cells, Organoids, and Ai/Ml-Based Approaches. e175824: Am Soc Clin Investig, 2023.
49. Han, JJ. Fda Modernization Act 2.0 Allows for Alternatives to Animal Testing. *Artif Organs.* 2023, 47, 3: 449-50.
50. Adashi, EY, O'Mahony, DP, and Cohen, IG. The Fda Modernization Act 2.0: Drug Testing in Animals Is Rendered Optional. *The American Journal of Medicine.* 2023, 136, 9: 853-54.
51. Council, NR, Earth, Do, Studies, L, Research, IfLA, Studies, BoE, Testing, CoT, and Agents, AoE. *Toxicity Testing in the 21st Century: A Vision and a Strategy*: National Academies Press, 2007.
52. Andersen, ME, and Krewski, D. Toxicity Testing in the 21st Century: Bringing the Vision to Life. *Toxicological sciences.* 2009, 107, 2: 324-30.
53. Ankley, GT, Bennett, RS, Erickson, RJ, Hoff, DJ, Hornung, MW, Johnson, RD, Mount, DR, Nichols, JW, Russom, CL, and Schmieder, PK. Adverse Outcome Pathways: A Conceptual Framework to Support Ecotoxicology Research and Risk Assessment.

Environmental Toxicology and Chemistry: An International Journal. 2010, 29, 3: 730-41.

54. OECD. Revised Guidance Document on Developing and Assessing Adverse Outcome Pathways, 2017.
55. OECD. Handbook Supplement to the Guidance Document for Developing and Assessing Adverse Outcome Pathways, 2018.
56. OECD. The Adverse Outcome Pathway for Skin Sensitisation Initiated by Covalent Binding to Proteins. 2012.
57. Fenner, J, and Clark, RA. Anatomy, Physiology, Histology, and Immunohistochemistry of Human Skin. *Skin tissue engineering and regenerative medicine.* 2016, 1.
58. Gilaberte, Y, Prieto-Torres, L, Pastushenko, I, and Juarranz, Á. Chapter 1 - Anatomy and Function of the Skin. In *Nanoscience in Dermatology*, edited by MR Hamblin, Avci, P and Prow, TW, 1-14. Boston: Academic Press, 2016.
59. Epstein Jr, E, and Munderloh, N. Human Skin Collagen. Presence of Type I and Type Iii at All Levels of the Dermis. *Journal of Biological Chemistry.* 1978, 253, 5: 1336-37.
60. Pfisterer, K, Shaw, LE, Symmank, D, and Weninger, W. The Extracellular Matrix in Skin Inflammation and Infection. *Frontiers in Cell and Developmental Biology.* 2021, 9.
61. Starcher, B, Aycock, RL, and Hill, CH. Multiple Roles for Elastic Fibers in the Skin. *Journal of Histochemistry & Cytochemistry.* 2005, 53, 4: 431-43.
62. Kabashima, K, Honda, T, Ginhoux, F, and Egawa, G. The Immunological Anatomy of the Skin. *Nature Reviews Immunology.* 2019, 19, 1: 19-30.
63. Yin, H, Hu, M, and Li, D. Regulation of Epidermal Stratification and Development by Basal Keratinocytes. *Journal of cellular physiology.* 2023, 238, 4: 742-48.
64. Nestle, FO, Di Meglio, P, Qin, J-Z, and Nickoloff, BJ. Skin Immune Sentinels in Health and Disease. *Nature Reviews Immunology.* 2009, 9, 10: 679-91.
65. Fehres, CM, Garcia-Vallejo, JJ, Unger, WW, and Van Kooyk, Y. Skin-Resident Antigen-Presenting Cells: Instruction Manual for Vaccine Development. *Frontiers in Immunology.* 2013, 4.
66. Yousef, H, Alhajj, M, and Sharma, S. Anatomy, Skin (Integument), Epidermis. 2017.
67. Kashem, SW, Haniffa, M, and Kaplan, DH. Antigen-Presenting Cells in the Skin. *Annu Rev Immunol.* 2017, 35469-99.
68. Ryan, CA, Kimber, I, Basketter, DA, Pallardy, M, Gildea, LA, and Gerberick, GF. Dendritic Cells and Skin Sensitization: Biological Roles and Uses in Hazard Identification. *Toxicology and Applied Pharmacology.* 2007, 221, 3: 384-94.
69. Hardonnière, K, Szely, N, El Ali, Z, Pallardy, M, and Kerdine-Römer, S. Models of Dendritic Cells to Assess Skin Sensitization. *Front Toxicol.* 2022, 4851017.
70. Valladeau, J, and Saeland, S. Cutaneous Dendritic Cells. Paper presented at the Seminars in immunology 2005.
71. Deckers, J, Hammad, H, and Hoste, E. Langerhans Cells: Sensing the Environment in Health and Disease. *Front Immunol.* 2018, 993.
72. Valladeau, J, Ravel, O, Dezutter-Dambuyant, C, Moore, K, Kleijmeer, M, Liu, Y, Duvert-Frances, V, Vincent, C, Schmitt, D, and Davoust, J. Langerin, a Novel C-Type Lectin Specific to Langerhans Cells, Is an Endocytic Receptor That Induces the Formation of Birbeck Granules. *Immunity.* 2000, 12, 1: 71-81.
73. Romani, N, Brunner, PM, and Stingl, G. Changing Views of the Role of Langerhans Cells. *Journal of investigative dermatology.* 2012, 132, 3, Part 2: 872-81.
74. Fukunaga, A, Khaskhely, NM, Sreevidya, CS, Byrne, SN, and Ullrich, SE. Dermal Dendritic Cells, and Not Langerhans Cells, Play an Essential Role in Inducing an Immune Response. *J Immunol.* 2008, 180, 5: 3057-64.
75. Kissenpfennig, A, Henri, S, Dubois, B, Laplace-Builhé, C, Perrin, P, Romani, N, Tripp, CH, Douillard, P, Leserman, L, Kaiserlian, D, Saeland, S, Davoust, J, and Malissen, B.

Dynamics and Function of Langerhans Cells in Vivo: Dermal Dendritic Cells Colonize Lymph Node Areas Distinct from Slower Migrating Langerhans Cells. *Immunity.* 2005, 22, 5: 643-54.

76. Matejuk, A. Skin Immunity. *Arch Immunol Ther Exp (Warsz).* 2018, 66, 1: 45-54.
77. Zaba, LC, Fuentes-Duculan, J, Steinman, RM, Krueger, JG, and Lowes, MA. Normal Human Dermis Contains Distinct Populations of Cd11c+Bdca-1+ Dendritic Cells and Cd163+Fxiiia+ Macrophages. *J Clin Invest.* 2007, 117, 9: 2517-25.
78. Zaba, LC, Krueger, JG, and Lowes, MA. Resident and "Inflammatory" Dendritic Cells in Human Skin. *Journal of investigative dermatology.* 2009, 129, 2: 302-08.
79. Bos, JD, and Meinardi, MM. The 500 Dalton Rule for the Skin Penetration of Chemical Compounds and Drugs. *Exp Dermatol.* 2000, 9, 3: 165-9.
80. Lepoittevin, J-P. Metabolism Versus Chemical Transformation or Pro-Versus Prehaptens? *Contact Dermatitis.* 2006, 54, 2: 73-74.
81. Chipinda, I, Hettick, JM, and Siegel, PD. Haptenation: Chemical Reactivity and Protein Binding. *Journal of allergy.* 2011, 2011.
82. Aleksic, M, Pease, CK, Basketter, DA, Panico, M, Morris, HR, and Dell, A. Investigating Protein Haptenation Mechanisms of Skin Sensitisers Using Human Serum Albumin as a Model Protein. *Toxicology in Vitro.* 2007, 21, 4: 723-33.
83. Vandebriel, RJ, Pennings, JLA, Baken, KA, Pronk, TE, Boorsma, A, Gottschalk, R, and Van Loveren, H. Keratinocyte Gene Expression Profiles Discriminate Sensitizing and Irritating Compounds. *Toxicological sciences.* 2010, 117, 1: 81-89.
84. Natsch, A, and Emter, R. Skin Sensitizers Induce Antioxidant Response Element Dependent Genes: Application to the in Vitro Testing of the Sensitization Potential of Chemicals. *Toxicological sciences.* 2007, 102, 1: 110-19.
85. Natsch, A. The Nrf2-Keap1-Are Toxicity Pathway as a Cellular Sensor for Skin Sensitizers—Functional Relevance and a Hypothesis on Innate Reactions to Skin Sensitizers. *Toxicological sciences.* 2009, 113, 2: 284-92.
86. Itoh, K, Wakabayashi, N, Katoh, Y, Ishii, T, Igarashi, K, Engel, JD, and Yamamoto, M. Keap1 Represses Nuclear Activation of Antioxidant Responsive Elements by Nrf2 through Binding to the Amino-Terminal Neh2 Domain. *Genes Dev.* 1999, 13, 1: 76-86.
87. Natsch, A, and Emter, R. Nrf2 Activation as a Key Event Triggered by Skin Sensitisers: The Development of the Stable Keratinosens Reporter Gene Assay. *Alternatives to Laboratory Animals.* 2016, 44, 5: 443-51.
88. Vandebriel, RJ, Pennings, JL, Baken, KA, Pronk, TE, Boorsma, A, Gottschalk, R, and Van Loveren, H. Keratinocyte Gene Expression Profiles Discriminate Sensitizing and Irritating Compounds. *Toxicological sciences.* 2010, 117, 1: 81-89.
89. Thierse, H-J, Gamerdinger, K, Junkes, C, Guerreiro, N, and Weltzien, HU. T Cell Receptor (Tcr) Interaction with Haptens: Metal Ions as Non-Classical Haptens. *Toxicology.* 2005, 209, 2: 101-07.
90. Viemann, D, Schmidt, M, Tenbrock, K, Schmid, S, Müller, V, Klimmek, K, Ludwig, S, Roth, J, and Goebeler, M. The Contact Allergen Nickel Triggers a Unique Inflammatory and Proangiogenic Gene Expression Pattern Via Activation of NF-kB and Hypoxia-Inducible Factor-1α1. *The Journal of Immunology.* 2007, 178, 5: 3198-207.
91. Kavasi, R-M, Berdiaki, A, Spyridaki, I, Papoutsidakis, A, Corsini, E, Tsatsakis, A, Tzanakakis, GN, and Nikitovic, D. Contact Allergen (Ppd and Dncb)-Induced Keratinocyte Sensitization Is Partly Mediated through a Low Molecular Weight Hyaluronan (Lmwha)/Tlr4/NF-kB Signaling Axis. *Toxicology and Applied Pharmacology.* 2019, 377114632.
92. Watanabe, H, Gaide, O, Pétrilli, V, Martinon, F, Contassot, E, Roques, S, Kummer, JA, Tschopp, J, and French, LE. Activation of the Il-1β-Processing Inflammasome Is Involved in Contact Hypersensitivity. *Journal of investigative dermatology.* 2007, 127, 8: 1956-63.

93. Galbiati, V, Cornaghi, L, Papale, A, Donetti, E, Marinovich, M, and Corsini, E. Study on the Inflammasome Nlrp3 and Blimp-1/Nlrp12 after Keratinocyte Exposure to Contact Allergens. *Toxicology Letters.* 2019, 313130-36.
94. Mizumoto, N, Mummert, ME, Shalhevet, D, and Takashima, A. Keratinocyte Atp Release Assay for Testing Skin-Irritating Potentials of Structurally Diverse Chemicals. *Journal of investigative dermatology.* 2003, 121, 5: 1066-72.
95. Esser, PR, Wölfle, U, Dürr, C, von Loewenich, FD, Schempp, CM, Freudenberg, MA, Jakob, T, and Martin, SF. Contact Sensitizers Induce Skin Inflammation Via ROS Production and Hyaluronic Acid Degradation. *PLOS ONE.* 2012, 7, 7: e41340.
96. Jung, D, Che, J-H, Lim, K-M, Chun, Y-J, Heo, Y, and Seok, SH. Discrimination of Skin Sensitizers from Non-Sensitizers by Interleukin-1α and Interleukin-6 Production on Cultured Human Keratinocytes. *Journal of Applied Toxicology.* 2016, 36, 9: 1129-36.
97. Coquette, A, Berna, N, Vandenbosch, A, Rosdy, M, De Wever, B, and Poumay, Y. Analysis of Interleukin-1α (Il-1α) and Interleukin-8 (IL-8) Expression and Release in in Vitro Reconstructed Human Epidermis for the Prediction of in Vivo Skin Irritation and/or Sensitization. *Toxicology in Vitro.* 2003, 17, 3: 311-21.
98. Zepter, K, Häffner, A, Soohoo, LF, De Luca, D, Tang, H-P, Fisher, P, Chavinson, J, and Elmets, CA. Induction of Biologically Active Il-1 Beta-Converting Enzyme and Mature Il-1 Beta in Human Keratinocytes by Inflammatory and Immunologic Stimuli. *Journal of immunology (Baltimore, Md.: 1950).* 1997, 159, 12: 6203-08.
99. Mohamadzadeh, M, Miiller, M, Hultsch, T, Enk, A, Saloga, J, and Knop, J. Enhanced Expression of Il-8 in Normal Human Keratinocytes and Human Keratinocyte Cell Line Hacat in Vitro after Stimulation with Contact Sensitizers., Tolerogens and Irritants. *Experimental Dermatology.* 1994, 3, 6: 298-303.
100. Aiba, S. Maturation of Dendritic Cells Induced by Cytokines and Haptens. *The Tohoku journal of experimental medicine.* 1998, 184, 3: 159-72.
101. Corsini, E, and Galli, CL. Epidermal Cytokines in Experimental Contact Dermatitis. *Toxicology.* 2000, 142, 3: 203-12.
102. Rustemeyer, T, Van Hoogstraten, IM, Von Blomberg, BME, and Scheper, RJ. Mechanisms of Allergic Contact Dermatitis. *Kanerva's occupational dermatology.* 2020,151-90.
103. Toebak, MJ, Gibbs, S, Bruynzeel, DP, Scheper, RJ, and Rustemeyer, T. Dendritic Cells: Biology of the Skin. *Contact Dermatitis.* 2009, 60, 1: 2-20.
104. Stoitzner, P, Tripp, CH, Eberhart, A, Price, KM, Jung, JY, Bursch, L, Ronchese, F, and Romani, N. Langerhans Cells Cross-Present Antigen Derived from Skin. *Proceedings of the National Academy of Sciences.* 2006, 103, 20: 7783-88.
105. Dolan, BP, Gibbs, KD, and Ostrand-Rosenberg, S. Dendritic Cells Cross-Dressed with Peptide MHC Class I Complexes Prime Cd8+ T Cells. *The Journal of Immunology.* 2006, 177, 9: 6018-24.
106. Mantegazza, AR, Magalhaes, JG, Amigorena, S, and Marks, MS. Presentation of Phagocytosed Antigens by Mhc Class I and II. *Traffic.* 2013, 14, 2: 135-52.
107. Betts, RJ, Perkovic, A, Mahapatra, S, Del Bufalo, A, Camara, K, Howell, AR, Martinozzi Teissier, S, De Libero, G, and Mori, L. Contact Sensitizers Trigger Human Cd1-Autoreactive T-Cell Responses. *European journal of immunology.* 2017, 47, 7: 1171-80.
108. Tuschl, H, and Kovac, R. Langerhans Cells and Immature Dendritic Cells as Model Systems for Screening of Skin Sensitizers. *Toxicol In Vitro.* 2001, 15, 4-5: 327-31.
109. Aiba, S, Terunuma, A, Manome, H, and Tagami, H. Dendritic Cells Differently Respond to Haptens and Irritants by Their Production of Cytokines and Expression of Co-Stimulatory Molecules. *European journal of immunology.* 1997, 27, 11: 3031-38.

110. Matos, TJ, Duarte, CB, Gonçalo, M, and Lopes, MC. Role of Oxidative Stress in Erk and P38 Mapk Activation Induced by the Chemical Sensitizer Dnfb in a Fetal Skin Dendritic Cell Line. *Immunology & Cell Biology.* 2005, 83, 6: 607-14.

111. Aiba, S, Manome, H, Nakagawa, S, Mollah, ZU, Mizuashi, M, Ohtani, T, Yoshino, Y, and Tagami, H. P38 Mitogen-Activated Protein Kinase and Extracellular Signal-Regulated Kinases Play Distinct Roles in the Activation of Dendritic Cells by Two Representative Haptens, Nicl2 and 2,4-Dinitrochlorobenzene. *J Invest Dermatol.* 2003, 120, 3: 390-9.

112. Arrighi, JF, Rebsamen, M, Rousset, F, Kindler, V, and Hauser, C. A Critical Role for P38 Mitogen-Activated Protein Kinase in the Maturation of Human Blood-Derived Dendritic Cells Induced by Lipopolysaccharide, Tnf-Alpha, and Contact Sensitizers. *J Immunol.* 2001, 166, 6: 3837-45.

113. Ade, N, Antonios, D, Kerdine-Romer, S, Boisleve, F, Rousset, F, and Pallardy, M. Nf-Kappab Plays a Major Role in the Maturation of Human Dendritic Cells Induced by NiSO(4) but Not by Dncb. *Toxicol Sci.* 2007, 99, 2: 488-501.

114. Boislève, F, Kerdine-Römer, S, Rougier-Larzat, N, and Pallardy, M. Nickel and Dncb Induce Ccr7 Expression on Human Dendritic Cells through Different Signalling Pathways: Role of TNF-a and MAPK. *Journal of investigative dermatology.* 2004, 123, 3: 494-502.

115. Trompezinski, S, Migdal, C, Tailhardat, M, Le Varlet, B, Courtellemont, P, Haftek, M, and Serres, M. Characterization of Early Events Involved in Human Dendritic Cell Maturation Induced by Sensitizers: Cross Talk between MAPK Signalling Pathways. *Toxicology and Applied Pharmacology.* 2008, 230, 3: 397-406.

116. Ghiringhelli, F, Apetoh, L, Tesniere, A, Aymeric, L, Ma, Y, Ortiz, C, Vermaelen, K, Panaretakis, T, Mignot, G, Ullrich, E, Perfettini, JL, Schlemmer, F, Tasdemir, E, Uhl, M, Génin, P, Civas, A, Ryffel, B, Kanellopoulos, J, Tschopp, J, André, F, Lidereau, R, McLaughlin, NM, Haynes, NM, Smyth, MJ, Kroemer, G, and Zitvogel, L. Activation of the Nlrp3 Inflammasome in Dendritic Cells Induces IL-1beta-Dependent Adaptive Immunity against Tumors. *Nat Med.* 2009, 15, 10: 1170-8.

117. Termeer, CC, Hennies, Jr, Voith, U, Ahrens, T, M Weiss, J, Prehm, P, and Simon, JC. Oligosaccharides of Hyaluronan Are Potent Activators of Dendritic Cells. *The Journal of Immunology.* 2000, 165, 4: 1863-70.

118. Tang, A, Amagai, M, Granger, LG, Stanley, JR, and Uddy, MC. Adhesion of Epidermal Langerhans Cells to Keratinocytes Mediated by E-Cadherin. *Nature.* 1993, 361, 6407: 82-85.

119. Wang, B, Amerio, P, and Sauder, DN. Role of Cytokines in Epidermal Langerhans Cell Migration. *Journal of Leukocyte Biology.* 1999, 66, 1: 33-39.

120. Kabashima, K, Shiraishi, N, Sugita, K, Mori, T, Onoue, A, Kobayashi, M, Sakabe, J-i, Yoshiki, R, Tamamura, H, Fujii, N, Inaba, K, and Tokura, Y. Cxcl12-Cxcr4 Engagement Is Required for Migration of Cutaneous Dendritic Cells. *The American Journal of Pathology.* 2007, 171, 4: 1249-57.

121. Ouwehand, K, Santegoets, SJ, Bruynzeel, DP, Scheper, RJ, de Gruijl, TD, and Gibbs, S. Cxcl12 Is Essential for Migration of Activated Langerhans Cells from Epidermis to Dermis. *Eur J Immunol.* 2008, 38, 11: 3050-9.

122. Pablos, JL, Amara, A, Bouloc, A, Santiago, B, Caruz, A, Galindo, M, Delaunay, T, Virelizier, JL, and Arenzana-Seisdedos, F. Stromal-Cell Derived Factor Is Expressed by Dendritic Cells and Endothelium in Human Skin. *The American Journal of Pathology.* 1999, 155, 5: 1577-86.

123. Tal, O, Lim, HY, Gurevich, I, Milo, I, Shipony, Z, Ng, LG, Angeli, V, and Shakhar, G. Dc Mobilization from the Skin Requires Docking to Immobilized Ccl21 on Lymphatic Endothelium and Intralymphatic Crawling. *Journal of Experimental Medicine.* 2011, 208, 10: 2141-53.

124. Braun, A, Worbs, T, Moschovakis, GL, Halle, S, Hoffmann, K, Bölter, J, Münk, A, and Förster, R. Afferent Lymph–Derived T Cells and Dcs Use Different Chemokine Receptor Ccr7–Dependent Routes for Entry into the Lymph Node and Intranodal Migration. *Nature Immunology.* 2011, 12, 9: 879-87.

125. Ohl, L, Mohaupt, M, Czeloth, N, Hintzen, G, Kiafard, Z, Zwirner, J, Blankenstein, T, Henning, G, and Förster, R. Ccr7 Governs Skin Dendritic Cell Migration under Inflammatory and Steady-State Conditions. *Immunity.* 2004, 21, 2: 279-88.

126. Porcelli, S, Brenner, MB, Greenstein, JL, Terhorst, C, Balk, SP, and Bleicher, PA. Recognition of Cluster of Differentiation 1 Antigens by Human CD4− CD8− Cytolytic T Lymphocyte. *Nature.* 1989, 341, 6241: 447-50.

127. de Lalla, C, Lepore, M, Piccolo, FM, Rinaldi, A, Scelfo, A, Garavaglia, C, Mori, L, De Libero, G, Dellabona, P, and Casorati, G. High-Frequency and Adaptive-Like Dynamics of Human Cd1 Self-Reactive T Cells. *European journal of immunology.* 2011, 41, 3: 602-10.

128. Gérard, A, Cope, AP, Kemper, C, Alon, R, and Köchl, R. Lfa-1 in T Cell Priming, Differentiation, and Effector Functions. *Trends in Immunology.* 2021, 42, 8: 706-22.

129. Chen, L, and Flies, DB. Molecular Mechanisms of T Cell Co-Stimulation and Co-Inhibition. *Nature Reviews Immunology.* 2013, 13, 4: 227-42.

130. Vocanson, M, Hennino, A, Rozieres, A, Poyet, G, and Nicolas, JF. Effector and Regulatory Mechanisms in Allergic Contact Dermatitis. *Allergy.* 2009, 64, 12: 1699-714.

131. Pickard, C, Smith, AM, Cooper, H, Strickland, I, Jackson, J, Healy, E, and Friedmann, PS. Investigation of Mechanisms Underlying the T-Cell Response to the Hapten 2,4-Dinitrochlorobenzene. *Journal of investigative dermatology.* 2007, 127, 3: 630-37.

132. Sakuratani, Y, Horie, M, and Leinala, E. Integrated Approaches to Testing and Assessment: Oecd Activities on the Development and Use of Adverse Outcome Pathways and Case Studies. *Basic & Clinical Pharmacology & Toxicology.* 2018, 12320-28.

133. Schmeisser, S, Miccoli, A, von Bergen, M, Berggren, E, Braeuning, A, Busch, W, Desaintes, C, Gourmelon, A, Grafström, R, Harrill, J, Hartung, T, Herzler, M, Kass, GEN, Kleinstreuer, N, Leist, M, Luijten, M, Marx-Stoelting, P, Poetz, O, van Ravenzwaay, B, Roggeband, R, Rogiers, V, Roth, A, Sanders, P, Thomas, RS, Marie Vinggaard, A, Vinken, M, van de Water, B, Luch, A, and Tralau, T. New Approach Methodologies in Human Regulatory Toxicology – Not If, but How and When! *Environment International.* 2023, 178108082.

134. OECD. *Guidance Document on the Validation and International Acceptance of New or Updated Test Methods for Hazard Assessment*, Oecd Series on Testing and Assessment, No 34, 2005.

135. de Ávila, RI, Lindstedt, M, and Valadares, MC. The 21st Century Movement within the Area of Skin Sensitization Assessment: From the Animal Context Towards Current Human-Relevant in Vitro Solutions. *Regulatory Toxicology and Pharmacology.* 2019, 108104445.

136. Basketter, DA, and Gerberick, GF. Skin Sensitization Testing: The Ascendancy of Non-Animal Methods. *Cosmetics.* 2022, 9, 2: 38.

137. Bas, A, Burns, N, Gulotta, A, Junker, J, Drasler, B, Lehner, R, Aicher, L, Constant, S, Petri-Fink, A, and Rothen-Rutishauser, B. Understanding the Development, Standardization, and Validation Process of Alternative in Vitro Test Methods for Regulatory Approval from a Researcher Perspective. *Small.* 2021, 17, 15: 2006027.

138. Taylor, K. Recent Developments in Alternatives to Animal Testing. *Animal experimentation: working towards a paradigm change.* 2019,585-609.

139. Bialas, I, Zelent-Kraciuk, S, and Jurowski, K. The Skin Sensitisation of Cosmetic Ingredients: Review of Actual Regulatory Status. *Toxics.* 2023, 11, 4: 392.

140. Gerberick, GF, Vassallo, JD, Bailey, RE, Chaney, JG, Morrall, SW, and Lepoittevin, JP. Development of a Peptide Reactivity Assay for Screening Contact Allergens. *Toxicol Sci.* 2004, 81, 2: 332-43.

141. Gerberick, GF, Vassallo, JD, Foertsch, LM, Price, BB, Chaney, JG, and Lepoittevin, JP. Quantification of Chemical Peptide Reactivity for Screening Contact Allergens: A Classification Tree Model Approach. *Toxicol Sci.* 2007, 97, 2: 417-27.

142. Fujita, M, Yamamoto, Y, Tahara, H, Kasahara, T, Jimbo, Y, and Hioki, T. Development of a Prediction Method for Skin Sensitization Using Novel Cysteine and Lysine Derivatives. *J Pharmacol Toxicol Methods.* 2014, 70, 1: 94-105.

143. Yamamoto, Y, Fujita, M, Watanabe, S, Yamaga, H, Wakabayashi, K, Tahara, Y, Horie, N, Fujimoto, K, Takeuchi, K, Kamiya, K, Kawakami, T, Kojima, K, Sozu, T, Kojima, H, Kasahara, T, and Ono, A. Within- and between-Laboratory Reproducibility and Predictive Capacity of Amino Acid Derivative Reactivity Assay (Adra) Using a 0.5 Mg/Ml Test Chemical Solution: Results of the Study for Reproducibility Confirmation Implemented in Five Participating Laboratories. *Journal of Applied Toxicology.* 2022, 42, 6: 1078-90.

144. Wareing, B, Kolle, SN, Birk, B, Alépée, N, Haupt, T, Kathawala, R, Kern, PS, Nardelli, L, Raabe, H, Rucki, M, Ryan, CA, Verkaart, S, Westerink, WMA, Landsiedel, R, and Natsch, A. The Kinetic Direct Peptide Reactivity Assay (Kdpra): Intra- and Inter-Laboratory Reproducibility in a Seven-Laboratory Ring Trial. *ALTEX - Alternatives to animal experimentation.* 2020, 37, 4: 639-51.

145. OECD. *Test No. 442c: In Chemico Skin Sensitisation*, 2023.

146. Natsch, A, Gfeller, H, Rothaupt, M, and Ellis, G. Utility and Limitations of a Peptide Reactivity Assay to Predict Fragrance Allergens in Vitro. *Toxicology in Vitro.* 2007, 21, 7: 1220-26.

147. OECD. *Test No. 442d: In Vitro Skin Sensitisation*, 2022.

148. Emter, R, Ellis, G, and Natsch, A. Performance of a Novel Keratinocyte-Based Reporter Cell Line to Screen Skin Sensitizers in Vitro. *Toxicol Appl Pharmacol.* 2010, 245, 3: 281-90.

149. Andreas, N, Caroline, B, Leslie, F, Frank, G, Kimberly, N, Allison, H, Heather, I, Robert, L, Stefan, O, Hendrik, R, Andreas, S, and Roger, E. The Intra- and Inter-Laboratory Reproducibility and Predictivity of the Keratinosens Assay to Predict Skin Sensitizers in Vitro: Results of a Ring-Study in Five Laboratories. *Toxicol In Vitro.* 2011, 25, 3: 733-44.

150. Ramirez, T, Mehling, A, Kolle, SN, Wruck, CJ, Teubner, W, Eltze, T, Aumann, A, Urbisch, D, van Ravenzwaay, B, and Landsiedel, R. Lusens: A Keratinocyte Based Are Reporter Gene Assay for Use in Integrated Testing Strategies for Skin Sensitization Hazard Identification. *Toxicol In Vitro.* 2014, 28, 8: 1482-97.

151. OECD. *Test No. 442e: In Vitro Skin Sensitisation*, 2023.

152. Ashikaga, T, Yoshida, Y, Hirota, M, Yoneyama, K, Itagaki, H, Sakaguchi, H, Miyazawa, M, Ito, Y, Suzuki, H, and Toyoda, H. Development of an in Vitro Skin Sensitization Test Using Human Cell Lines: The Human Cell Line Activation Test (H-Clat): I. Optimization of the H-Clat Protocol. *Toxicology in Vitro.* 2006, 20, 5: 767-73.

153. Piroird, C, Ovigne, JM, Rousset, F, Martinozzi-Teissier, S, Gomes, C, Cotovio, J, and Alépée, N. The Myeloid U937 Skin Sensitization Test (U-Sens) Addresses the Activation of Dendritic Cell Event in the Adverse Outcome Pathway for Skin Sensitization. *Toxicol In Vitro.* 2015, 29, 5: 901-16.

154. Takahashi, T, Kimura, Y, Saito, R, Nakajima, Y, Ohmiya, Y, Yamasaki, K, and Aiba, S. An in Vitro Test to Screen Skin Sensitizers Using a Stable Thp-1-Derived Il-8 Reporter Cell Line, Thp-G8. *Toxicol Sci.* 2011, 124, 2: 359-69.

155. Kimura, Y, Fujimura, C, Ito, Y, Takahashi, T, Nakajima, Y, Ohmiya, Y, and Aiba, S. Optimization of the Il-8 Luc Assay as an in Vitro Test for Skin Sensitization. *Toxicol In Vitro.* 2015, 29, 7: 1816-30.

156. Johansson, H, Albrekt, AS, Borrebaeck, CA, and Lindstedt, M. The Gard Assay for Assessment of Chemical Skin Sensitizers. *Toxicol In Vitro.* 2013, 27, 3: 1163-9.

157. Johansson, H, Gradin, R, Johansson, A, Adriaens, E, Edwards, A, Zuckerstätter, V, Jerre, A, Burleson, F, Gehrke, H, and Roggen, EL. Validation of the Gard™Skin Assay for Assessment of Chemical Skin Sensitizers: Ring Trial Results of Predictive Performance and Reproducibility. *Toxicol Sci.* 2019, 170, 2: 374-81.

158. OECD. *Guideline No. 497: Defined Approaches on Skin Sensitisation*, 2023.

159. Gądarowska, D, Kalka, J, Daniel-Wójcik, A, and Mrzyk, I. Alternative Methods for Skin-Sensitization Assessment. *Toxics.* 2022, 10, 12: 740.

160. Robinson, MK, Gerberick, GF, Ryan, CA, McNamee, P, White, IR, and Basketter, DA. The Importance of Exposure Estimation in the Assessment of Skin Sensitization Risk. *Contact Dermatitis.* 2000, 42, 5: 251-59.

161. Roberts, DW, and Patlewicz, G. Chemistry Based Nonanimal Predictive Modeling for Skin Sensitization. *Ecotoxicology Modeling.* 2009,61-83.

162. Adler, S, Basketter, D, Creton, S, Pelkonen, O, van Benthem, J, Zuang, V, Andersen, KE, Angers-Loustau, A, Aptula, A, Bal-Price, A, Benfenati, E, Bernauer, U, Bessems, J, Bois, FY, Boobis, A, Brandon, E, Bremer, S, Broschard, T, Casati, S, Coecke, S, Corvi, R, Cronin, M, Daston, G, Dekant, W, Felter, S, Grignard, E, Gundert-Remy, U, Heinonen, T, Kimber, I, Kleinjans, J, Komulainen, H, Kreiling, R, Kreysa, J, Leite, SB, Loizou, G, Maxwell, G, Mazzatorta, P, Munn, S, Pfuhler, S, Phrakonkham, P, Piersma, A, Poth, A, Prieto, P, Repetto, G, Rogiers, V, Schoeters, G, Schwarz, M, Serafimova, R, Tähti, H, Testai, E, van Delft, J, van Loveren, H, Vinken, M, Worth, A, and Zaldivar, J-M. Alternative (Non-Animal) Methods for Cosmetics Testing: Current Status and Future Prospects—2010. *Archives of Toxicology.* 2011, 85, 5: 367-485.

163. Vandebriel, RJ, and Loveren, Hv. Non-Animal Sensitization Testing: State-of-the-Art. *Critical reviews in toxicology.* 2010, 40, 5: 389-404.

164. Urbisch, D, Mehling, A, Guth, K, Ramirez, T, Honarvar, N, Kolle, S, Landsiedel, R, Jaworska, J, Kern, PS, Gerberick, F, Natsch, A, Emter, R, Ashikaga, T, Miyazawa, M, and Sakaguchi, H. Assessing Skin Sensitization Hazard in Mice and Men Using Non-Animal Test Methods. *Regulatory Toxicology and Pharmacology.* 2015, 71, 2: 337-51.

165. Kleinstreuer, NC, Hoffmann, S, Alépée, N, Allen, D, Ashikaga, T, Casey, W, Clouet, E, Cluzel, M, Desprez, B, Gellatly, N, Göbel, C, Kern, PS, Klaric, M, Kühnl, J, Martinozzi-Teissier, S, Mewes, K, Miyazawa, M, Strickland, J, van Vliet, E, Zang, Q, and Petersohn, D. Non-Animal Methods to Predict Skin Sensitization (Ii): An Assessment of Defined Approaches**. *Critical reviews in toxicology.* 2018, 48, 5: 359-74.

166. Strickland, J, Truax, J, Corvaro, M, Settivari, R, Henriquez, J, McFadden, J, Gulledge, T, Johnson, V, Gehen, S, Germolec, D, Allen, DG, and Kleinstreuer, N. Application of Defined Approaches for Skin Sensitization to Agrochemical Products. *Front Toxicol.* 2022, 4852856.

167. Caloni, F, De Angelis, I, and Hartung, T. Replacement of Animal Testing by Integrated Approaches to Testing and Assessment (Iata): A Call for in Vivitrosi. *Archives of Toxicology.* 2022, 96, 7: 1935-50.

168. Asselineau, D, Bernard, BA, Bailly, C, Darmon, M, and Pruniéras, M. Human Epidermis Reconstructed by Culture: Is It "Normal"? *Journal of investigative dermatology.* 1986, 86, 2: 181-86.

169. Nakamura, M, Haarmann-Stemmann, T, Krutmann, J, and Morita, A. Alternative Test Models for Skin Ageing Research. *Exp Dermatol.* 2018, 27, 5: 495-500.

170. OECD. *Test No. 431: In Vitro Skin Corrosion: Reconstructed Human Epidermis (Rhe) Test Method*, 2019.

171. OECD. *Test No. 439: In Vitro Skin Irritation: Reconstructed Human Epidermis Test Method*, 2021.

172. Cottrez, F, Boitel, E, Ourlin, J-C, Peiffer, J-L, Fabre, I, Henaoui, I-S, Mari, B, Vallauri, A, Paquet, A, Barbry, P, Auriault, C, Aeby, P, and Groux, H. Sens-Is, a 3d Reconstituted Epidermis Based Model for Quantifying Chemical Sensitization Potency: Reproducibility and Predictivity Results from an Inter-Laboratory Study. *Toxicology in Vitro.* 2016, 32248-60.

173. Cottrez, F, Boitel, E, Auriault, C, Aeby, P, and Groux, H. Genes Specifically Modulated in Sensitized Skins Allow the Detection of Sensitizers in a Reconstructed Human Skin Model. Development of the Sens-Is Assay. *Toxicology in Vitro.* 2015, 29, 4: 787-802.

174. Saito, K, Nukada, Y, Takenouchi, O, Miyazawa, M, Sakaguchi, H, and Nishiyama, N. Development of a New in Vitro Skin Sensitization Assay (Epidermal Sensitization Assay; Episensa) Using Reconstructed Human Epidermis. *Toxicology in Vitro.* 2013, 27, 8: 2213-24.

175. Brandmair, K, Dising, D, Finkelmeier, D, Schepky, A, Kuehnl, J, Ebmeyer, J, and Burger-Kentischer, A. A Novel Three-Dimensional Nrf2 Reporter Epidermis Model for Skin Sensitization Assessment. *Toxicology.* 2024, 503153743.

176. Rodrigues Neves, C, and Gibbs, S. Progress on Reconstructed Human Skin Models for Allergy Research and Identifying Contact Sensitizers. *Three Dimensional Human Organotypic Models for Biomedical Research.* 2021,103-29.

177. Zghoul, N, Fuchs, R, Lehr, C-M, and Schaefer, UF. Reconstructed Skin Equivalents for Assessing Percutaneous Drug Absorption from Pharmaceutical Formulations. *ALTEX-Alternatives to animal experimentation.* 2001, 18, 2: 103-06.

178. Van Gele, M, Geusens, B, Brochez, L, Speeckaert, R, and Lambert, J. Three-Dimensional Skin Models as Tools for Transdermal Drug Delivery: Challenges and Limitations. *Expert Opinion on Drug Delivery.* 2011, 8, 6: 705-20.

179. Schäfer-Korting, M, Bock, U, Diembeck, W, Düsing, H-J, Gamer, A, Haltner-Ukomadu, E, Hoffmann, C, Kaca, M, Kamp, H, and Kersen, S. The Use of Reconstructed Human Epidermis for Skin Absorption Testing: Results of the Validation Study. *Alternatives to Laboratory Animals.* 2008, 36, 2: 161-87.

180. Hagvall, L, Munem, M, Hoang Philipsen, M, Dowlatshahi Pour, M, Hedberg, Y, and Malmberg, P. Skin Permeation Studies of Chromium Species – Evaluation of a Reconstructed Human Epidermis Model. *Toxicology in Vitro.* 2023, 91105636.

181. Poumay, Y, Dupont, F, Marcoux, S, Leclercq-Smekens, M, Hérin, M, and Coquette, A. A Simple Reconstructed Human Epidermis: Preparation of the Culture Model and Utilization in in Vitro Studies. *Archives of dermatological research.* 2004, 296203-11.

182. Pupovac, A, Senturk, B, Griffoni, C, Maniura-Weber, K, Rottmar, M, and McArthur, SL. Toward Immunocompetent 3d Skin Models. *Advanced Healthcare Materials.* 2018, 7, 12: 1701405.

183. Régnier, M, Staquet, MJ, Schmitt, D, and Schmidt, R. Integration of Langerhans Cells into a Pigmented Reconstructed Human Epidermis. *J Invest Dermatol.* 1997, 109, 4: 510-2.

184. Regnier, M, Patwardhan, A, Scheynius, A, and Schmidt, R. Reconstructed Human Epidermis Composed of Keratinocytes, Melanocytes and Langerhans Cells. *Medical and Biological Engineering and Computing.* 1998, 36821-24.

185. Bechetoille, N, Dezutter-Dambuyant, C, Damour, O, André, V, Orly, I, and Perrier, E. Effects of Solar Ultraviolet Radiation on Engineered Human Skin Equivalent Containing Both Langerhans Cells and Dermal Dendritic Cells. *Tissue Eng.* 2007, 13, 11: 2667-79.

186. Bock, S, Said, A, Müller, G, Schäfer-Korting, M, Zoschke, C, and Weindl, G. Characterization of Reconstructed Human Skin Containing Langerhans Cells to Monitor Molecular Events in Skin Sensitization. *Toxicol In Vitro.* 2018, 4677-85.

187. Laubach, V, Zöller, N, Rossberg, M, Görg, K, Kippenberger, S, Bereiter-Hahn, J, Kaufmann, R, and Bernd, A. Integration of Langerhans-Like Cells into a Human Skin Equivalent. *Arch Dermatol Res.* 2011, 303, 2: 135-9.

188. Ouwehand, K, Spiekstra, SW, Waaijman, T, Scheper, RJ, de Gruijl, TD, and Gibbs, S. Technical Advance: Langerhans Cells Derived from a Human Cell Line in a Full-Thickness Skin Equivalent Undergo Allergen-Induced Maturation and Migration. *J Leukoc Biol.* 2011, 90, 5: 1027-33.

189. Kosten, IJ, Spiekstra, SW, de Gruijl, TD, and Gibbs, S. Mutz-3 Derived Langerhans Cells in Human Skin Equivalents Show Differential Migration and Phenotypic Plasticity after Allergen or Irritant Exposure. *Toxicol Appl Pharmacol.* 2015, 287, 1: 35-42.

190. Look, SA, Fenical, W, Jacobs, RS, and Clardy, J. The Pseudopterosins: Anti-Inflammatory and Analgesic Natural Products from the Sea Whip Pseudopterogorgia Elisabethae. *Proc Natl Acad Sci U S A.* 1986, 83, 17: 6238-40.

191. Look, SA, Fenical, W, Matsumoto, GK, and Clardy, J. The Pseudopterosins: A New Class of Antiinflammatory and Analgesic Diterpene Pentosides from the Marine Sea Whip Pseudopterogorgia Elisabethae (Octocorallia). *The Journal of Organic Chemistry.* 1986, 51, 26: 5140-45.

192. Berrué, F, McCulloch, MWB, and Kerr, RG. Marine Diterpene Glycosides. *Bioorganic & medicinal chemistry.* 2011, 19, 22: 6702-19.

193. Ata, A, Win, HY, Holt, D, Holloway, P, Segstro, EP, and Jayatilake, GS. New Antibacterial Diterpenes from Pseudopterogorgia Elisabethae. *Helvetica Chimica Acta.* 2004, 87, 5: 1090-98.

194. Roussis, V, Wu, Z, Fenical, W, Strobel, SA, Van Duyne, GD, and Clardy, J. New Anti-Inflammatory Pseudopterosins from the Marine Octocoral Pseudopterogorgia Elisabethae. *The Journal of Organic Chemistry.* 1990, 55, 16: 4916-22.

195. Ata, A, Kerr, RG, Moya, CE, and Jacobs, RS. Identification of Anti-Inflammatory Diterpenes from the Marine Gorgonian Pseudopterogorgia Elisabethae. *Tetrahedron.* 2003, 59, 23: 4215-22.

196. Duque, C, Puyana, M, Narváez, G, Osorno, O, Hara, N, and Fujimoto, Y. Pseudopterosins P–V, New Compounds from the Gorgonian Octocoral Pseudopterogorgia Elisabethae from Providencia Island, Colombian Caribbean. *Tetrahedron.* 2004, 60, 47: 10627-35.

197. Rodríguez, II, Shi, YP, García, OJ, Rodríguez, AD, Mayer, AM, Sánchez, JA, Ortega-Barria, E, and González, J. New Pseudopterosin and Seco-Pseudopterosin Diterpene Glycosides from Two Colombian Isolates of Pseudopterogorgia Elisabethae and Their Diverse Biological Activities. *J Nat Prod.* 2004, 67, 10: 1672-80.

198. Dayan, N, Grove, G, and Sivalenka, R. Anti-Inflammatory Activity of Pseudopterosins by Laser Doppler Blood Flow Evaluation. *International Journal of Cosmetic Science.* 2009, 31, 6: 480-80.

199. Mayer, AMS, Jacobson, PB, Fenical, W, Jacobs, RS, and Glaser, KB. Pharmacological Characterization of the Pseudopterosins: Novel Anti-Inflammatory Natural Products Isolated from the Caribbean Soft Coral, Pseudopterogorgia Elisabethae. *Life Sciences.* 1998, 62, 26: PL401-PL07.

200. Scherl, DS, Afflitto, J, and Gaffar, A. Influence of Oas-1000 on Mediators of Inflammation. *Journal of Clinical Periodontology.* 1999, 26, 4: 246-51.

201. Sperlich, J, Kerr, R, and Teusch, N. The Marine Natural Product Pseudopterosin Blocks Cytokine Release of Triple-Negative Breast Cancer and Monocytic Leukemia Cells by Inhibiting Nf-Kb Signaling. *Mar Drugs.* 2017, 15, 9.

202. Sperlich, J, and Teusch, N. Pseudopterosin Inhibits Proliferation and 3d Invasion in Triple-Negative Breast Cancer by Agonizing Glucocorticoid Receptor Alpha. *Molecules.* 2018, 23, 8.

203. Haimes, HB, and Jimenez, PA. Use of Pseudopterosins for Promoting Wound Healing. Google Patents, 1997.

204. Day, DR, Jabaiah, S, Jacobs, RS, and Little, RD. Cyclodextrin Formulation of the Marine Natural Product Pseudopterosin a Uncovers Optimal Pharmacodynamics in Proliferation Studies of Human Umbilical Vein Endothelial Cells. *Mar Drugs.* 2013, 11, 9: 3258-71.

205. Moya, CE, and Jacobs, RS. Pseudopterosins Appear to Enhance the Wound Healing Process through an Adenosine Receptor Mediated Mechanism. *The FASEB Journal.* 2008, 22, S1: 729.7-29.7.

206. Moya, CE, and Jacobs, RS. Mechanism of Action of the Pseudopterosins and Their Role in Wound Healing. *The FASEB Journal.* 2007, 21, 5: A427-A27.

207. Mayer, AMS, Glaser, KB, Cuevas, C, Jacobs, RS, Kem, W, Little, RD, McIntosh, JM, Newman, DJ, Potts, BC, and Shuster, DE. The Odyssey of Marine Pharmaceuticals: A Current Pipeline Perspective. *Trends in Pharmacological Sciences.* 2010, 31, 6: 255-65.

208. Vimrx Pharmaceuticals New Drug Application Vm 301 for Use in Phase I/IIa Clinical Trials. Ind 60,606. 12 July 2000.

209. Rouhi, AM. Science/Technology: Supply Issues Complicate Trek of Chemicals from Sea to Market▪ Reliable Supply Is a Vexing Problem in Converting Bioactive Marine Chemicals into Commercial Products. *Chemical & Engineering News.* 1995, 7342-44.

210. Chen, J, Namiki, S, Toma-Hirano, M, Miyatake, S, Ishida, K, Shibata, Y, Arai, N, Arai, K-i, and Kamogawa-Schifter, Y. The Role of Cd11b in Phagocytosis and Dendritic Cell Development. *Immunology letters.* 2008, 120, 1-2: 42-48.

211. Ten Broeke, T, Wubbolts, R, and Stoorvogel, W. Mhc Class Ii Antigen Presentation by Dendritic Cells Regulated through Endosomal Sorting. *Cold Spring Harbor perspectives in biology.* 2013, 5, 12: a016873.

212. de Witte, L, Nabatov, A, Pion, M, Fluitsma, D, de Jong, MAWP, de Gruijl, T, Piguet, V, van Kooyk, Y, and Geijtenbeek, TBH. Langerin Is a Natural Barrier to HIV-1 Transmission by Langerhans Cells. *Nature Medicine.* 2007, 13, 3: 367-71.

213. Hunger, RE, Sieling, PA, Ochoa, MT, Sugaya, M, Burdick, AE, Rea, TH, Brennan, PJ, Belisle, JT, Blauvelt, A, Porcelli, SA, and Modlin, RL. Langerhans Cells Utilize Cd1a and Langerin to Efficiently Present Nonpeptide Antigens to T Cells. *J Clin Invest.* 2004, 113, 5: 701-8.

214. Mewes, KR, Raus, M, Bernd, A, Zöller, NN, Sättler, A, and Graf, R. Elastin Expression in a Newly Developed Full-Thickness Skin Equivalent. *Skin Pharmacol Physiol.* 2007, 20, 2: 85-95.

215. Mewes, KR, Zöller, NN, Bernd, A, Prießner, A, DeWever, B, Graf, R, and Schröder, KR. Expression of Dermal Extracellular Matrix Proteins in a Newly Developed Full-Thickness Skin Model. Paper presented at the Cells and Culture, Dordrecht, 2010// 2010.

216. van der Vlist, M, de Witte, L, de Vries, RD, Litjens, M, de Jong, MAWP, Fluitsma, D, de Swart, RL, and Geijtenbeek, TBH. Human Langerhans Cells Capture Measles Virus through Langerin and Present Viral Antigens to Cd4+ T Cells but Are Incapable of Cross-Presentation. *European journal of immunology.* 2011, 41, 9: 2619-31.

217. Jubin, K, Martin, Y, Lawrence-Watt, DJ, and Sharpe, JR. A Fully Autologous Co-Culture System Utilising Non-Irradiated Autologous Fibroblasts to Support the Expansion of Human Keratinocytes for Clinical Use. *Cytotechnology.* 2011, 63, 6: 655-62.

218. Schultz, TW, Dimitrova, G, Dimitrov, S, and Mekenyan, OG. The Adverse Outcome Pathway for Skin Sensitisation: Moving Closer to Replacing Animal Testing. *Altern Lab Anim.* 2016, 44, 5: 453-60.

219. Worbs, T, Hammerschmidt, SI, and Förster, R. Dendritic Cell Migration in Health and Disease. *Nat Rev Immunol.* 2017, 17, 1: 30-48.

220. Tiberio, L, Del Prete, A, Schioppa, T, Sozio, F, Bosisio, D, and Sozzani, S. Chemokine and Chemotactic Signals in Dendritic Cell Migration. *Cellular & Molecular Immunology.* 2018, 15, 4: 346-52.

221. Macanas-Pirard, P, Quezada, T, Navarrete, L, Broekhuizen, R, Leisewitz, A, Nervi, B, and Ramírez, PA. The Ccl2/Ccr2 Axis Affects Transmigration and Proliferation but Not Resistance to Chemotherapy of Acute Myeloid Leukemia Cells. *PLOS ONE.* 2017, 12, 1: e0168888.

222. Tarnowski, M, Liu, R, Wysoczynski, M, Ratajczak, J, Kucia, M, and Ratajczak, MZ. Cxcr7: A New Sdf-1-Binding Receptor in Contrast to Normal CD34(+) Progenitors Is Functional and Is Expressed at Higher Level in Human Malignant Hematopoietic Cells. *Eur J Haematol.* 2010, 85, 6: 472-83.

223. Quan, C, Cho, MK, Shao, Y, Mianecki, LE, Liao, E, Perry, D, and Quan, T. Dermal Fibroblast Expression of Stromal Cell-Derived Factor-1 (SDF-1) Promotes Epidermal Keratinocyte Proliferation in Normal and Diseased Skin. *Protein Cell.* 2015, 6, 12: 890-903.

224. Coutant, KD, de Fraissinette, AdB, Cordier, A, and Ulrich, P. Modulation of the Activity of Human Monocyte-Derived Dendritic Cells by Chemical Haptens, a Metal Allergen, and a Staphylococcal Superantigen. *Toxicological sciences: an official journal of the Society of Toxicology.* 1999, 52, 2: 189-98.

225. Kiertscher, SM, and Roth, MD. Human CD14+ Leukocytes Acquire the Phenotype and Function of Antigen-Presenting Dendritic Cells When Cultured in Gm-Csf and Il-4. *Journal of Leukocyte Biology.* 1996, 59, 2: 208-18.

226. Chapuis, F, Rosenzwajg, M, Yagello, M, Ekman, M, Biberfeld, P, and Gluckman, JC. Differentiation of Human Dendritic Cells from Monocytes in Vitro. *European journal of immunology.* 1997, 27, 2: 431-41.

227. Chanput, W, Mes, JJ, and Wichers, HJ. Thp-1 Cell Line: An in Vitro Cell Model for Immune Modulation Approach. *International Immunopharmacology.* 2014, 23, 1: 37-45.

228. Kleiveland, CR. Peripheral Blood Mononuclear Cells. In *The Impact of Food Bioactives on Health: In Vitro and Ex Vivo Models*, edited by K Verhoeckx, Cotter, P, López-Expósito, I, Kleiveland, C, Lea, T, Mackie, A, Requena, T, Swiatecka, D and Wichers, H, 161-67. Cham: Springer International Publishing, 2015.

229. Berges, C, Naujokat, C, Tinapp, S, Wieczorek, H, Höh, A, Sadeghi, M, Opelz, G, and Daniel, V. A Cell Line Model for the Differentiation of Human Dendritic Cells. *Biochemical and Biophysical Research Communications.* 2005, 333, 3: 896-907.

230. Larsson, K, Lindstedt, M, and Borrebaeck, CAK. Functional and Transcriptional Profiling of Mutz-3, a Myeloid Cell Line Acting as a Model for Dendritic Cells. *Immunology.* 2006, 117, 2: 156-66.

231. Czernek, L, Chworos, A, and Duechler, M. The Uptake of Extracellular Vesicles Is Affected by the Differentiation Status of Myeloid Cells. *Scandinavian journal of immunology.* 2015, 82, 6: 506-14.

232. Galbiati, V, Marinovich, M, and Corsini, E. Mechanistic Understanding of Dendritic Cell Activation in Skin Sensitization: Additional Evidences to Support Potency Classification. *Toxicology Letters.* 2020, 32250-57.

233. Ogasawara, N, Kojima, T, Go, M, Fuchimoto, J, Kamekura, R, Koizumi, J-i, Ohkuni, T, Masaki, T, Murata, M, and Tanaka, S. Induction of Jam-a During Differentiation of Human Thp-1 Dendritic Cells. *Biochemical and Biophysical Research Communications.* 2009, 389, 3: 543-49.

234. Riaz, B, Islam, SMS, Ryu, HM, and Sohn, S. Cd83 Regulates the Immune Responses in Inflammatory Disorders. *Int J Mol Sci.* 2023, 24, 3.

235. Delgado, E, Finkel, V, Baggiolini, M, Mackay, CR, Steinman, RM, and Granelli-Piperno, A. Mature Dendritic Cells Respond to Sdf-1, but Not to Several B-Chemokines. *Immunobiology.* 1998, 198, 5: 490-500.

236. Ricart, BG, John, B, Lee, D, Hunter, CA, and Hammer, DA. Dendritic Cells Distinguish Individual Chemokine Signals through CCR7 and CXCR4. *The Journal of Immunology.* 2011, 186, 1: 53-61.

237. Sallusto, F, Schaerli, P, Loetscher, P, Schaniel, C, Lenig, D, Mackay, CR, Qin, S, and Lanzavecchia, A. Rapid and Coordinated Switch in Chemokine Receptor Expression During Dendritic Cell Maturation. *European journal of immunology.* 1998, 28, 9: 2760-69.

238. Sándor, N, Kristóf, K, Paréj, K, Pap, D, Erdei, A, and Bajtay, Z. Cr3 Is the Dominant Phagocytotic Complement Receptor on Human Dendritic Cells. *Immunobiology.* 2013, 218, 4: 652-63.

239. Mire-Sluis, AR. Expression of Potency: Why Units of Biological Activity Not Mass? *Pharmacy and Pharmacology Communications.* 1997, 3, 1: 15-18.

240. Riemann, H, Schwarz, A, Grabbe, S, Aragane, Y, Luger, TA, Wysocka, M, Kubin, M, Trinchieri, G, and Schwarz, T. Neutralization of Il-12 in Vivo Prevents Induction of Contact Hypersensitivity and Induces Hapten-Specific Tolerance. *The Journal of Immunology.* 1996, 156, 5: 1799-803.

241. Macatonia, SE, Hosken, NA, Litton, M, Vieira, P, Hsieh, C-S, Culpepper, JA, Wysocka, M, Trinchieri, G, Murphy, KM, and O'Garra, A. Dendritic Cells Produce Il-12 and Direct the Development of Th1 Cells from Naive CD4+ T Cells. *Journal of immunology (Baltimore, Md.: 1950).* 1995, 154, 10: 5071-79.

242. Wojno, EDT, Hunter, CA, and Stumhofer, JS. The Immunobiology of the Interleukin-12 Family: Room for Discovery. *Immunity.* 2019, 50, 4: 851-70.

243. Ling, P, Gately, MK, Gubler, U, Stern, AS, Lin, P, Hollfelder, K, Su, C, Pan, YC, and Hakimi, J. Human IL-12 P40 Homodimer Binds to the Il-12 Receptor but Does Not Mediate Biologic Activity. *J Immunol.* 1995, 154, 1: 116-27.

244. Mitjans, M, Viviani, B, Lucchi, L, Galli, CL, Marinovich, M, and Corsini, E. Role of P38 Mapk in the Selective Release of Il-8 Induced by Chemical Allergen in Naïve Thp-1 Cells. *Toxicology in Vitro.* 2008, 22, 2: 386-95.

245. Straube, F, Grenet, O, Bruegger, P, and Ulrich, P. Contact Allergens and Irritants Show Discrete Differences in the Activation of Human Monocyte-Derived Dendritic Cells: Consequences for in Vitro Detection of Contact Allergens. *Archives of Toxicology.* 2005, 79, 1: 37-46.

246. Toebak, MJ, Pohlmann, PR, Sampat-Sardjoepersad, SC, von Blomberg, BME, Bruynzeel, DP, Scheper, RJ, Rustemeyer, T, and Gibbs, S. Cxcl8 Secretion by Dendritic Cells Predicts Contact Allergens from Irritants. *Toxicology in Vitro.* 2006, 20, 1: 117-24.

247. Mitjans, M, Galbiati, V, Lucchi, L, Viviani, B, Marinovich, M, Galli, CL, and Corsini, E. Use of IL-8 Release and P38 Mapk Activation in Thp-1 Cells to Identify Allergens and to Assess Their Potency in Vitro. *Toxicol In Vitro.* 2010, 24, 6: 1803-9.

248. Hennen, J, Aeby, P, Goebel, C, Schettgen, T, Oberli, A, Kalmes, M, and Blömeke, B. Cross Talk between Keratinocytes and Dendritic Cells: Impact on the Prediction of Sensitization. *Toxicological sciences.* 2011, 123, 2: 501-10.

249. Groeber, F, Schober, L, Schmid, FF, Traube, A, Kolbus-Hernandez, S, Daton, K, Hoffmann, S, Petersohn, D, Schäfer-Korting, M, Walles, H, and Mewes, KR. Catch-up Validation Study of an in Vitro Skin Irritation Test Method Based on an Open Source Reconstructed Epidermis (Phase II). *Toxicology in Vitro.* 2016, 36254-61.

250. Stein, M, Bernd, A, Ramirez-Bosca, A, Kippenberger, S, and Holzmann, H. Measurement of Anti-Inflammatory Effects of Glucocorticoids on Human Keratinocytes in Vitro. *Arzneim-Forsch/Drug Res.* 1997, 471266-70.

251. Michel, M, L'Heureux, N, Auger, FA, and Germain, L. From Newborn to Adult: Phenotypic and Functional Properties of Skin Equivalent and Human Skin as a Function of Donor Age. *Journal of cellular physiology.* 1997, 171, 2: 179-89.

252. Tan, Kenneth KB, Salgado, G, Connolly, John E, Chan, Jerry KY, and Lane, EB. Characterization of Fetal Keratinocytes, Showing Enhanced Stem Cell-Like Properties: A Potential Source of Cells for Skin Reconstruction. *Stem Cell Reports.* 2014, 3, 2: 324-38.

253. Umegaki, R, Murai, K, Kino-Oka, M, and Taya, M. Correlation of Cellular Life Span with Growth Parameters Observed in Successive Cultures of Human Keratinocytes. *Journal of Bioscience and Bioengineering.* 2002, 94, 3: 231-36.

254. Rheinwald, JG, and Green, H. Serial Cultivation of Strains of Human Epidermal Keratinocytes: The Formation of Keratinizing Colonies from Single Cells. *Cell.* 1975, 6, 3: 331-43.

255. Mateu, R, Živicová, V, Krejčí, ED, Grim, M, Strnad, H, Vlček, Č, Kolář, M, Lacina, L, Gál, P, Borský, J, Smetana, K, and Dvořánková, B. Functional Differences between Neonatal and Adult Fibroblasts and Keratinocytes: Donor Age Affects Epithelial-Mesenchymal Crosstalk in Vitro. *International Journal of Molecular Medicine.* 2016, 381063 - 74.

256. Rousselle, P, Braye, F, and Dayan, G. Re-Epithelialization of Adult Skin Wounds: Cellular Mechanisms and Therapeutic Strategies. *Advanced Drug Delivery Reviews.* 2019, 146344-65.

257. Plikus, MV, Gay, DL, Treffeisen, E, Wang, A, Supapannachart, RJ, and Cotsarelis, G. Epithelial Stem Cells and Implications for Wound Repair. Paper presented at the Seminars in cell & developmental biology 2012.

258. Cohen, DE, and Heidary, N. Treatment of Irritant and Allergic Contact Dermatitis. *Dermatol Ther.* 2004, 17, 4: 334-40.

259. Tramontana, M, Hansel, K, Bianchi, L, Sensini, C, Malatesta, N, and Stingeni, L. Advancing the Understanding of Allergic Contact Dermatitis: From Pathophysiology to Novel Therapeutic Approaches. *Frontiers in Medicine.* 2023, 10.

260. Reichardt, SD, Amouret, A, Muzzi, C, Vettorazzi, S, Tuckermann, JP, Lühder, F, and Reichardt, HM. The Role of Glucocorticoids in Inflammatory Diseases. *Cells.* 2021, 10, 11: 2921.

261. Hengge, UR, Ruzicka, T, Schwartz, RA, and Cork, MJ. Adverse Effects of Topical Glucocorticosteroids. *Journal of the American Academy of Dermatology.* 2006, 54, 1: 1-15.

262. Mehta, AB, Nadkarni, NJ, Patil, SP, Godse, KV, Gautam, M, and Agarwal, S. Topical Corticosteroids in Dermatology. *Indian J Dermatol Venereol Leprol.* 2016, 82, 4: 371-8.

263. Coondoo, A, Phiske, M, Verma, S, and Lahiri, K. Side-Effects of Topical Steroids: A Long Overdue Revisit. *Indian Dermatol Online J.* 2014, 5, 4: 416-25.

264. Correa, H, Aristizabal, F, Duque, C, and Kerr, R. Cytotoxic and Antimicrobial Activity of Pseudopterosins and Seco-Pseudopterosins Isolated from the Octocoral Pseudopterogorgia Elisabethae of San Andrés and Providencia Islands (Southwest Caribbean Sea). *Mar Drugs.* 2011, 9, 3: 334-43.

265. Caplan, SL, Zheng, B, Dawson-Scully, K, White, CA, and West, LM. Pseudopterosin A: Protection of Synaptic Function and Potential as a Neuromodulatory Agent. *Mar Drugs.* 2016, 14, 3.

266. Moya, CE, and Jacobs, RS. Pseudopterosin a Inhibits Phagocytosis and Alters Intracellular Calcium Turnover in a Pertussis Toxin Sensitive Site in Tetrahymena Thermophila. *Comparative Biochemistry and Physiology Part C: Toxicology & Pharmacology.* 2006, 143, 4: 436-43.

267. Niu, X, Yu, C, Jiang, G, Wu, J, Tan, X, Zhang, W, and Hou, L. Pseudopterosin A ameliorates Ischaemia-Induced Brain Injury by Acting on Akt Signalling Pathway. *Folia Neuropathol.* 2018, 56, 2: 104-11.

268. Nguyen, HL, and Yiannias, JA. Contact Dermatitis to Medications and Skin Products. *Clinical Reviews in Allergy & Immunology.* 2019, 56, 1: 41-59.

269. Saito, K, Miyazawa, M, Nukada, Y, Sakaguchi, H, and Nishiyama, N. Development of an in Vitro Skin Sensitization Test Based on Ros Production in Thp-1 Cells. *Toxicology in Vitro.* 2013, 27, 2: 857-63.

270. Arkusz, J, Stępnik, M, Sobala, W, and Dastych, J. Prediction of the Contact Sensitizing Potential of Chemicals Using Analysis of Gene Expression Changes in Human Thp-1 Monocytes. *Toxicology Letters.* 2010, 199, 1: 51-59.

271. Silberberg-Sinakin, I, and Thorbecke, GJ. Contact Hypersensitivity and Langerhans Cells. *J Invest Dermatol.* 1980, 75, 1: 61-7.

272. Zoio, P, and Oliva, A. Skin-on-a-Chip Technology: Microengineering Physiologically Relevant in Vitro Skin Models. *Pharmaceutics.* 2022, 14, 3: 682.

273. Risueño, I, Valencia, L, Jorcano, JL, and Velasco, D. Skin-on-a-Chip Models: General Overview and Future Perspectives. *APL Bioeng.* 2021, 5, 3: 030901.

274. Zhang, Q, Sito, L, Mao, M, He, J, Zhang, YS, and Zhao, X. Current Advances in Skin-on-a-Chip Models for Drug Testing. *Microphysiol Syst.* 2018, 2.

275. Fernandez-Carro, E, Angenent, M, Gracia-Cazaña, T, Gilaberte, Y, Alcaine, C, and Ciriza, J. Modeling an Optimal 3d Skin-on-Chip within Microfluidic Devices for Pharmacological Studies. *Pharmaceutics.* 2022, 14, 7: 1417.

6 Appendix

List of Abbreviations

°C	degree Celsius
µg	Microgram
µM	Micromolar
ACD	Allergic contact dermatitis
ADRA	Amino Acid Derivative Reactivity Assay
AI	Artificial Intelligence
AO	Adverse outcome
AOP	Adverse Outcome Pathway
APC	Antigen-presenting cell
ARE	Antioxidant response element
ATCC	American Type Culture Collection
BA	Buehler assay
CCL	C-C chemokine ligand
CCR	C-C chemokine receptor
CD	Cluster of Differentiation
cDNA	complementary Deoxyribonucleic acid
CHS	Contact hypersensitivity
CLP	Classification, Labelling and Packing Regulation
Ct	Crossing threshold
CTL-4	Cytotoxic T-lymphocyte-associated protein 4
CXCL	C-X-C chemokine ligand
CXCR	C-X-C chemokine receptor
d	Day(s)
DA	Defined approach
DAPI	4′,6-Diamidin-2-phenylindol
DC	Dendritic cell
DDC	Dermal dendritic cell
Dex	Dexamethasone
DMEM	Dulbeccos Modified Eagle Medium
DMSO	Dimethylsulfoxide
DNA	Deoxyribonucleic acid
DNCB	1-Chlor-2,4-dinitrobenzol
DPRA	Direct Peptide Reactivity Assay
DSMZ	Deutsche Sammlung von Mikroorganismen und Zellkulturen

EU	European Union
EURL ECVAM	European Union Reference Laboratory on Alternatives to Animal Testing
FDA	Food and Drug Administration
FT	Full-thickness
GAPDH	Glyceraldehyde 3-phosphate dehydrogenase
GARD	Genomic Allergen Rapid Detection
GHS	Global Harmonized System
GM-CSF	Granulocyte-macrophage colony-stimulating factor
GMFI	Geometric mean fluorescence intensity
GMPT	Guinea Pig maximization test
GPS	Genomic Prediction Signature
h	hour
HA	Hyaluronic acid
h-CLAT	human cell line activation test
HIF-1	Hypoxia-inducible factor-1
HLA-DR	Human Leukocyte Antigen – DR isotype
HMOX-1	Heme oxygenase 1
ICAM-1	Intracellular adhesion molecule 1
ICD	Irritant contact dermatitis
iDCs	Immature dendritic cells
IF	Immunofluorescence
IL	Interleukin
IS	Immunological synapse
IκBα	Inhibitor protein kappa B alpha
kDPRA	Kinetic Direct Peptide Reactivity Assay
KE	Key event
KEAP-1	Kelch-like ECH-associated protein 1
LC	Langerhans cell
LFA-1	Leukocyte function-associated antigen 1
LLNA	Local lymph node assay
LPS	Lipopolysaccharide
MAPK	Mitogen activated protein kinase
MARCH	Membrane-associated RING-CH
mDCs	Mature dendritic cells
mg	Milligram
MHC	Major histocompatibility complex
MIE	Molecular initiating event

min	Minutes
mL	Millilitre
mM	Millimolar
mRNA	Messenger ribonucleic acid
NF-κB	Nuclear factor kappa light chain enhancer of activated B cells
ng	Nanogram
$NiSO_4$	Nickel sulfate
NLRP3	NOD-like receptor family pyrin domain-containing 3
NRC	National Research Council
Nrf2	Nuclear factor erythroid 2
OECD	Organisation for Economic Co-operation and Development
PBMC	Peripheral blood monocytes
PBS	Dulbecco's phosphate buffered saline
REACH	Regulation on registration, evaluation, authorisation and restriction of chemicals
RFI	Relative fluorescence intensity
rh	recombinant human
RIPA	Radioimmunoprecipitation assay
ROS	Reactive oxygen species
RPMI	Roswell Park Memorial Institute
RT-qPCR	Real-time quantitative polymerase-chain reaction
SDF-1	Stromal cell-derived factor 1
T-bet	T-box expressed in T cells
TG	Test guideline
TGF-β	Transforming growth factor β
Th	T helper
TLR	Toll like receptor
TNCB	Trinitrochlorobenzene
TNF-α	Tumor necrosis factor α
U-SENS	U937 Cell Line Activation Test
UV	Ultraviolet

List of Figures

List of Tables

Publications and participation at scientific conferences

Publications

Johanna Maria Hölken and Nicole Elisabeth Teusch. “Recent developments of 3D models of the tumor microenvironment for cutaneous melanoma: Bridging the gap between the bench and the bedside?” Journal of Translational Science (2020). doi: 10.15761/JTS.1000388

Johanna Maria Hölken and Nicole Teusch, “The monocytic cell line THP-1 as a validated and robust surrogate model for human dendritic cells” International Journal of Molecular Science (2023). doi: 10.3390/ijms24021452

Johanna Maria Hölken, Katja Friedrich, Marion Merkel, Nelli Blasius, Ursula Engels, Timo Buhl, Karsten Rüdiger Mewes, Lars Vierkotten and Nicole Elisabeth Teusch. “A human 3D immune competent full-thickness skin model mimicking dermal dendritic cell activation” Frontiers in Immunology (2023). doi: 10.3389/fimmu.2023.1276151

Johanna Maria Hölken, Anna-Lena Wurz, Katja Friedrich, Patricia Böttcher, Dounia Asskali, Holger Stark, Jörg Breitkreutz, Timo Buhl, Lars Vierkotten, Karsten Rüdiger Mewes and Nicole Teusch. “Incorporating immune cell surrogates into a full-thickness tissue equivalent of human skin to characterize dendritic cell activation” *Submitted to Scientific Reports*

Conference Participations

09/2023 **10th Polish-German Symposium on Pharmaceutical Science**, Düsseldorf, Germany, Poster: Engineering a human 3D immune competent skin model for drug discovery

04/2023 **3D Cell Culture**, DECHEMA, Freiburg, Germany, Oral presentation and Poster: Development of a human 3D immune competent skin model for the analysis of dendritic cell activation to identify skin sensitizers

02/2023 **Skin-Immune Crosstalk**, Breckenridge, CO, United States, Poster: Development of a human 3D immune competent skin model for the analysis of dendritic cell activation to identify skin sensitizers

05/2021 **3D Cell Culture**, DECHEMA, Freiburg, Germany (online), Virtual conference participation

Danksagung

In erster Linie danke ich Frau Prof. Dr. Nicole Teusch für die Möglichkeit an dem Thema der vorliegenden Arbeit zu forschen. Danke für Deine Unterstützung und Betreuung während der gesamten Promotion; für die Möglichkeit der Teilnahme an internationalen Konferenzen; für die wertvollen wissenschaftlichen Diskussionen; für den Freiraum, eigene Ideen und Ansätze auszuprobieren; die Möglichkeit meinen wissenschaftlichen Horizont zu erweitern und über mich selbst hinauszuwachsen und mich persönlich und wissenschaftlich weiterzuentwickeln.

Des Weiteren möchte ich mich ganz herzlich bei Prof. Dr. Stefanie Scheu für die kurzfristige Übernahme der Begutachtung dieser Arbeit bedanken.

Mein Dank gilt allen Kooperationspartnern im 3D-ImmunoSkin-Team, namentlich: Dirk Peterson, Karsten Mewes, Lars Vierkotten, Marion Merkel, Nelli Blasius, Patricia Böttcher, Laura Steinmeyer, Timo Buhl, Moritz Hollstein und Marvin Nüsken. Danke für Eure Unterstützung und die wertvollen wissenschaftlichen Diskussionen in den Meetings. An dieser Stelle ein besonderer Dank an Marion und Nelli für die technische Unterstützung und an Karsten und Lars, die mit ihrer Expertise bei allen Fragen rund um die Hautmodelle jederzeit zur Verfügung standen.

Mein herzlicher Dank gilt auch Prof. Dr. Eckhart Lammert für die Übernahme der Mentorenschaft und für die übergangsweise Bereitstellung seiner Labore nach unserem Umzug von der Universität Osnabrück an die HHU.

Danke an alle ehemaligen und aktuellen Mitglieder des AK-Teusch-Teams, die mich auf dem Weg der Promotion begleitet haben, namentlich: Irene Reimche, Jan Hänsel, Karin Peter, Meike Siendenkersting, Janina Krause, Gabriele Baron-Ruppert, Daria Janssen, Arta Kuci, Dina El-Kashef, Ying Gao, Katja Schiedlauske, Alina Deipenbrock, Vanessa Wiegand, Katja Friedrich, Simone Miljanovic, Claudia Eckelskemper, Deborah Obidake, Büsra Kirmizigül, Anna-Lena Wurz und Kyra Moustakas.

Ein besonderer Dank gilt hier Anna-Lena, die mit ihrer Motivation und ihrem Engagement während ihrer Masterarbeit wesentlich zu diesem Projekt beigetragen hat.

Mein ganz besonderer Dank geht auch an Katja F., für die maßgebliche Unterstützung im Projekt, für die stets warmherzigen, aufmunternden und motivierenden Worte und für die lustigen Teepausen im Büro.

Danke auch an Katja S. und Alina für Eure Hilfsbereitschaft, den gegenseitigen Austausch und die gemeinsamen Tee- und Quatschpausen, die ich ganz sicher vermissen werde.

Vielen Dank für die tolle gemeinsame Zeit, die ich nicht vergessen werde!

Danke an meine Studienfreundinnen aus dem Bachelor und Master, für Euren Zuspruch und Ansporn, wenn es im Labor mal wieder stressig war, Experimente mal nicht funktioniert haben oder die Nerven im Peer-Review-Prozess blank lagen. Danke an meine langjährigen Freunde aus der Kindheit und Schulzeit, für Euren Rückhalt und dass ihr mich regelmäßig daran erinnert, dass meine Versuche im Labor zwar super cool sind, aber das Leben außerhalb des Labors auch.

Mein größter Dank geht an meine Familie. DANKE für Eure Liebe, Euer Verständnis und Eure Geduld an der ein oder anderen Stelle während dieser Arbeit und die stets offenen Ohren. Danke an Papa, Clara und Thea für Euer Bemühen, mein Projekt und meine Versuche bis ins kleinste Detail zu verstehen und mir stets bei den Lösungsansätzen behilflich zu sein. Danke für Eure Unterstützung und Euren unerschütterlichen Humor, egal was das Leben so bereithält. In Erinnerung an meine Mama, die mich immer ermutigt hat, meinen Weg zu gehen.

Eidesstattliche Erklärung

Hiermit erkläre ich, Johanna Maria Hölken, an Eides statt, dass die vorliegende Dissertation von mir selbstständig und ohne unzulässige fremde Hilfe unter Beachtung der „Grundsätze zur Sicherung guter wissenschaftlicher Praxis an der Heinrich-Heine-Universität Düsseldorf“ erstellt worden ist. Die Dissertation wurde in der vorgelegten oder in ähnlicher Form noch bei keiner anderen Fakultät eingereicht. Ich habe bisher keine erfolglosen und erfolgreichen Promotionsversuche unternommen.

Münster, 15.05.2024

Johanna Maria Hölken